

ANALYSIS OF FOUNDATION WITH  
WIDELY SPACED BATTER PILES

by

Katsuyuki Awoshika  
Lymon C. Reese

Research Report Number 117-3F

Development of Method of Analysis of Deep  
Foundations Supporting Bridge Bents

Research Project 3-5-68-117

conducted for

The Texas Highway Department

in cooperation with the  
U. S. Department of Transportation  
Federal Highway Administration

by the

CENTER FOR HIGHWAY RESEARCH  
THE UNIVERSITY OF TEXAS AT AUSTIN

February 1971

The opinions, findings, and conclusions expressed in this publication are those of the authors and not necessarily those of the Federal Highway Administration.

## PREFACE

This report is the last of three reports dealing with the findings of Research Project 3-5-68-117, "Development of Method of Analysis of Deep Foundations Supporting Bridge Bents." The first report combines the existing methods of analysis of a grouped pile foundation with typical soil criteria for automatic generation of lateral soil resistance ( $p$ - $y$ ) curves. The second report presents the methods of predicting the axial and lateral behavior of a single pile in sand to facilitate the analysis of grouped pile foundation.

This final report gives a new method of analysis of grouped pile foundations. This new method eliminates some limitations inherent in methods previously available. The evaluation of the theory for grouped pile behavior is made by comparing analytical and experimental results. This report also summarizes design procedures for a grouped pile foundation.

The authors wish to acknowledge the technical aid given by Messrs. Harold H. Dalrymple, Olen Hudson, and Fred Koch. The invaluable assistance and advice of Messrs. H. D. Butler and Warren Grasso of the Texas Highway Department and Mr. Bob Stanford of the Federal Highway Administration are gratefully appreciated.

This page replaces an intentionally blank page in the original.

-- CTR Library Digitization Team

## LIST OF REPORTS

Report No. 117-1, "A Method for the Analysis of Pile Supported Foundations Considering Nonlinear Soil Behavior," by Frazier Parker, Jr., and William R. Cox, presents the documentation of a procedure which was developed for the analysis of pile supported foundations and the use of the procedure to analyze two bridge bents that were designed and built by the Texas Highway Department.

Report No. 117-2, "Experimental and Analytical Studies of Behavior of Single Piles in Sand Under Lateral and Axial Loading," by Frazier Parker, Jr., and Lymon C. Reese, presents criteria for describing families of nonlinear axial and lateral pile-soil interaction curves for piles in sand, and solves example problems using the proposed criteria.

Report No. 117-3F, "Analysis of Foundation with Widely Spaced Batter Piles," by Katsuyuki Awoshika and Lymon C. Reese, presents a theory for a grouped pile foundation with an experimental evaluation.

This page replaces an intentionally blank page in the original.

-- CTR Library Digitization Team

## ABSTRACT

A theory for solving the displacement of a two-dimensional foundation with widely spaced batter piles under any arbitrary static loading is presented. The theory is capable of dealing with a highly nonlinear soil-pile interaction system as well as the nonlinear pile material. The pile in the foundation may possess variable sectional properties along its axis and may have any degree of fixity to the pile cap.

The theory consists of a numerical procedure for seeking the equilibrium of the applied load and the pile reactions using formulated finite difference methods to compute the pile-top reactions of an axially loaded pile and a laterally loaded pile.

An experiment was conducted on small-sized steel pipe piles which were two inches in diameter and embedded eight feet in a submerged, dense fine sand. A number of single piles were tested to examine the behavior of an axially loaded pile and a laterally loaded pile. Then, the behavior of grouped pile foundations with four piles was compared with analytical predictions which were based on information about the axial behavior of a single pile and the soil criteria for a laterally loaded single pile.

Good agreement was obtained between theory and experiment. The analytical procedure which is presented can be immediately useful in computing the behavior of a pile supported foundation under inclined and eccentric loading.

**KEY WORDS: FOUNDATION, GROUPED PILES, PILES, DESIGN, COMPUTERS, BRIDGE, OFFSHORE STRUCTURE**

This page replaces an intentionally blank page in the original.

-- CTR Library Digitization Team



## SUMMARY

A theory is proposed which presents the possibility of making a very general analysis of grouped pile foundations. The method allows the computation of lateral load, bending moment, and axial load sustained by each pile in a grouped pile foundation. The most economical design of a pile foundation, including pile material, pile dimensions, and the arrangement of the piles in a foundation, can be found by successive application of the proposed analytical procedure.

This page replaces an intentionally blank page in the original.

-- CTR Library Digitization Team

## IMPLEMENTATION STATEMENT

The result of the research is materialized by developing a set of three computer programs. A computer program GROUP is written for the analysis or the design of a grouped pile foundation. The analysis of axial and lateral behavior of a single pile may be made by computer programs AXP and LLP, respectively.

These computer programs are documented in the report with example problems, so that they are available for analysis and design purposes.

The analytical procedure which is presented can be immediately useful in computing the behavior of a pile supported foundation under inclined and eccentric loading.

This page replaces an intentionally blank page in the original.

-- CTR Library Digitization Team

## TABLE OF CONTENTS

	<u>Page</u>
PREFACE . . . . .	iii
LIST OF REPORTS . . . . .	v
ABSTRACT. . . . .	vii
SUMMARY . . . . .	ix
IMPLEMENTATION STATEMENT . . . . .	xi
NOMENCLATURE . . . . .	xix
CHAPTER I, INTRODUCTION . . . . .	1
Description of the Problem . . . . .	1
Review of Theories . . . . .	2
Review of Experiments . . . . .	8
State of the Art and Scope of Study . . . . .	10
CHAPTER II, MECHANICS OF GROUPED PILE FOUNDATION . . . . .	13
Basic Structural System . . . . .	13
Terminology . . . . .	17
Assumptions . . . . .	17
Two-Dimensionality. . . . .	17
Nondeformability of Pile Cap . . . . .	18
Wide Pile Spacing . . . . .	18
No Interaction Between Axially Loaded Pile and Laterally Loaded Pile . . . . .	19
Two-Dimensional Grouped Pile Foundation . . . . .	20
Coordinate Systems and Sign Conventions . . . . .	20
Transformation of Coordinates . . . . .	22
Displacement . . . . .	22
Force . . . . .	25

	<u>Page</u>
Successive Displacement Correction Method . . . . .	26
Force Correction Vector . . . . .	28
Stiffness Matrix . . . . .	29
Displacement Correction Vector . . . . .	30
Computational Procedure . . . . .	31
Laterally Loaded Pile . . . . .	33
Differential Equations for a Beam Column . . . . .	34
Finite Difference Approximation . . . . .	36
Recursive Solution of Difference Equations . . . . .	38
Boundary Conditions at Pile Top . . . . .	39
Displacement Boundary Condition, Pinned Connection. . . . .	40
Displacement Boundary Condition, Fixed Connection . . . . .	42
Displacement Boundary Condition, Elastically Restrained Connection . . . . .	42
Force Boundary Condition . . . . .	43
Boundary Conditions at Pile Tip . . . . .	45
Solution of a Laterally Loaded Pile Problem . . . . .	46
Axially Loaded Pile . . . . .	47
Basic Equations . . . . .	49
Finite Difference Equation . . . . .	53
Boundary Condition . . . . .	54
Recursive Solution . . . . .	55
Elasto-Plastic Pile Strength . . . . .	56
Interaction Diagram . . . . .	57
Moment Curvature Relationship . . . . .	59
CHAPTER III, SOIL CRITERIA FOR SOIL PILE INTERACTION SYSTEM . . . . .	61
Laterally Loaded Pile . . . . .	61
Soil Modulus . . . . .	61
Clay . . . . .	63
McClelland and Focht's Criteria . . . . .	63
Skempton's Criteria . . . . .	65

	<u>Page</u>
Reese's Criteria . . . . .	66
Matlock's Criteria . . . . .	70
Sand . . . . .	74
Reese's Criteria . . . . .	74
Parker and Reese's Criteria . . . . .	77
Summary . . . . .	80
Axially Loaded Pile . . . . .	81
Load Transfer and Point Resistance . . . . .	81
Clay . . . . .	82
Coyle and Reese's Criteria . . . . .	82
Skempton's Criteria . . . . .	85
Sand . . . . .	86
Coyle and Sulaiman's Criteria . . . . .	86
Parker and Reese's Criteria . . . . .	87
Meyerhof's Criteria . . . . .	90
Summary . . . . .	91
CHAPTER IV, DESIGN OF EXPERIMENT . . . . .	93
Aim and Outline of Experiment . . . . .	93
Test Setup . . . . .	93
Piles . . . . .	95
Measurement . . . . .	100
Sand . . . . .	100
CHAPTER V, ANALYSIS OF EXPERIMENT ON SINGLE PILES. . . . .	107
Axially Loaded Pile . . . . .	107

	<u>Page</u>
Axial Load Versus Pile-Top Displacement . . . . .	107
Load Transfer . . . . .	118
Experimental Load Transfer and Point Resistance . . .	118
Analysis of Load Transfer . . . . .	122
Conclusion . . . . .	127
Laterally Loaded Pile . . . . .	128
Measurement of Displacement and Moment . . . . .	128
Experimental Lateral Soil Resistance Curves . . . . .	132
Theoretical Lateral Soil Resistance Curves. . . . .	137
Effect of Batter . . . . .	142
Conclusion . . . . .	144
CHAPTER VI, ANALYSIS OF EXPERIMENT ON GROUPED PILE FOUNDATION . .	145
Cap 1 . . . . .	146
Test 22-1 . . . . .	146
Test 22-2 . . . . .	154
Test 22-3 . . . . .	156
Cap 2 . . . . .	159
Displacement . . . . .	161
Force . . . . .	165
Discussion . . . . .	171
CHAPTER VII, NUMERICAL EXAMPLES . . . . .	173
Example 1, Test Grouped Pile Foundation, Cap 2 . . . . .	173
Example 2, Copano Bay Causeway Bent . . . . .	177
CHAPTER VIII, CONCLUSIONS AND RECOMMENDATIONS . . . . .	183
REFERENCES . . . . .	187
APPENDIX A. Computer Program GROUP . . . . .	193
APPENDIX B. Computer Program LLP . . . . .	263



	<u>Page</u>
APPENDIX C. Computer Program AXP . . . . .	291
APPENDIX D. Displacement Measurement of Pile Cap . . . . .	317

This page replaces an intentionally blank page in the original.

-- CTR Library Digitization Team

## NOMENCLATURE

<u>Symbol</u>	<u>Units (Typical)</u>	<u>Definition</u>
A	inch <sup>2</sup>	cross-sectional area of pile
A <sub>s</sub>	dimensionless	Terzaghi's coefficient for lateral soil modulus
b	inch	width of pile
C	inch-pound	rotational spring constant at pile top
D <sub>R</sub>	dimensionless	relative density of a sand
D <sub>10</sub>	mm	soil diameter at which 10 per cent of the soil weight is finer
D <sub>60</sub>	mm	soil diameter at which 60 per cent of the soil weight is finer
$\bar{dF}$		force correction vector
$\bar{dR}$		total pile reaction variation vector
$\bar{dU}$		displacement correction vector
$\bar{dV}$		displacement variation vector
E	pounds per inch <sup>2</sup>	Young's modulus
E <sub>s</sub>	pounds per inch <sup>2</sup>	soil modulus
G <sub>s</sub>	dimensionless	specific gravity of soil particle
h	inch	increment length of a pile element
I	inch <sup>4</sup>	moment of inertia
J <sub>i</sub>		number of piles in the ith individual pile group
K		stiffness matrix
F		resultant load vector on pile cap

<u>Symbol</u>	<u>Units (Typical)</u>	<u>Definition</u>
$l$	inch	circumference of a cylindrical pile or a perimeter encompassing an H pile
$M$	inch-pound	moment in a beam column
$M_i$	inch-pound	moment on top of pile in the $i$ th individual pile group
$M'_i$	inch-pound	moment exerted on pile cap by the pile in the $i$ th individual pile group with regard to the origin of the structural coordinate system
$M_o$	inch-pound	applied moment on the pile cap around the origin of the structural coordinate system
$M_t$	inch-pound	moment on pile top
$M_y$	inch-pound	yield moment
$M_{y0}$	inch-pound	yield moment for pure bending
$P$	pound	axial force in a beam column
$P_i$	pound	axial reaction of pile in the $i$ th individual pile group
$P'_i$	pound	vertical pile reaction on pile cap from the pile in the $i$ th individual pile group
$\bar{P}_i$		reaction vector of the pile in the $i$ th individual pile group
$\bar{P}'_i$		reaction vector of the pile in the $i$ th individual pile group in structural coordinate system
$P_o$	pound	vertical component of resultant load on the pile cap acting at the origin of structural coordinate system
$P_u$	pound	ultimate axial load
$P_{uo}$	pound	ultimate axial load for pure axial loading

<u>Symbol</u>	<u>Units (Typical)</u>	<u>Definition</u>
$p$	pounds per inch	distributed spring force on a beam column
$P_f$	pounds per inch	ultimate lateral soil resistance by flow around type failure
$P_u$	pounds per inch	ultimate lateral soil resistance
$P_w$	pounds per inch	ultimate lateral soil resistance by wedge type failure
$Q$	pound	shear force in a beam column
$Q_i$	pound	lateral reaction of pile in the $i$ th individual pile group
$Q'_i$	pound	horizontal pile reaction on pile cap from the pile cap acting at the origin of structural coordinate system
$Q_o$	pound	horizontal component of resultant load on the pile cap acting at the origin of structural coordinate system
$q$	pounds per inch	distributed load on a beam column
$\bar{R}$		total pile reaction vector
$S$	dimensionless	slope of a beam column
$S_i$	dimensionless	slope at $i$ th station of a pile
$s$	dimensionless	shape factor
$T$	psi	load transfer
$T_{D,i}$		displacement transformation matrix for the pile in the $i$ th individual pile group
$T_{F,i}$		force transformation matrix of the pile in the $i$ th individual pile group
$U$	inch	vertical displacement (X axis) of pile cap
$\bar{U}$		displacement vector of the pile cap

<u>Symbol</u>	<u>Units (Typical)</u>	<u>Definition</u>
$u_i$	inch	pile-top displacement in $x_i$ axis of member coordinate system
$u'_i$	inch	pile-top displacement in $x'_i$ axis of the local coordinate system
$\bar{u}_i$		displacement vector of head of pile in the $i$ th individual pile group
$V$	inch	horizontal displacement (Y axis) of pile cap
$v_i$	inch	pile-top displacement in $y_i$ axis of member coordinate system
$v'_i$	inch	pile-top displacement in $y'_i$ axis of the local coordinate system
$X$	inch	vertical axis of the structural coordinate system
$x_i$	inch	an axis which coincides with pile axis of the $i$ th individual pile group
$x'_i$	inch	vertical axis of the local structural coordinate system of the $i$ th individual pile group
$Y$	inch	horizontal axis of the structural coordinate system
$y$	inch	lateral pile deflection
$y_i$	inch	an axis perpendicular to pile axis of the $i$ th individual pile group
$y'_i$	inch	horizontal axis of the local structural coordinate system of the $i$ th individual pile group
$y_t$	inch	lateral deflection of the top of pile
$y_{50}$	inch	lateral pile deflection corresponding to $p_u/2$

<u>Symbol</u>	<u>Units (Typical)</u>	<u>Definition</u>
Z	inch <sup>3</sup>	section modulus
Z <sub>t</sub>	pound	transverse force on pile top
z	inch	axial pile displacement
α	radian	rotational angle of pile cap
β	inch <sup>-1</sup>	characteristic length $4\sqrt{\frac{E_s}{4EI}}$
γ	pcf	unit weight of soil
γ <sub>min</sub>	pcf	minimum dry density
γ <sub>max</sub>	pcf	maximum dry density
ε	dimensionless	strain
ε <sub>50</sub>	dimensionless	strain corresponding to $\sigma_{\Delta f}/2$
λ	dimensionless	scale factor for the suffixed quantity
λ <sub>i</sub>	radian	batter angle of a pile in the ith individual pile group
μ	pounds per inch <sup>3</sup>	secant modulus of the load transfer curve
ν	pounds per inch	secant modulus of a point resistance curve
1/ρ	inch <sup>-1</sup>	curvature
σ <sub>Δ</sub>	psi	deviator stress
σ <sub>Δf</sub>	psi	ultimate deviator stress
σ <sub>y</sub>	psi	yield stress
φ	degree	angle of internal friction of sand

CHAPTER I  
INTRODUCTION

Description of the Problem.

The behavior of a pile group may be influenced by two forms of group interaction: The first form of interaction is the "group effect" produced by piles which are in close proximity to one another. The second form of interaction is a result of the interaction between pile tops which are connected by a pile cap. In the first instance the interactive forces are transmitted by the soil, while in the second form of interaction, the forces are transmitted through the pile cap above the soil. However, if the piles are spaced widely apart the interaction between piles is influenced primarily by the pile cap and the group effect or the interactive influence of the soil is insignificant.

In this study the group behavior of piles produced by the pile cap is described and it is assumed that no group effect is produced by the proximity of the piles.

The aim of this research is the development of rational design procedures for a widely spaced group pile foundation, including both vertical and battered piles. Numerical methods are formulated in detail, and computer programs for making the necessary computations are presented and described. A principal phase of this research is the performance and analysis of experiments on small-sized piles. Before discussing the experiments and the design recommendations, the problem is described fully. A literature survey is given, and a comprehensive statement is made concerning the mechanics of the problem.



The behavior of a pile group as considered in this study requires a knowledge of the single-pile behavior. A companion study to this one (Parker and Reese, 1970) is concerned with the load-displacement characteristics of individual piles and detailed reference will be made to that study where appropriate.

### Review of Theories.

The development of computational methods has been limited because of lack of knowledge about single-pile behavior. In order to meet the practical needs of designing structures with grouped piles, various computational methods were developed by making assumptions that would permit analysis of the problem.

The simplest way to treat a grouped pile foundation is to assume that both the structure and the piles are rigid and that only the axial resistance of the piles is considered. The lateral resistance of piles is excluded from the computation. Under these assumptions, Culmann (Terzaghi, 1956) presented a graphical solution in 1866. The equilibrium state of the resultant external load and the axial reaction of each group of similar piles was obtained by drawing a force polygon. The application of Culmann's method is limited to the case of a foundation with three groups of similar piles. A supplemental method to this graphical solution was proposed in 1970 by Brennecke and Lohmeyer (Terzaghi, 1956). The vertical component of the resultant load is distributed in a trapezoidal shape in such a way that the total area equals the magnitude of the vertical component, and its center of gravity lies on the line of action of the vertical component of the resultant load. The vertical load is distributed to each pile,

assuming that the trapezoidal load is separated into independent blocks at the top of the piles, except at the end piles. Unlike Culmann's method, the later method can handle more than three groups of similar piles. But the Brennecke and Lohmeyer method is restricted to the case where all of the pile tops are on the same level.

The elastic displacement of pile tops was first taken into consideration by Westergaard in 1917 (Karol, 1960). Westergaard assumed linearly elastic displacement of pile tops under a compressive load, but the lateral resistance of the pile was not considered. He developed a method to find a center of rotation of a pile cap. With the center of rotation known, the displacements and forces in each pile could be computed.

Nökkentved (Hansen, 1959) presented in 1924 a method similar to that of Westergaard. He defined a point that was dependent only on the geometry of the pile arrangement, so that forces which pass through this point produce only unit vertical and horizontal translations of the pile cap. The method was also pursued by Vetter (Terzaghi, 1956) in 1939. Vetter introduced the "dummy pile" technique to simulate the effect of the lateral restraint and the rotational fixity of pile tops. Dummy piles are properly assumed to be imaginary elastic columns.

Later, in 1953, Vandepitte (Hansen, 1959) applied the concept of the elastic center in developing the ultimate design method, which was further formulated by Hansen (1959). The transitional stage in which some of the piles reach the ultimate bearing capacity, while the remainder of the piles in a foundation are in an elastic range, can be computed by a purely elastic method if the reactions of the piles in the ultimate stages are regarded as constant forces on the cap. The failure of the cap is reached after

successive failures of all but the last two piles. Then the cap can rotate around the intersection of the axis of the two elastic piles. Vandepitte resorted to a graphical solution to compute directly the ultimate load of a two-dimensional cap. Hansen extended the method to the three-dimensional case. Although the plastic design method is unique and rational, the assumptions to simplify the real soil-structure system may need examination. It was assumed that a pile had only axial resistance, that is, no lateral resistance, and no rotational restraint of the pile tops on the cap was considered. The axial load versus displacement of each individual pile was represented by a bilinear relationship.

The comprehensive modern structural treatment was presented by Hrennikoff (1950) for the two-dimensional case. He considered the axial, transverse, and rotational resistance of piles on the cap. The load displacement relationship of the pile top was assumed to be linearly elastic. One restrictive assumption was that all piles must have the same load-displacement relationship. Hrennikoff substituted a free-standing elastic column for an axially loaded pile. A laterally loaded pile was regarded as an elastic beam on an elastic foundation with a uniform stiffness. Even with these crude approximations of pile behavior, the method is significant in the sense that it presents the potentiality of the analytical treatment of the soil-pile interaction system. Hrennikoff's method consisted of obtaining influence coefficients for cap displacements by summing the influence coefficients of individual piles in terms of the spring constants which represent the pile-head reactions onto the pile cap. Almost all the subsequent work follows the approach taken by Hrennikoff.

Radosavljević (1957) also regarded a laterally loaded pile as an elastic beam in an elastic medium with a uniform stiffness. He advocated the use of the results of tests of single piles under axial loading. In this way a designer can choose the most practical spring constant for the axially loaded pile head, and he can consider nonlinear behavior also. Radosavljević showed a slightly different formulation than Hrennikoff in deriving the coefficients of the equations of the equilibrium of forces. Instead of using unit displacement of a cap, he used an arbitrary given set of displacements. Still, his structural approach is essentially analogous to Hrennikoff's method. Radosavljević's method is restricted to the case of identical piles in identical soil conditions.

Turzynski (1960) presented a formulation by the matrix method for the two-dimensional case. Neglecting the lateral resistance of pile and soil, he considered only the axial resistance of piles. Further, he assumed piles as elastic columns pinned at the top and the tip. He derived a stiffness matrix and inverted it to obtain the flexibility matrix. Except for the introduction of the matrix method, Turzynski's method does not serve a practical use because of its oversimplification of the soil-pile interaction system.

Asplund (1956) formulated the matrix method for both two-dimensional and three-dimensional cases. His method also starts out from calculations of a stiffness matrix to obtain a flexibility matrix by inversion. In an attempt to simplify the final flexibility matrix, Asplund defined a pile group center by which the flexibility matrix is diagonalized. He stressed the importance of the pile arrangement for an economically grouped pile foundation, and he contended that the pile group center method helped to

visualize better the effect of the geometrical factors. He employed the elastic center method for the treatment of laterally loaded piles. Any transverse load through the elastic center causes only the transverse displacement of the pile head, and rotational load around the elastic center gives only the rotation of the pile head. In spite of the elaborate structural formulation, there is no particular correlation with the soil-pile system. Laterally loaded piles are merely regarded as elastic beams on an elastic bed with a uniform spring constant.

Francis (1964) computed the two-dimensional case using the influence coefficient method. The lateral resistance of soil was considered either uniform throughout or increasing in proportion to depth. Assuming a fictitious point of fixity at a certain depth, elastic columns fixed at both ends are substituted for laterally loaded piles. The axial loads on individual piles are assumed to have an effect only on the elastic stability without causing any settlement or uplift at the pile tips.

Aschenbrenner (1967) presented a three-dimensional analysis based on the influence coefficient method. This analysis is an extension of Hrennikoff's method to the three-dimensional case. Aschenbrenner's method is restricted to pin-connected piles.

Saul (1968) gave the most general formulation of the matrix method for a three-dimensional foundation with rigidly connected piles. He employed the cantilever method to describe the behavior of laterally loaded piles. He left it to the designer to set the soil criteria for determining the settlement of axially loaded piles and the resistance of laterally loaded piles. Saul indicated the possible application of his method to dynamically loaded foundations.

Reese and Matlock (1960, 1966a) presented a method for coupling the analysis of the grouped pile foundation with the analysis of laterally loaded piles by the finite difference method. Reese and Matlock's method presumes the use of electronic computers. The finite difference method of analyzing a laterally loaded pile developed by them can handle a pile of varying size and flexural rigidity in any complex profile of highly nonlinear soils. The method can account for the behavior of any soil system providing the soil behavior can be described analytically or numerically. Any type of boundary conditions of the pile head can be treated; namely, the fixed, pinned, or elastically restrained pile head. A nonlinear curve showing axial load versus pile-head deflection is employed in the analysis. The curve may either be derived by computations based on proper assumptions, or it may be obtained from field loading tests. The formulation of equations giving the movement of the pile cap is done by the influence coefficient method, similar to Hrennikoff's method. Reese and Matlock devised a convenient way to represent the pile-head moment and lateral reaction by spring forces only in terms of the lateral pile-top displacement. The effect of pile-head rotation on the pile-head reactions are included implicitly in the force-displacement relationship. This convenient method, however, does not readily converge for the special case where the lateral displacement of the pile cap is relatively small. The significance of this method lies in the fact that it can predict the bent cap behavior continuously for the incremental load until the bent cap fails by excessive movement, and also, that nonlinear relationships between pile-head loads and displacements are incorporated in the analysis.

Using Reese and Matlock's method, example problems were worked out by Robertson (1961) and by Parker and Cox (1969). Robertson compared the method with Vetter's method and Hrennikoff's method. Parker and Cox integrated into the method typical soil criteria for laterally loaded piles.

Reese and O'Neill (1967) developed the theory of the general three-dimensional grouped pile foundation using matrix formulations. Their theory is an extension of the theory of Hrennikoff (1950), in which springs are used to represent the piles. Representation of piles by springs imposes the superposition of two independent modes of deflection of a laterally loaded pile. The spring constants for the lateral reaction and the moment at the pile top must be obtained for a mode of deflection, where a pile head is given only translational displacement without rotation and also for a mode of deflection where a pile head is given only rotation without translation. While the soil-pile interaction system has highly nonlinear relationships, the pile material also exhibits nonlinear characteristics when it is loaded near its ultimate strength. The principle of superposition does not apply to the nonlinear system. Therefore, the most general and advanced theory by Reese and O'Neill still has the theoretical weakness of superposing the nonlinear soil-pile interaction system and the limitation to the linearly elastic pile material.

#### Review of Experiments.

Very little experimental work has been reported on the testing of grouped pile foundations with batter piles and under inclined loading.

As early as 1936, Feagin (1957) conducted a series of full-scale tests on eight concrete monoliths with different combinations of vertical and batter piles. Timber piles 32 feet in length with top diameters of 12 to 14 inches and tip diameters of 8 to 10 inches were driven into fine to coarse sands containing some occasional gravel. The batter piles were at 20-degree angles to the vertical. Inclined loading and horizontal loading were both applied to the concrete monoliths. The tests supported the qualitative description of battered piles rather than validating a theory.

In 1945 Tschebotarioff (1953) carried out lateral load tests on model single piles and three-pile and seven-pile dolphins. The scale of the model was 1:10. Tapered wood piles were used. The piles were driven 29 inches into a layered soil consisting of 14 inches of submerged loose sand with a relative density of less than 20 per cent and an underlying consolidated clay with an unconfined compressive strength of 0.15 tsf. Tschebotarioff tried to find the soil reactions on piles and emphasized the difference between the "in" batter and the "out" batter piles.

Wen (1955) also used models to find the lateral and vertical load distribution in piles of a laterally loaded bent. The model piles were made of white oak. The piles had a 1 1/2-inch square section and were 45 inches long. He tested two- and three-pile bents. The piles were instrumented with wire strain gages to give the stress distribution. Dry sand was used as the model soil. Unfortunately, no specific description is given about the density and the angle of the internal friction of the sand.

Prakash (1961) carried out model tests using aluminum tubes, one-half inch in diameter. Dense, dry sand of a relative density of 90 per cent



was used, filling a 48-inch-diameter by 48-inch-high tank. He instrumented piles with strain gages. He tested four-pile foundation caps and nine-pile foundation caps. Single piles were tested to give the comparison between tests. Prakash's paper deals only with the behavior of piles under lateral loading. There is no mention of the axial resistance of piles nor the distribution of applied forces at the cap between individual piles.

#### State of the Art and Scope of Study.

The foregoing review of the past research shows that the most general and advanced structural theory available at present has the theoretical weakness of superposing two modes of nonlinear deflection of a laterally loaded pile, and is limited to linearly elastic material.

The review of the past experimental work reveals a deficiency in experiments on grouped pile foundations both in quantity and in quality. The need for well-planned experiments is great.

This study is divided into two parts. Part one is devoted to development of a new structural theory which eliminates the superposition of two independent modes of nonlinear deflection for a laterally loaded pile and is capable of considering nonlinear pile material.

In part two, experimental work on small-sized steel pipe piles in a submerged dense sand is described. Emphasis in the experimental work was on developing an understanding of the behavior of a single pile. Studies of the behavior of a foundation consisting of a group of four piles were then undertaken. The responses of the single piles were analyzed in terms of the soil properties so that a contribution could be made to establish more general soil criteria (Parker and Reese, 1970).

The main purpose of this study is the organization of a rational design procedure for a two-dimensional foundation with widely spaced, battered, nonlinearly elastic piles subjected to any arbitrary static loading. A computer program GROUP was developed for the computation of grouped pile foundations. A program LLP and a program AXP were written to investigate the single pile behavior under a lateral load and under an axial load, respectively. Combined with the criteria of typical soils for predicting single pile behavior, the complete routine of design is presented. In the Appendices A, B, and C the documentation of the computer programs is given.

This page replaces an intentionally blank page in the original.

-- CTR Library Digitization Team

CHAPTER II  
MECHANICS OF GROUPED PILE FOUNDATION

A structural theory is formulated herein for computing the behavior of a two-dimensional grouped pile foundation with arbitrarily arranged piles that possess nonlinear force-displacement characteristics. Coupled with the structural theory of a pile cap are the theories of a laterally loaded pile and an axially loaded pile. In this chapter each theory is developed separately. Solution of all of the theories depends on the use of digital computers for the actual computations. Computer programs are introduced in Appendices A, B, and C, with documentation.

Basic Structural System

Figure 2.1a illustrates the general system of a two-dimensional grouped pile foundation. A group of piles are connected to an arbitrarily shaped pile cap with arbitrary spacing and arbitrary inclination. Such sectional properties of a pile as the width, the area and the moment of inertia can vary, not only from pile to pile, but also along the axis of a pile. The pile material may be different from pile to pile but it is assumed that the same material is used within a pile.

There are three conceivable cases of pile connection to the pile cap. Pile 1 in Fig. 2.1a illustrates a pin connection. Pile 2 shows a fixed head pile with its head clamped by the pile cap. Pile 3 represents an elastically restrained pile top, which is the typical case of an offshore bent whose piles and the superstructure consist of a unit structural system (Fig. 2.2). The pile head is fixed to the pile cap by two

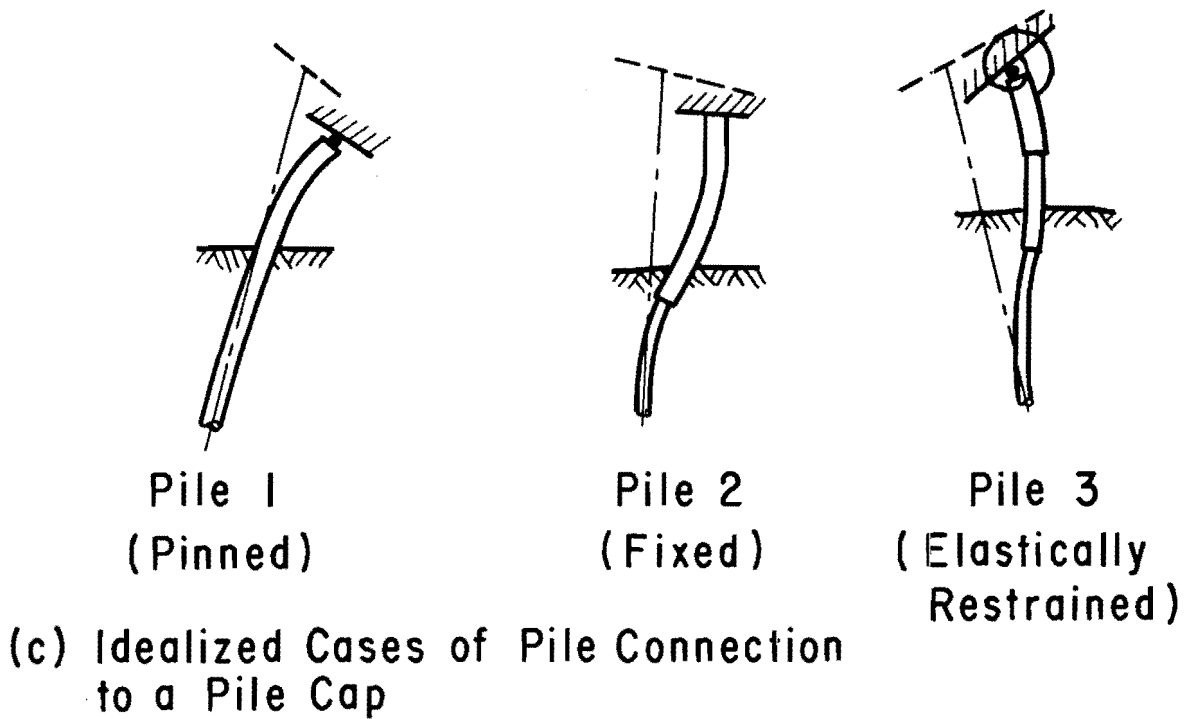
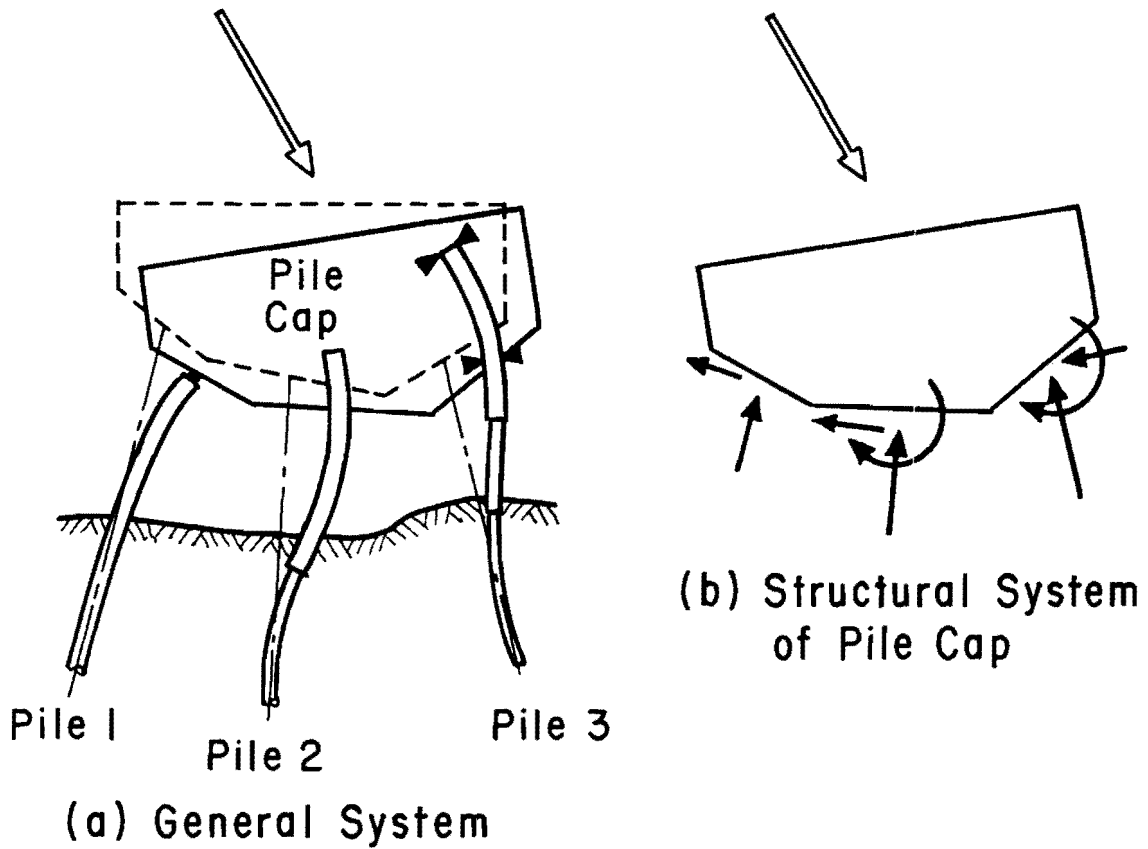


Fig. 2.1. Basic Structural System

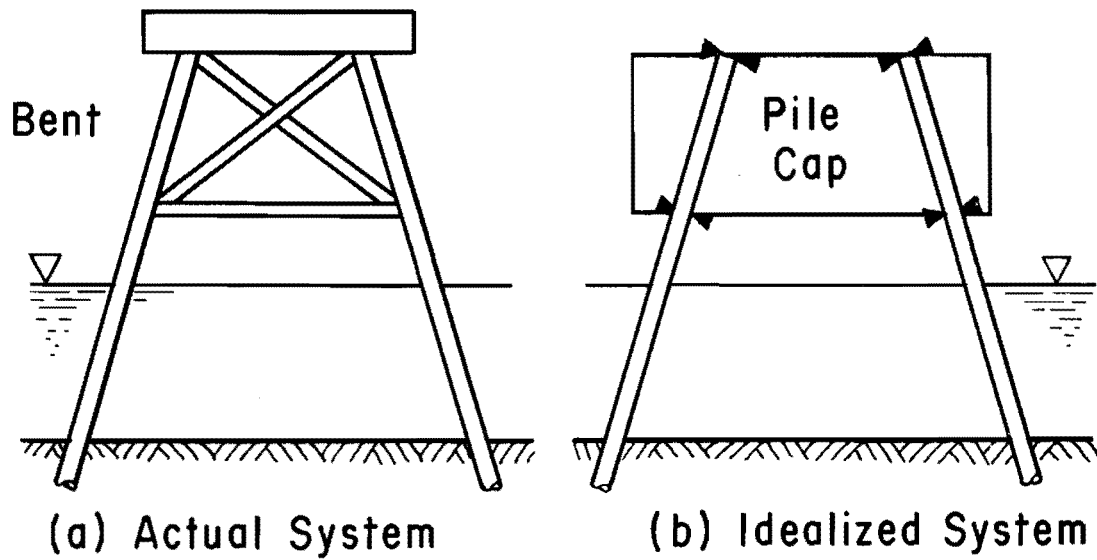


Fig. 2.2. Typical Offshore Structure

### Reinforced Concrete Pile Cap

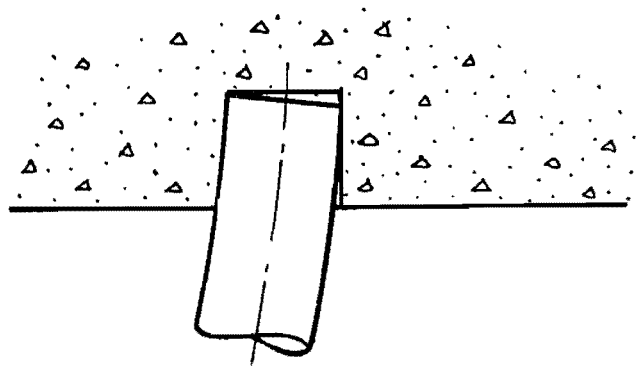


Fig. 2.3. Typical Pile Head in a Pile Cap

knife-edge supports, but the pile can be deflected freely between these supports. The elastic restraint is provided by the flexural rigidity of the pile itself. The treatment of a laterally loaded pile with an elastically restrained top gives a useful tool for handling the real foundation. The piles are usually embedded into a monolithic reinforced concrete pile cap with the assumption that a complete fixity of the pile to the pile cap is obtained (Fig. 2.3). However, the elasticity of the reinforced concrete and the local failure due to the stress concentration allows the rotation of a pile head within the pile cap. The magnitude of the restraint on the pile from the pile cap is usually unknown; yet it is important to check the behavior of the grouped pile foundation for the possible range of elastic restraint.

The pile cap is subjected to the two-dimensional external loads. The line of action of the resultant external load may be inclined and may assume any arbitrary position with respect to the plane of symmetry. The external loads cause the displacement of the pile cap in the plane of symmetry, which subsequently brings forth the axial, the lateral, and the rotational displacements of each individual pile (Fig. 2.1c). The forced displacements on individual piles in turn give reactions to the pile cap as illustrated in Fig. 2.1b. These pile reactions are highly nonlinear in nature. They are functions of the pile properties, the soil properties, and the boundary conditions at the pile top. The structural theory of the grouped pile foundation used a numerical method to seek the compatible displacement of the pile cap, which satisfies the equilibrium of the applied external loads and the nonlinear pile reactions.

### Terminology

It is necessary to distinguish some of the basic terms used throughout the study.

A grouped pile foundation consists of a group of piles and a pile cap (Fig. 2.1a). A pile cap may be a monolithic reinforced concrete block or, at times, a bent as it is shown in Fig. 2.2. Any structure above the pile cap is called a superstructure.

For a pile group to be analyzed as two-dimensional, the group must have a plane of symmetry, and the resultant of the applied loads must be in that plane. The two-dimensional problem may be illustrated by drawing an elevation of the plane of symmetry. Such a drawing is shown in Fig. 2.1a. The individual piles shown in Fig. 2.1a can represent several similar piles. Similar piles in a location in the plane of symmetry with the same pile properties and the same inclination are referred to as individual pile groups. There can be more than two individual pile groups at a location if the properties vary, or if the inclination angle, or the type of connection to the pile cap is changed. The individual pile group is a collection of individual piles or single piles.

### Assumptions

Some of the basic assumptions employed for the treatment of the grouped pile foundation are discussed below.

Two-Dimensionality. The first assumption is the two-dimensional arrangement of the bent cap and the piles. The usual design practice is to arrange piles symmetrically with a plane or planes with loads acting in this plane of symmetry. The assumption of a two-dimensional



case reduces considerably the number of variables to be handled. However, there is no essential difference in the theory between the two-dimensional case and the three-dimensional case. If the validity of the theory for the former is established, the theory can be extended to the latter by adding more components of forces and displacements mechanically with regard to the new dimension (Reese and O'Neill, 1970).

Nondeformability of Pile Cap. The second major assumption is the nondeformability of the pile cap. A pile head encased in a monolithic pile cap (Fig. 2.3), or supported by a pair of knife-edge supports (Fig. 2.2) can rotate or deflect within the pile cap. But the shape of the pile cap itself is assumed to be always the same. That means the relative positions of the pile top remain the same for any pile-cap displacement. If the pile cap is deformable, the structural theory of the grouped pile foundation must include the compatibility condition of the pile cap itself. While no treatment of a foundation with a deformable pile cap is included in this study, the theory could be extended to such a case if the pile cap consists of a structural member such that the analytical computation of the deformation of the pile cap is possible.

Wide Pile Spacing. It is assumed at the outset that the individual piles are so widely spaced that there is no influence of one pile on another. Interaction between piles in a closely spaced group occurs both under axial and under lateral loads. Such interaction is usually referred to as group effect. While some research has been carried out on the group effect, this phenomenon is little understood. Currently, design recommendations for the group effect are limited to a special case where a foundation consists only of vertical piles subjected only

to vertical load near the centroid of the foundation. A very small number of full-scale field tests have been performed on a closely spaced pile group under axial load. Therefore, recommendations for design of such groups must be considered as preliminary and tentative.

The analysis of a general grouped pile foundation involves not only axially loaded piles, but also laterally loaded piles. The pile may be inclined at an arbitrary angle in an arbitrary direction. There is no way, at present, to evaluate the group effect on the behavior of closely spaced piles subjected to lateral loading either parallel to a row of piles or perpendicular to it.

The assumption of wide spacing of the piles in a foundation eliminates from the analysis the complication of the group effect. Yet, the analytical and the experimental establishment of the correlation between single pile behavior and that of a grouped pile foundation is believed to be the logical first step towards the more general theory.

No Interaction Between Axially Loaded Pile and Laterally Loaded Pile.

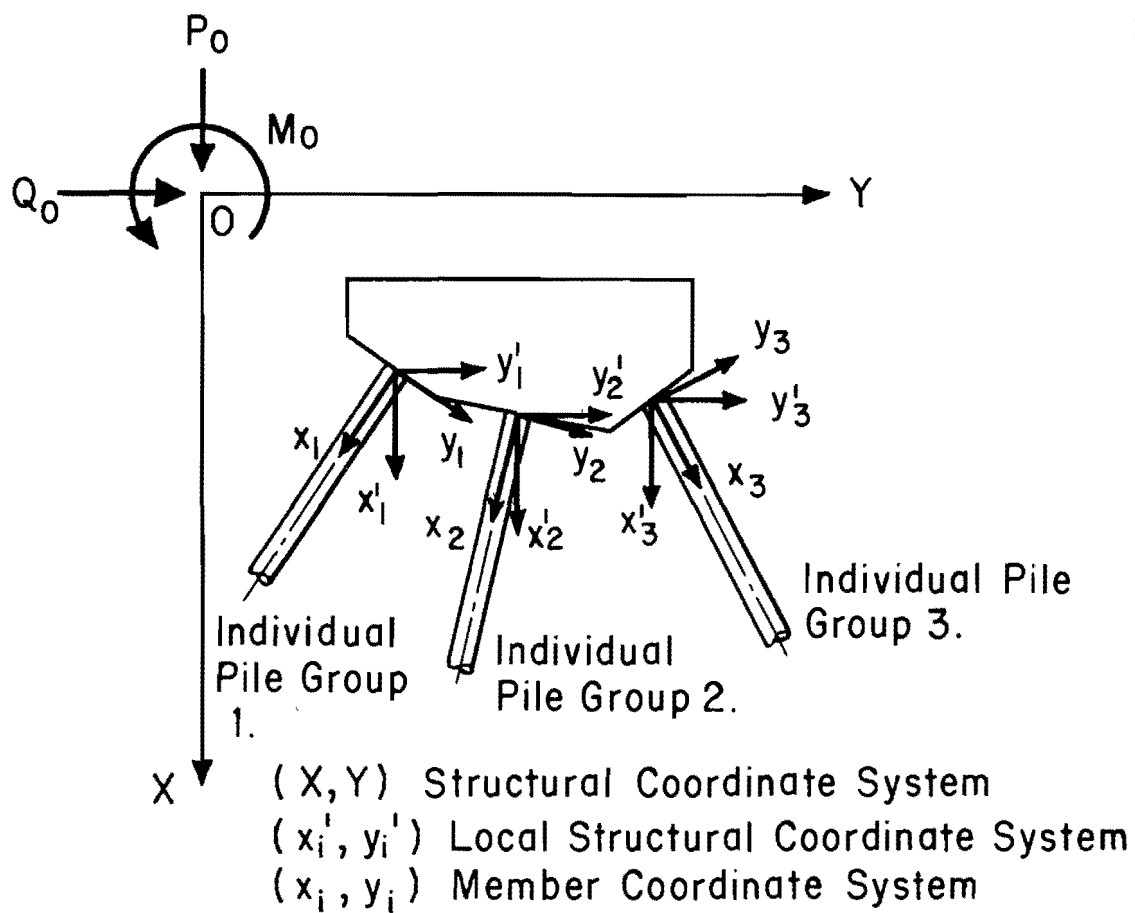
The assumption is made that there is no interaction between the axial pile behavior and the lateral pile behavior. That is, the relationship between axial load and displacement is not affected by the presence of lateral deflection of the pile and vice versa. The validity of this assumption is discussed by Parker and Reese (1970). However, if theory were available to allow the single-pile problem to be treated as an interaction system involving both axial and lateral deflection, the present theory of a grouped pile foundation can accommodate the pile behavior without any change.

### Two-Dimensional Grouped Pile Foundation

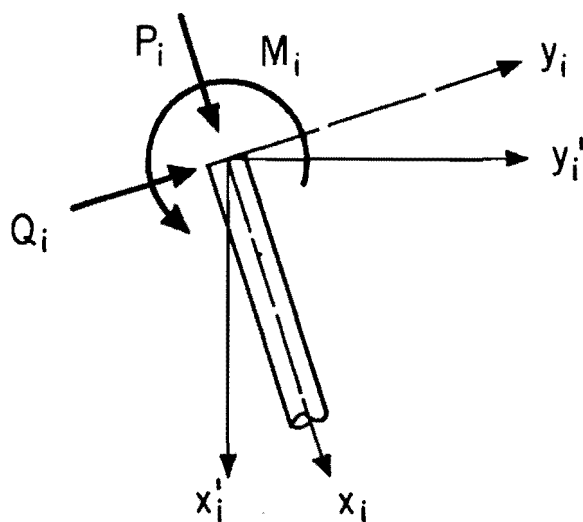
The equilibrium of the applied loads and the pile reactions on a pile cap is sought by the successive correction of pile-cap displacements. After each correction of the displacement, the difference between the load and the pile reaction is calculated. The next displacement correction is obtained through the calculation of a new stiffness matrix at the previous pile-cap position. The elements of a stiffness matrix are obtained by giving a small virtual increment to each component of displacement, one at a time. The proper magnitude of the virtual increment may be set at  $10^{-5}$  times a unit displacement to attain acceptable accuracy.

#### Coordinate Systems and Sign Conventions

Figure 2.4a shows the coordinate systems and sign conventions. The superstructure and the pile cap are referred to the global structural coordinate system  $(X, Y)$  where  $X$  and  $Y$  axes are vertical and horizontal, respectively. The resultant external forces are acting at the origin  $O$  of this global structural coordinate system. The positive directions of the components of the resultant load  $P_o$ ,  $Q_o$ , and  $M_o$  are shown by the arrows. The positive curl of the moment was determined by the usual right-hand rule. The pile head of each individual pile group is referred to the local structural coordinate system  $(x'_i, y'_i)$ , whose origin is the pile head and with axes running parallel to those of the global structural coordinate system. The member coordinate system  $(x_i, y_i)$  is further assigned to each pile. The origin of the member



(a) Coordinate Systems



(b) Pile Forces

Fig. 2.4. Coordinate System and Sign Convention

coordinate system is the pile head. Its  $x_i$  axis coincides with the pile axis and the  $y_i$  axis is perpendicular to the  $x_i$  axis. The  $x_i$  axis makes an angle  $\lambda_i$  with the vertical. The angle  $\lambda_i$  is positive when it is measured counterclockwise.

Figure 2.4b shows the positive directions of the forces,  $P_i$ ,  $Q_i$ , and  $M_i$  exerted from the pile cap onto the top of an individual pile in the  $i$ th individual pile group. The forces  $P_i$  and  $Q_i$  are acting on the  $x_i$  and  $y_i$  axes of the member coordinate system.

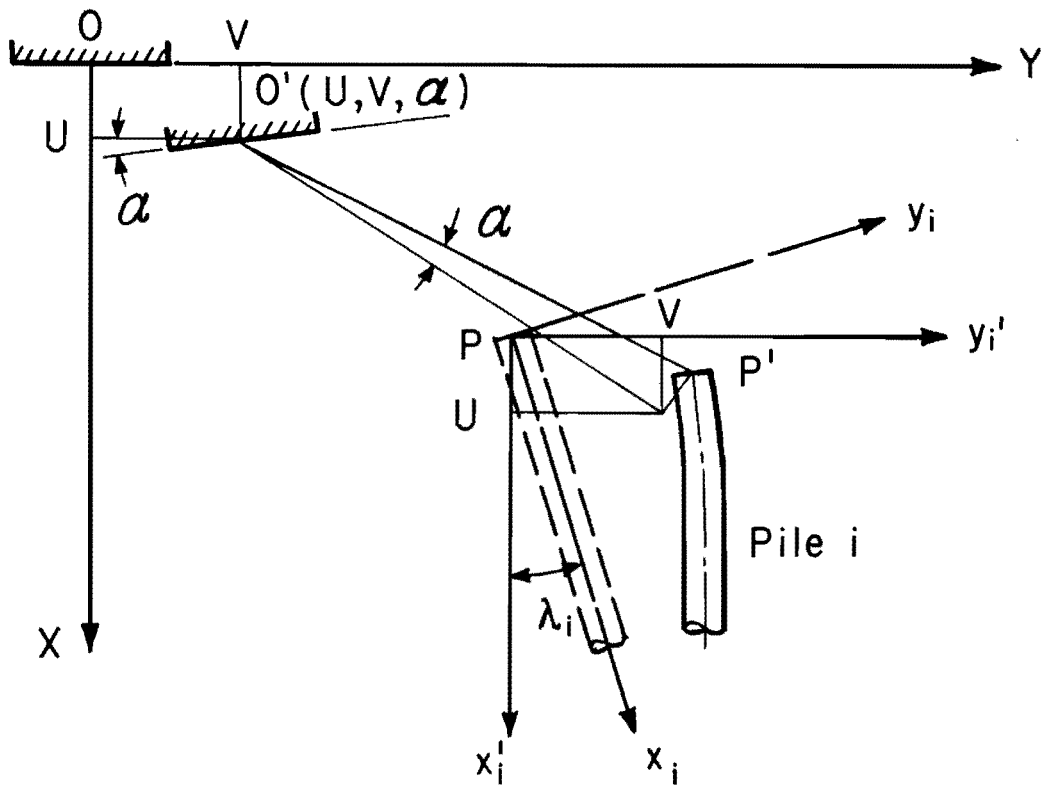
#### Transformation of Coordinates

Displacement. Figure 2.5 illustrates the pile-head displacement in the structural, the local structural, and the member coordinate systems. Due to the pile-cap displacement from point  $O$  to point  $O'$  with a rotation  $\alpha$ , the  $i$ th pile moves from the original position  $P$  to the new position  $P'$  and rotates through the same angle  $\alpha$ . The components of pile-cap displacement are expressed by  $(U, V, \alpha)$  with regard to the structural coordinate system. The pile-head displacement is denoted by  $(u'_i, v'_i, \alpha)$  in the local coordinate system and by  $(u_i, v_i, \alpha)$  in the member coordinate system.

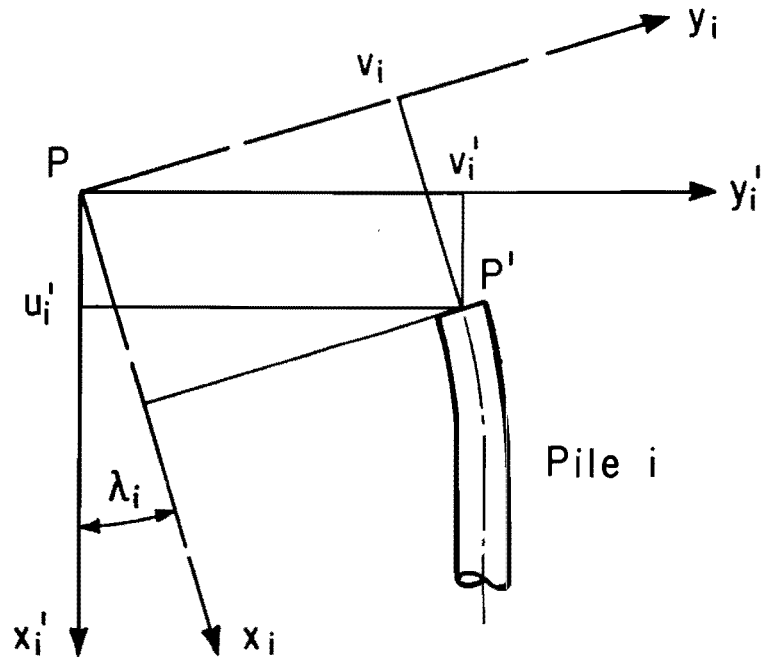
The coordinate transformation between the structural and the local structural coordinate system is derived from the simple geometrical consideration:

$$u'_i = U - Y_i \alpha \quad \dots \dots \dots (2.1)$$

$$v'_i = V + X_i \alpha \quad \dots \dots \dots (2.2)$$



(a) Pile Head Displacement due to Pile Cap Displacement



(b) Transformation of Displacement Between Local Structural Coordinate System and Member Coordinate System

Fig. 2.5. Transformation of Displacement

where

$(X_i, Y_i)$  = location of  $i$ th pile head in the structural coordinate system.

The transformation of pile-head displacement from the local structural coordinate system to the member coordinate system is obtained from the geometrical relationship (Fig. 2.5b).

$$u_i = u'_i \cos \lambda_i + v'_i \sin \lambda_i \dots \dots \dots (2.3)$$

$$v_i = v'_i \cos \lambda_i - u'_i \sin \lambda_i \dots \dots \dots (2.4)$$

Substitution of Eqs. 2.1 and 2.2 into Eqs. 2.3 and 2.4 yields the transformation relationship between the pile-cap displacement in the structural coordinate system and the corresponding pile-top displacement of the  $i$ th individual pile group in the member coordinate system.

$$u_i = U \cos \lambda_i + V \sin \lambda_i + \alpha (X_i \sin \lambda_i - Y_i \cos \lambda_i) \dots (2.5)$$

$$v_i = U \sin \lambda_i + U \cos \lambda_i + \alpha (X_i \cos \lambda_i + Y_i \sin \lambda_i) \dots (2.6)$$

In matrix notation

$$\begin{bmatrix} u_i \\ v_i \\ \alpha_i \end{bmatrix} = \begin{bmatrix} \cos \lambda_i & \sin \lambda_i & X_i \sin \lambda_i - Y_i \cos \lambda_i \\ -\sin \lambda_i & \cos \lambda_i & X_i \cos \lambda_i + Y_i \sin \lambda_i \\ 0 & 0 & 1 \end{bmatrix} \begin{bmatrix} U \\ V \\ \alpha \end{bmatrix} \dots (2.7)$$

The matrix expression above is written concisely

$$\bar{u}_i = T_{D,i} \bar{U} \dots \dots \dots (2.8)$$

where

$\bar{u}_i$  = displacement vector of the head of the pile in the  $i$ th individual pile group,

$T_{D,i}$  = displacement transformation matrix of the pile, and

$\bar{U}$  = displacement vector of the pile cap.

Force. Figure 2.4 illustrates the load acting on the pile cap and the pile reactions. The load is expressed in three components ( $P_o$ ,  $Q_o$ ,  $M_o$ ) with regard to the structural coordinate system. The reactions in the  $i$ th individual pile group are expressed in terms of the member coordinate system ( $P_i$ ,  $Q_i$ ,  $M_i$ ). Decomposition of the reactions of the  $i$ th pile with respect to the structural coordinate system gives the transformation of the pile reaction from the member coordinate system to the structural coordinate system

$$P'_i = P_i \cos \lambda_i - Q_i \sin \lambda_i \dots \dots \dots (2.9)$$

$$Q'_i = P_i \sin \lambda_i + Q_i \cos \lambda_i \dots \dots \dots (2.10)$$

$$M'_i = P_i (X_i \sin \lambda_i - Y_i \cos \lambda_i) + Q_i (X_i \cos \lambda_i + Y_i \sin \lambda_i) + M_i \dots \dots \dots (2.11)$$



Matrix notation expresses the equations above

$$\begin{pmatrix} P'_i \\ Q'_i \\ M'_i \end{pmatrix} = \begin{pmatrix} \cos \lambda_i & -\sin \lambda_i & 0 \\ \sin \lambda_i & \cos \lambda_i & 0 \\ X_i \sin \lambda_i - Y_i \cos \lambda_i & X_i \cos \lambda_i + Y_i \sin \lambda_i & 1 \end{pmatrix} \begin{pmatrix} P_i \\ Q_i \\ M_i \end{pmatrix} \dots (2.12)$$

or more concisely

$$\bar{P}'_i = T_{F,i} \bar{P}_i \dots \dots \dots (2.13)$$

where

- $\bar{P}'_i$  = reaction vector of the pile of ith individual pile group in the structural coordinate system,
- $T_{F,i}$  = force transformation matrix of the pile, and
- $\bar{P}_i$  = reaction vector of the pile in the member coordinate system.

It is observed that the force transformation matrix  $T_{F,i}$  is obtained by transposing the displacement transformation matrix  $T_{D,i}$ .

Thus,

$$T_{F,i} = T_{D,i}^T \dots \dots \dots (2.14)$$

Successive Displacement Correction Method

Figure 2.6 illustrates the successive displacement correction method of obtaining the equilibrium of forces of a pile cap.

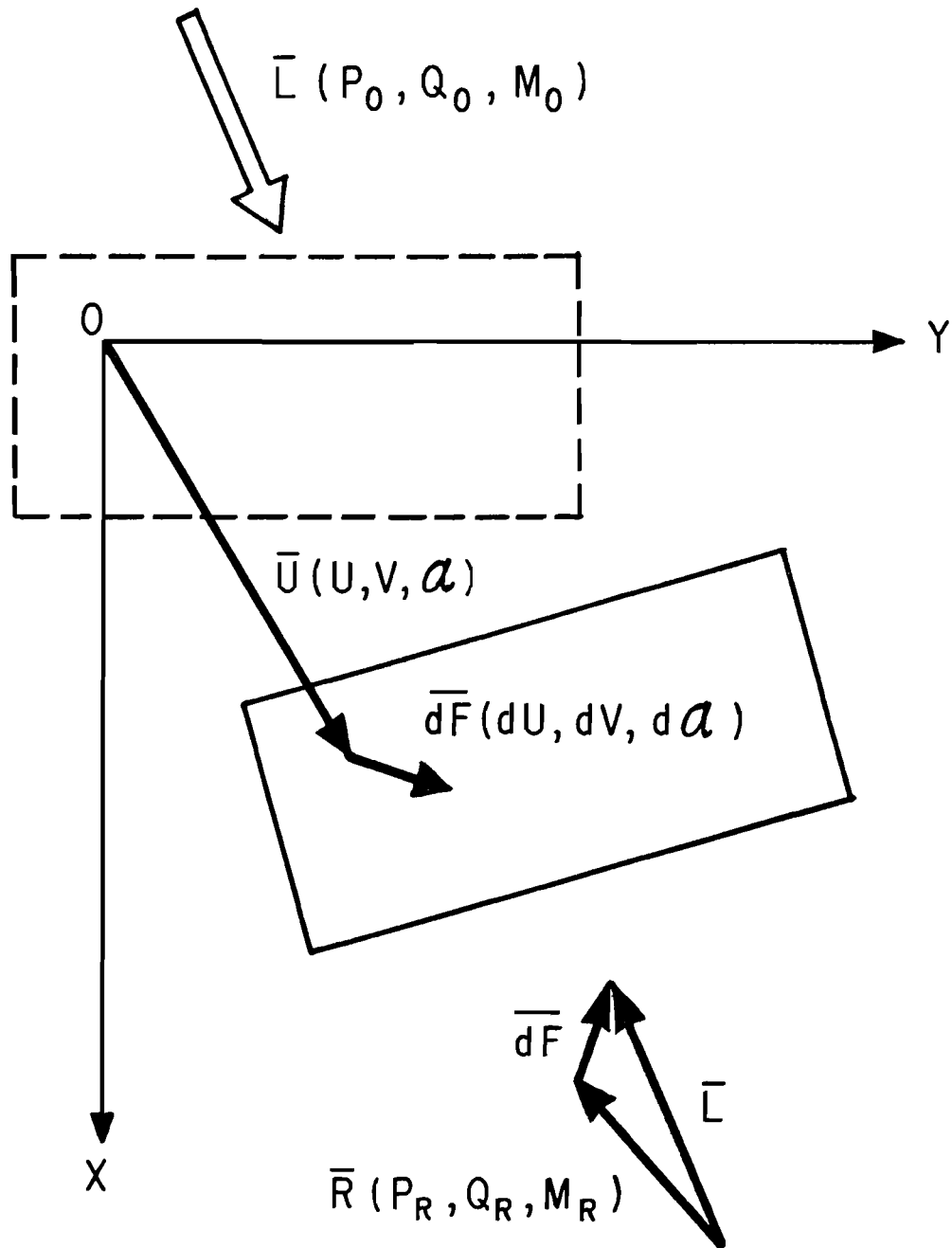


Fig. 2.6. Successive Displacement Correction Method

Force Correction Vector. After successive correction, the pile cap moves from the initial position 0 to the last position 0' with new displacement components (U, V,  $\alpha$ ). If the three components of the displacement of a pile cap are given, the displacement of each pile head may be computed by Eq. 2.8. Then the theories of a laterally loaded pile and an axially loaded pile presented in the following sections may be used to solve for the reaction vector  $f_i$  of each pile numerically. If axial load versus pile-top displacement curves are available, the axial pile reactions may be directly obtained by reading the curves. The summation of the reaction vector with respect to the structural coordinate system is given by

$$\bar{R} = \sum_{i=1}^n J_i \bar{P}'_i = \sum_{i=1}^n J_i T_{F,i} \bar{P}_i \dots \dots \dots (2.15)$$

where

$\bar{R}$  = total reaction vector with elements ( $P_R, Q_R, M_R$ ) and  
 $J_i$  = number of piles in an individual pile group.

The difference between the applied load and the pile reactions or the force correction is calculated by

$$\bar{dF} = \bar{L} - \bar{R} \dots \dots \dots (2.16)$$

where

$\bar{L}$  = load vector with three elements ( $P_o, Q_o, M_o$ ) and

$\bar{dF}$  = force correction vector also with three elements  
(dP, dQ, dM).

Stiffness Matrix. Each element of the reaction vector is a highly nonlinear function of the pile cap displacement (U, V,  $\alpha$ ). Then

$$P_R = P_R (U, V, \alpha) \dots \dots \dots (2.17)$$

$$Q_R = Q_R (U, V, \alpha) \dots \dots \dots (2.18)$$

$$M_R = M_R (U, V, \alpha) \dots \dots \dots (2.19)$$

The total differentiation of each of the above quantities is written out as

$$dP_R = \frac{\partial P_R}{\partial U} dU + \frac{\partial P_R}{\partial V} dV + \frac{\partial P_R}{\partial \alpha} d\alpha \dots \dots \dots (2.20)$$

$$dQ_R = \frac{\partial Q_R}{\partial U} dU + \frac{\partial Q_R}{\partial V} dV + \frac{\partial Q_R}{\partial \alpha} d\alpha \dots \dots \dots (2.21)$$

$$dM_R = \frac{\partial M_R}{\partial U} dU + \frac{\partial M_R}{\partial V} dV + \frac{\partial M_R}{\partial \alpha} d\alpha \dots \dots \dots (2.22)$$

In matrix notation

$$\begin{pmatrix} dP_R \\ dQ_R \\ dM_R \end{pmatrix} = \begin{pmatrix} \frac{\partial P_R}{\partial U} & \frac{\partial P_R}{\partial V} & \frac{\partial P_R}{\partial \alpha} \\ \frac{\partial Q_R}{\partial U} & \frac{\partial Q_R}{\partial V} & \frac{\partial Q_R}{\partial \alpha} \\ \frac{\partial M_R}{\partial U} & \frac{\partial M_R}{\partial V} & \frac{\partial M_R}{\partial \alpha} \end{pmatrix} \begin{pmatrix} dU \\ dV \\ d\alpha \end{pmatrix} \dots \dots \dots (2.23)$$

or in concise form

$$\bar{dR} = K \bar{dV} \dots \dots \dots (2.24)$$

where

$\bar{dR}$  = vector of the variation of the total pile reaction,

$K$  = stiffness matrix, and

$\bar{dV}$  = displacement variation vector.

The elements of the stiffness matrix  $K$  or the partial derivatives of the total reaction forces with respect to each element of the pile-cap displacement are obtained by giving small displacement  $dX$ ,  $dY$ , and  $d\alpha$  one at a time to the pile cap (Fig. 2.6).

Giving a small displacement  $dU$  in the  $X$  direction, three elements in the first column of the stiffness matrix  $K$  are determined.

$$\frac{\partial P_R}{\partial U} = \frac{P_R(U + dU, V, \alpha) - P_R(U, V, \alpha)}{dU} \dots \dots \dots (2.25)$$

$$\frac{\partial Q_R}{\partial U} = \frac{Q_R(U + dU, V, \alpha) - Q_R(U, V, \alpha)}{dU} \dots \dots \dots (2.26)$$

$$\frac{\partial M_R}{\partial U} = \frac{M_R(U + dU, V, \alpha) - M_R(U, V, \alpha)}{dU} \dots \dots \dots (2.27)$$

The rest of the elements are obtained in a similar fashion.

Displacement Correction Vector: Equating the reaction variation vector  $\bar{dR}$  with the force correction vector  $\bar{dF}$  and substituting the

displacement variation vector  $\bar{dV}$  with the displacement correction vector  $\bar{dU}$ , the necessary correction of the displacement is obtained from Eq. 2.24.

$$\bar{dU} = K^{-1} \bar{dF} \dots \dots \dots (2.28)$$

The new displacement of the pile cap is given by adding the displacement correction vector  $\bar{dU}$  to the displacement vector  $\bar{U}$ .

The size of the stiffness matrix  $K$  is only three by three. Therefore, the inversion of the matrix  $K$  is most conveniently done by the Cramer rule. That is, the element of the flexibility matrix or the inverted matrix  $K^{-1}$  is expressed by a formula.

$$K_{ij}^{-1} = \frac{A_{ij}}{\det K} \dots \dots \dots (2.29)$$

where

$K_{ij}^{-1}$  = element in the inverted stiffness matrix,

$\det K$  = determinant of the matrix  $K$ , and

$A_{ij}$  = cofactor of the matrix  $K$

Computational Procedure

The principle of the successive displacement correction method for obtaining the equilibrium state of the applied loads and the pile reactions on the pile cap has been developed in the three previous sections of this study.

The solution is obtained through the iterative numerical procedure. A computer program GROUP (Appendix A) is developed for this purpose. The logic of the computer program is described in steps in the following.

1. Give an initial displacement to the pile cap.
2. Compute the corresponding pile-top displacements.
3. Compute the pile reaction for the given pile-top displacements.
4. Sum up the pile reactions.
5. Compute the difference between the applied load and the pile reactions to obtain the force correction vector.
6. Give small virtual displacement to obtain the stiffness matrix.
7. Invert the stiffness matrix to get a flexibility matrix.
8. Multiply the flexibility matrix (Step 7) with the force correction vector (Step 5) to get the displacement correction vector.
9. Correct the pile-cap displacement by adding the displacement correction vector.

Repeat Steps two through nine until the displacement correction vector becomes sufficiently small.

The successive displacement correction method requires the pile-top reaction to be solved for the forced displacement at pile top. Under the assumption of the independency between the lateral and axial behaviors of a pile, the pile reactions on the pile cap are conveniently solved independently for these two different modes.

The analytical prediction of the axial and lateral behaviors of a pile may be made by finite difference methods. The remaining portion

of this chapter is devoted to formulation of the finite difference methods for a laterally loaded pile and for an axially loaded pile.

The computer program GROUP is internally equipped with the finite difference method for a laterally loaded pile but not with that for an axially loaded pile. There are two reasons for this decision. Firstly, the axial pile reaction versus displacement relationship is expressed by a single curve, while the lateral and rotational pile reactions consists of families of curves in terms of multiparameters such as the lateral and rotational displacements and the type of pile connections to pile cap. Secondly, the present state of knowledge about soil criteria for an axially loaded pile does not readily allow the choice of proper soil criteria for an accurate prediction of axial pile behavior. It may still be more practical to obtain the load versus axial displacement curve by such direct means as loading test than resorting to the analytical method.

#### Laterally Loaded Pile

The analysis of the laterally loaded pile by the finite difference method has been undertaken extensively by Reese and Matlock since 1960 (Reese and Matlock, 1960; Matlock and Reese, 1962; Matlock, 1963; Matlock and Ingram, 1963; Matlock and Hailburton, 1966; Reese, 1966; Reese, 1970; Matlock, 1970). Their work proved the versatility and the theoretical unequivocability of the finite difference method in dealing with the highly nonlinear soil-pile interaction system with any arbitrary change in the soil formation and pile properties.



There is already a computer program to solve a laterally loaded pile by the finite difference method (Reese, 1970). However, a new solution of the finite difference equations is necessary before it is applied to the successive displacement method. The existing finite difference method can solve a laterally loaded pile for given combinations of load and moment, load and slope or load and spring constant, but not for given displacements.

The new solution of the finite difference equations is presented in the following section.

#### Differential Equations for a Beam Column

Figure 2.7b shows an element of a beam column. The basic differential equation is derived by examining this element (Timoshenko and Gere, 1961). The equilibrium for forces in  $y$  direction gives

$$Q - p \, dx - (Q + dQ) + q \, dx = 0 \quad \text{or}$$

$$\frac{dQ}{dx} = q - p \dots \dots \dots (2.30)$$

where

$Q$  = shear force,

$q$  = distributed load, and

$p$  = distributed spring force which is expressed by the soil modulus  $E_s$

$$p = E_s \, y \dots \dots \dots (2.31)$$

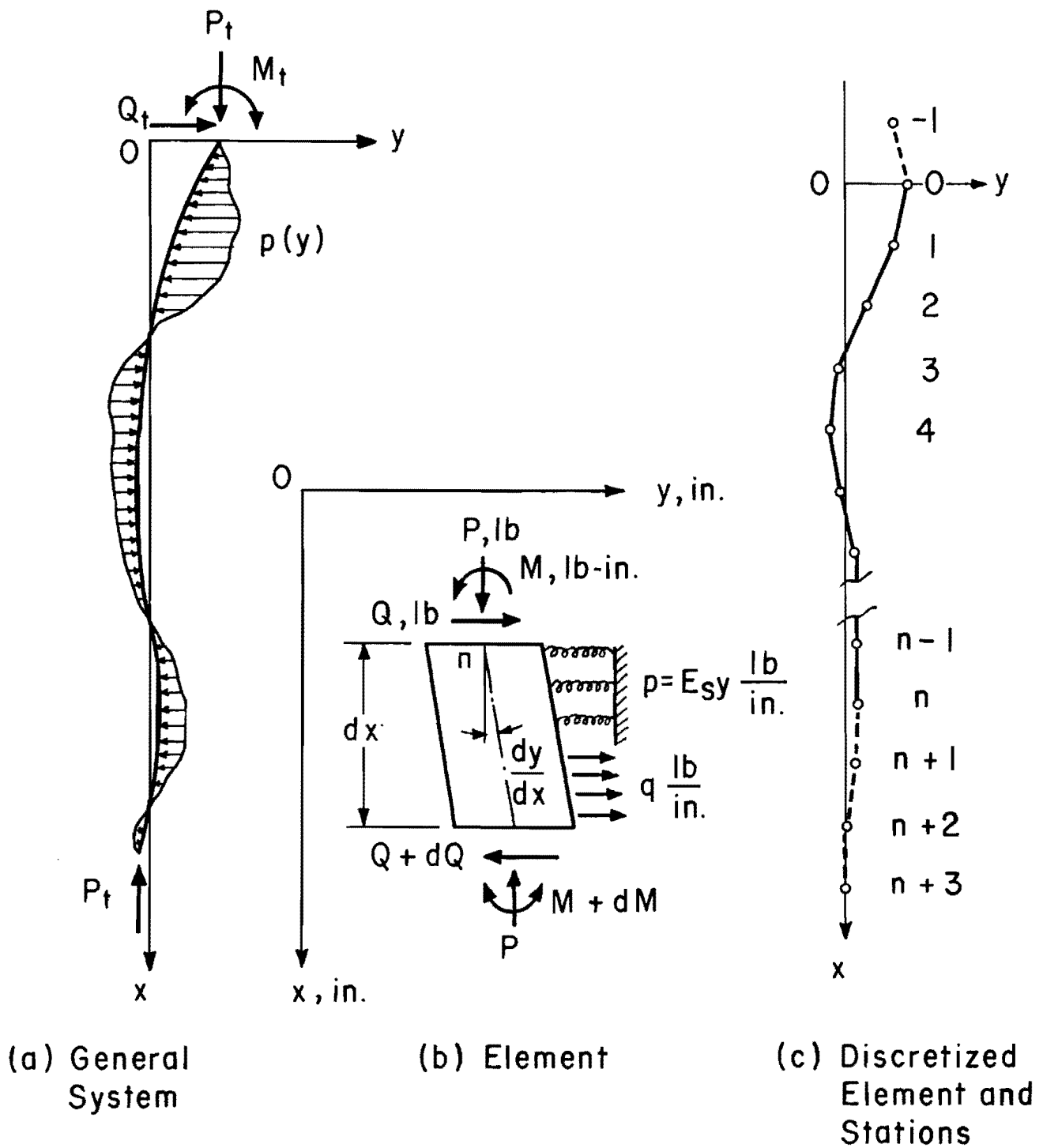


Fig. 2.7. Beam Column

Taking the equilibrium of moment about point  $n$  (Fig. 2.7b),

$$M + q \, dx \frac{dx}{2} - (Q + dQ) \, dx - (M + dM) - P \, dx \frac{dy}{dx} \, dx = 0$$

neglecting the second-order terms,

$$Q = P \frac{dy}{dx} - \frac{dM}{dx} \dots \dots \dots (2.32)$$

where

$M$  = bending moment and

$P$  = axial force in the beam column.

Standard textbooks on the strength of material give an expression for the moment-curvature relationship of a beam when shear and axial deformation are neglected.

$$EI \frac{d^2 y}{dx^2} = - M \dots \dots \dots (2.33)$$

Differentiating Eq. 2.32 with respect to  $x$  and substituting Eq. 2.30 the basic differential equation for a beam-column is obtained.

$$\frac{d^2 M}{dx^2} = E_s y - q + \frac{d}{dx} \left( P \frac{dy}{dx} \right) \dots \dots \dots (2.34)$$

### Finite Difference Approximation

The beam column is divided into  $n$  discrete elements of length  $h$  as shown in Fig. 2.7c. Stations  $-1$ , and  $n+1$  through  $n+3$  are imaginary

or fictitious where the actual beam column does not exist. These imaginary stations are necessary for technical reasons to apply the central difference equations at all stations. The flexural rigidity at the imaginary stations are considered zero and the deflections are set in such a way as to satisfy the boundary conditions at the top and bottom of the pile.

The finite difference approximation of the second derivative of  $y$  is expressed by

$$\left(\frac{d^2 y}{dx^2}\right)_i = \frac{y_{i+1} - 2y_i + y_{i-1}}{h^2} \dots \dots \dots (2.35)$$

Therefore, the moment at station  $i$  is approximated by

$$M_i = -(EI)_i \frac{y_{i+1} - 2y_i + y_{i-1}}{h^2} \dots \dots \dots (2.36)$$

Applying the finite difference approximation also to the moment  $M$ , Eq. 2.34 is converted to

$$\frac{M_{i+1} - 2M_i + M_{i-1}}{h^2} = E_s y - q + P \frac{d^2 y}{dx^2} \dots \dots \dots (2.37)$$

Substituting Eqs. 2.35 and 2.36 into the above equation, we obtain the general finite difference expression for a beam column.

$$a_i y_{i-2} + b_i y_{i-1} + c_i y_i + d_i y_{i+1} + e_i y_{i+2} = f_i \dots (2.38)$$

where

$$-1 \leq i \leq n+1$$

and where

$$a_i = EI_{i-1} \dots \dots \dots (2.39)$$

$$b_i = - 2 EI_i - 2 EI_{i-1} + P_t h^2 \dots \dots \dots (2.40)$$

$$c_i = EI_{i+1} + 4 EI_i + EI_{i-1} - 2 P_t h^2 + E_s h^4 \dots \dots \dots (2.41)$$

$$d_i = - 2 EI_{i+1} - 2 EI_i + P_t h^2 \dots \dots \dots (2.42)$$

$$e_i = EI_{i+1} \dots \dots \dots (2.43)$$

$$f_i = q h^4 \dots \dots \dots (2.44)$$

Recursive Solution of Difference Equations

Assuming that deflection  $y_{i-1}$  is expressed in terms of deflections at two subsequent stations

$$y_{i-1} = A_{i-1} + B_{i-1} y_i + C_{i-1} y_{i+1} \dots \dots \dots (2.45)$$

The deflection at station  $i$  is obtained by substituting Eq. 2.45 into Eq. 2.38

$$y_i = A_i + B_i y_{i+1} + C_i y_{i+2} \dots \dots \dots (2.46)$$

where the continuity coefficients  $A_i$ ,  $B_i$ , and  $C_i$  are expressed by

$$A_i = D_i (A_{i-1} E_i + a_i A_{i-2} - f_i) \dots \dots \dots (2.47)$$

$$B_i = D_i (C_{i-1} E_i + d_i) \dots \dots \dots (2.48)$$

$$C_i = D_i e_i \dots \dots \dots (2.49)$$

and where

$$D_i = -1/ (B_{i-1} E_i + a_i C_{i-2} + c_i) \dots \dots \dots (2.50)$$

$$E_i = a_i B_{i-2} + b_i \dots \dots \dots (2.51)$$

for  $-1 \leq i \leq n+1$ .

It is shown in the following section that the pile-top boundary conditions are expressed by finite difference equations similar to Eq. 2.45 at stations  $-1$  and  $0$ . Then the continuity coefficients  $A_i$ ,  $B_i$ , and  $C_i$  are computed for stations  $1$  through  $n+1$ . The deflection at the imaginary station  $y_{n+2}$  and  $y_{n+3}$  are assumed to be zero. Therefore, the round-trip path of the recursive solution of a set of banded simultaneous equations is completed.

#### Boundary Conditions at Pile Top

The analysis of a grouped pile foundation requires the pile-top reactions of a laterally loaded pile. The general finite difference equation (Eq. 2.38) must be solved in such a way as to satisfy the displacement boundary condition at pile top which is imposed by the pile-cap displacement. The pile-top reactions are computed, subsequently, from the pile deflection at discrete stations along the pile.

The lateral deflection at the pile top coincides with the lateral displacement of the pile cap in the member coordinate system. However, the slope or the rotation of the pile head is not always equal to the rotation of the pile cap. It is dependent on the kind of pile connection to the pile cap. In the following, the displacement boundary conditions are expressed in terms of the lateral deflection at the finite difference station near the pile top for a pinned, for a fixed, and for an elastically restrained connection.

Usually a laterally loaded single pile is given a lateral load and a moment at the pile head. In order to facilitate the analysis of a single laterally loaded pile, it is convenient to solve for the displacement of a pile subjected to the force boundary conditions. The finite difference expressions of the force boundary conditions are added in this section after displacement boundary conditions.

Displacement Boundary Condition, Pinned Connection. A pinned pile head cannot carry any moment. Equation 2.36 gives the finite difference expression for this condition (Fig. 2.8a)

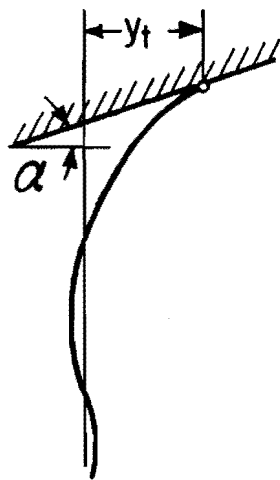
$$y_1 - 2y_0 + y_{-1} = 0 \dots \dots \dots (2.52)$$

Another condition is the deflection at the pile top.

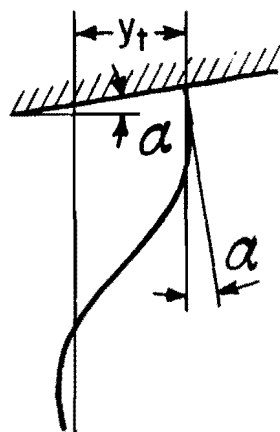
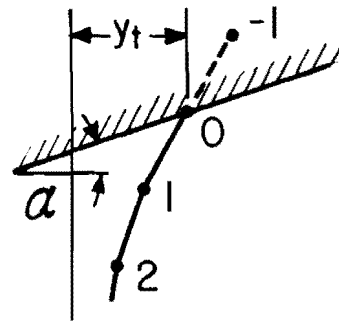
$$y_0 = y_t \dots \dots \dots (2.53)$$

where

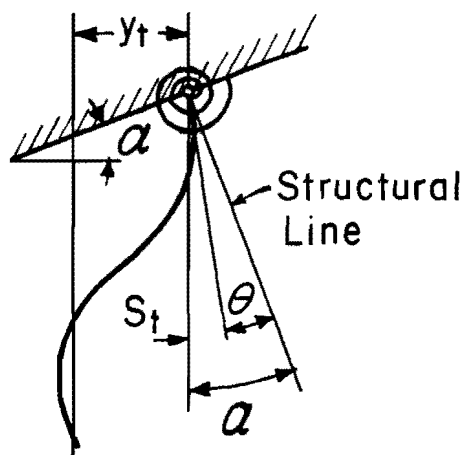
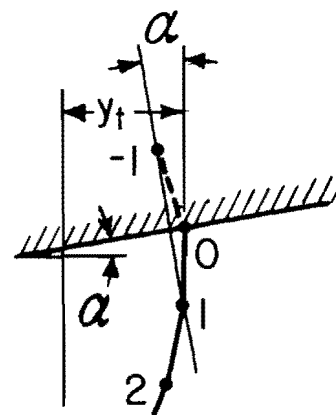
$$y_t = \text{given lateral deflection of the top of the pile.}$$



(a) Pinned Top



(b) Fixed Top



(c) Elastically Restrained Top

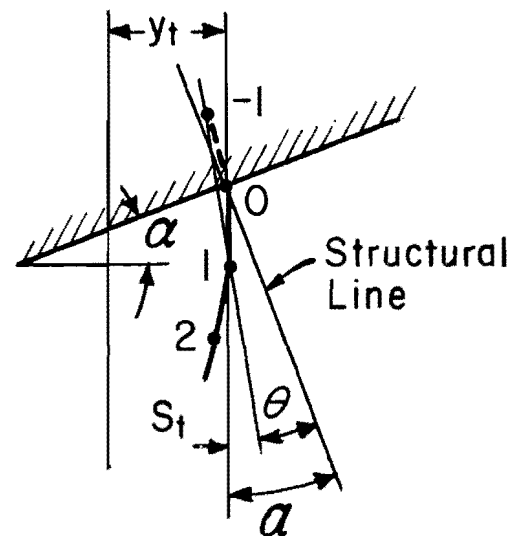


Fig. 2.8. Boundary Conditions at Pile Top



Displacement Boundary Condition, Fixed Connection. For a pile which is perfectly fixed to an infinitely stiff bent cap, the slope at the top of the pile is equal to the rotation angle of the bent cap. Therefore, from the central difference expression of the slope (Fig. 2.8b),

$$\frac{y_1 - y_{-1}}{2h} = \alpha \dots \dots \dots (2.54)$$

where

$\alpha$  = rotation angle of pile cap.

The other condition is the deflection at the pile top.

$$y_0 = y_t \dots \dots \dots (2.55)$$

Displacement Boundary Condition, Elastically Restrained Connection.

A pile may have its top elastically restrained by a rotational spring force which is proportional to the deviation angle  $\theta$  from the structural line (Fig. 2.8c). The structural line is fixed to the pile cap and tangent to the pile before loading. Thus, one of the boundary conditions is written

$$\frac{M_t}{\theta} = C \dots \dots \dots (2.56)$$

where

$M_t$  = moment at pile top and

$C$  = rotational spring constant (inch-pounds).

The sum of deviation angle  $\theta$  and slope at the pile head  $S_t$  makes the pile cap rotation angle  $\alpha$ .

$$\alpha = \theta + S_t \dots \dots \dots (2.57)$$

Applying a central difference expression for the slope, Eqs. 2.56 and 2.57 give

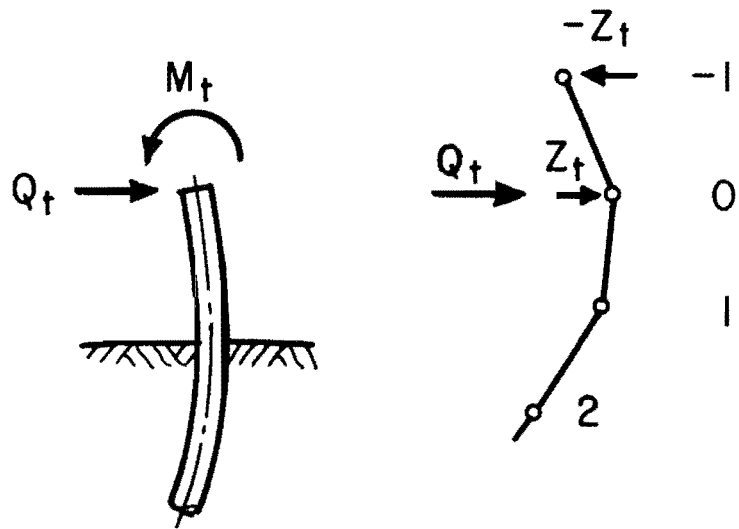
$$\left(EI_o - \frac{Ch}{2}\right) y_1 - 2 EI_o h^2 y_o + \left(EI_o + \frac{Ch}{2}\right) y_{-1} + C \alpha h^2 = 0 \dots \dots \dots (2.58)$$

The lateral deflection at the pile also constitutes a boundary condition

$$y_o = y_t \dots \dots \dots (2.59)$$

Force Boundary Condition. If the boundary conditions are given in terms of forces, the lateral load and the moment at pile top, these forces are simulated by imaginary forces  $Z_t$  and  $-Z_t$  at station 0 and at the fictitious station -1. A couple is formed, equal to the applied moment, and a lateral load exists at station 0 of the discretized model (Fig. 2.9).

These transverse forces are taken into the solution by modifying the continuity coefficient given by Eq. 2.47. It is soon observed that the effect of the transverse load  $q$  appears only in the term of  $f_i$  (Eq. 2.44). Therefore, the continuity coefficient  $A$  is rewritten for stations -1 and 0 as follows (Matlock and Haliburton, 1966)



(a) Actual Laterally Loaded Pile

(b) Discretized Model

Fig. 2.9. Force Boundary Conditions at Pile Top

$$A'_{-1} = A_{-1} + D_{-1} (h^3 Z_t) \dots \dots \dots (2.60)$$

$$A'_0 = A_0 + D_0 (-h^3 Z_t - h^3 Q_t) \dots \dots \dots (2.61)$$

where

$$Z_t = \frac{M_t}{h} \dots \dots \dots (2.62)$$

and where

$A'_{-1}$  and  $A'_0$  = revised continuity coefficients and

$Q_t$  = horizontal load at pile top.

The concentrated load  $Q_t$  is equivalent to the product of increment  $h$  and the distributed load  $q$ .

#### Boundary Conditions at Pile Tip

At the pile tip a laterally loaded pile is subjected neither to a lateral load nor to a bending moment. These force boundary conditions may be applied explicitly to the pile tip by deriving the finite difference representations of these conditions. However, the same effect is obtained by providing the additional fictitious station  $n+2$  and  $n+3$  at the tip of the pile. These two fictitious stations assume no lateral deflection and no flexural rigidity. The latter method is preferred in the numerical method because it eliminates the special treatment of the continuity coefficients (Eqs. 2.47, 2.48 and 2.49) at the

pile tip. Thus, the path of the recursive computation, which starts from the pile top to make a return path at station  $n+1$ , is streamlined.

#### Solution of a Laterally Loaded Pile Problem

Once the lateral deflections at all discrete stations are calculated, the slope  $S$ , the moment  $M$ , the shear force  $Q$ , the distributed horizontal reaction  $q$ , and the distributed horizontal spring force  $p$  are calculated by the following finite difference equations.

$$S_i = \frac{y_{i+1} - y_{i-1}}{2h} \dots \dots \dots (2.63)$$

$$M_i = -EI_i \frac{y_{i+1} - 2y_i + y_{i-1}}{h^2} \dots \dots \dots (2.64)$$

$$Q_i = P_t S_i - \frac{M_{i+1} - M_{i-1}}{2h} \dots \dots \dots (2.65)$$

$$q_i = E_{s,i} y_i + P_t \frac{y_{i+1} - 2y_i + y_{i-1}}{h^2} - \frac{M_{i+1} - 2M_i + M_{i-1}}{h^2} \dots \dots \dots (2.66)$$

$$P_i = E_{s,i} y_i \dots \dots \dots (2.67)$$

Lateral reaction at the top of the pile is given by  $q_0 h$ . The lateral reaction should be equal to the summation of soil reactions along the pile.

$$q_o h = \sum_{i=0}^n E_{s,i} y_i \dots \dots \dots (2.68)$$

Check computations by a computer program showed that the inherent error to the finite difference approximation always amounts to several per cent for the distributed load  $q_o$ , while the summation of the soil resistance or spring force coincided well with the shear force  $Q$  immediately below the pile top. Therefore, the lateral pile reaction is calculated by summing the soil resistance along the pile shaft.

#### Axially Loaded Pile

There are basically two analytical methods to calculate the load versus settlement curve of an axially loaded pile. One method takes the theory of elasticity approach. The theories suggested by D'Appolonia and Romualdi (1963), Thurman and D'Appolonia (1965), Poulos and Davis (1968), Poulos and Mattes (1969), and Mattes and Poulos (1969) belong to the theory of elasticity method. All of these theories resort to the so-called Mindlin equation, which gives a solution for the vertical deformation at any point in a semi-infinite, elastic, and isotropic solid due to a downward force in the interior of a solid. The pile displacement at a certain point is calculated by superimposing the influences of the load transfer (skin friction) along the pile and the pile-tip resistance at that point. The compatibility of those forces and the displacement of a pile is obtained by solving a set of simultaneous equations. This method takes the stress distribution within the soil into consideration; therefore, the elasticity method presents the

possibility of solving for the behavior of a group of closely spaced piles under axial loading (D'Appolonia, 1968; Poulos, 1968).

The drawback to the elasticity method lies in the basic assumptions which must be made. The actual ground condition rarely satisfies the assumption of uniform and isotropic material. In spite of the highly non-linear stress-strain characteristics of soils, the only soil properties considered in the elasticity method are the Young's modulus  $E$  and the Poisson's ratio  $\nu$ . The use of only two constants,  $E$  and  $\nu$ , to represent soil characteristics is too much of an oversimplification. In actual field conditions, the parameter  $\nu$  may be relatively constant, but the parameter  $E$  can vary through several orders of magnitude.

The other method to calculate the load versus settlement curve for an axially loaded pile may be called the finite difference method. Finite difference equations are employed to achieve compatibility between pile displacement and the load transfer along a pile and between displacement and resistance at the tip of the pile. This method was first used by Seed and Reese (1957); other studies are reported by Coyle and Reese (1966) and Coyle and Sulaiman (1967). The finite difference method assumes the Winkler concept. That is to say, the load transfer at a certain pile section and the pile tip resistance are independent of the pile displacements elsewhere. The finite difference method should give good prediction of the pile behavior in clayey soils, since the shear strength characteristics of clayey soils are rather insensitive to the change in stress. In the case of sandy soils, however, the shear strength characteristics are directly affected by the stress change due to the pile displacement in another place. The close agreement between the prediction

and the loading test results in clays (Coyle and Reese, 1966) and the scattering of prediction from the loading test in sands (Coyle and Sulaiman, 1967) may possibly be explained by the relative sensitivity of a soil to changes in patterns of stress. Admitting the deficiency in the displacement-shear force criteria of sands, the finite difference method is still a practical and potential method because the method can deal with any complex composition of soil layers with any nonlinear displacement versus shear force relationship. Furthermore, the method can accommodate improvements in soil criteria with no modification of the basic theory.

In the next sections the derivation of the finite difference expressions is shown. The fundamental technique employed here is the same as that employed by previous investigations. The difference lies in the computation procedure. The method shown herein gives a solution first for the pile displacement at all stations. Then, the pile force at each station is calculated. Convergence of the iterative computation is quite fast even near the ultimate load.

### Basic Equations

Figure 2.10a shows the mechanical system for an axially loaded pile. The pile head is subjected to an axial force  $P_t$ , and the pile head undergoes a displacement  $z_t$ . The pile-tip displacement is  $z_{tip}$  and the pile displacement at the depth  $x$  is  $z$ . Displacement  $z$  is positive downward and the compressive force  $P$  is positive.

Considering an element  $dx$  (Fig. 2.10a) the strain in the element due to the axial force  $P$  is calculated by neglecting the second order form  $dP$ .



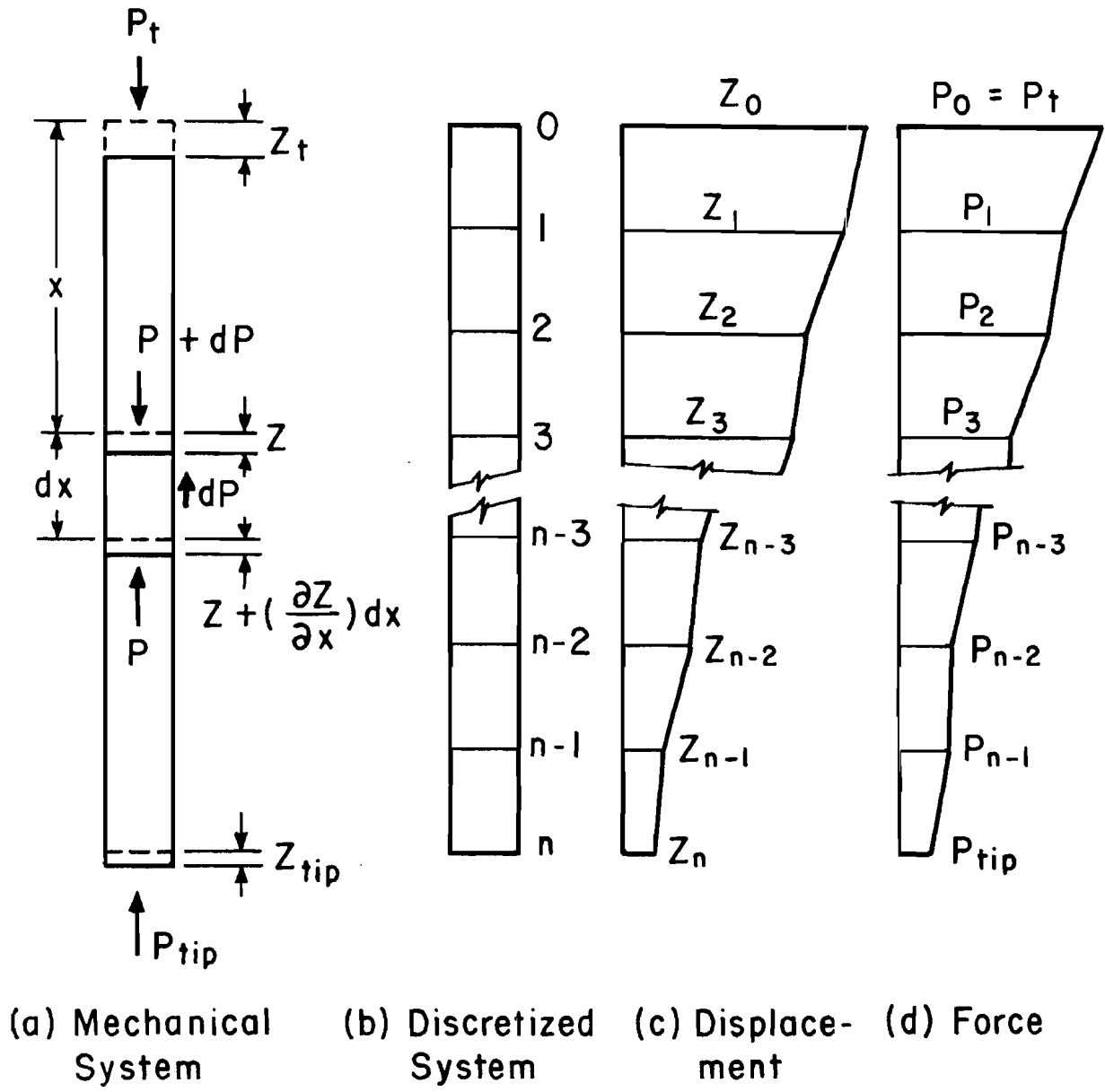


Fig. 2.10. Axially Loaded Pile

$$\frac{dz}{dx} = - \frac{P}{EA} \dots \dots \dots (2.69)$$

or

$$P = - EA \left( \frac{dz}{dx} \right) \dots \dots \dots (2.70)$$

where

- P = axial force in the pile in pounds (downward positive),
- E = Young's modulus of pile material in psi, and
- A = cross-sectional area of the pile in square inches.

The total load transfer through an element  $dx$  is expressed by using the modulus  $\mu$  in the load transfer curve (Fig. 2.11a).

$$dP = - \mu z \ell dx \dots \dots \dots (2.71)$$

or

$$\frac{dP}{dx} = - \mu z \ell \dots \dots \dots (2.72)$$

where

- $\ell$  = circumference of a cylindrical pile or the perimeter encompassing an H pile.

Differentiating Eq. 2.70 with respect to  $x$ , it is equated with Eq. 2.72.

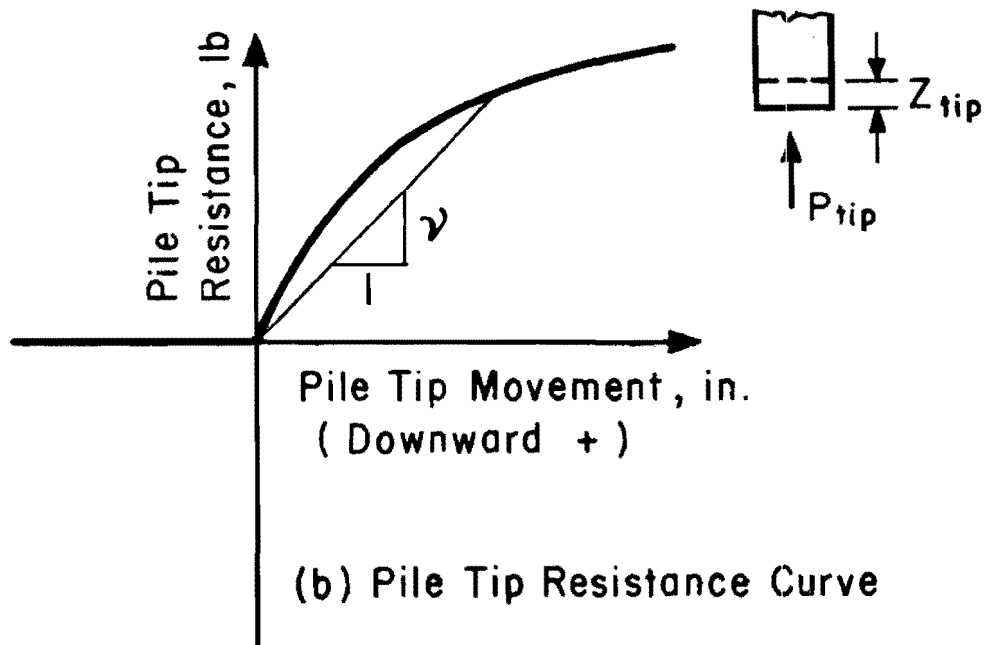
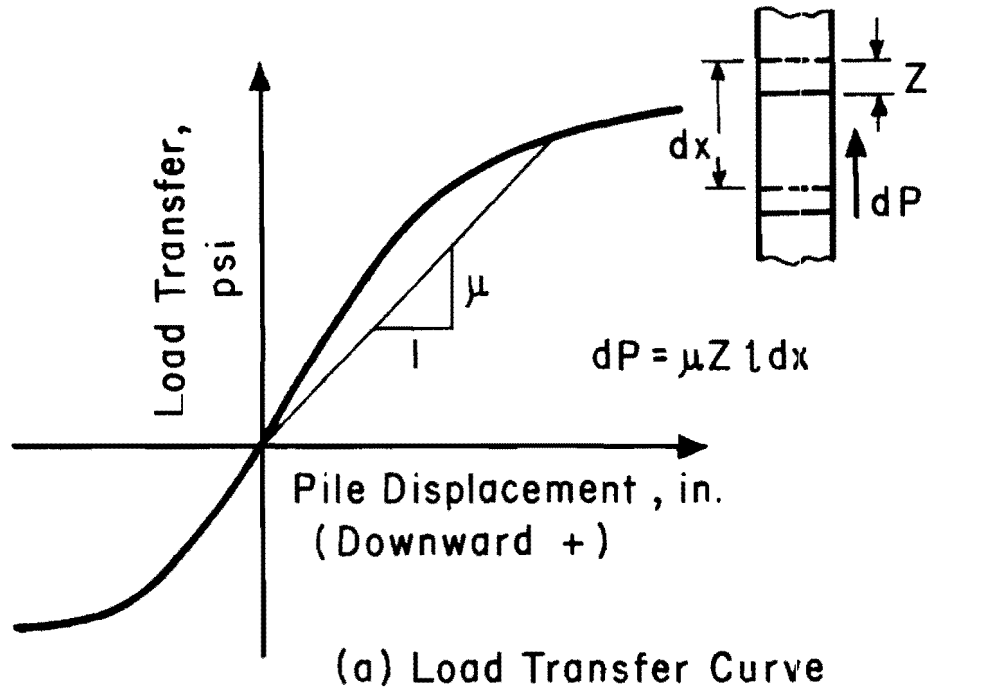


Fig. 2.11. Load Transfer and Pile-Tip Resistance

$$\frac{d}{dx} EA \frac{dz}{dx} = \mu z l \quad \dots \dots \dots (2.73)$$

The pile-tip resistance is given by the product of a secant modulus  $\nu$  and the pile-tip movement  $z_{tip}$ . (See the pile-tip movement versus resistance curve, Fig. 2.11b).

$$P_{tip} = \nu z_{tip} \quad \dots \dots \dots (2.74)$$

Equation 2.73 constitutes the basic differential equation which must be solved. Boundary conditions at the tip and at the top of the pile must be established. The boundary condition at the tip of the pile is given by Eq. 2.74. At the top of the pile the boundary condition may be either a force or a displacement. Treatment of these two cases is presented later.

#### Finite Difference Equation

Equation 2.75 gives in difference equation form the differential equation (Eq. 2.73) for solving the axial pile displacement at discrete stations.

$$a_i z_{i+1} + b_i z_i + c_i z_{i-1} = 0 \quad \dots \dots \dots (2.75)$$

for  $0 \leq i \leq n$

where

$$a_i = 1/4 EA_{i+1} + EA_i - 1/4 EA_{i-1} \quad \dots \dots \dots (2.76)$$

$$b_i = - \mu \ell h^2 - 2 EA_i \dots \dots \dots (2.77)$$

$$c_i = - 1/4 EA_{i+1} + EA_i + 1/4 EA_{i-1} \dots \dots \dots (2.78)$$

and where

$h =$  increment length or  $dx$  (Fig. 2.10a).

Boundary Condition

There are two kinds of boundary conditions at the pile top. One is the specified axial force at the pile top. The other is the specified displacement at the pile top.

If the axial force at pile head is specified, a forward difference equation of the first derivative of  $z$  with respect to  $x$  gives the condition that must be satisfied by the displacement near the pile top.

$$P_t = - EA_o \frac{z_1 - z_0}{2h} \dots \dots \dots (2.79)$$

where

$P_t =$  given axial load on the pile top.

If a displacement is specified at the pile top

$$z_t = z_0 \dots \dots \dots (2.80)$$

where

$z_t =$  forced axial displacement of the pile top.

The boundary condition at pile tip is given by the point resistance force. Using the secant modulus  $v$  of the pile-tip movement versus point resistance curve (Fig. 2.11b), the backward difference equation of the first derivative of  $z$  with respect to  $x$  gives the force boundary condition at the pile tip.

$$v z_n = - EA_n \frac{z_n - z_{n-1}}{h} \dots \dots \dots (2.81)$$

Assuming the reduced form of the basic equation at station  $n-1$

$$z_{n-1} = B_{n-1} + C_{n-1} z_n \dots \dots \dots (2.82)$$

Solving Eqs. 2.81 and 2.82 simultaneously for  $z_n$

$$z_n = \frac{B_{n-1}}{\frac{vh}{EA_n} + 1 - C_{n-1}} \dots \dots \dots (2.83)$$

Recursive Solution

Assume that the basic equation 2.75 is reduced to a form

$$z_{i-1} = B_{i-1} + C_{i-1} z_i \dots \dots \dots (2.84)$$

up to  $i-1$  th station. Substitution of Eq. 2.84 into Eq. 2.75 yields another reduced form at station  $i$

$$z_i = B_i + C_i z_{i+1} \dots \dots \dots (2.85)$$

where

$$B_i = \frac{c_i B_{i-1}}{D} \dots \dots \dots (2.86)$$

$$C_i = \frac{a_i}{D} \dots \dots \dots (2.87)$$

$$D = -b_i - c_i C_{i-1} \dots \dots \dots (2.88)$$

Applying the pile top boundary condition Eq. 2.79 or Eq. 2.80 at station 0, all the continuity coefficients  $B_i$  and  $C_i$  are computed for stations 1 through n. The displacement  $z$  at the last station n is computed from the boundary condition at the pile tip (Eq. 2.83). All the rest of  $z$ 's are obtained by the back substitution into Eq. 2.84.

Once the displacement  $z$  is obtained at all the difference stations, the axial force within a pile is computed by Eq. 2.89

$$P_i = -EA_i \frac{z_{i+1} - z_{i-1}}{2h} \dots \dots \dots (2.89)$$

Equation 2.89 is the central difference expression of Eq. 2.70.

#### Elasto-Plastic Pile Strength

The behavior of a grouped pile foundation is influenced by the structural strength of the pile itself. A pile in a grouped pile foundation is subjected both to a bending moment and to an axial force. The structural strength of a pile may be determined either by elastic instability or by yielding of the pile material. Elastic instability or the

buckling of a pile is predicted by the numerical procedure developed earlier for the laterally loaded pile as a beam column. The failure of a pile due to the yielding of the pile material requires the consideration of the interaction of the bending moment and the axial force on the pile section.

Interaction Diagram. The interaction diagram of the ultimate axial strength  $P_u$  and the plastic moment  $M_p$  takes various shapes depending on the geometry of the cross-section of the pile and, more importantly, on the stress-strain relationships of the pile materials. Figure 2.12a shows a typical interaction diagram of a steel pile. Figure 2.12 b shows a typical interaction diagram of a reinforced concrete pile or a prestressed concrete pile.

The computer program GROUP can accommodate an interaction diagram of any shape. The program GROUP has an option to generate simplified interaction diagrams for steel piles (Fig. 2.13). In Fig. 2.13,  $M_y$  and  $P_u$  refer to the yield moment and the axial yield load and  $M_{yo}$  and  $P_{uo}$  are the values corresponding to pure bending and to pure axial loading. It is assumed that the interaction diagram is valid for both compression and tension. The computation of  $M_{yo}$  and  $P_{uo}$  is made by Eqs. 2.90 and 2.91.

$$M_{yo} = \sigma_y Z \dots \dots \dots (2.90)$$

$$P_{uo} = \sigma_y A \dots \dots \dots (2.91)$$



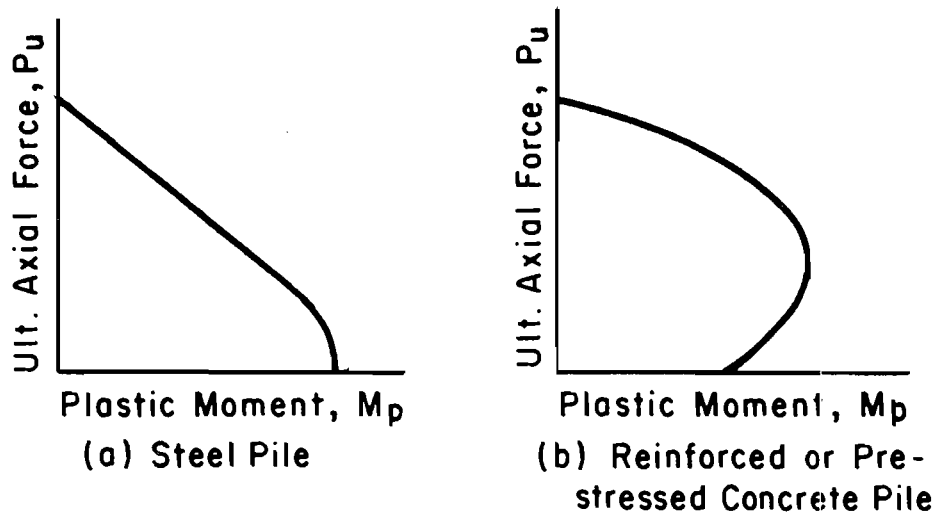


Fig. 2.12. Typical Interaction Diagram

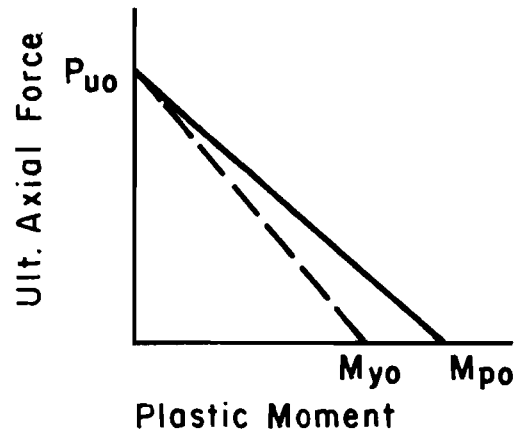


Fig. 2.13. Simplified Interaction Diagram for Steel Piles

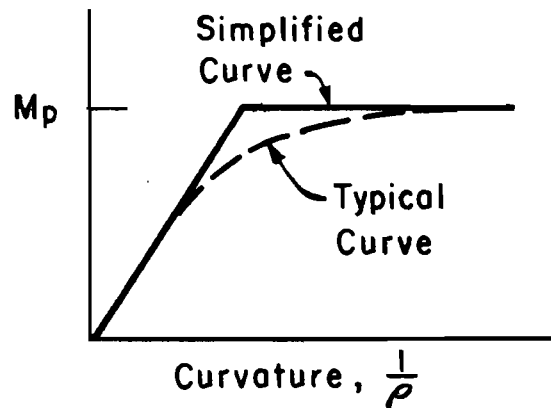


Fig. 2.14. Moment Curvature Relationship

where

$\sigma_y$  = yield stress of a steel in psi,

Z = section modulus of a steel in cubic inches, and

A = cross-sectional area of a steel section in square inches.

The relationship between  $M_{yo}$  and  $M_{po}$  is defined by a shape factor  $s$ .

$$M_{po} = s M_{yo} \dots \dots \dots (2.92)$$

The shape factor  $s$  is a function of the shape of the steel section and it is given for typical steel sections in Table 2.1 (Beedle, 1961).

TABLE 2.1 SHAPE FACTOR FOR STEEL PILES

Section	Shape Factor $s$
Wide Flange (Strong Axis)	1.14
Wide Flange (Weak Axis)	1.50
Pipe	1.27

In Fig. 2.13  $P_{uo}$  and  $M_{po}$  are connected by a straight line. It is a conservative procedure, because the actual curve is always on the right-hand side of the straight line (Beedle, 1961).

Moment Curvature Relationships. The real moment curvature relationship may be represented by such a curved line as shown by a broken line

in Fig. 2.14. In the computer program GROUP, a simplified bilinear moment-curvature curve is employed as it is shown by a solid line in Fig. 2.14. In the elastic range the flexural rigidity coincides with  $EI$ , where  $E$  is the Young's modulus and  $I$  is the moment of inertia. Once the full plasticity is developed in a section, the secant modulus of the moment-curvature curve replaces the flexural rigidity.

## CHAPTER III

### SOIL CRITERIA FOR SOIL PILE INTERACTION SYSTEM

The structural theories for single piles presented in the previous chapter requires soil criteria which give the nonlinear spring-force representations of the lateral resistance and the axial resistance.

The actual pile-soil systems are complex, involving such things as the time effect on soil behavior, dynamic or repeated loading, settlement of the surrounding soil due to negative skin friction, interference from other piles or from adjacent structures and so on. Presently available soil criteria, however, can handle only static, short-term loading.

In this chapter the soil criteria for lateral loading and axial loading are presented. The soil criteria are developed for sand and for clay, the two typical types of the soil. Other soils will normally exhibit characteristics somewhere between those for clay and sand.

#### Laterally Loaded Pile

##### Soil Modulus

The finite difference method of solving the problem of a laterally loaded pile is based on the assumption of the Winkler mechanism, where the soil can be replaced by a set of independent springs. The spring force action on a segment of a laterally loaded pile is represented by the subgrade reaction per unit length of a pile

$$p = E_s y \dots \dots \dots (3.1)$$

where

$y$  = horizontal deflection of pile in inches

$E_s$  = soil modulus in pounds per square inch.

The soil modulus  $E_s$  is generally not a constant but is a nonlinear function of depth  $x$  and the pile deflection  $y$ .

$$E_s = f(x, y) \dots \dots \dots (3.2)$$

If the correct relationship between  $p$  and  $y$ , and the right moment-curvature relationship for the pile section are given, the finite difference method can describe any state of a laterally loaded pile.

Before the age of electronic computers, simplified forms were assumed for the variation of the soil modulus  $E_s$  with depth in order to get closed-form solutions of the differential equation of the beam, or the beam-column, on an elastic foundation. The simplest theory assumes that the soil modulus  $E_s$  is constant (Chang, 1937) or that the soil modulus  $E_s$  increases in proportion to depth (Terzaghi, 1955). In attempts to represent the nonlinear nature of the soil reaction, various efforts were made to express  $E_s$  by an exponential function of depth and pile deflection (Palmer and Brown, 1954, and Shinohara and Kubo, 1961). The mathematical treatment of these methods was cumbersome and the estimation of the constants to be used were left to guess work. A realistic approach to establishing  $p$ - $y$  relationships must be based on the true load-deformation characteristics of the in situ soils. The soil criteria introduced in the following are all trying to correlate the relationship of the pile deformation and soil resistance with the basic soil properties determinable by standard soil tests or methods of exploration.

### Clay

McClelland and Focht's Criteria. McClelland and Focht (1958) found a correlation between a  $p$ - $y$  curve and a stress-strain curve from the consolidated-undrained triaxial test ( $Q_c$  test) on small specimens. The approach is similar to Skempton's (1951) work on the vertical settlement of a foundation. McClelland and Focht opened the way to developing  $p$ - $y$  curves for a clay where the clay consists of layers with different shear strength characteristics. The relationship between a  $p$ - $y$  curve and a stress-strain curve from a  $Q_c$  triaxial test is expressed by

$$p = 5.5 b \sigma_{\Delta} \dots \dots \dots (3.3)$$

and

$$y = 1/2 b \epsilon \dots \dots \dots (3.4)$$

where

- $b$  = pile diameter or frontal size in inches,
- $\sigma_{\Delta}$  = deviator stress in  $Q_c$  triaxial test with confining pressure as close to the actual overburden pressure as possible in psi,
- $\epsilon$  = strain in  $Q_c$  triaxial test.

The above relationship is illustrated in the nondimensional form in Fig. 3.1.

The procedure to get a set of  $p$ - $y$  curves from stress-strain curves is summarized as follows.

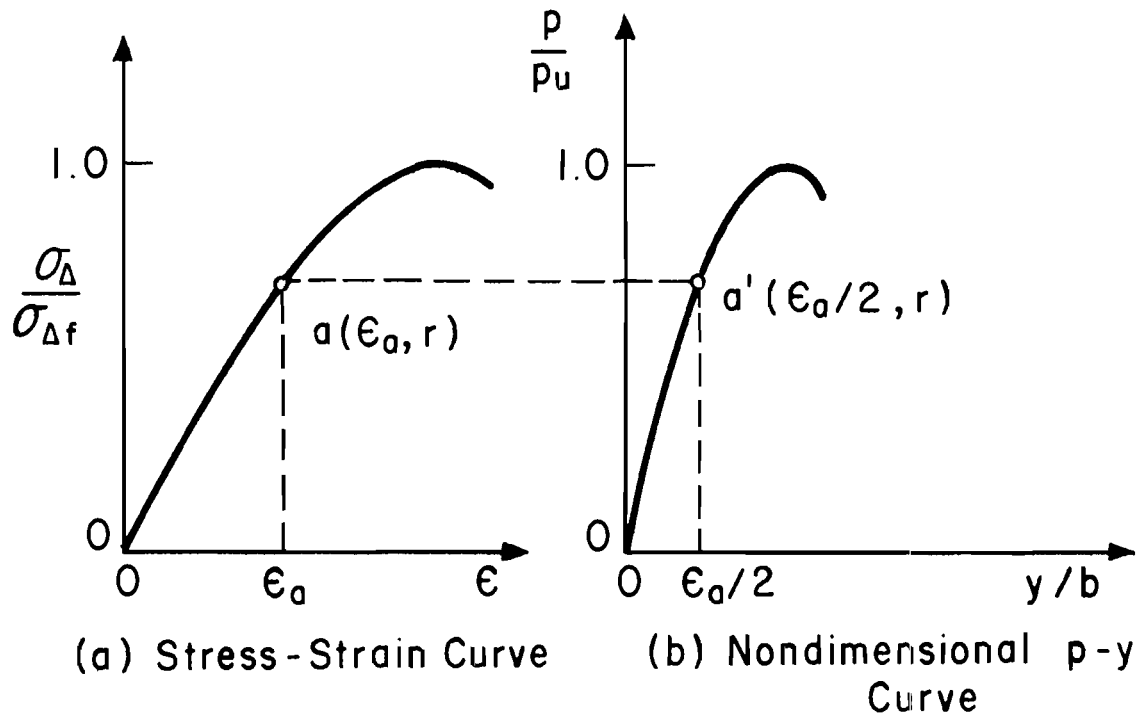


Fig. 3.1. McClelland and Focht's Criteria for p-y Curves in Clays

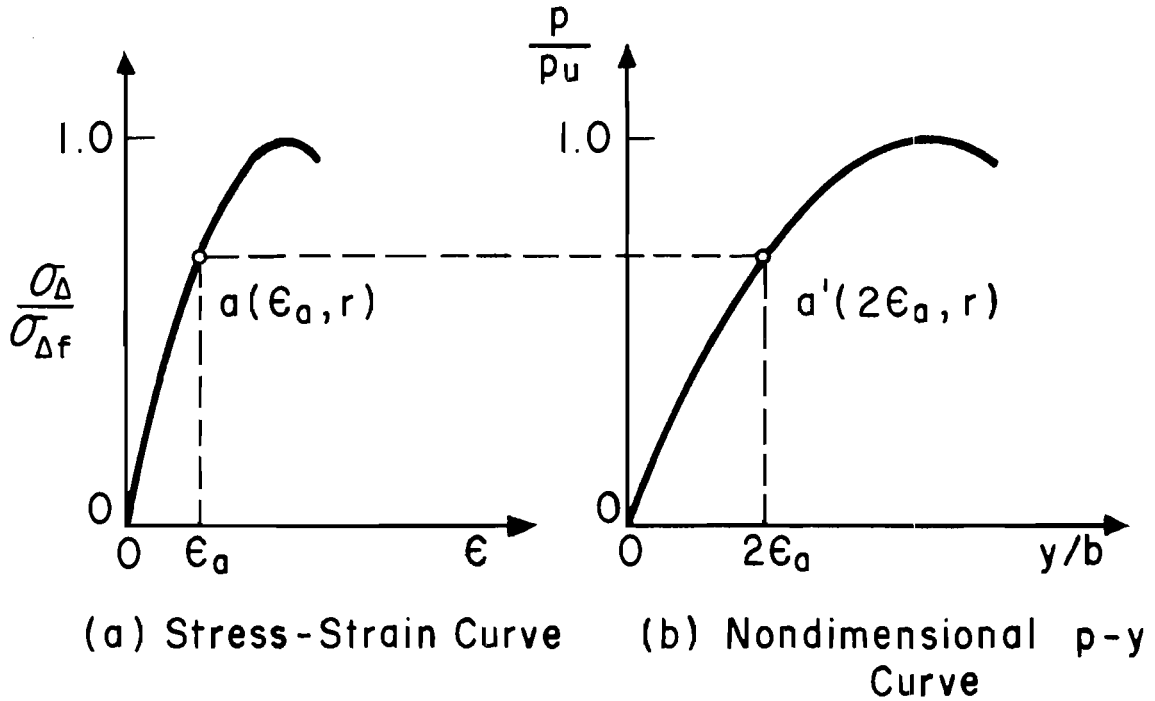


Fig. 3.2. Skempton's Criteria for p-y Curves in Clays

1. Plot a nondimensional stress-strain curve (Fig. 3.1a) with the strain  $\epsilon$  as abscissa and the ratio of the deviator stress to the ultimate deviator stress  $\sigma_{\Delta}/\sigma_{\Delta f}$  as ordinate.
2. Compute the ultimate lateral soil resistance  $p_u$  by Eq. 3.5.

$$p_u = 5.5 b \sigma_{\Delta f} \dots \dots \dots (3.5)$$

3. Construct a nondimensional coordinate system with the ratio of pile deflection to the pile diameter, or pile width,  $y/b$  as abscissa and the ratio of soil resistance per unit length of pile to its ultimate value  $p/p_u$  as ordinate. (Fig. 3.1b)
4. Draw a nondimensional  $p$ - $y$  curve, or  $p/p_u$  versus  $y/b$  curve, by transferring the stress-strain curve from Fig. 3.1a to Fig. 3.1b. After the transfer, the ordinate of the curve remains the same as the stress-strain curve, but the abscissa of the curve is reduced to one-half that of the stress-strain curve. Any arbitrary point  $a$  ( $\epsilon, r$ ) on a stress-strain curve (Fig. 3.1a) is transferred as point  $a'$  ( $\epsilon/2, r$ ) on the nondimensional  $p$ - $y$  curve, where  $r$  is greater than zero but less than unity.
5. Convert the nondimensional  $p$ - $y$  curve in Fig. 3.1b into a dimensional  $p$ - $y$  curve by multiplying the ordinate with  $p_u$  (Eq. 3.5) and multiplying the abscissa with  $b$ .
6. Repeat steps 1 through 5 for various depths to obtain a set of  $p$ - $y$  curves along a pile.

Skempton's Criteria, which is described later, may be used for the analytical generation of  $p$ - $y$  curves. Skempton (1951) correlated the



load settlement curve of a shallow foundation with the stress-strain curve of an undrained triaxial compression test. In order to make use of Skempton's equation to obtain  $p$ - $y$  curves for piles in clay, one must assume that the bearing pressure versus settlement for a long strip footing at a great depth is identical to that for the soil resistance versus deflection for a laterally loaded pile. The relationship obtained by Skempton is essentially the same as that established by McClelland and Focht. The only difference between the two is the factor which transfers the stress-strain curve of an undrained triaxial compression test to a nondimensional  $p$ - $y$  curve. McClelland and Focht multiply the abscissa of a stress-strain curve with a factor of 0.5 to get the abscissa of a nondimensional  $p$ - $y$  curve, while Skempton uses a factor of 2.

Reese's Criteria. The criteria by McClelland and Focht considers only a flow-around type of failure of soil in a horizontal plane around a pile. Reese (1958) argued that the behavior of a laterally loaded pile is greatly influenced by the soil near the ground surface which fails by moving upward in the form of a wedge. He derived an expression of the ultimate soil resistance for the wedge-type failure by considering the equilibrium of forces on the wedge.

$$p_w = \gamma b x + 2 c b + 2.83 c x \dots \dots \dots (3.6)$$

where

$p_w$  = ultimate lateral soil resistance by wedge-type failure in  
pounds per inch,

$\gamma$  = effective unit weight of soil in pci,

$b$  = diameter or width of pile in inches,

$x$  = depth in inches,

$c$  = cohesion of a clay in psi.

He also derived an expression for the ultimate soil reaction of a flow-around type of failure by considering the failure of the soil mass around the pile.

$$p_f = N_c c b \dots \dots \dots (3.7)$$

where

$p_f$  = ultimate lateral soil resistance per unit length of pile  
by flow-around type failure,

$N_c$  = coefficient of the bearing capacity, whose value is usually  
assumed to be 11.

The smaller value of  $p_w$  and  $p_f$  governs the actual ultimate lateral soil resistance.

Reese proposed to simulate the stress-strain curves by parabolas in the absence of  $Q_c$  triaxial compression test (Fig. 3.2b). The curve is assumed to become flat when the ultimate deviator stress is reached. The reference point is chosen at one-half of the ultimate deviator stress, that is, 0.5 on the ordinate. The corresponding strain  $\epsilon_{50}$  is assumed to take different values depending on the type of clay. After Skempton (1951), the following values for  $\epsilon_{50}$  are recommended.

TABLE 3.1 STRAIN OF CLAY IN TRIAXIAL COMPRESSION TEST

$\epsilon_{50}$	clay
0.005	brittle or stiff clay
0.02	soft clays
0.01	other clays

The parabolic stress-strain curve may be expressed by Eq. 3.8.

$$\frac{\sigma_{\Delta}}{\sigma_{\Delta f}} = m \sqrt{\epsilon} \dots \dots \dots (3.8)$$

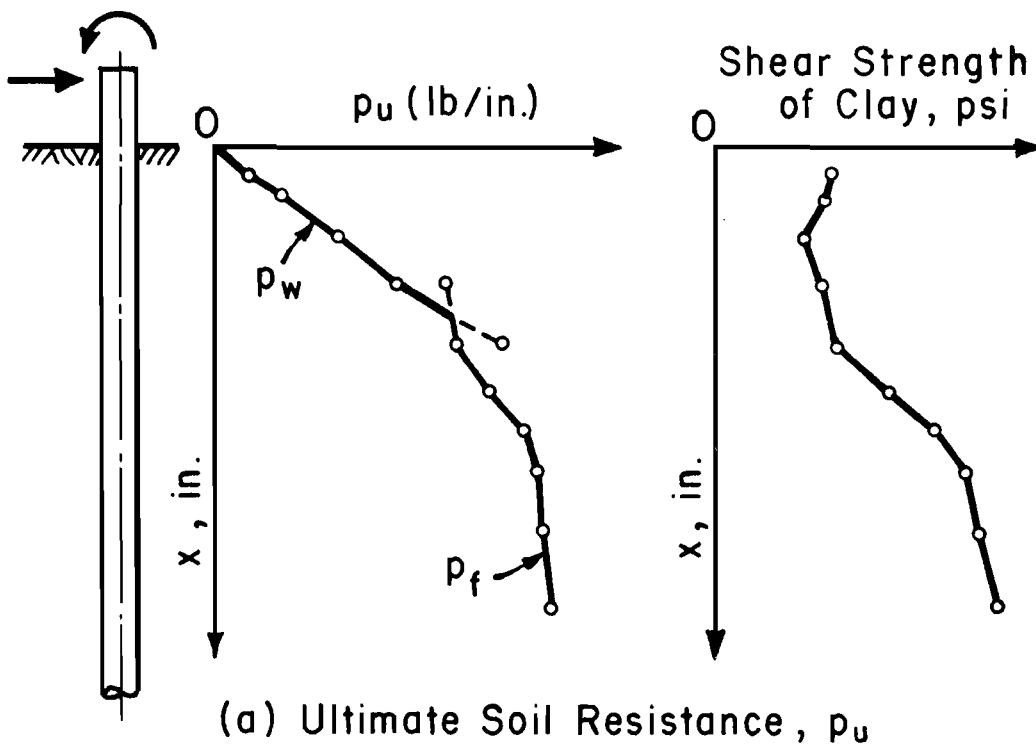
where

$m$  = coefficient to define a parabola.

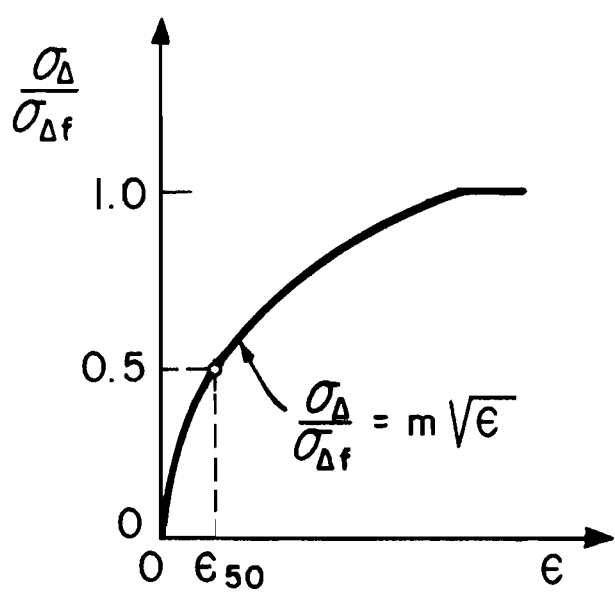
The conversion from the stress-strain curve to the  $p$ - $y$  curve can be done according to either McClelland and Focht's criteria or Skempton's criteria.

The procedure for constructing the  $p$ - $y$  curves out of the parabolic shape of stress-strain curve is summarized as follows.

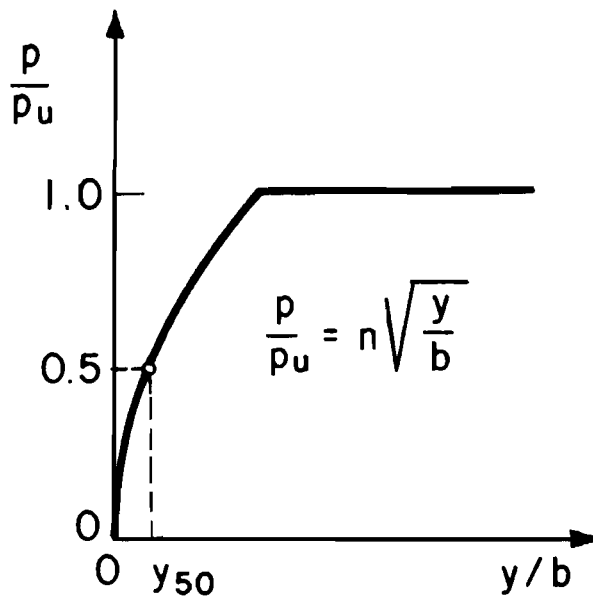
1. Calculate the two types of ultimate soil resistance per unit length of pile  $p_w$  and  $p_f$ , using Eqs. 3.6 and 3.7 and the best estimate of the shear strength of the clay. As it is shown in Fig. 3.3a, Eq. 3.6 determines the ultimate soil resistance at the upper portion and Eq. 3.7 controls the lower portion of a pile. The smaller value of  $p_w$  and  $p_f$  determines the ultimate lateral soil resistance  $p_u$ .



(a) Ultimate Soil Resistance,  $p_u$



(b) Stress-Strain Curve



(c) Nondimensional  $p$ - $y$  Curve

Fig. 3.3. Reese's Criteria for  $p$ - $y$  Curves in Clays

2. Determine the coefficient of parabola  $n$  for a nondimensional  $p$ - $y$  curve in Fig. 3.3c.

$$\frac{p}{p_u} = n \sqrt{\frac{y}{b}} \dots \dots \dots (3.9)$$

the parabola passes through the point  $(y_{50}, 0.5)$ . The magnitude of the abscissa  $y_{50}$  is given by McClelland and Focht

$$y_{50} = 1/2 \epsilon_{50} \dots \dots \dots (3.10)$$

or by Skempton

$$y_{50} = 2 \epsilon_{50} \dots \dots \dots (3.11)$$

thus

$$n = \frac{0.5}{\sqrt{y_{50}}} \dots \dots \dots (3.12)$$

3. Draw a parabola on the nondimensional coordinate system of  $(y/b)$  and  $(p/p_u)$ .
4. Cut the parabola at  $p/p_u = 1.0$  and connect with a horizontal line.
5. Compute the  $p$  and  $y$  values from the nondimensional  $p$ - $y$  curve by multiplying the ordinate with  $p_u$  determined in Step 1 and multiplying the abscissa with  $b$ .

Matlock's Criteria. Based on field tests as well as on laboratory tests, Matlock (1970) developed soil criteria for constructing  $p$ - $y$  curves

for static and cyclic loading in soft clay. Figures 3.4a and 3.4b show a summary of the procedure, both for static loading and for cyclic loading.

Matlock assumed that the ultimate resistance per unit length of pile is expressed by Eq. 3.13.

$$p_u = N_p c b \dots \dots \dots (3.13)$$

where

$c$  = cohesion of a clay in psi,

$b$  = pile diameter in inches,

$N_p$  = dimensionless coefficient of ultimate bearing capacity.

The value of the coefficient  $N_p$  for the depth where only the flow-around failure occurs is

$$N_p = 9 \dots \dots \dots (3.14)$$

Near the ground surface where the overburden pressure is not enough to prevent the forming of the upward wedge, the coefficient  $N_p$  is given by

$$N_p = 3 + \frac{\gamma x}{c} + J \frac{x}{b} \dots \dots \dots (3.15)$$

where

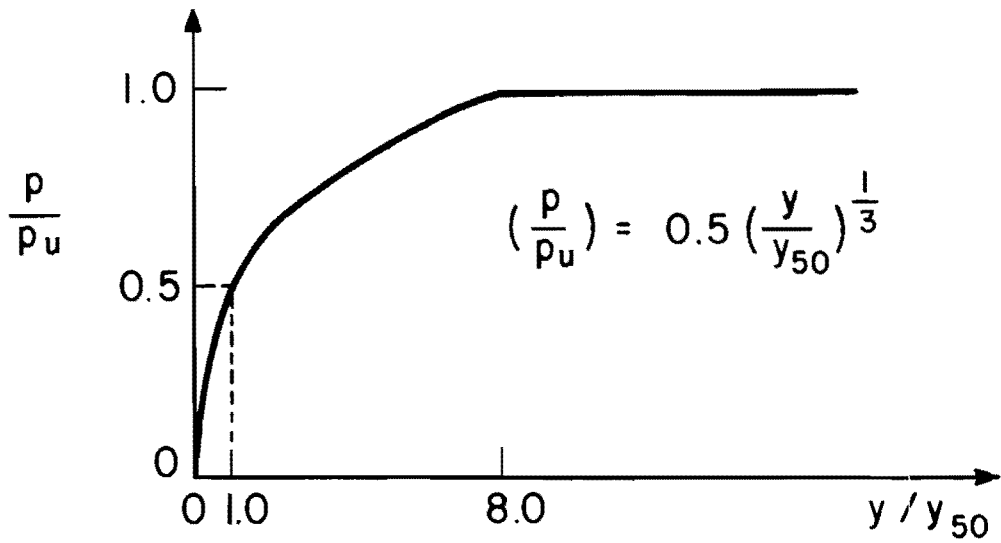
$\gamma$  = effective unit weight of clay in pci,

$x$  = depth in inches,

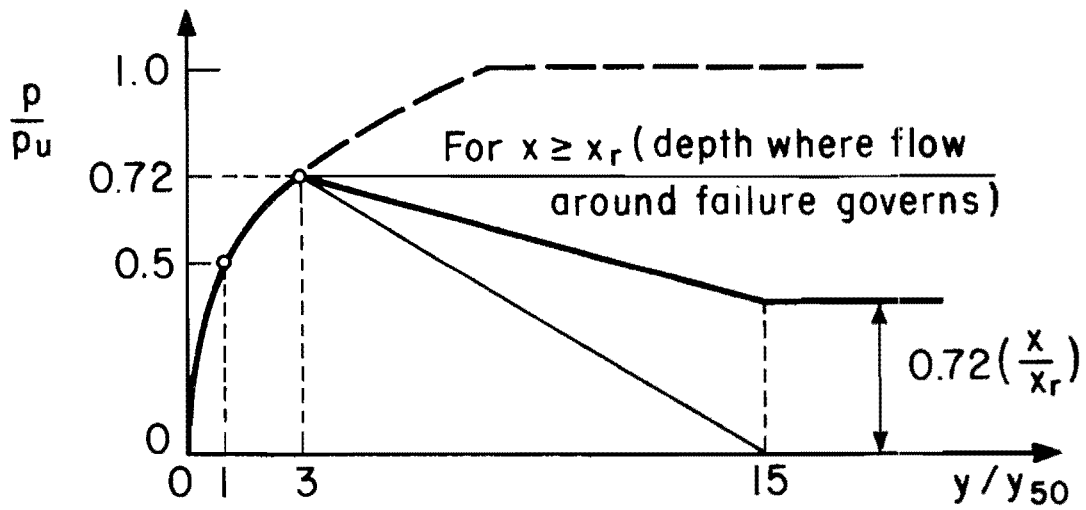
$c$  = cohesion of a clay in psi,

$b$  = pile diameter in inches,

$J$  = dimensionless constant determined from the type of clay.



(a) Static Loading



(b) Cyclic Loading

(after Matlock)

Fig. 3.4. Matlock's Criteria for  $p$ - $y$  Curves in Soft Clays

Matlock's experimental value of the constant  $J$  ranged from 0.25 to 0.5. Reference to Eq. 3.6 shows that Matlock's criteria is similar to that of Reese.

Near the ground surface the ultimate resistance per unit length of pile is determined by the lesser value of  $p_u$  computed from Eqs. 3.13, 3.14, and 3.15. The  $p$ - $y$  curve for the static loading is constructed by the following procedure.

1. Choose  $\epsilon_{50}$ , the strain corresponding to one-half of the ultimate deviator stress  $\sigma_{\Delta f}$  or one-half of the unconfined compression strength  $q_u$ . (Skempton's criteria give typical values of  $\epsilon_{50}$  (Table 3.1) if a stress-strain curve is unavailable.)
2. Calculate the pile deflection  $y_{50}$  which corresponds to the strain  $\epsilon_{50}$  on the stress-strain curve, by a formula

$$y_{50} = 2.5 \epsilon_{50} b \dots \dots \dots (3.16)$$

where

$b$  = diameter or width of a pile in inches.

3. Draw a nondimensional cubic curve

$$\frac{p}{p_u} = 0.5 \left( \frac{y}{y_{50}} \right)^{1/3} \dots \dots \dots (3.18)$$

between  $0 \leq p/p_u \leq 1$



4. Connect the curve with a horizontal line

$$\frac{p}{p_u} = 1 \dots \dots \dots (3.18)$$

5. Calculate the values of  $p$  and  $y$  from the nondimensional  $p$ - $y$  curve by multiplying the ordinate with  $p_u$  and multiplying the abscissa with  $y_{50}$ .

The  $p$ - $y$  curve for the cyclic loading is constructed in a similar manner. Figure 3.4b reflects the deterioration of soil strength by the effect of repeated loading.

### Sand

Reese's Criteria. Reese's criteria for obtaining a set of  $p$ - $y$  curves for sand are based on formulas for the ultimate lateral soil resistance per unit length of pile and on recommendations by Terzaghi (1955) for the shape of the early part of the  $p$ - $y$  curve. The detailed development of the formulas for the ultimate lateral soil resistance is given by Parker and Reese (1970).

In the following, a brief summary is given of the method for determining the ultimate lateral soil resistance and for the construction of the basic bilinear  $p$ - $y$  curves.

The ultimate lateral soil resistance at depth is given by the equation for a flow-around type failure of sand. The equation is derived by considering the successive failure of the square block soil elements as in the case of clay (Reese, 1958).

$$p_f = \gamma b x \left\{ K_P^3 + 2K_O \tan \phi (K_P^2 + 1) - K_A \right\} \dots \dots \dots (3.19)$$

where

$p_f$  = ultimate soil resistance per unit length of pile in pounds per inch,

$\gamma$  = effective unit weight of soil in pci,

$x$  = depth in inches,

$b$  = pile width in inches,

$K_A = \tan^2 (45^\circ - \phi/2)$  coefficient of active earth pressure,

$K_P = \tan^2 (45^\circ + \phi/2)$  coefficient of passive earth pressure,

$K_O$  = coefficient of earth pressure at rest which is assumed to be 0.5,

$\phi$  = angle of internal friction of a sand in degree.

The examination of Eq. 3.19 reveals that the first term within the parenthesis  $K_P^3$  is by far the major contributing factor in determining the ultimate lateral soil resistance per unit length of pile. Therefore, the ultimate lateral soil resistance by flow-around type failure  $p_f$  is proportional to the cube of the coefficient of the passive earth pressure.

Near the ground surface the ultimate soil resistance on a pile is obtained by computing the force exerted from a soil wedge moving upward. The ultimate lateral soil resistance by wedge type failure  $p_w$  is obtained by differentiating the total force exerted from the soil wedge onto the pile with respect to depth,  $x$ .

$$p_w = \gamma x \left\{ b (K_P - K_A) + x \tan \beta \left[ K_P \tan \alpha + K_O (\tan \phi - \tan \alpha) \right] \right\} \dots \dots (3.20)$$

where

$$\beta = 45^\circ + \frac{\phi}{2},$$

$\alpha$  = angle to define the shape of wedge, and is assumed to be equal to one-half of  $\phi$ .

The early portion of the p-y curve is constructed from Terzaghi's (1955) recommendation. Terzaghi used the theory of elasticity to derive the relationship between the horizontal deflection of a vertical pile and the soil resistance.

$$\frac{p}{y} = E_s = k x \dots \dots \dots (3.21)$$

where

p = lateral soil resistance in pounds per inch,

y = lateral pile deflection in inches,

$E_s$  = soil modulus in pounds per inch<sup>2</sup>,

k = coefficient of lateral soil reaction in pounds per inch<sup>3</sup>.

Terzaghi (1955) gave the values of k as Table 3.2.

x = depth from ground surface in inches.

TABLE 3.2 RANGE OF VALUES OF k, POUNDS PER INCH<sup>3</sup>

Relative Density of Sand	Loose	Medium	Dense
Dry or Moist Sand	3.5 - 10.4	12.8 - 40.1	50.8 - 101.6
Submerged Sand	2.1 - 6.4	8.0 - 26.7	32.1 - 64.1

The procedures for constructing the bilinear  $p$ - $y$  curves are summarized as follows.

1. Compute the two types of ultimate lateral soil resistance per unit length of pile by Eqs. 3.19 and 3.20 along the pile.
2. Take the smaller value as the governing ultimate value (Fig. 3.5a).
3. Choose the appropriate value of  $k$ , depending on the state of the sand (Table 3.2).
4. Construct a bilinear  $p$ - $y$  curve as it is shown in Fig. 3.5b.
5. Repeat Steps 3 and 4 for various depth to obtain a set of  $p$ - $y$  curves.

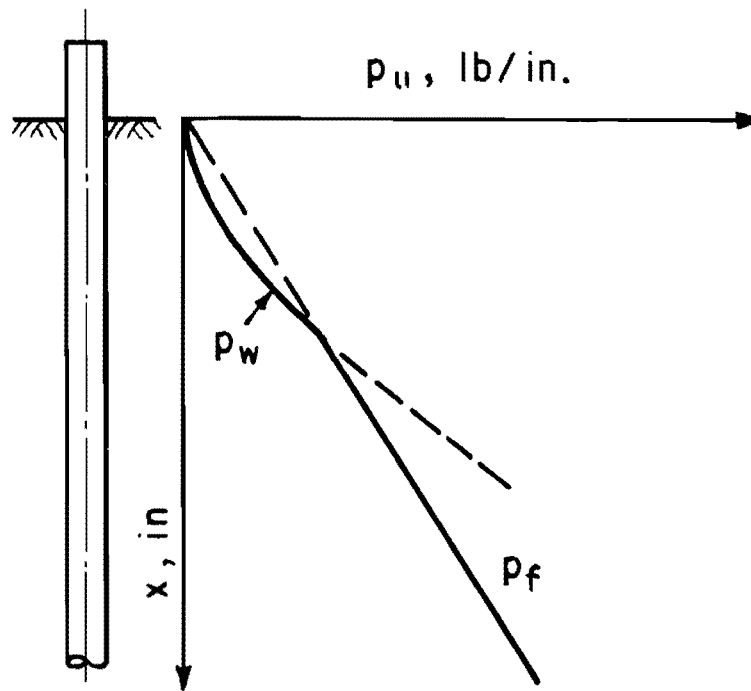
Parker and Reese's Criteria. A proposal was made by Parker and Reese (1970) to smooth the bilinear  $p$ - $y$  curves, obtained by Reese's method, by use of a hyperbolic function of the form

$$p = p_u \tanh \left( \frac{k y}{p_u} \right) \dots \dots \dots (3.22)$$

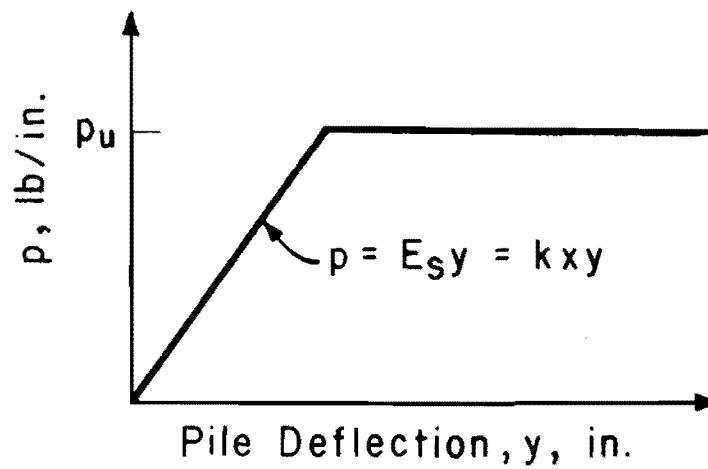
where

- $p$  = lateral soil resistance in pounds per inch,
- $p_u$  = ultimate lateral soil resistance in pounds per inch,
- $k$  = coefficient of lateral soil resistance in pounds per inch<sup>3</sup> (Table 3.2),
- $y$  = lateral deflection of pile in inches.

The hyperbolic  $p$ - $y$  curve generated by Eq. 3.22 is asymptotic to the bilinear  $p$ - $y$  curve obtained from Reese's criteria (Fig. 3.6).



(a) Ultimate Lateral Soil Resistance,  $p_u$



(b) Bilinear  $p$ - $y$  Curve

Fig. 3.5. Reese's Criteria for  $p$ - $y$  Curves in Sands

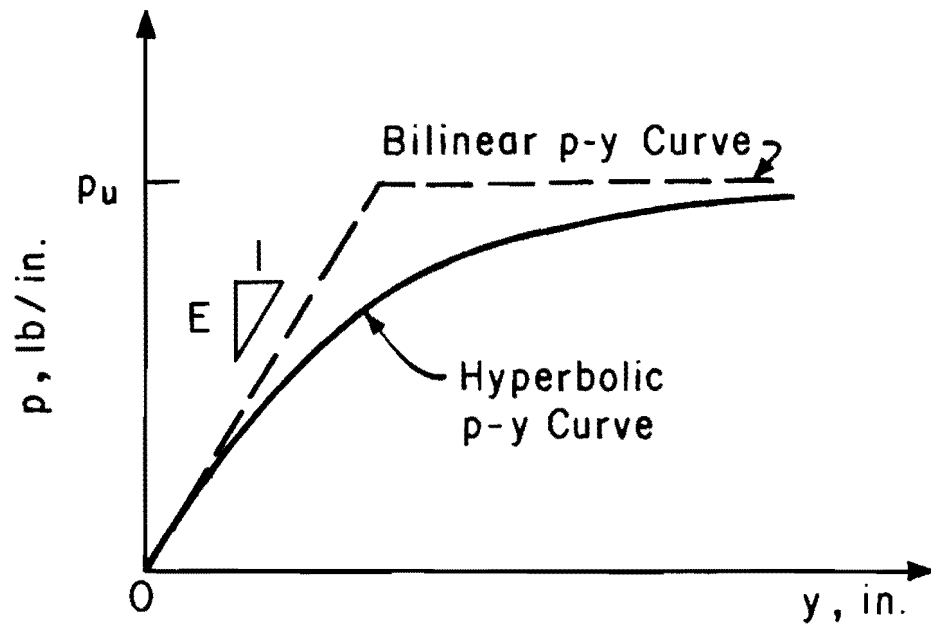


Fig. 3.6. Hyperbolic p-y Curve

Summary

The most realistic  $p$ - $y$  curves or the lateral soil resistance versus pile deflection curves are those based on theory as far as possible. Both the flow-around type failure of a soil in a horizontal plane and the wedge-type failure of a soil are taken into consideration. The wedge-type failure occurs near the ground surface. The flow-around type failure occurs at enough depth from the ground surface where there is sufficient restraint to prevent the upward movement of the soil.

Perhaps the most important consideration regarding  $p$ - $y$  curves is whether or not there are validating experimental results. Matlock's criteria are based on a series of carefully performed experiments, including cyclic lateral loading, and furthermore employ theoretical expressions for ultimate resistance. Matlock's criteria are believed to be the best currently available for clays. Only Matlock has given recommendations for  $p$ - $y$  curves for cyclic loading for clays. While Matlock's recommendations are specifically for soft clays, perhaps the most common soil for marine structures, this idea can also be applied with some caution to medium and stiff clays.

The only soil criteria for sand available in the literature are those by Reese and Parker. Reese considered the flow-around type failure and the wedge-type failure of a soil. The criteria by Parker and Reese smooth the simple bilinear  $p$ - $y$  curves obtained from Reese's criteria. These criteria are weakened somewhat by a lack of experimental verification, particularly on large-sized piles; however, theoretical computations using these methods agree well with experimental results that are available.

## Axially Loaded Pile

### Load Transfer and Point Resistance

The finite difference method for solving the problem of an axially loaded pile employs a set of load transfer curves along the pile and the point resistance curve at the top of pile.

The load transfer curve refers to a relationship between the skin friction developed on the side of a pile and the absolute axial displacement of a pile section. The point resistance curve expresses the total axial soil resistance on the base of the pile-tip in terms of the pile-tip movement.

The properties of soil which determine the load transfer curve and the point resistance curve may be considerably affected by pile driving. In the case of clays, Seed and Reese (1957) reported that soon after the pile driving a loss in shear strength was observed in clays adjacent to the pile equal to 70 per cent of that for total remolding. They also observed that the recovery of shear strength with the passage of time resulted in a five-fold increase in the load-carrying capacity of a pile, even in insensitive clays. As is pointed out by Kishida (1967), the pile driving in a loose sand results in the increase in the relative density and increase in the confining pressure, both of which are major factors affecting the load transfer curves and the point resistance curve. The action of arching observed in sands around a pile (Robinsky and Morrison, 1964) may be another important factor to be considered.

In spite of all these complex factors, presently available soil criteria are based only on the soil properties before pile driving. In view of the fact that the effect of different methods of pile installation



on the soil properties with the passage of time are excluded from the soil criteria, the soil criteria described in the following must be regarded as tentative.

### Clay

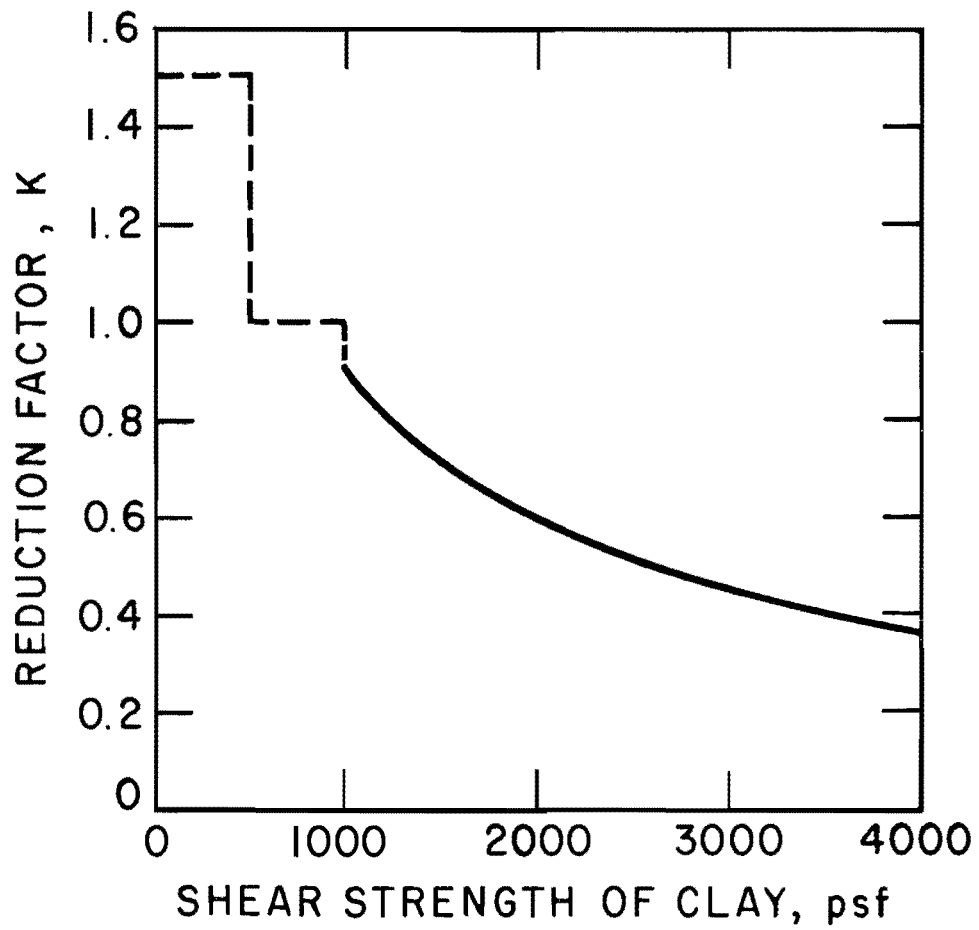
Coyle and Reese's Criteria. Coyle and Reese (1966) developed soil criteria for the load transfer curves for a pile in clays.

After Woodward, Lundgren, and Boitano (1961), Coyle and Reese proposed a reduction factor  $K$  to express the relationship between the cohesion of a clay and the maximum load transfer on a pile. Figure 3.7 shows that the reduction factor  $K$  is less than unity if the shear strength of a clay is over 1,000 psi. Similar observation is also made by Tomlinson (1957).

Coyle and Reese expressed the rate of load transfer developed on the side of a pile as a function of absolute pile movement. Curves were given for various depths. (Fig. 3.8).

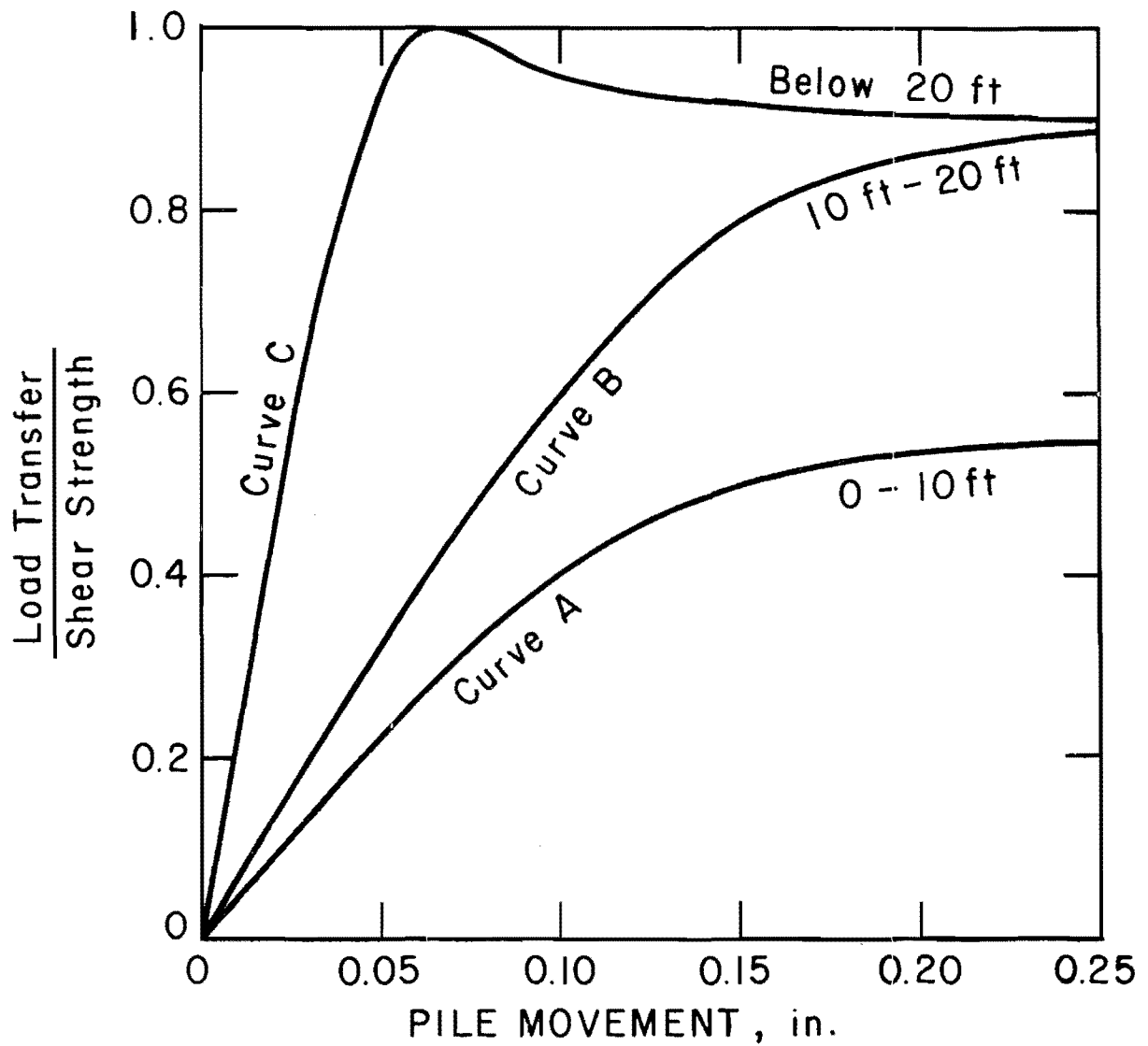
The procedure for developing a load transfer curve for the side of a pile is summarized as follows:

1. Estimate the distribution of cohesion of the clays along the length of the pile from available soil data.
2. Compute the maximum load transfer as a function of depth from Fig. 3.7.
3. Select the curve A, B, or C in Fig. 3.8 depending on the depth.
4. Multiplying the ordinate of the selected curve in Fig. 3.8 with the maximum load transfer obtained in Step 2, compute a load transfer curve.



(after Coyle and Reese)

Fig. 3.7. Reduction Factor for Maximum Adhesion



(after Coyle and Reese)

Fig. 3.8. Nondimensional Load Transfer Curves of a Pile in Clays

5. Repeat Steps 2 through 4 for varying depths to obtain a set of load transfer curves along a pile.

Skempton's Criteria. The point resistance curve for a pile in a clay may be generated by Skempton's (1951) criteria. Starting with the theory of elasticity, Skempton found a correlation between the load-settlement curve of the shallow foundation and the stress-strain curve for the undrained triaxial compression test. The validity of the same correlation for a deep foundation was attested by examining the effect of the foundation depth on the pertinent variables in the basic equation. The correlation is expressed by simple equations.

$$\frac{z}{b} = 2 \epsilon \dots \dots \dots (3.23)$$

$$\epsilon = \frac{\sigma_{\Delta}}{E} \dots \dots \dots (3.24)$$

where

$z$  = settlement of a foundation in inches,

$b$  = diameter of a circular foundation in inches,

$\epsilon$  = dimensionless strain in the undrained triaxial compression test;

$\sigma_{\Delta}$  = deviator stress of the undrained triaxial compression test in psi, with the ambient pressure as close as possible to the overburden pressure,

$E$  = Young's modulus of the soil or the secant modulus in the stress-strain curve.

If a stress-strain curve from undrained triaxial test is available, it is readily transformed to a point resistance curve as it is described in the early part of this Chapter. If no stress-strain curve is available, a parabola is assumed in a similar fashion as it is shown in Figs. 3.3b and 3.3c.

### Sand

Meager studies have been made for sands to establish generally applicable soil criteria for generating a set of load transfer curves along a pile and a point resistance curve at the tip of the pile. Two soil criteria are described, as follows.

Coyle and Sulaiman's Criteria. Coyle and Sulaiman (1967) experimentally investigated the load transfer curves of a pile in sand. The ultimate load transfer or skin friction on the side of a pile wall is expressed in the simplest form by

$$T_f = K_o \gamma x \tan \delta \dots \dots \dots (3.25)$$

where

- $T_f$  = maximum load transfer on the pile in psi,
- $K_o$  = earth pressure coefficient whose value may lie somewhere between the active earth pressure coefficient  $K_A$  and the passive earth pressure coefficient  $K_p$ ,
- $\gamma$  = effective unit weight of the soil in pci,
- $x$  = depth from the ground surface in inches,
- $\delta$  = friction angle between the pile and the contacting sand.

Assuming that the earth pressure coefficient  $K_o$  is equal to one and the friction angle is equal to the angle of internal friction of the sand before disturbance, Coyle and Sulaiman found the relationship between the load transfer of a pile in a sand and the pile displacement.

Their conclusion, however, is contradictory to the experimental observation by Parker and Reese (1970). Coyle and Sulaiman state that at shallow depth there is a considerable increase in the actual maximum load transfer over that calculated by Eq. 3.25 with the assumption of constant  $K_o$  and constant  $\delta$  throughout the length of pile. They further assert that the maximum load transfer is reached at the lower portion of the pile with smaller pile displacement than at the upper portion of the pile. The observation by Parker and Reese indicated that the actual maximum load transfer at shallow depth is close to that obtained from Eq. 3.25 with the same  $K_o$  and  $\delta$  at all depths. Parker and Reese also found that the pile displacement necessary to reach the maximum load transfer increases linearly with depth.

Parker and Reese's Criteria. Empirical criteria were established by Parker and Reese (1970) for generating a set of load transfer curves along a pile in sand. The criteria correlates the load transfer curve with the stress-strain curve of a triaxial compression test. Their criteria includes a recommendation for the estimation of point resistance curve.

The stepwise description of the procedure for generating a set of load transfer curves and a point resistance curve is given in the following.

1. Determine the relative density of sand and the stress-strain curve of a triaxial test with the ambient pressure equal to the overburden pressure.

2. Obtain the correction factor for the maximum load transfer as a function of relative density of sand (Fig. 3.9).
3. Obtain modified correlation coefficients, which relate the deviator stress in the triaxial test with the load transfer on the side of the pile. The modified correlation coefficient for uplift loading is calculated by dividing the value obtained by Eq. 3.26 with the correction factor (Step 2).

$$U_t = \frac{N_t}{\tan^2(45^\circ + \phi/2) - 1} \dots \dots \dots (3.26)$$

where

$U_t$  = correlation coefficient for uplift loading

$N_t$  = tension skin friction coefficient which is a function of the earth pressure coefficient and the friction angle. The value of 4.06 is assumed by Parker and Reese.

The modified correlation coefficient for a compression pile is calculated by dividing the value of Eq. 3.27 with the correction factor (Step 2).

$$U_c = \frac{N_c}{\tan^2(45^\circ + \phi/2) - 1} \dots \dots \dots (3.27)$$

where

$U_c$  = correlation coefficient for downward loading,

$N_c$  = compression skin friction coefficient which is a

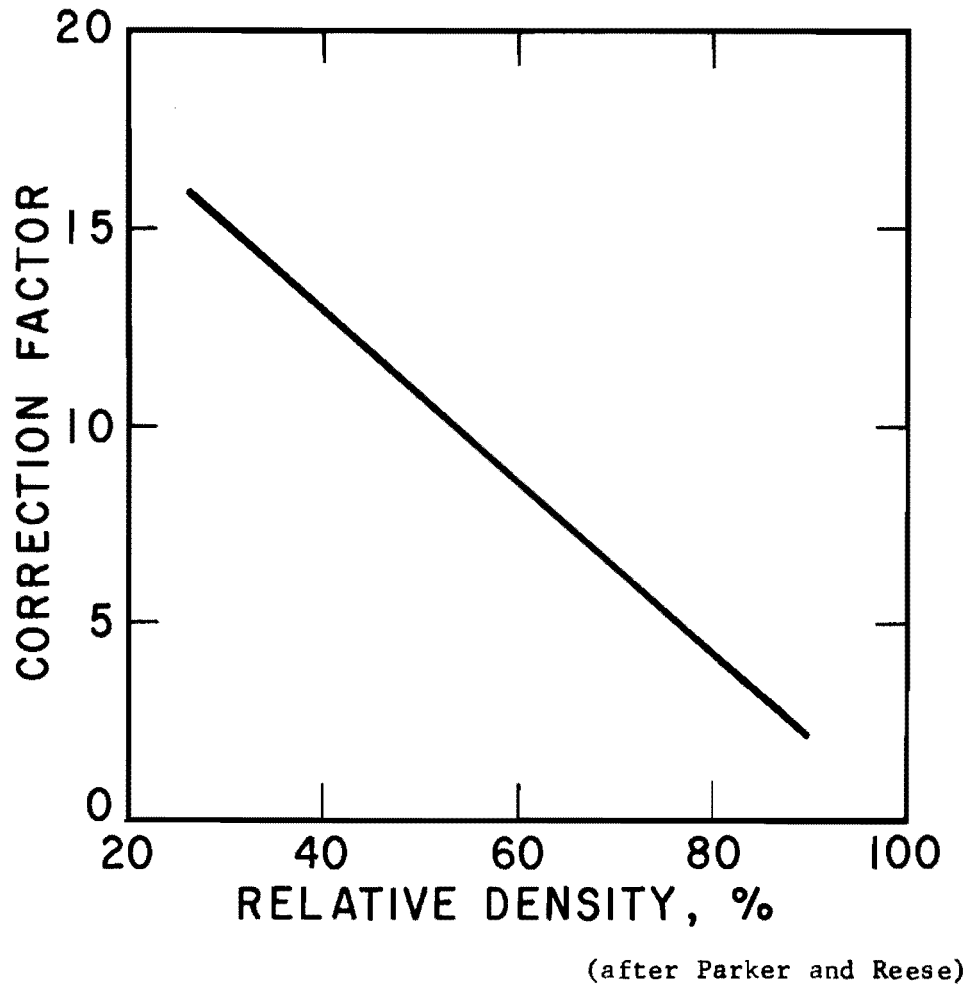


Fig. 3.9. Correction Factor for Maximum Load Transfer



function of the earth pressure coefficient and the friction angle. Parker and Reese assume the value 5.3 or the value computed from  $7.0 - 0.04 x$ .

4. Compute a load transfer curve from a stress-strain curve.

Multiplying the deviator stresses with the modified correlation coefficient (Step 3), the values of load transfer is obtained.

The displacement of the pile is computed by multiplying the axial strain in the triaxial test with the value obtained from Eq. 3.28 or 3.29

$$R_t = 0.15 + 0.012 x \dots \dots \dots (3.28)$$

$$R_c = 0.4 + 0.016 x \dots \dots \dots (3.29)$$

where

$R_t$  = factor correlating upward pile movement to axial strain,

$R_c$  = factor correlating downward pile movement to axial strain.

5. Repeat Steps 1 through 4 for depth up to 15 times the pile diameter. The curve for this depth is used for the remainder of the pile.
6. Construct a point resistance curve by combining any one of the bearing capacity formulas with the theory of elasticity solution for the settlement of a rigid footing on an elastic material (Skempton, 1951).

Meyerhof's Criteria. After Skempton, Yassin, and Gibson (1953), Meyerhof (1959) proposed a simple criterion (Eq. 3.30) for generating a point resistance of a pile in sands.

$$z = \frac{p_b}{30 p_{bu}} \dots \dots \dots (3.30)$$

where

- $z$  = settlement in inches,
- $p_b$  = base pressure in psi,
- $b$  = diameter of the base in square inches,
- $p_{bu}$  = unit ultimate bearing capacity in psi.

Considering the diversity of values of  $p_{bu}$  by various bearing capacity formulas (Vesić, 1963; McClelland, Focht, and Emrich, 1969), the unit ultimate bearing capacity of a pile point may be readily obtained from the empirical relationship with the standard penetration test (Meyerhof, 1956).

$$p_{bu} = 60 N \dots \dots \dots (3.31)$$

where

- $N$  = number of blows per foot penetration in the standard penetration test.

### Summary

A set of load transfer curves along a pile in clays can be computed from the criteria by Coyle and Reese. A point resistance curve for a pile in clays can be constructed from Skempton's criteria.

The load transfer curves along a pile in sands should be computed by the procedure given by Parker and Reese. A point resistance curve for a

pile in sands may be computed either according to the recommendation by Parker and Reese or according to Meyerhof's criteria.

Existing soil criteria can only make a rough prediction of the axial behavior of a pile. For a more accurate prediction of axial behavior of a pile, future development is needed of the theory for the mechanism of load transfer and of point resistance.

CHAPTER IV  
DESIGN OF EXPERIMENT

Aim and Outline of Experiment

The experiment was conducted to develop information on the behavior of single piles in sand (Parker and Reese, 1970) and on the behavior of grouped pile foundations. Results from the tests of the single piles were used in the theory for the behavior of grouped pile foundations (Chapter II) and analytical predictions were made which were then compared with the experimental results. The aim of this program was to provide an evaluation of the theory of grouped pile foundations.

The experiment consisted of two phases. First, a number of single piles were tested to obtain necessary information on the load displacement relationships of axially and laterally loaded piles (Chapter V). In the second phase, grouped pile foundations were tested under various types of static loads. Results from the tests of the grouped pile foundations were compared with the analytical predictions (Chapter VI).

Although it was desirable to perform the experiment on full-scale piles in a variety of typical soils, economic considerations required the experiment to be limited to small-sized piles, which were steel pipe piles of two-inch diameter. These piles were embedded eight feet in a submerged dense sand.

The design of the experiments are briefly described in the following.

Test Setup

The test was carried out in a reinforced concrete tank (Fig. 4.1). A temporary shed was built over the tank to shield the test piles and

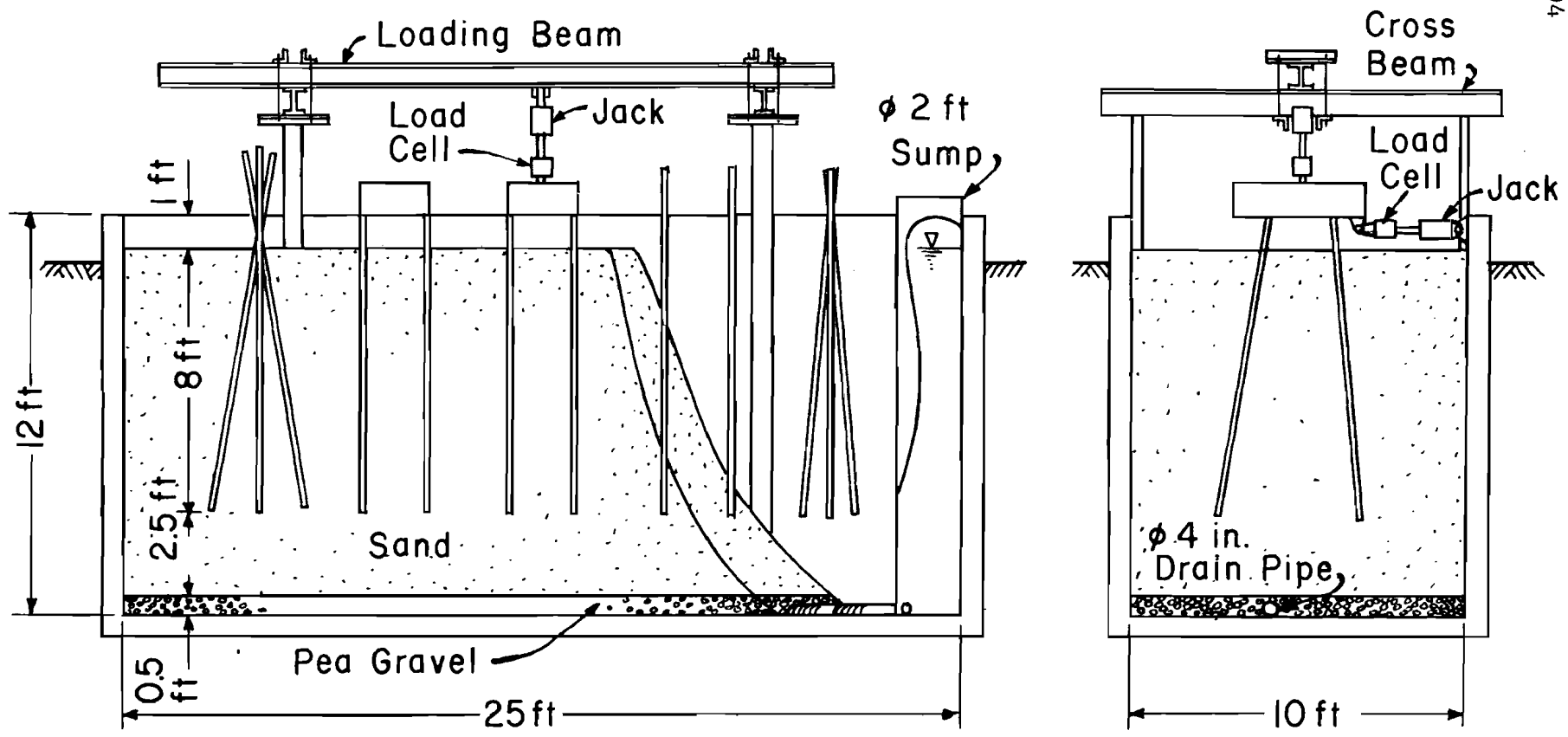


Fig. 4.1. Test Setup

equipment from the weather. The inside dimensions of the tank were 10 feet wide, 12 feet deep and 25 feet long. The wall thickness was eight inches.

A four-inch diameter drainage pipe was installed diagonally on the bottom of the tank. The drainage pipe was placed in a six-inch thick pea gravel layer, and was connected to a two-foot diameter sump at a corner of the tank. A small submersible water pump provided drainage which was necessary during the placing of the sand.

Four eight-inch wide channels were fastened to the tank wall with anchor bolts to provide the loading anchors (Fig. 4.1). A moveable loading beam was placed atop two cross beams. Vertical jack reaction was taken by the loading beam. Horizontal jack reaction was taken by the sidewall of the tank.

For vertical loading a double-acting hydraulic jack was used. The jack was capable of developing 37 kips with 6-inch travel. Horizontal load was supplied by a similar jack but with maximum capacity of 9.5 kips. The hydraulic pressure was given by an electric power pump. The exact load was monitored by reading a digital voltmeter hooked to a load cell; operators regulated the oil flow to maintain the load at the desired level. The control of the oil flow was done through adjusting a series of valves.

### Piles

The dimensions of test piles were determined after a series of considerations to the lateral and axial behavior of a small-sized pile in sand.

While the tests did not attempt to model a prototype, it is instructive to consider some ideas on the modeling of piles. Shinohara and Kubo (1961) derived the scale factor for the flexural rigidity  $EI$  of a laterally loaded pile in sands for the two limiting cases. The first case assumes the lateral soil resistance per unit length of pile is proportional to depth  $x$ .

$$p = K_o \times b \dots \dots \dots (4.1)$$

where

- $p$  = lateral soil resistance per unit length of pile,
- $K_o$  = coefficient of the lateral soil reaction,
- $b$  = width of pile.

Then the scale factor for  $EI$  is expressed as follows.

$$\lambda_{EI} = \lambda_{K_o} \lambda_x \lambda_b \lambda_y^{-1} \dots \dots \dots (4.2)$$

where

$\lambda$  = scale factor for the subscripted quantity.

In the second case the lateral soil resistance per unit length of pile is assumed to be proportional to depth  $x$  and pile deflection  $y$ .

$$p = K_o \times y \times b \dots \dots \dots (4.3)$$

The corresponding scale factor for EI is expressed by Eq. 4.4.

$$\lambda_{EI} = \lambda_{K_0} \lambda_x^5 \lambda_b \dots \dots \dots (4.4)$$

Shinohara and Kubo indicated two alternatives to satisfy the modeling law Eq. 4.2 or Eq. 4.4. The first choice is the use of a geometrically similar model in the identical soil, in which the model pile must be made of more flexible material than the prototype pile. The second choice is the use of geometrically and materially similar model pile, for which a denser sand is used as a model soil. A practical modeling is made by combining these two choices, where a model pile is made of more flexible material and installed in a denser sand. This work by Shinohara and Kubo helped in the final selection of pile dimensions and soil properties, as well as the state of the sand.

Another guideline for the proper selection of the pile dimensions is obtained from examining the simple case of a laterally loaded pile in a soil with a uniform soil modulus  $E_s$ . The closed form solution of this pile singles out a parameter  $\beta$  (Chang, 1937).

$$\beta = 4 \sqrt{\frac{E_s}{4EI}} \dots \dots \dots (4.5)$$

The dimension of the parameter  $\beta$  is the reciprocal of length. It is easily checked that the pile can be regarded as semi-infinitely long if its length is at least four times the reciprocal of  $\beta$ . If the soil modulus  $E_s$  is assumed to be proportional to depth  $x$ , the soil



modulus at the one-third depth of the first stationary point of the pile may be used for the equivalent uniform soil modulus.

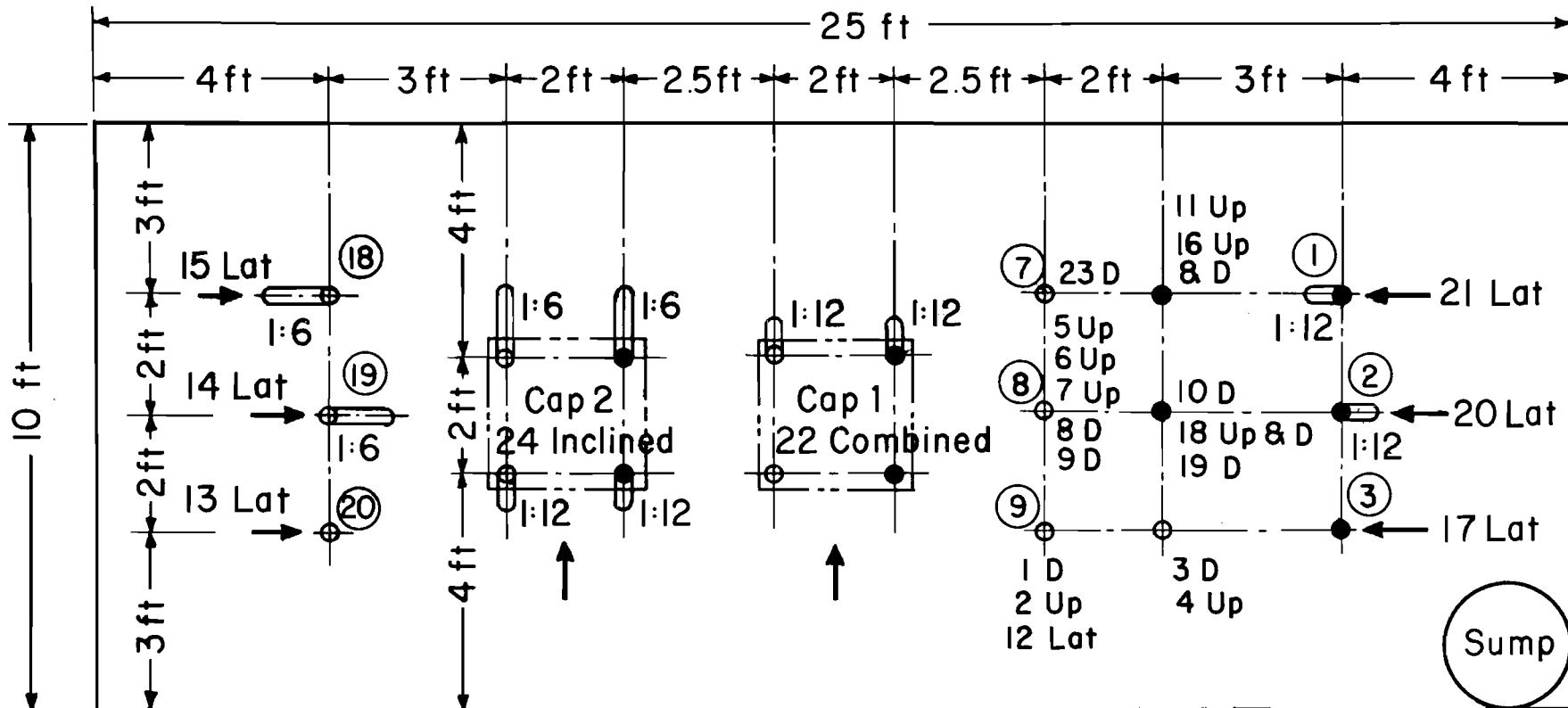
A rule of thumb for the dimension of an axially loaded small-sized pile is given by Vesic' (1965) who stated that the pile diameter of the model foundation must be at least 1.5 inches or about the size of the Dutch Cone Penetrometer to be quantitatively useful.

A seamless steel tube of two-inch outside diameter with 0.065-inch wall thickness was selected to make all of the piles used in the test. The size of the tube satisfies the rule of thumb given by Vesic'. In terms of the parameter  $\beta$  (Eq. 4.5), a pile embedded eight feet in a dense sand has a length of approximately five times the reciprocal of  $\beta$

The tube has a cross-sectional area of 0.380 inch<sup>2</sup>. Its radius of gyration is 0.698 inch. The moment of inertia is 0.185 inch<sup>4</sup>. The weight of the tube is 1.29 pounds per foot. A tensile test was performed on a strip cut from one of the piles. The yield stress was found to be 64 ksi and the ultimate stress was 78 ksi. Young's modulus of the steel was  $29 \times 10^6$  psi.

The arrangement of test piles and test foundations is shown in Fig. 4.2. The minimum distance between the piles was set 2 feet or 12 times the pile diameter to eliminate substantially any interference from other piles. The distance between the tip of pile and the base of the sand layer is 2 feet and 6 inches or 15 times the pile diameter. This distance was thought to be sufficient so that the effect of the underlying pea gravel layer on the pile behavior was negligible.

Twelve single piles and two grouped pile foundations with four piles were tested. The pile numbers are shown circled in Fig. 4.2. Figure 4.2



**LEGEND:**

- D Downward Loading
- Up Uplift Loading
- Lat Lateral Loading
- Uninstrumented Pile
- Instrumented Pile
- ↔ Lateral Load.

Fig. 4.2. Arrangement of Test Piles and Type of Test

also shows the sequential test number and the type of test performed. The axial loading tests, both upward and downward, were carried out on vertical piles. The lateral loading tests were performed not only on the vertical but also on the in-batter and out-batter piles. The batter piles have either 1 to 6 batter or 1 to 12 batter.

All the piles in the two foundations, designated Cap 1 and Cap 2 in Fig. 4.2, were designed to have fixed connections with the pile cap. To insure the fixed connection the pile head was clamped by a pair of steel angles welded on the side of a heavy steel channel which composes the pile cap. The gap between the pile and the steel angles was filled with epoxy resin. The rigid pile cap weighed about 500 pounds.

#### Measurement

Measurement of the displacement was done by dial gages. The measurement of the axial and bending strains in the pile was made by metal foil strain gages.

Detailed description of the instrumentation of the metal foil strain gages is given by Parker and Reese (1970).

The principle of computing the two-dimensional displacement of any arbitrary reference point of pile cap from the dial gage readings is given in Appendix D.

#### Sand

A sand was preferred to a clay as a test material because of the controllability and the reproducibility of the state of sand.

The state of sand was made as dense as possible, following the modeling law given by Shinohara and Kubo. The sand was fully submerged,

because the test setup did not allow for keeping the sand always dry. The standard method of placing sand is described by Parker and Reese (1970).

All the piles were installed and held at the scheduled positions when the sand fill reached a thickness of 2.5 feet. Thereafter, the compaction was done around the embedded piles for the remaining sand layer of eight feet in thickness.

The sand is classified as subangular to slightly subrounded, poorly graded, fine sand. The general properties of the sand are listed in Table 4.1.

TABLE 4.1 PROPERTIES OF SAND	
Effective Size $D_{10}$ . . . . .	.0.08-0.09 mm
Uniformity Coefficient. . . . .	2.4
Specific Gravity $G_s$ . . . . .	2.679
Minimum Density $\gamma_{min}$ . . . . .	1.32 g/cm <sup>3</sup> (82.4 pcf)
Maximum Density $\gamma_{max}$ . . . . .	1.64 g/cm <sup>3</sup> (102.3 pcf)

The in situ density of sand was uniform throughout the layer and remained constant through the test period. The dry density of the sand before the test was 100 pcf. After the test period, the average density was 101 pcf.

The angle of internal friction of the sand  $\phi$  was measured, using air-dried samples and also using undisturbed samples taken from the tank five months after the beginning of the test. Direct shear tests and tri-axial compression tests were performed on the air-dried samples of various

densities (Fig. 4.3 and 4.4). Both types of tests gave an angle of internal friction  $\phi$  of  $41^\circ$  for the sand at a density of 100 pcf. Ten undisturbed samples in a submerged state were tested in a triaxial compression device, using varying confining pressures and back pressures.

Figure 4.5 displays the test results. In Fig. 4.5  $\sigma_1$  is the axial compression in psi and  $\sigma_3$  is the confining pressure in psi. If no cohesion is assumed for the sand, the mean angle of internal friction is computed as  $47^\circ$ .

There is a considerable difference in the measurement of  $\phi$  between the air-dried samples and the undisturbed specimens. The problem of in situ strength of the sand will be discussed later in the analysis of single piles.

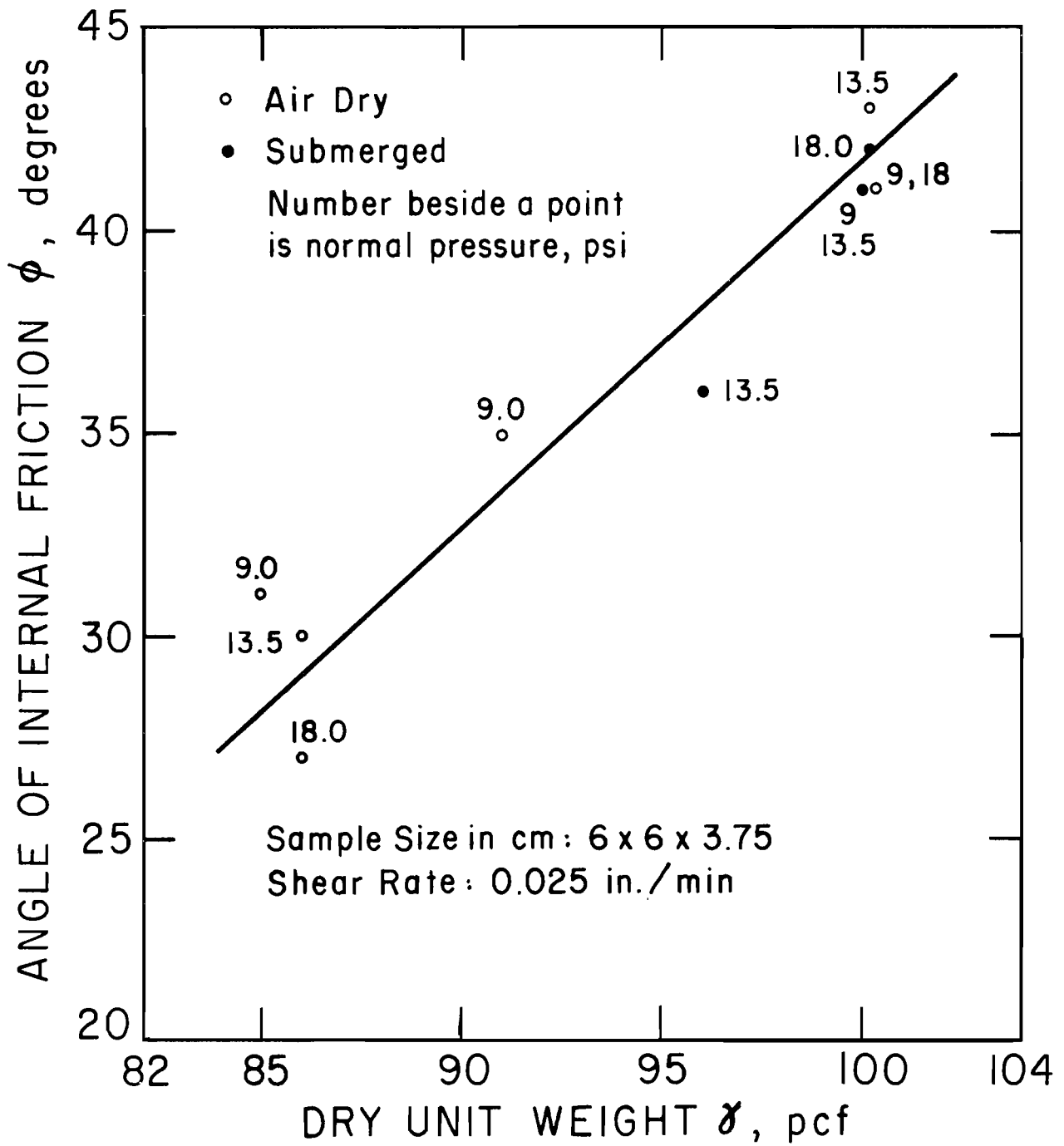


Fig. 4.3. Direct Shear Test

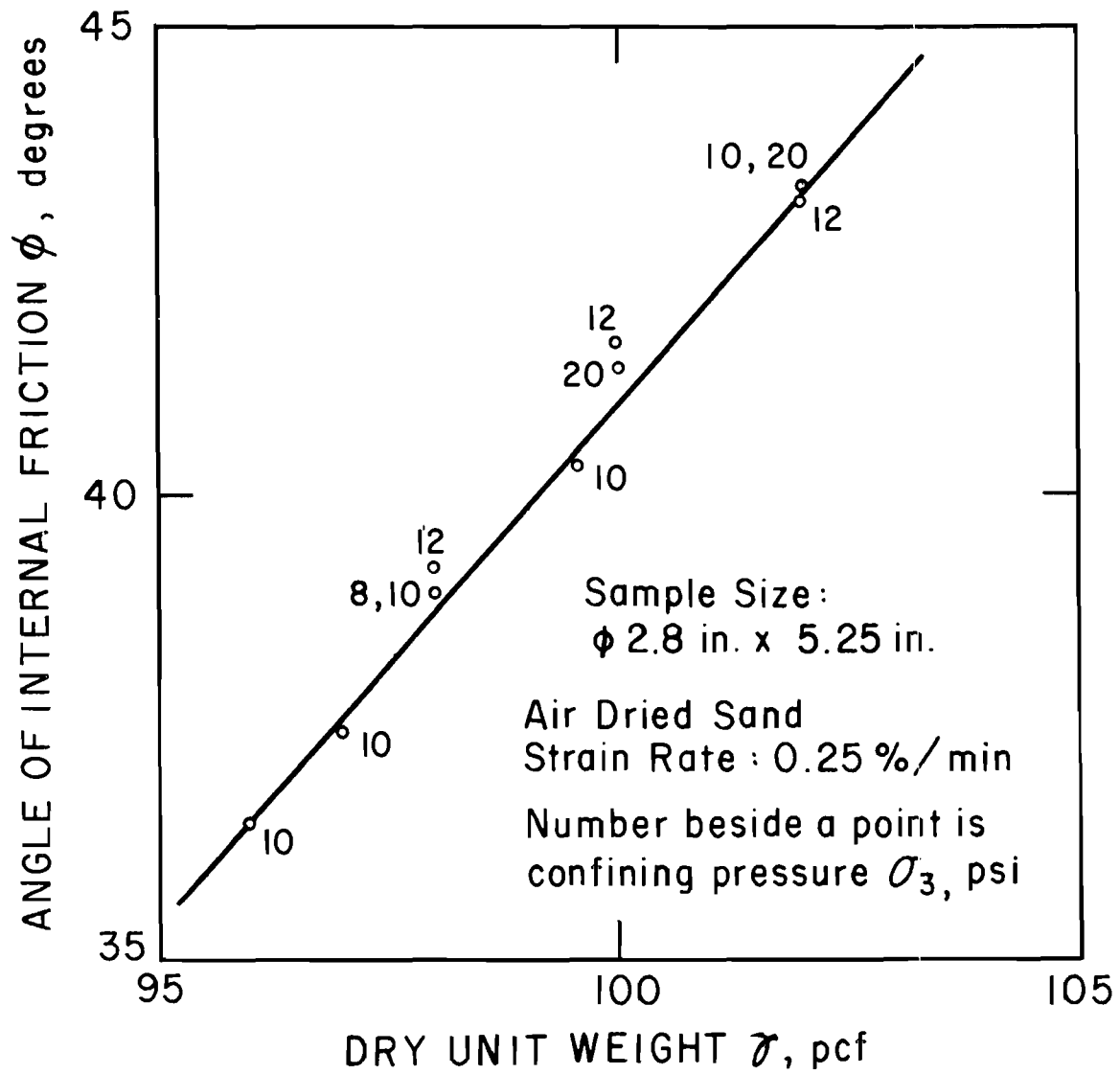


Fig. 4.4. Triaxial Compression Test

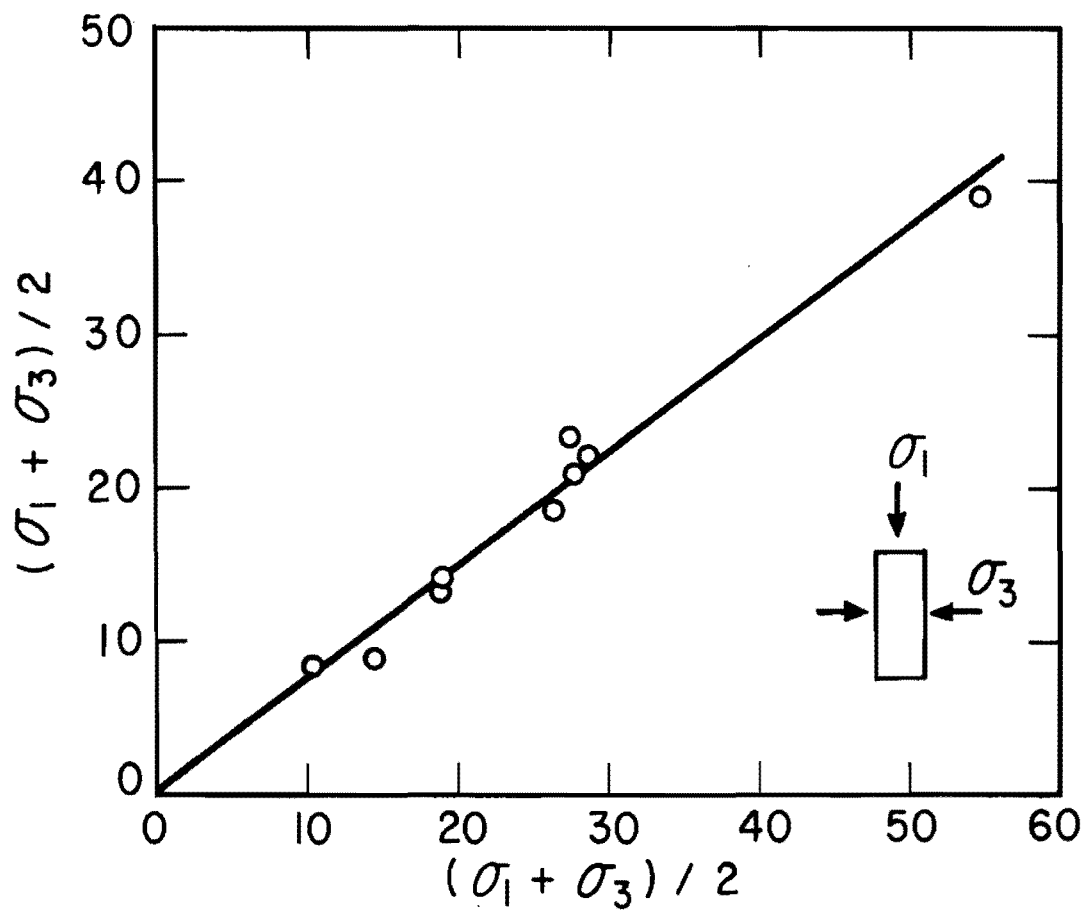


Fig. 4.5. Triaxial Compression Test on Undisturbed Specimens



This page replaces an intentionally blank page in the original.

-- CTR Library Digitization Team

## CHAPTER V

### ANALYSIS OF EXPERIMENTS ON SINGLE PILES

Two kinds of experiments were performed on single piles, axial loading and lateral loading. Axial loading tests were performed only on vertical piles, with the load being applied both downward and upward. Lateral loading tests were performed on vertical, in-batter and out-batter piles. The axial behavior and the lateral behavior of a pile are treated independently according to one of the basic assumptions that there is no interaction between these two types of behavior.

#### Axially Loaded Pile

In the analysis of grouped pile foundations, it is only necessary to have curves giving the axial load versus the displacement of the top of the pile.

The first portion of this section is devoted to a study of load displacement curves to find representative curves for the analysis of grouped pile foundation. In the latter half of this section, an analysis is made to explain the considerable influence on load displacement curves of load transfer along the sides of the pile.

Parker and Reese (1970) established an empirical correlation between load transfer curves for the test piles and stress-strain curves from triaxial compression tests.

#### Axial Load Versus Pile-Top Displacement

The test piles were usually loaded in increments, with a constant load being held until the movement of the top of the pile had stabilized.

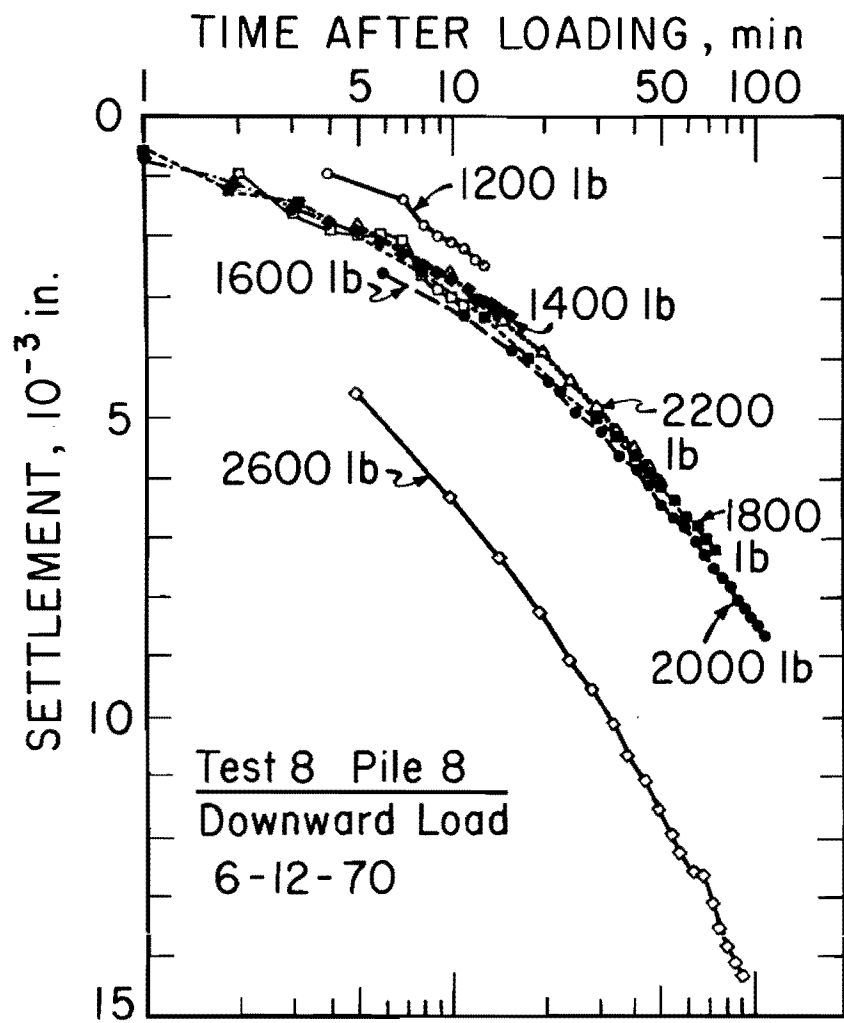


Fig. 5.1. Time versus Pile-Top Settlement

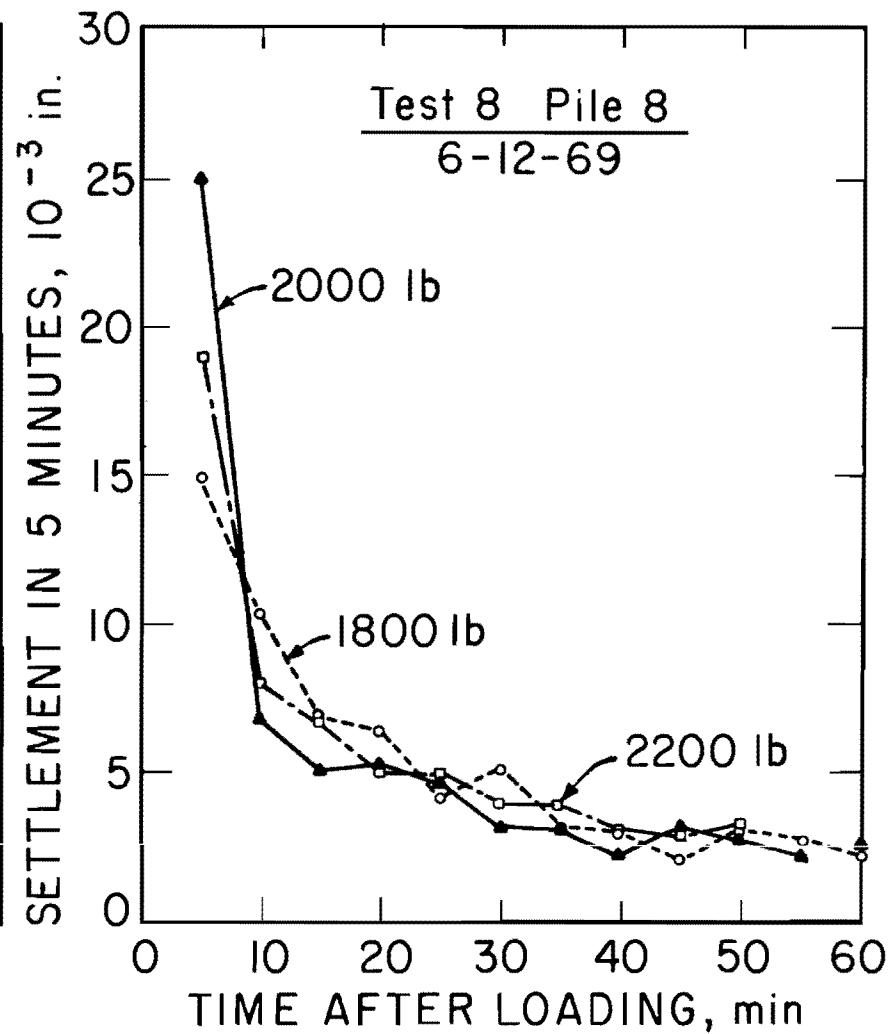


Fig. 5.2. Time versus Pile-Top Settlement

In some instances the load was increased continuously until failure by plunging of the pile. In another instance the load was increased cyclically.

Figure 5.1 is a semi-logarithmic plot of an example time-settlement relationship for incremental loading. The plot shows that, for the larger loads, settlement continues with time. Figure 5.2 is a plot in the normal scale of the pile-top movement for every five minutes, showing that, after about 30 minutes, the rate of pile-top displacement drops sharply to the level of about  $5 \times 10^{-4}$  inch per five minutes. A pile was regarded as stable when the rate of movement dropped to this level.

Figures 5.3 through 5.8 show plots of the axial load versus pile-top displacement for each of the axially loaded piles. The downward-loading curve is plotted in the fourth quadrant in accordance with the usual sign convention. The upward-loading curve is plotted in the second quadrant to be consistent with the former. This rule of plotting is kept for the rest of the analysis.

Examination of these curves for axial load versus pile-top displacement reveals some of the characteristics of the axial behavior of the pile.

1. There is a marked difference between the virgin loading curve and the subsequent loading curves. Tests 5, 6, and 7 in Fig. 5.5 show that the ultimate uplift resistance is one-half of that for the virgin loading. Test 2 (Fig. 5.3), Test 4 (Fig. 5.4), Test 8 (Fig. 5.5), Test 18 (loop landings) Fig. 5.6b) and Test 16 (Fig. 5.7b) show that if a pile is failed once, the ultimate

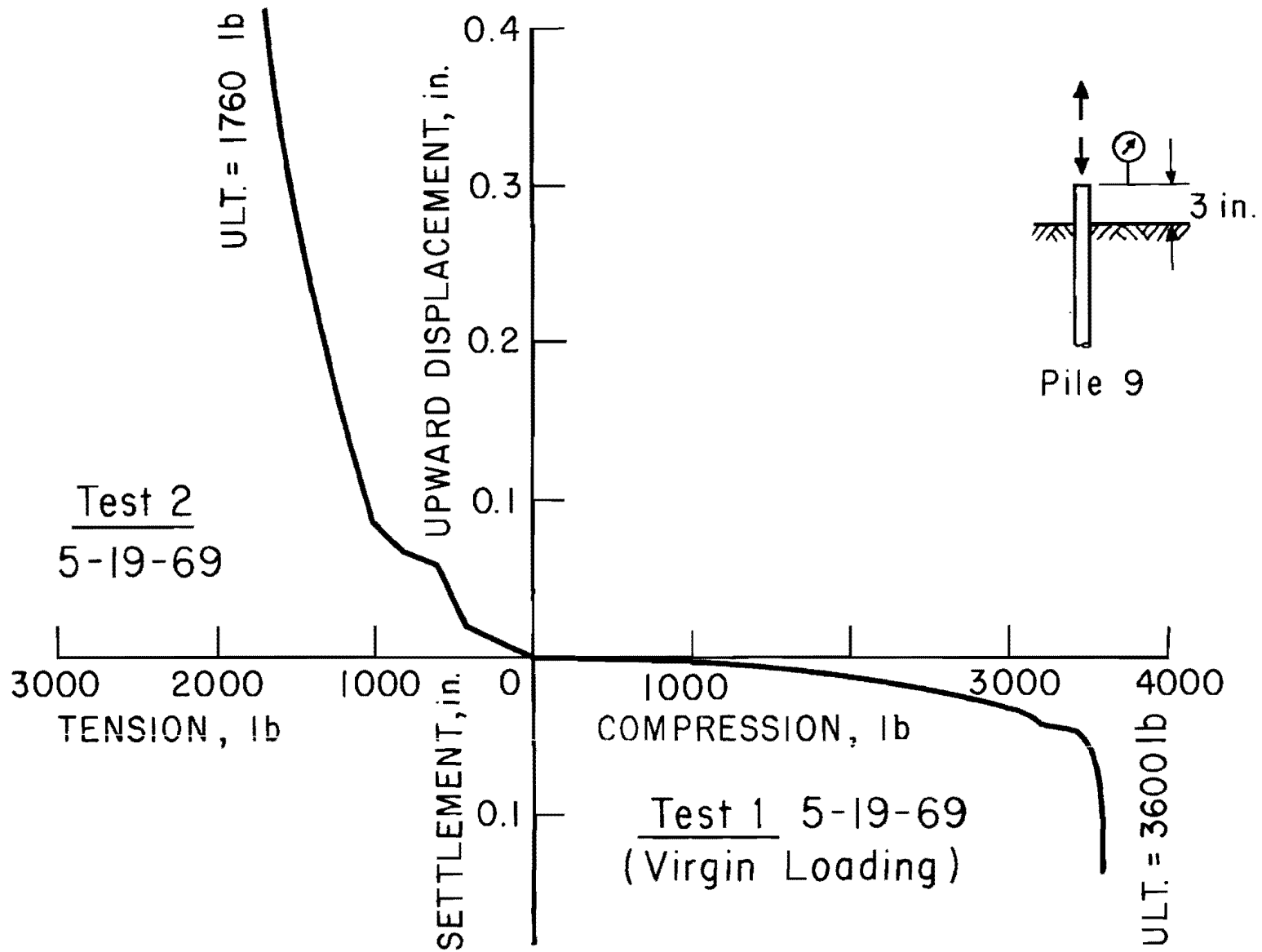


Fig. 5.3. Axial Load versus Pile-Top Displacement

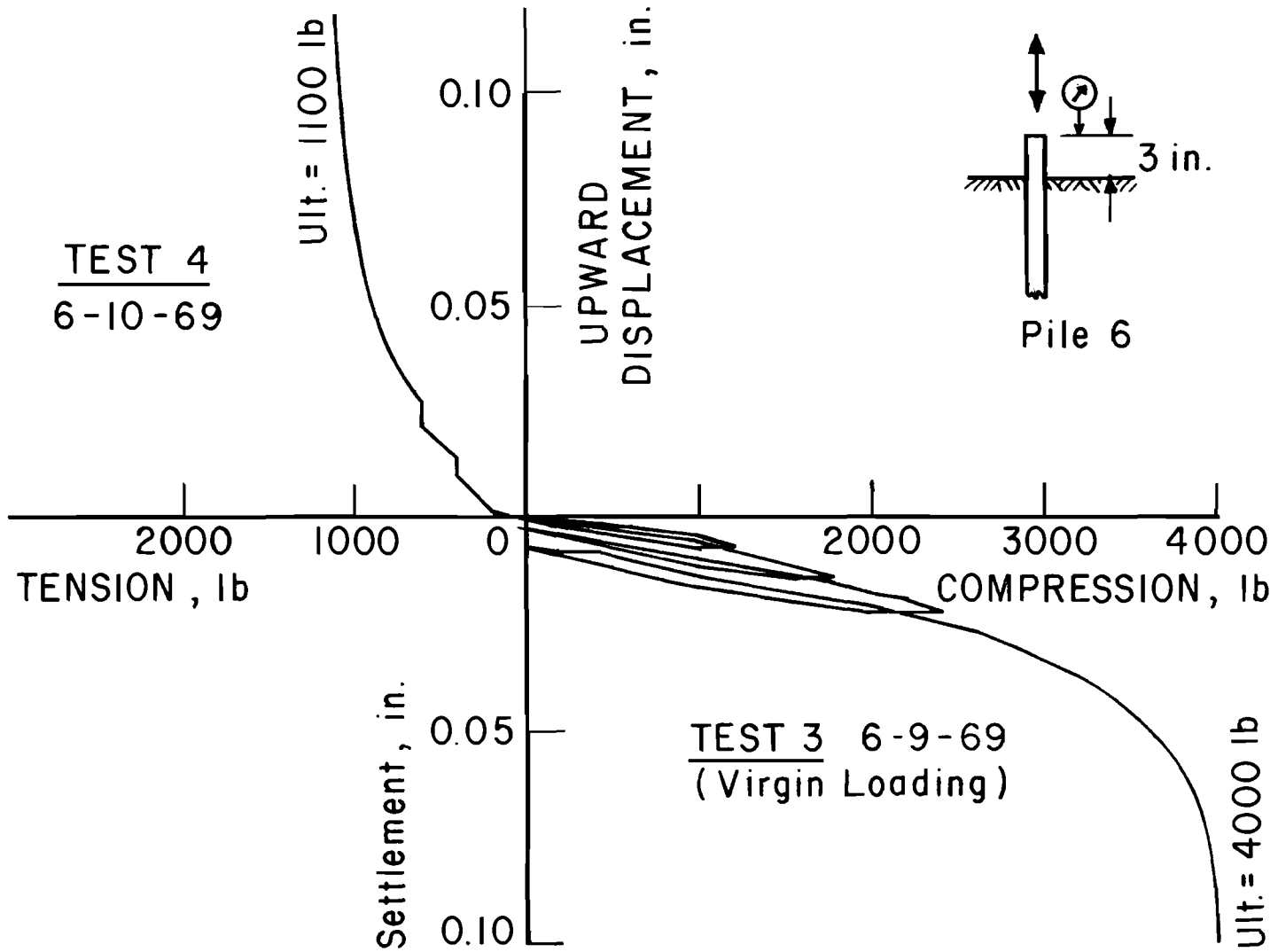


Fig. 5.4. Axial Load versus Pile-Top Displacement

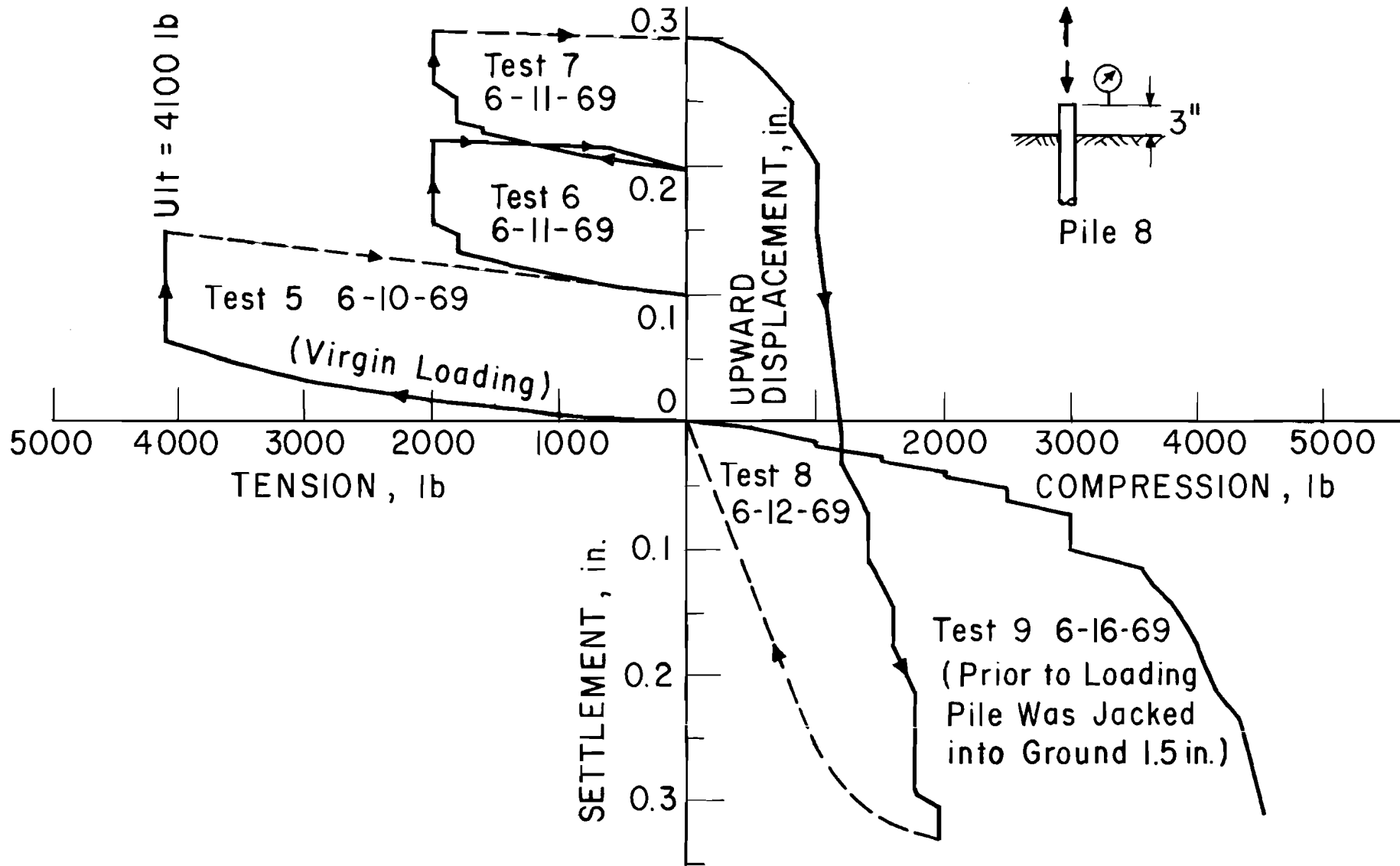
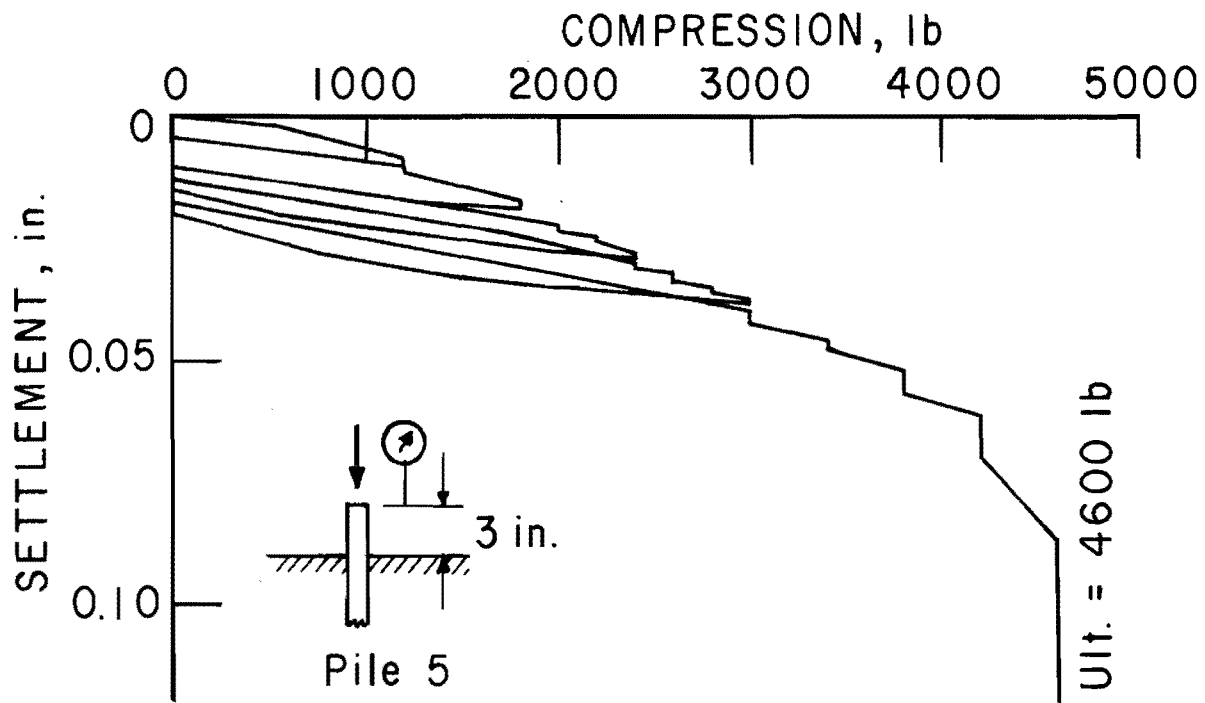
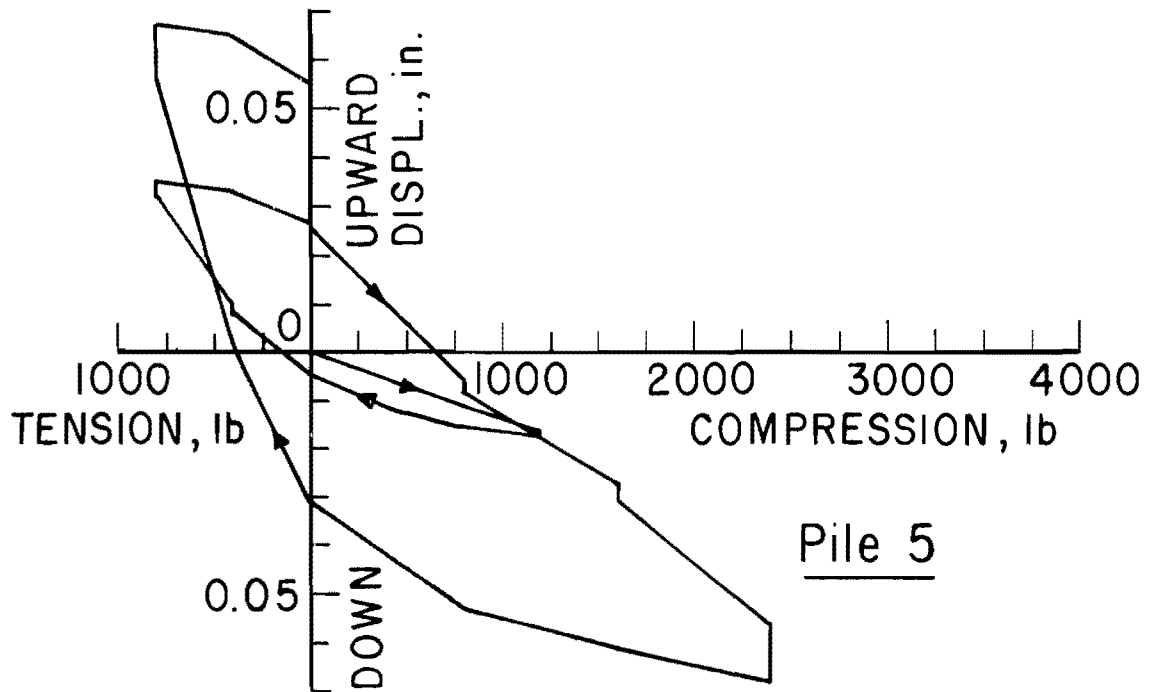


Fig. 5.5. Axial Load versus Pile-Top Displacement



(a) Test 10 6-20,24,25-69 (Virgin Loading)



(b) Test 18 7-15,22-69 (Loop Loading)

Fig. 5.6. Axial Load versus Pile-Top Displacement



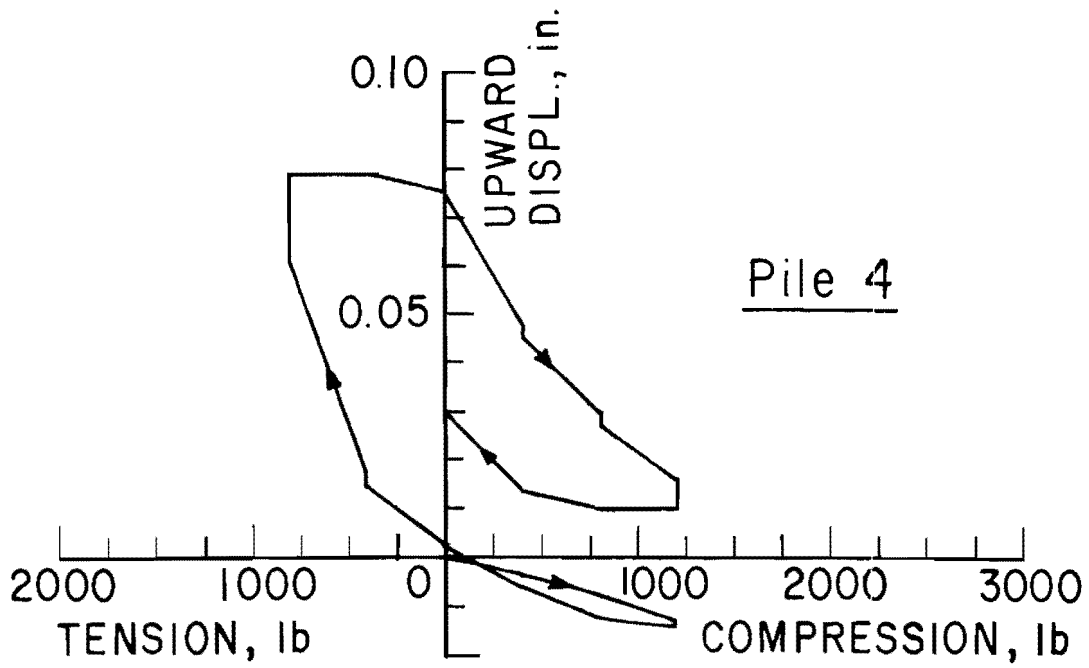
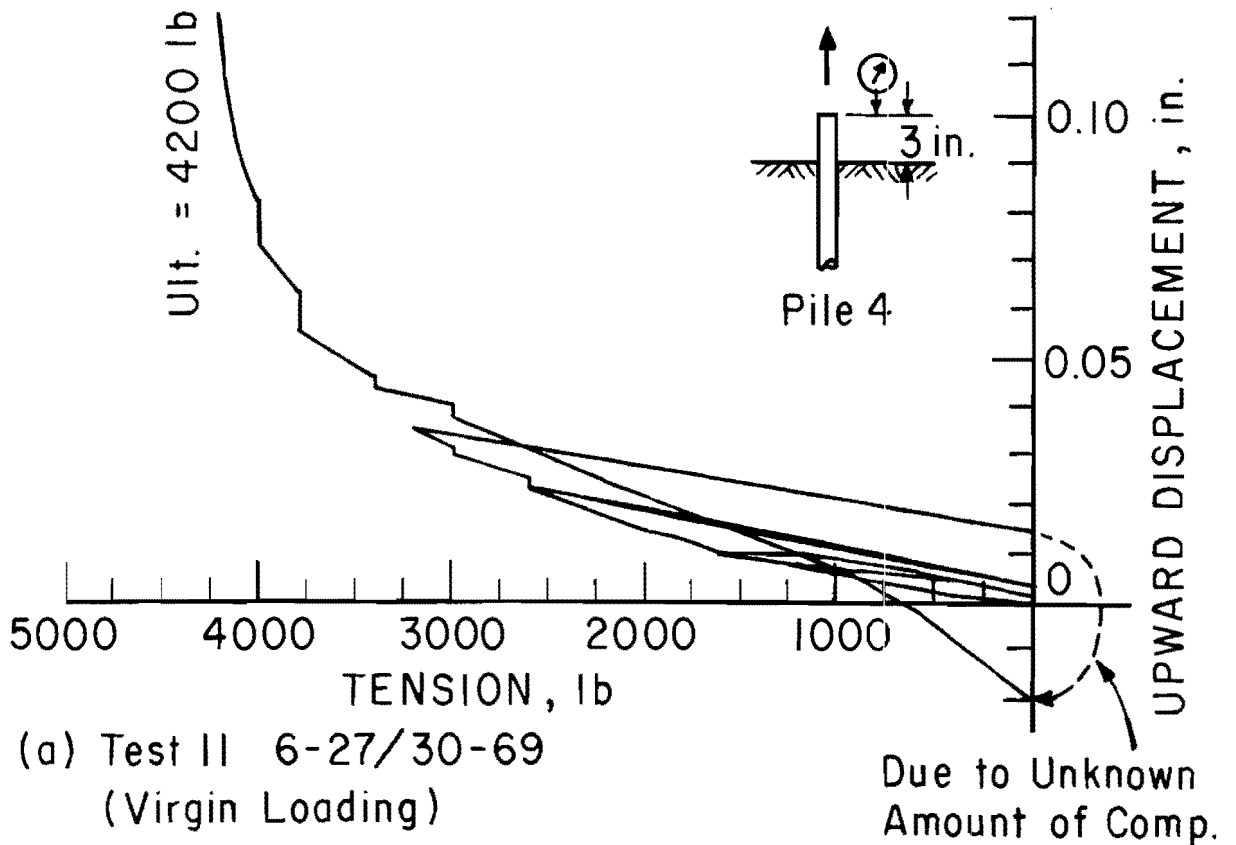


Fig. 5.7. Axial Load versus Pile-Top Displacement

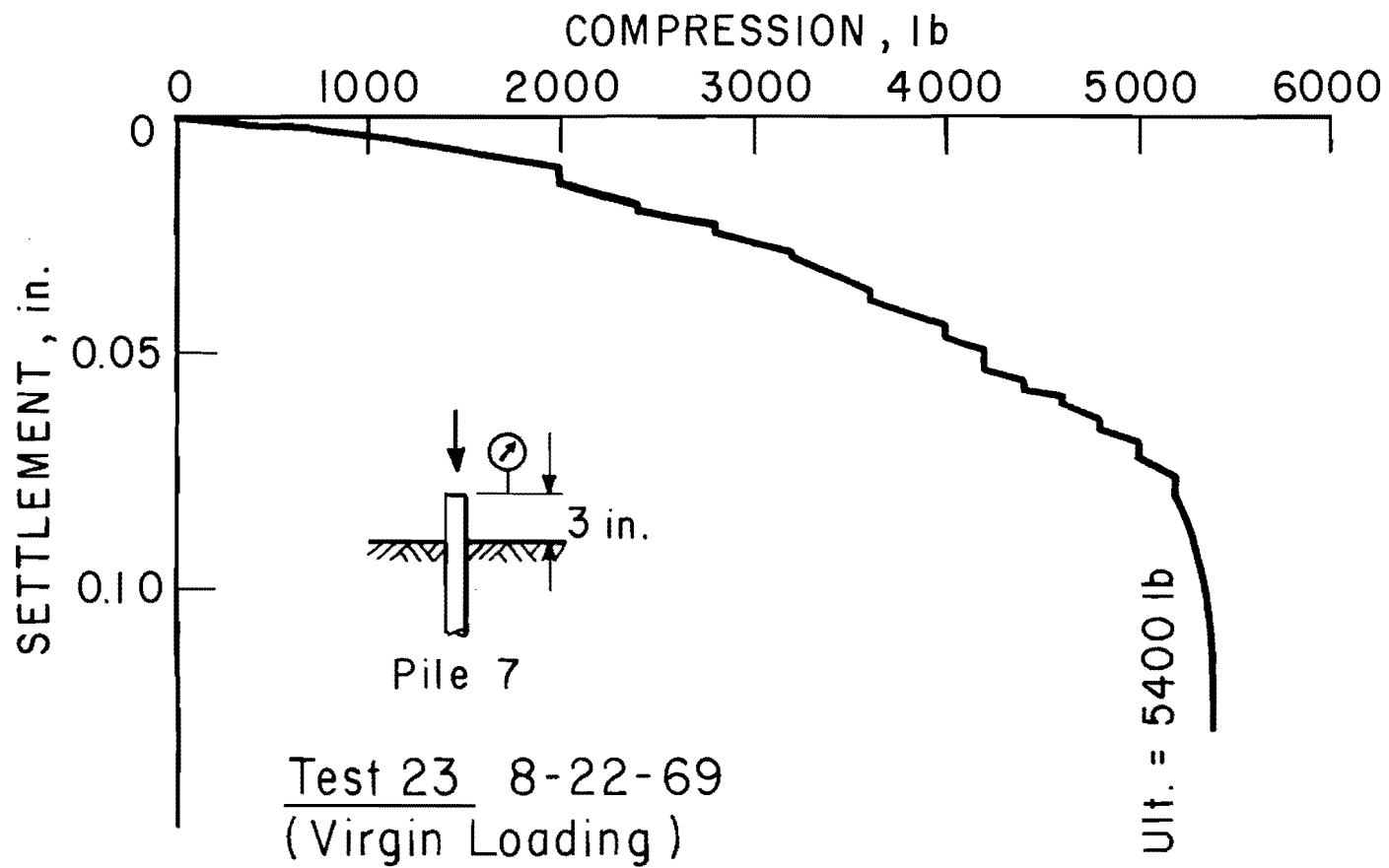


Fig. 5.8. Axial Load versus Pile-Top Displacement

bearing capacity in the reversed direction of loading is reduced to less than one-half the original value, and the rate of displacement becomes far greater than for the first loading. Test 9 (Fig. 5.5) indicates that downward ultimate bearing capacity is restored by jacking the pile 1.5 inches in the ground, but the rate of displacement is much greater than for the virgin loading.

2. The envelope of the cyclic virgin loading curve, such as Test 3 (Fig. 5.4), Test 10 (Fig. 5.6a), or Test 11 (Fig. 5.7a), is similar to the virgin loading curve of Test 1 (Fig. 5.3), Test 5 (Fig. 5.5), or Test 23 (Fig. 5.8) in which the load was increased continuously.
3. Comparison of the virgin downward-loading curves of Test 1 (Fig. 5.3), Test 3 (Fig. 5.4), Test 10 (Fig. 5.6a), and Test 23 (Fig. 5.8) with those of the virgin upward loadings, Test 5 (Fig. 5.5) and Test 11 (Fig. 5.6a) show that both of them are similar in their shapes.
4. The ultimate resistance of the pile increased with the passage of time. Figure 5.9 shows the plotting of the ultimate resistance of the bearing and uplift piles. It shows that the ultimate pile resistance increased 50 per cent in the time span of 3 months over the first test which was conducted soon after sand placement.

These observations on axial pile behavior stress the importance of awareness of loading history and the time of testing in applying the test results to the analysis of grouped pile foundations.

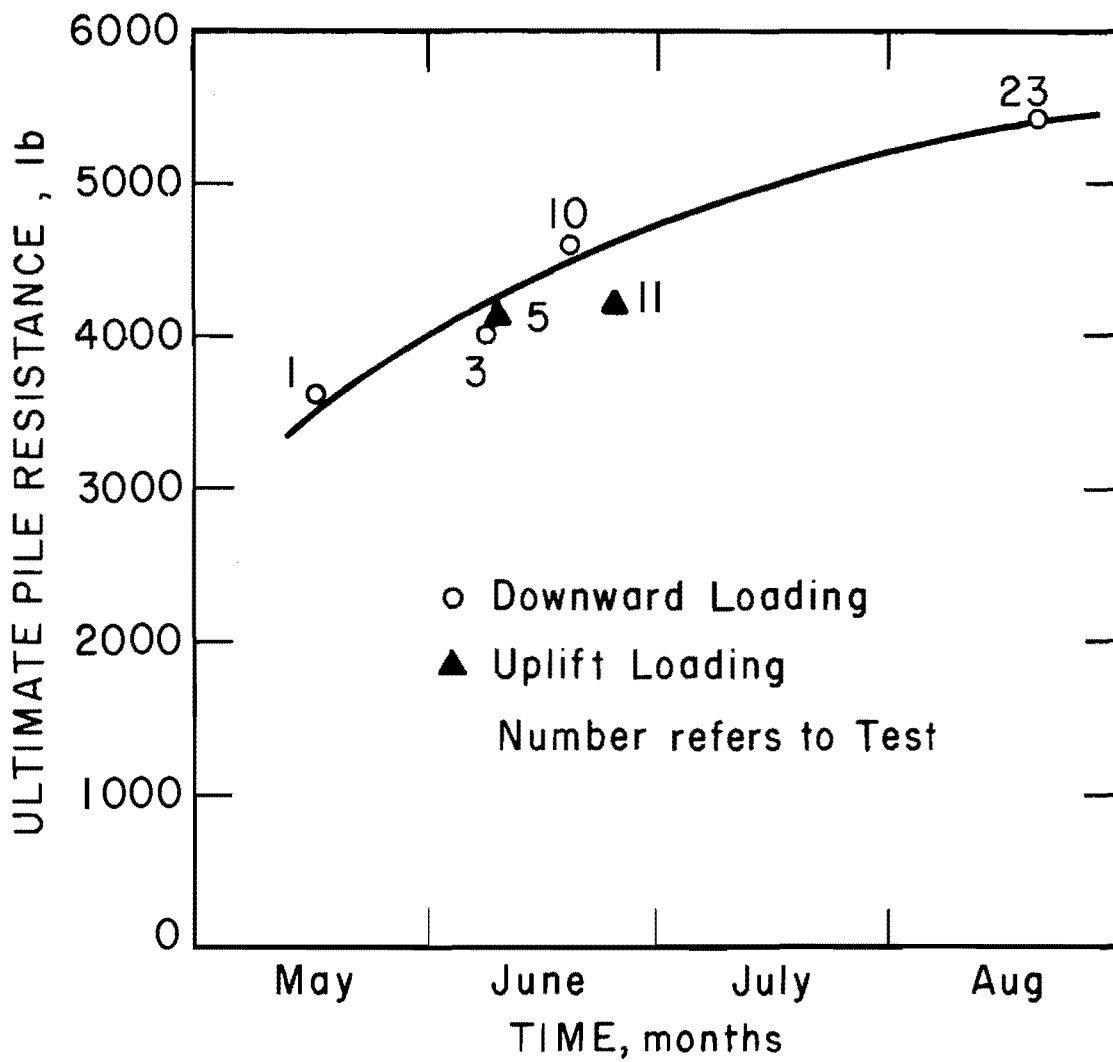


Fig. 5.9. Ultimate Axial Pile Resistance

### Load Transfer

Experimental Load Transfer and Point Resistance. Experimental load transfer curves are obtainable from axial forces computed from the measurement of axial strains along the pile by strain gages and from axial pile displacement obtained by the integration of the axial strain. Figure 5.10 illustrates a typical example of axial force computation at five gage locations. The solid lines in Fig. 5.10 show results obtained from loading measurements, and the broken lines show those from unloading measurements. The locked-in axial force in the pile after the removal of load, which was common throughout the experiments, is illustrated in Fig. 5.10.

Figures 5.11 and 5.12 are the load transfer curves computed by Parker and Reese (1970) for a bearing pile and for an uplift pile, respectively. The load transfer curves are developed at the five locations of the strain gages.

The point resistance is the unit vertical soil resistance on the base of the pile as a function of the settlement of the pile tip. Since no direct measurement of the point resistance was made, a point resistance curve can only be obtained by extrapolating the experimental axial force distribution curves.

The linear extrapolation of the bottom two measurements of the axial force gives a maximum point resistance of only about 160 pounds. The distance between the bottom strain gage and the tip of the pile was 12 inches or 6 times the pile diameter. The accuracy of the extrapolated

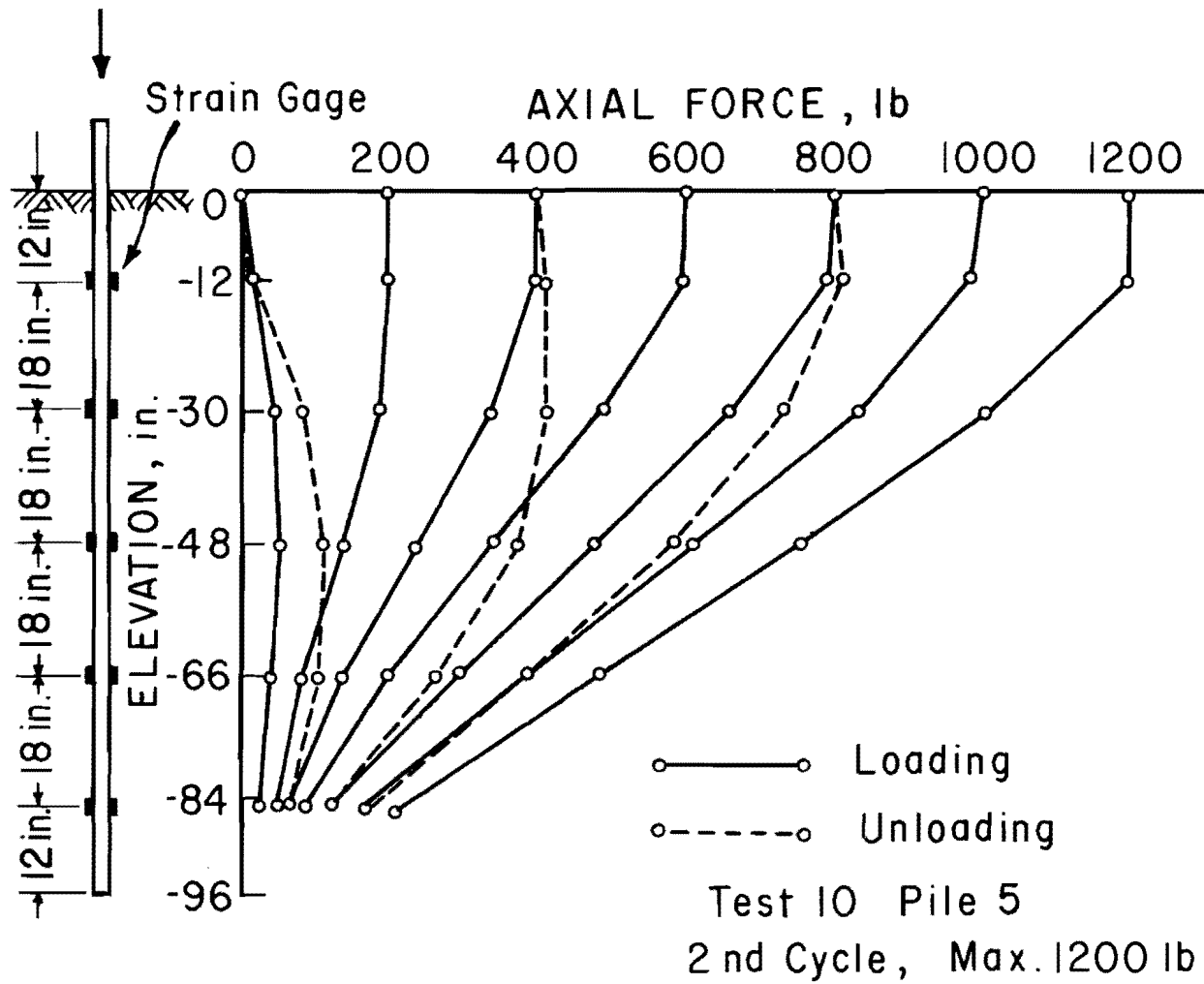
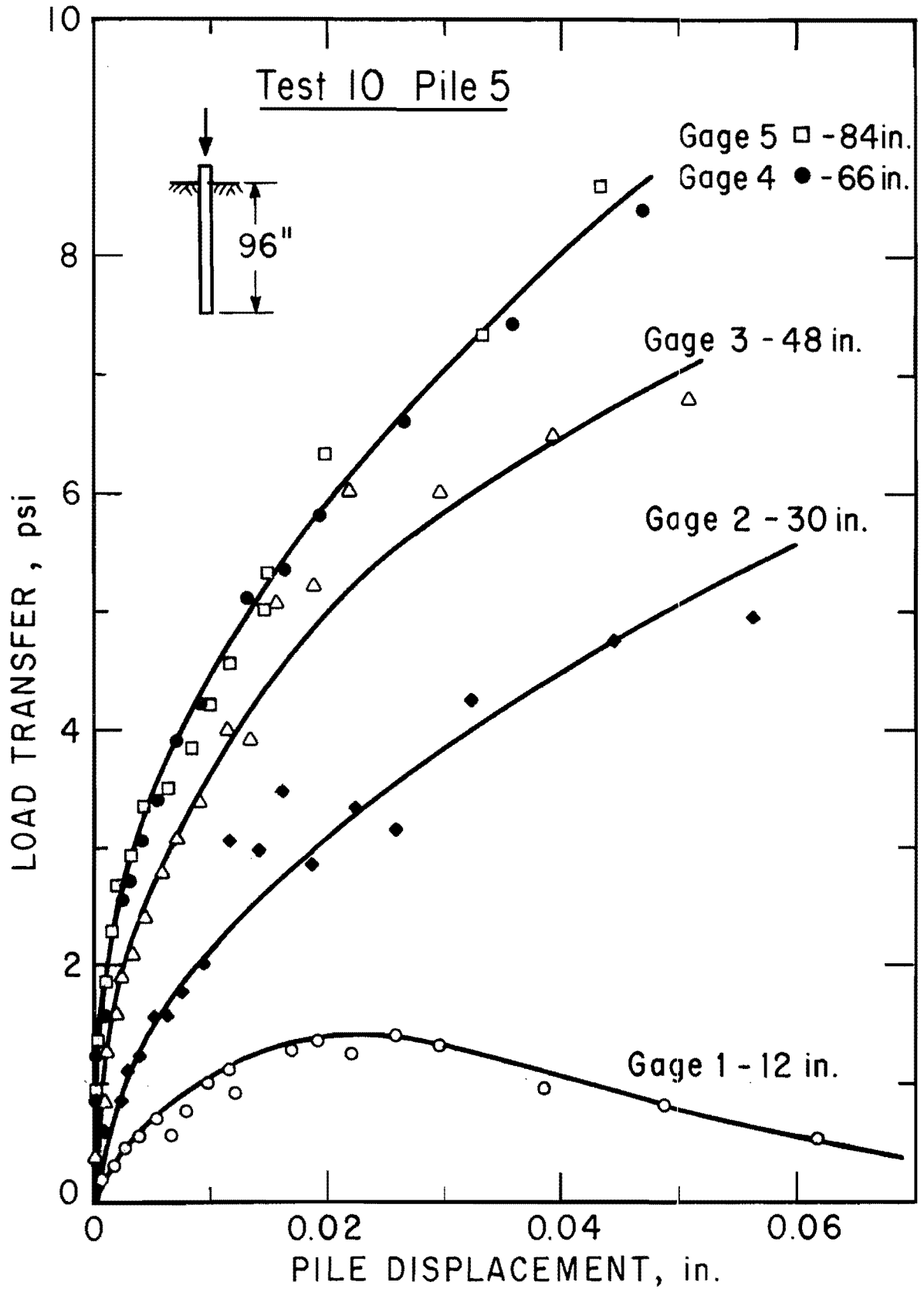


Fig. 5.10. Typical Axial Force Distribution



(after Parker and Reese)

Fig. 5.11. Load Transfer Curves of a Bearing Pile

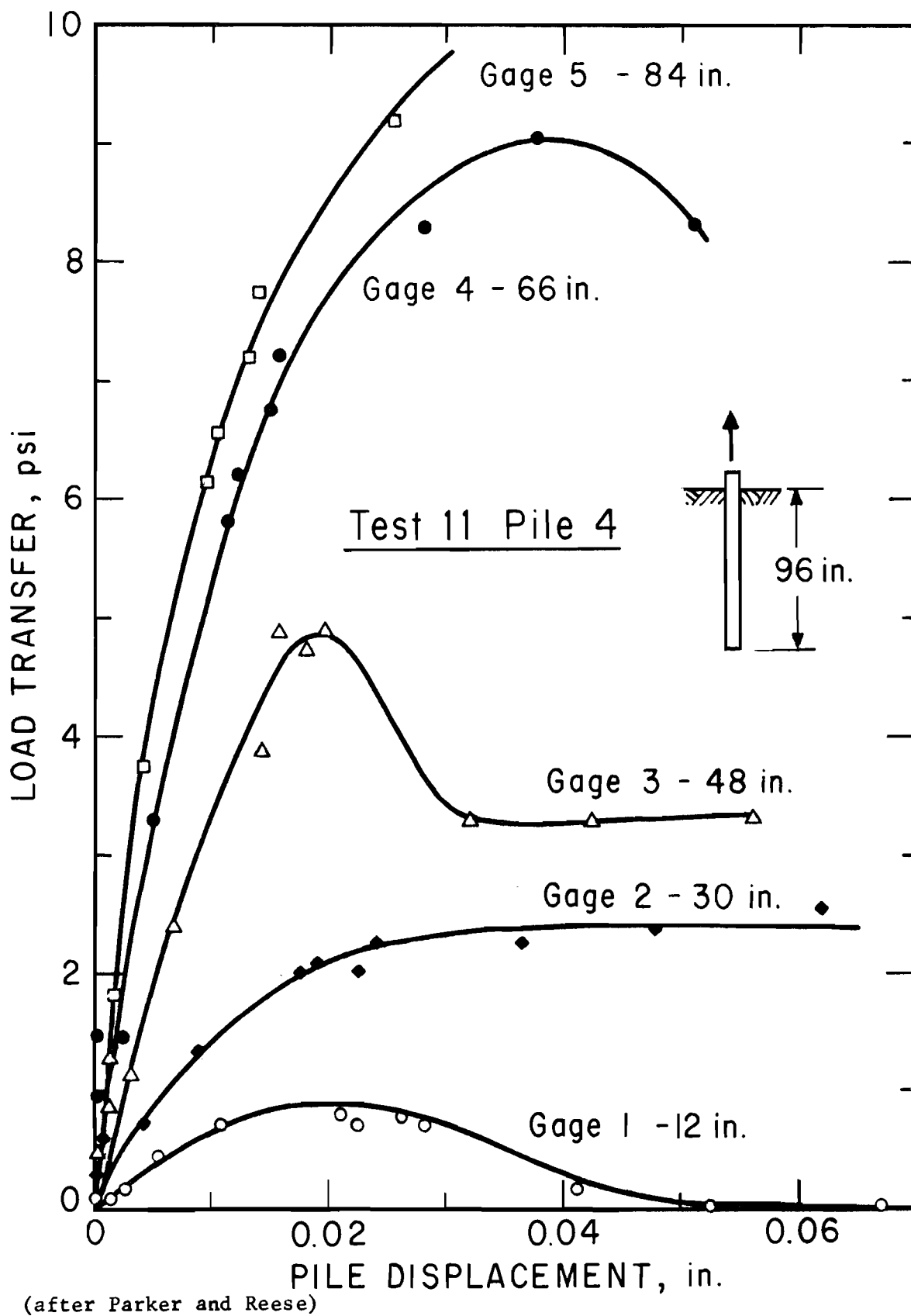


Fig. 5.12. Load Transfer Curves of an Uplift Pile



value of the point resistance may be somewhat questionable, but it can be said with certainty that the point resistance accounts for a quite small share of the total axial pile resistance.

Figures 5.13 and 5.14 compare the actual top displacement with the theoretical predictions made from the experimental load transfer curves (Figs. 5.11 and 5.12) and the assumption of no point resistance. The discrepancy between the experimental curve and the theoretical prediction may be attributed to the following reasons. First, there are inevitable experimental errors in the measurement in the axial force. Secondly, the number of gage locations were so few that errors were introduced in the numerical integration of axial strain. The comparison is also indicative of the sensitivity of the prediction of pile-top displacement to the accuracy of the load transfer curves.

Analysis of Load Transfer. The maximum value of the load transfer on a pile in a cohesionless soil is assumed to be expressed by a linear function of depth (Eq. 5.1)

$$T = K_o \gamma x \tan \delta \ell \dots \dots \dots (5.1)$$

where

- T = total load transfer in pounds per unit length of pile,
- $K_o$  = nondimensional coefficient of earth pressure on the side of a pile whose value lies somewhere between the active earth pressure coefficient  $K_A$  and the passive earth pressure  $K_p$  ,
- $\gamma$  = effective unit weight of sand in pcf,

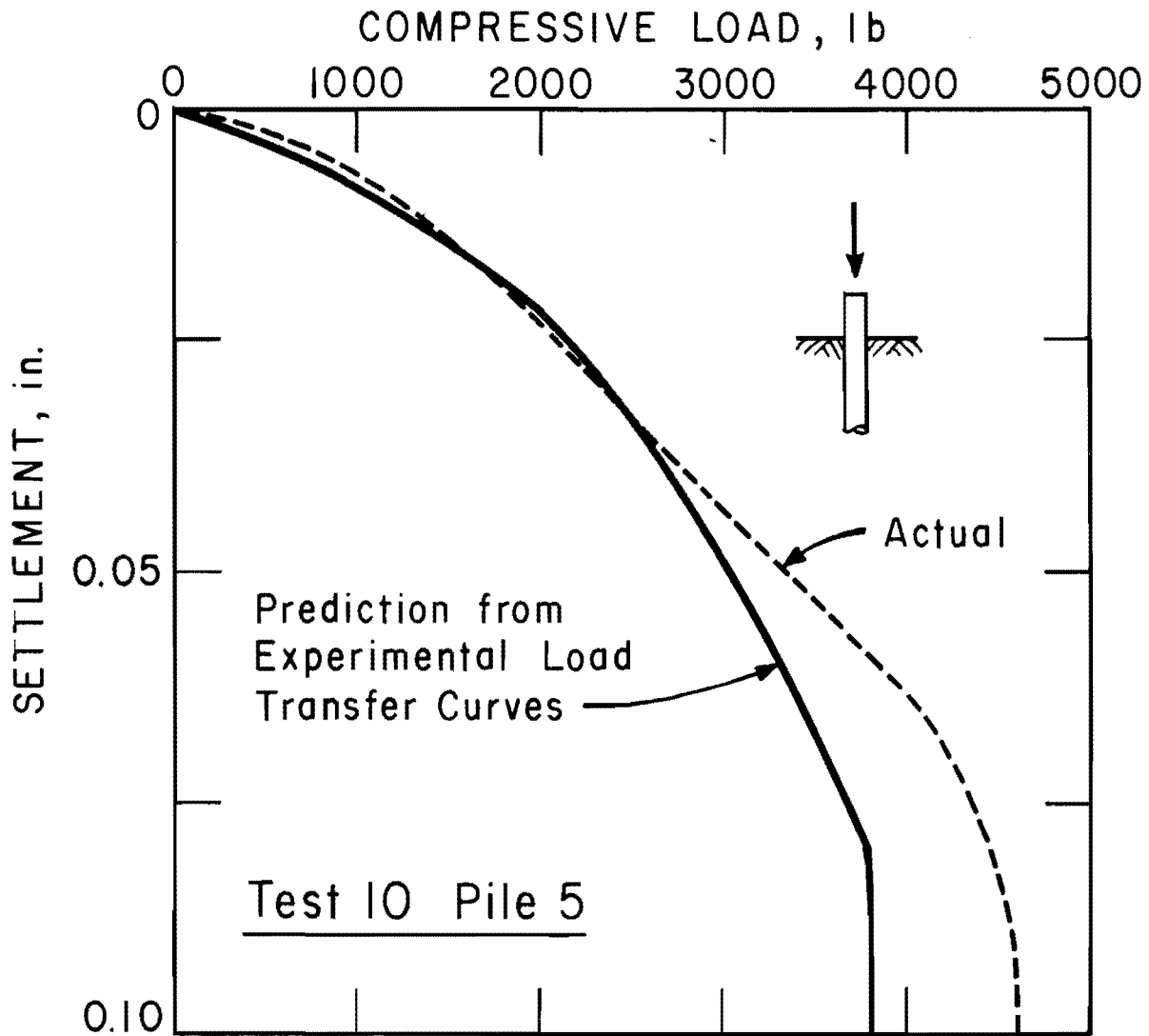


Fig. 5.13. Prediction of Load-Displacement Curve from Experimental Load Transfer Curves, Uplift Pile

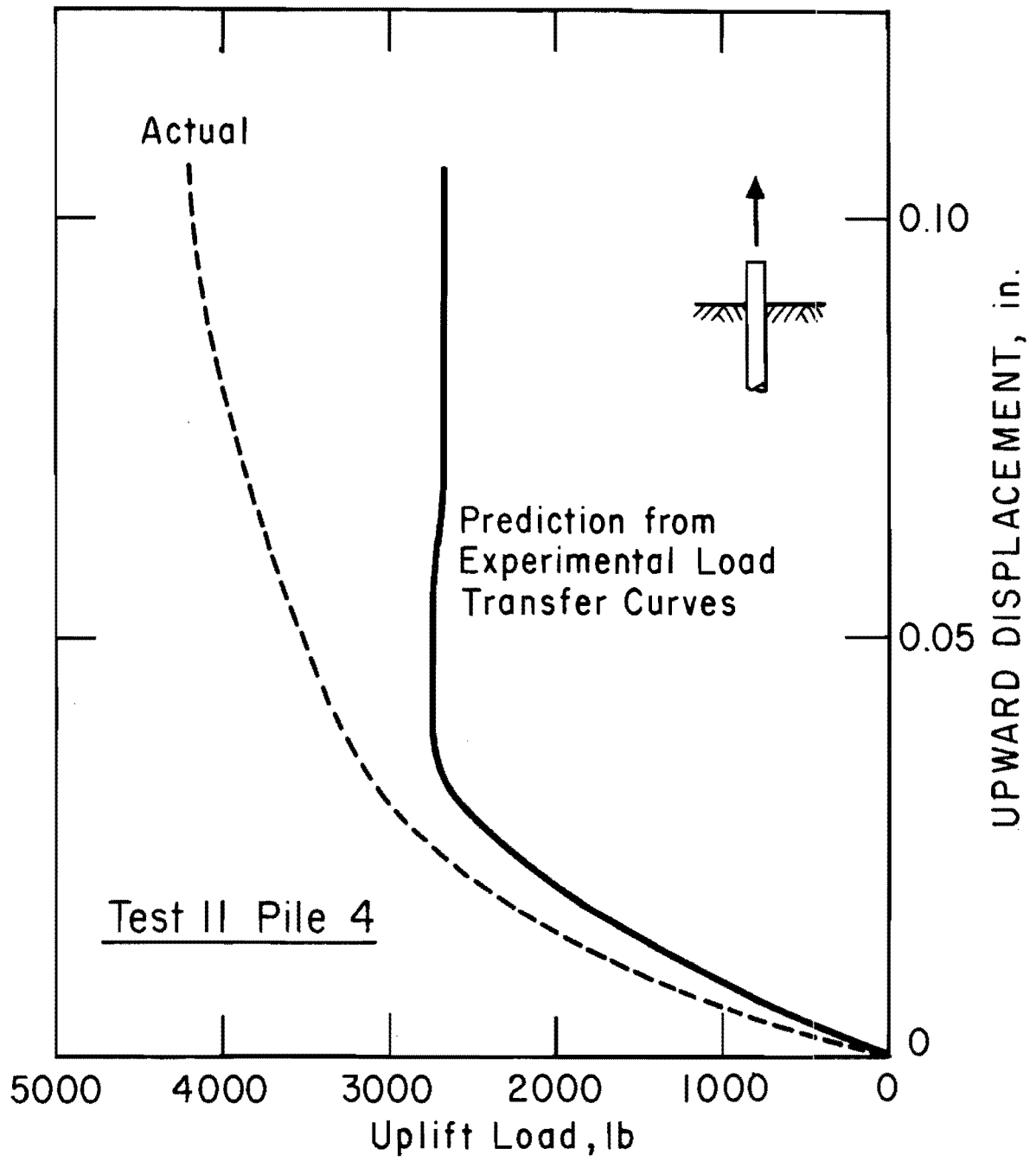


Fig. 5.14. Prediction of Load-Displacement Curve from Experimental Load-Transfer Curves, Uplift Pile

$x$  = depth from ground surface in feet,  
 $\delta$  = friction angle between the sand and the pile wall whose  
 value is greater than 0 but smaller than the angle of the  
 internal friction of the sand  $\phi$  ,  
 $l$  = circumference of the pile in feet.

In this case where point resistance is negligible, the ultimate bearing capacity of a pile in a sand is dependent on the relationship expressed by Eq. 5.1. The equation has two quantities, namely  $K_o$  and  $\delta$  . The maximum ultimate bearing capacity is computed by assuming the upper limit values for  $K_o$  and  $\delta$  . If the angle of internal friction of the sand is  $41^\circ$  as it was measured on air-dried samples, the maximum ultimate bearing capacity is 4,350 pounds. In this computation,  $K_o$  was taken as equal to  $K_p$  , with a numerical value of 4.8, and  $\delta$  was taken as equal to  $\phi$  , with a numerical value of  $41^\circ$ .

The actual loading tests gave ultimate bearing capacities ranging from 3,600 pounds at the beginning of the test period to 5,400 pounds at the end of the period (Fig. 5.9). The value of 5,400 pounds exceeds by about 25 per cent the value computed from Eq. 5.1.

One explanation for this lack of agreement is that the soil itself increased in strength and at the end of the test period had a strength greater than that for a  $\phi$  of  $41^\circ$ . The strength of a sand may be increased either by an increase in the angle of internal friction or by the development of cohesion due to chemical action. An increase in the angle of internal friction, however, is ruled out, because measurement of the in situ density of the sand was almost identical before and after

testing. It is thought that no appreciable cohesion developed in the sand, because examination of the sand at the end of the test period failed to reveal any substantial unconfined compressive strength.

Another explanation for the lack of agreement is that there was an increase in bond at the soil-pile interface. There is a strong possibility that the sand in the vicinity of the piles changed in properties because of corrosion of the pile material. The retraction of piles after the test program showed rusting on the walls of the piles. The piles had been sand blasted before installation. It was also observed that the sand in the vicinity of each pile had changed color to a dark gray. These observations give credence to the idea that chemical action produced a bonding at the pile-soil interface and perhaps also between soil grains in the vicinity of the pile wall. This hypothesis is supported by the fact that a great reduction in the axial pile resistance occurred as a result of the virgin loading. Therefore, the major factor contributing to the increase in the ultimate bearing capacity of the piles under axial load is thought to be the increased bond at the soil-pile interface.

The effect of the increase in the bond on the ultimate bearing capacity may be accounted for by an increase in the apparent angle of internal friction. If the apparent angle of internal friction is assumed to have increased to  $47^\circ$ , good agreement is obtained between the ultimate bearing capacity observed at the end of the test period and the ultimate bearing capacity computed from Eq. 5.1.

The discussions above conspicuously point out the difficulty of the theoretical determination of the ultimate pile resistance. The present state of the art is such that the ultimate resistance of a pile may only be approximated by theoretical computations.

### Conclusion

A series of axial loading tests on single piles revealed the characteristic behavior of axially loaded piles. This behavior is important in the analysis of the experiments on grouped pile foundations. Specific observations are:

1. The ultimate bearing capacity of the axially loaded piles in sand increased with the passage of time. This increase is probably due to the development of a chemical band at the pile-soil interface.
2. Each loading cycle leaves some permanent set.
3. The envelope of a load-displacement curve is smoothly curved. In each loading cycle except the first one, the early portion of the curve is almost straight until it touches the envelope.
4. If a pile is once failed, there is a drastic change in the behavior of the pile. Generally, the ultimate axial resistance is reduced and the rate of pile-top displacement is increased.
5. There is some variation in the virgin ultimate axial resistance of piles tested even with a short span of time.
6. The analytical method can describe only the limited aspect of the complex axial behavior of a pile.
7. More careful test planning is needed to determine the load

transfer and the point resistance in the test piles more accurately.

#### Laterally Loaded Pile

In the analysis of grouped pile foundations, it is necessary to have curves giving lateral pile-head deflection and the pile-head rotation as a function of pile-head loading. Such curves can be computed from the theory of the laterally loaded pile if curves are available for points along the pile giving soil resistance versus pile deflection (p-y curves). In the research study, p-y curves were obtained from results of experiments with instrumented laterally loaded piles. As discussed previously, other investigations have given recommendations for the theoretical development of p-y curves.

The analysis of laterally loaded single piles in the following compares the experimental pile behavior with the predictions made from the use of p-y curves derived from experiment and also with predictions made from theoretical p-y curves. The effect of batter on the lateral soil resistance curves is also included in the analysis.

#### Measurements of Displacement and Moment

All the lateral loading tests were performed in a period of a month at the later stage of testing.

Figures 5.15 through 5.20 show the lateral displacement and the slope of Pile 20, Pile 19, and Pile 18 measured at the point of horizontal load application, which is about eight inches above the ground surface. Pile 20 was vertical. Pile 19 and Pile 18 both had a 1 to 6

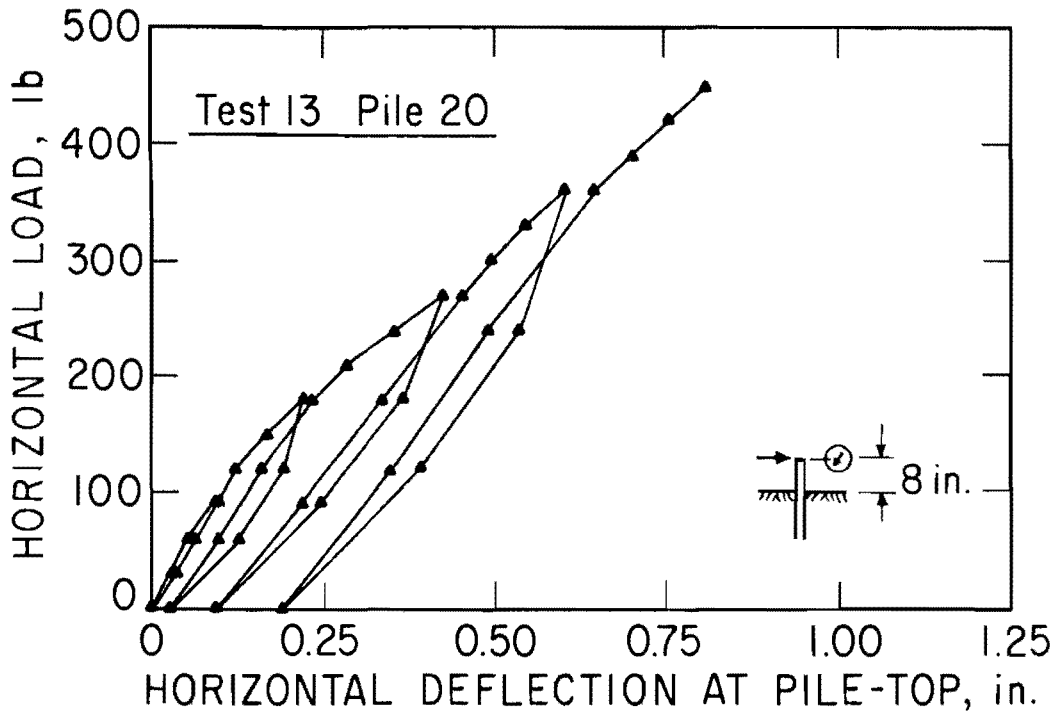


Fig. 5.15. Horizontal Load versus Pile-Top Deflection

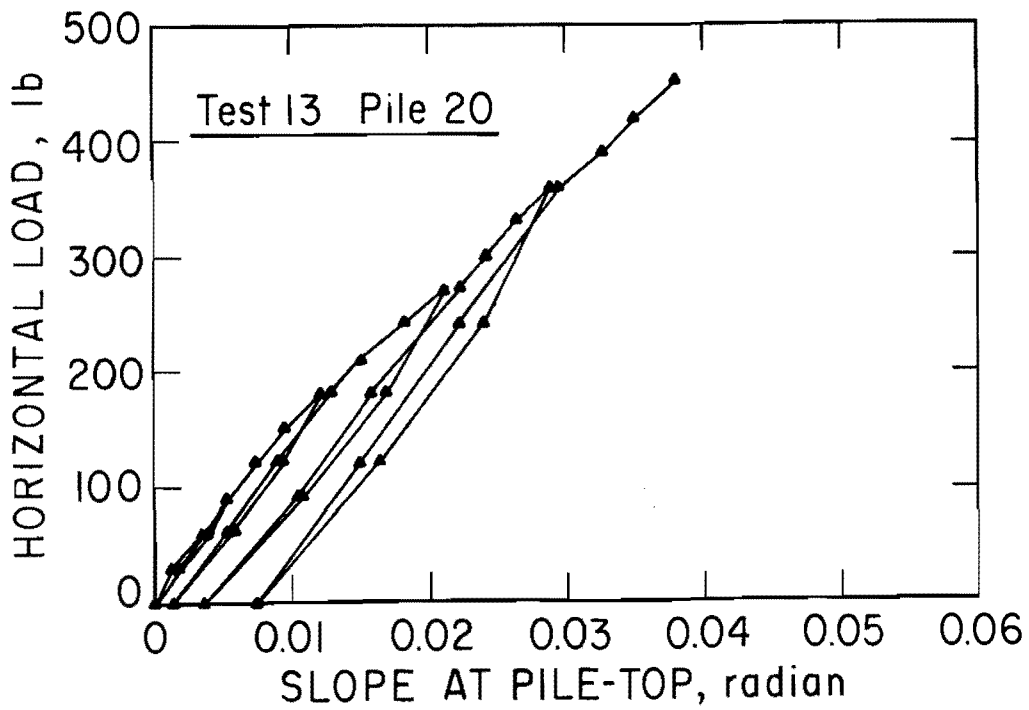


Fig. 5.16. Horizontal Load versus Pile-Top Slope



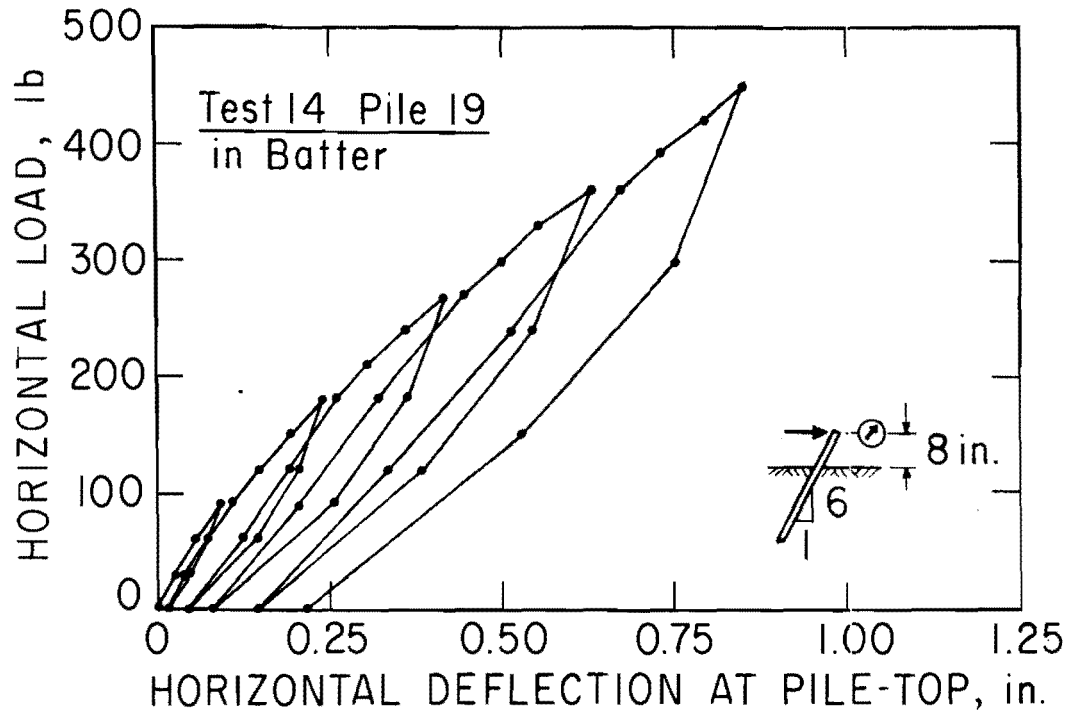


Fig. 5.17. Horizontal Load versus Pile-Top Deflection

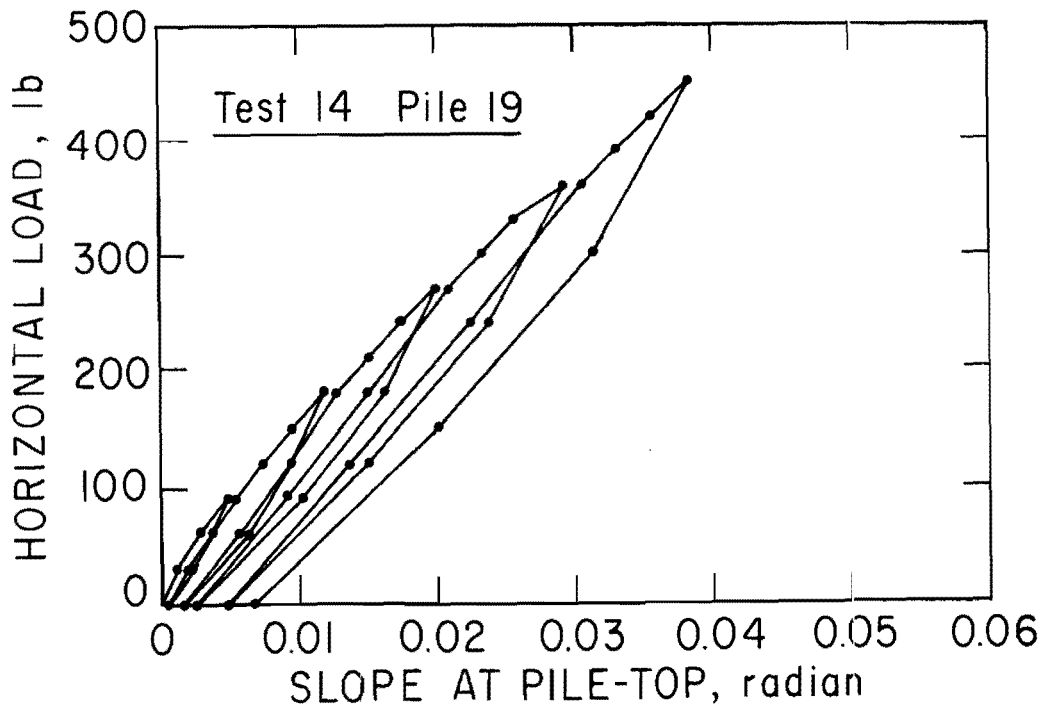


Fig. 5.18. Horizontal Load versus Pile-Top Slope

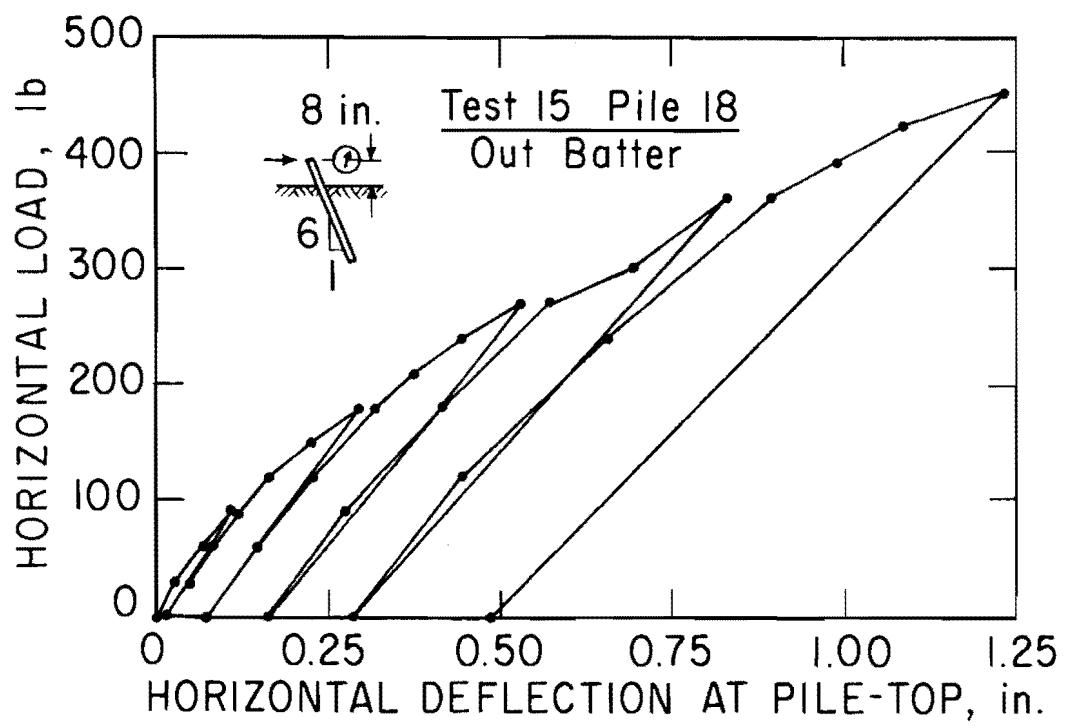


Fig. 5.19. Horizontal Load versus Pile-Top Deflection

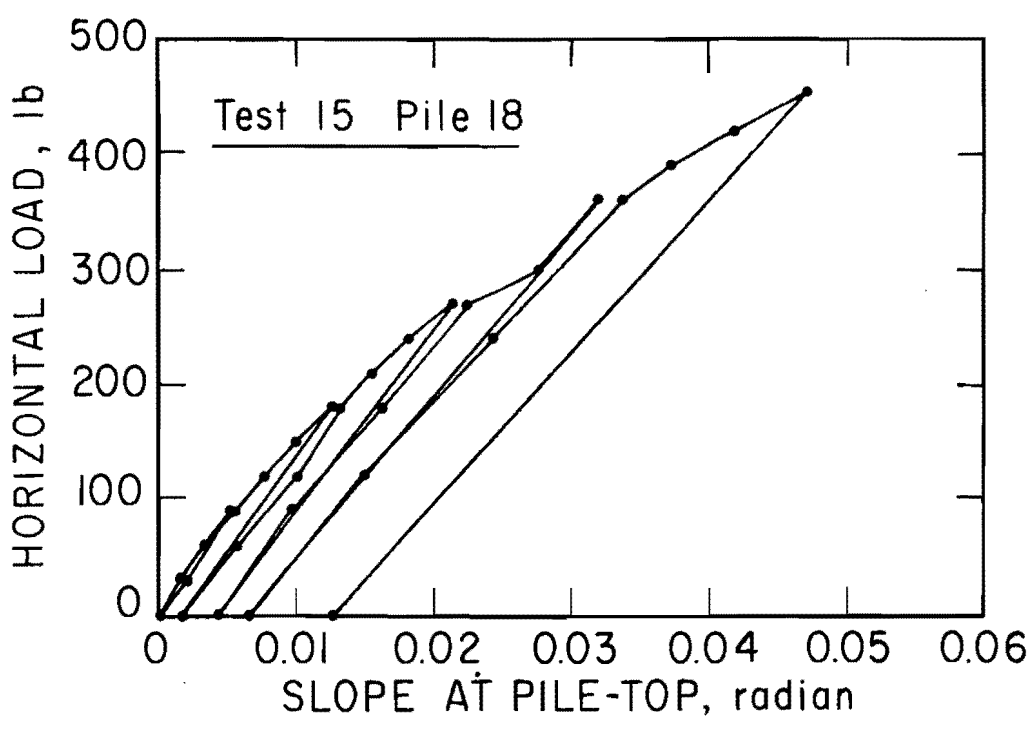


Fig. 5.20. Horizontal Load versus Pile-Top Slope

batter with Pile 19 being in-battered and Pile 18 being out-battered. The distinction of in-batter and out-batter is made with regard to the direction of horizontal load. (The terms "in-batter" and "out-batter" are defined by sketches in the figures.)

The horizontal load was increased or decreased in increments. The criterion for the stabilization of the lateral displacement of pile head under a constant load was set to be  $3 \times 10^{-3}$  inch per 5 minutes.

Figures 5.21 and 5.22 summarize the measurements of displacement and slope of Pile 1, Pile 2, and Pile 3. Pile 1 was a vertical pile. Pile 2 and Pile 3 were in-batter and out-batter piles with a 1 to 12 batter. The static load on these piles were also increased and decreased in steps. The plot shows only the envelopes of the displacement curves.

Pile 1, Pile 2, and Pile 3 were instrumented with strain gages to give bending strains. A typical family of bending moment distribution curves is shown in Fig. 5.23. The points of the maximum moment and the first zero moment shifted slightly downward as lateral load was increased. The plot of maximum bending moment of these three piles in Fig. 5.24 indicates that the lateral load versus the maximum bending moment relationships are still linear at 450 pounds lateral load. The largest bending stress in the pile is about 50 ksi.

#### Experimental Lateral Soil Resistance Curves

Experimental p-y curves are shown in Fig. 5.25. These curves were computed by Parker and Reese (1970). The computation was done by two different methods. One of the methods resorted to the numerical integration and differentiation of the bending moment distribution curves

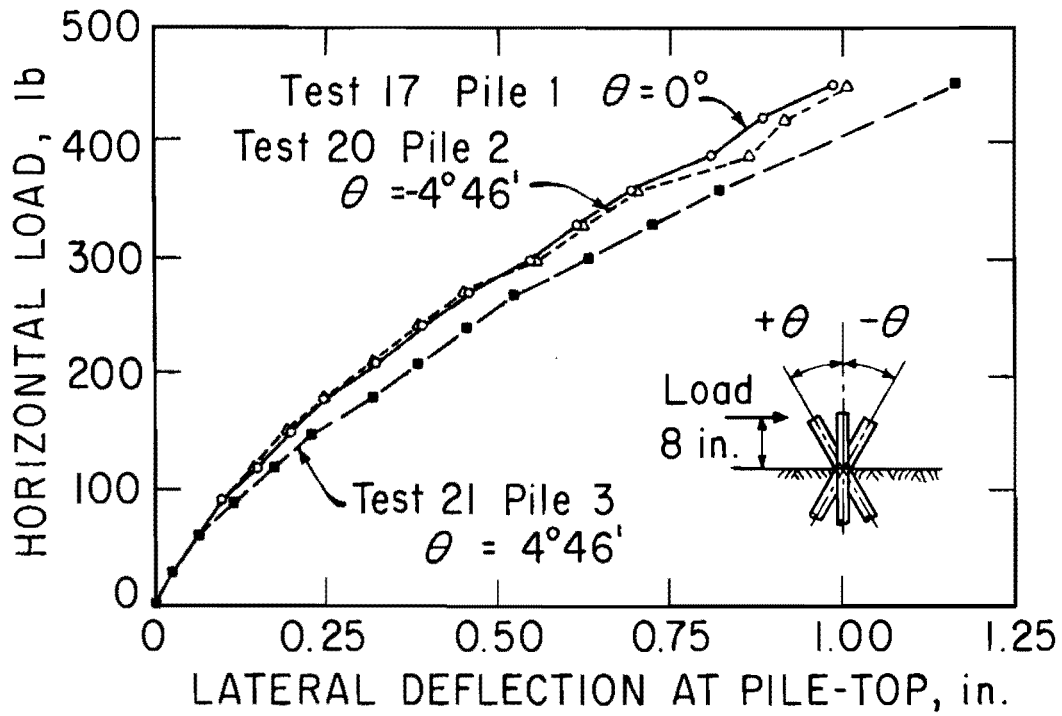


Fig. 5.21. Horizontal Load versus Pile-Top Deflection

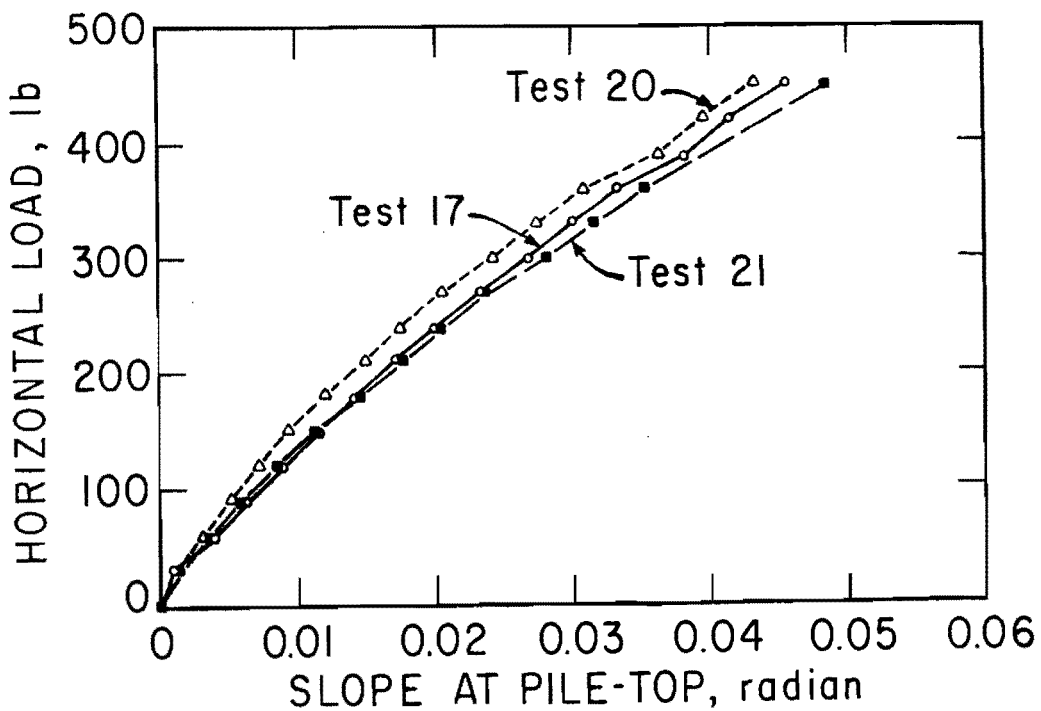


Fig. 5.22. Horizontal Load versus Pile-Top Slope

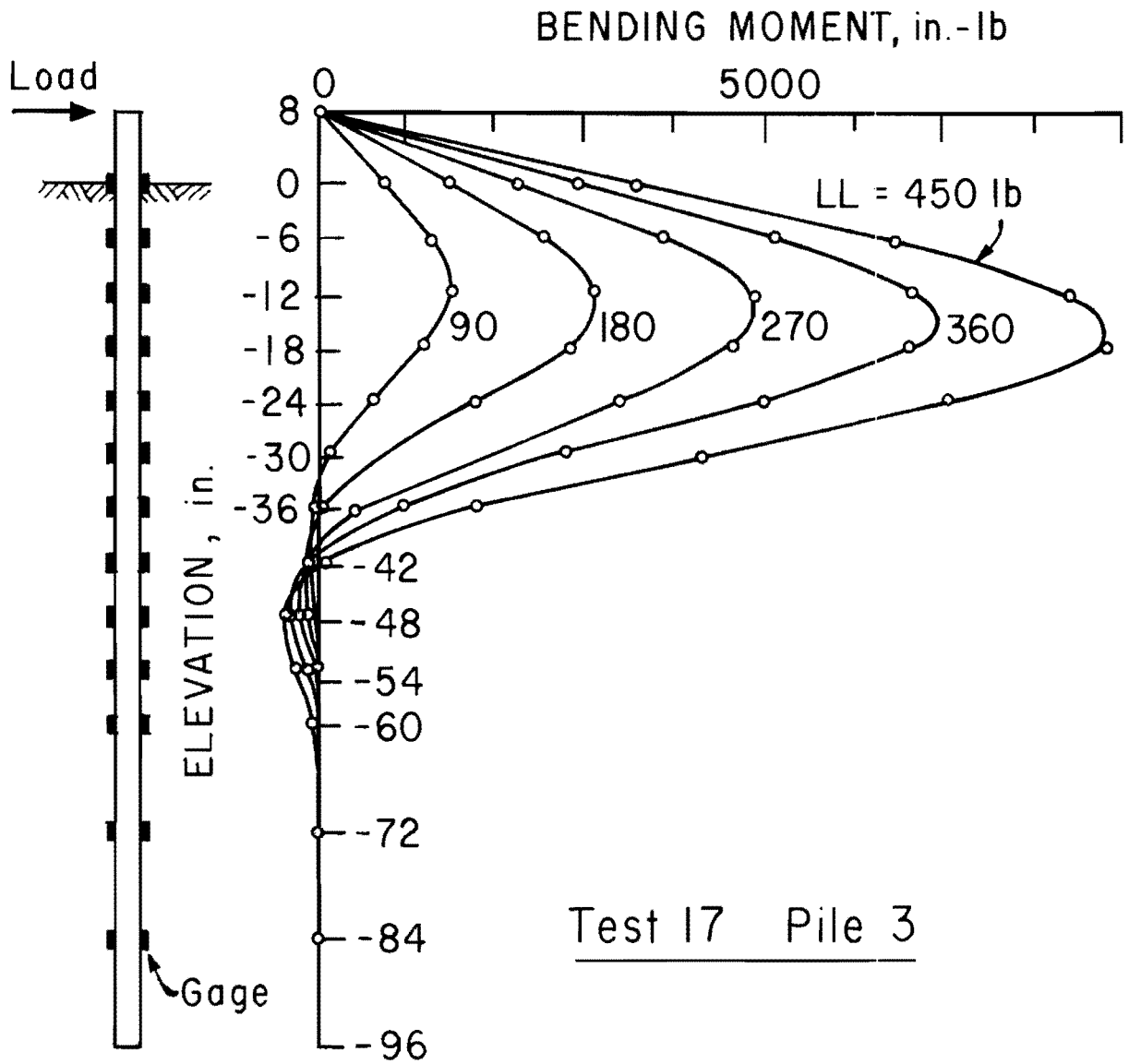


Fig. 5.23. Typical Moment Distribution Curves

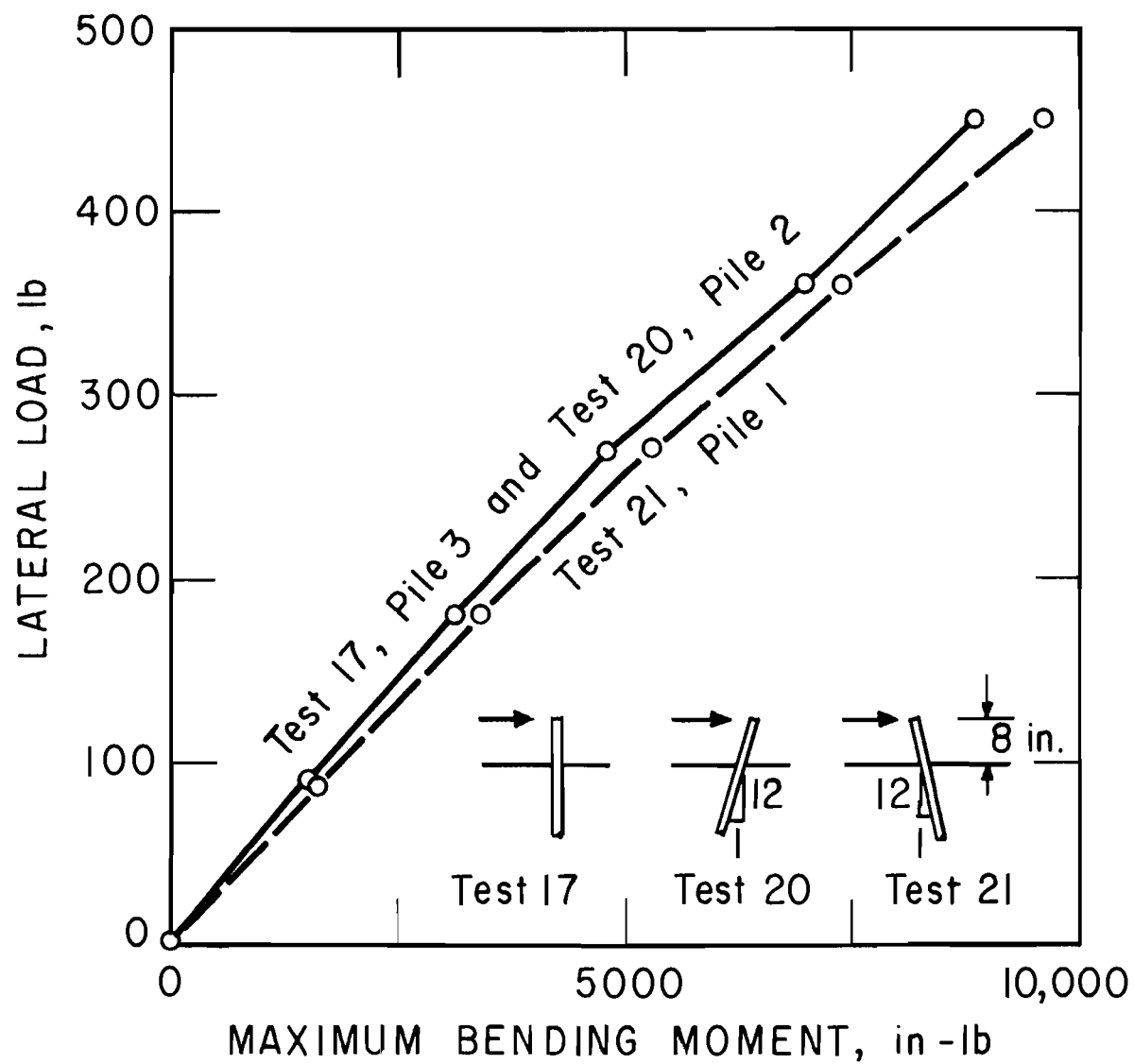


Fig. 5.24. Maximum Moment in Pile

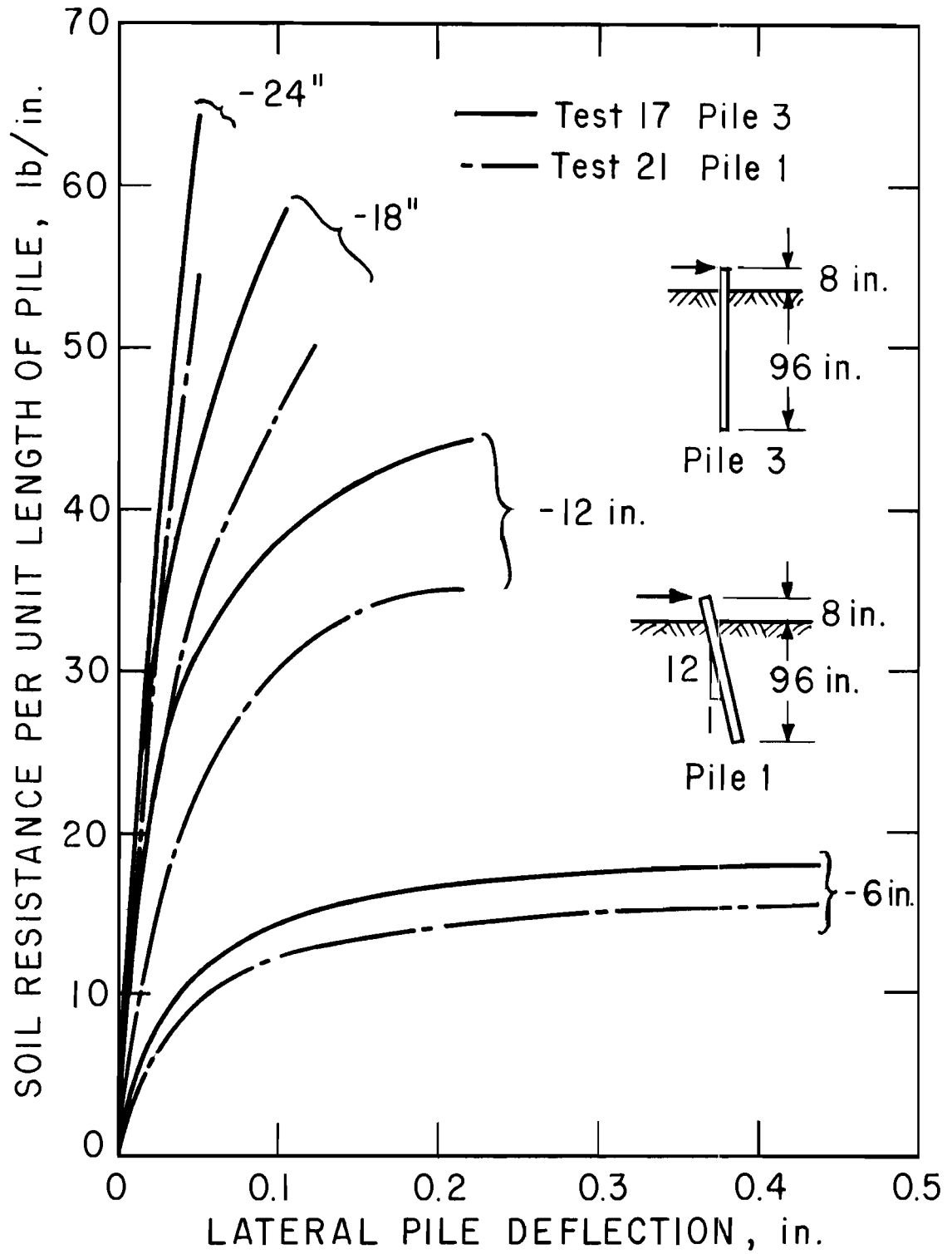


Fig. 5.25. Experimental p-y Curves

to obtain the pile deflection and the horizontal soil reaction per unit length of a pile. The other method involved the application of the non-dimensional analysis of a laterally loaded pile developed by Reese and Matlock (1956).

The experimental p-y curves are given to the depth of 24 inches. Below that depth the magnitude of the lateral pile deflection was insignificant. The experimental p-y curves indicate that the ultimate lateral soil resistance was developed to the depth of approximately 12 inches. It is also observed that there is a considerable difference in p-y curves between an out-battered pile (Pile 1) and a vertical pile (Pile 3).

The prediction of pile-head deflection from these experimental p-y curves, agrees well with the actual deflection curve (Fig. 5.26). The prediction of the maximum bending moment in the pile, which is another important quantity to describe the laterally loaded pile behavior, gives only two to five per cent discrepancy from the actual measurement for the maximum lateral load at pile top (450 pounds).

#### Theoretical Lateral Soil Resistance Curves

Some discussion is necessary concerning the selection of the value of the angle of internal friction to be used in the theoretical analysis of behavior of the piles under lateral loading. In Chapter IV it was reported that the value of  $\phi$  for air-dried samples was  $41^\circ$  at 100 pcf as obtained from triaxial tests and direct shear test. A value of  $\phi$  of  $47^\circ$  was obtained from triaxial tests on specimens trimmed from the soil removed from the tank at the end of the test program. The average dry



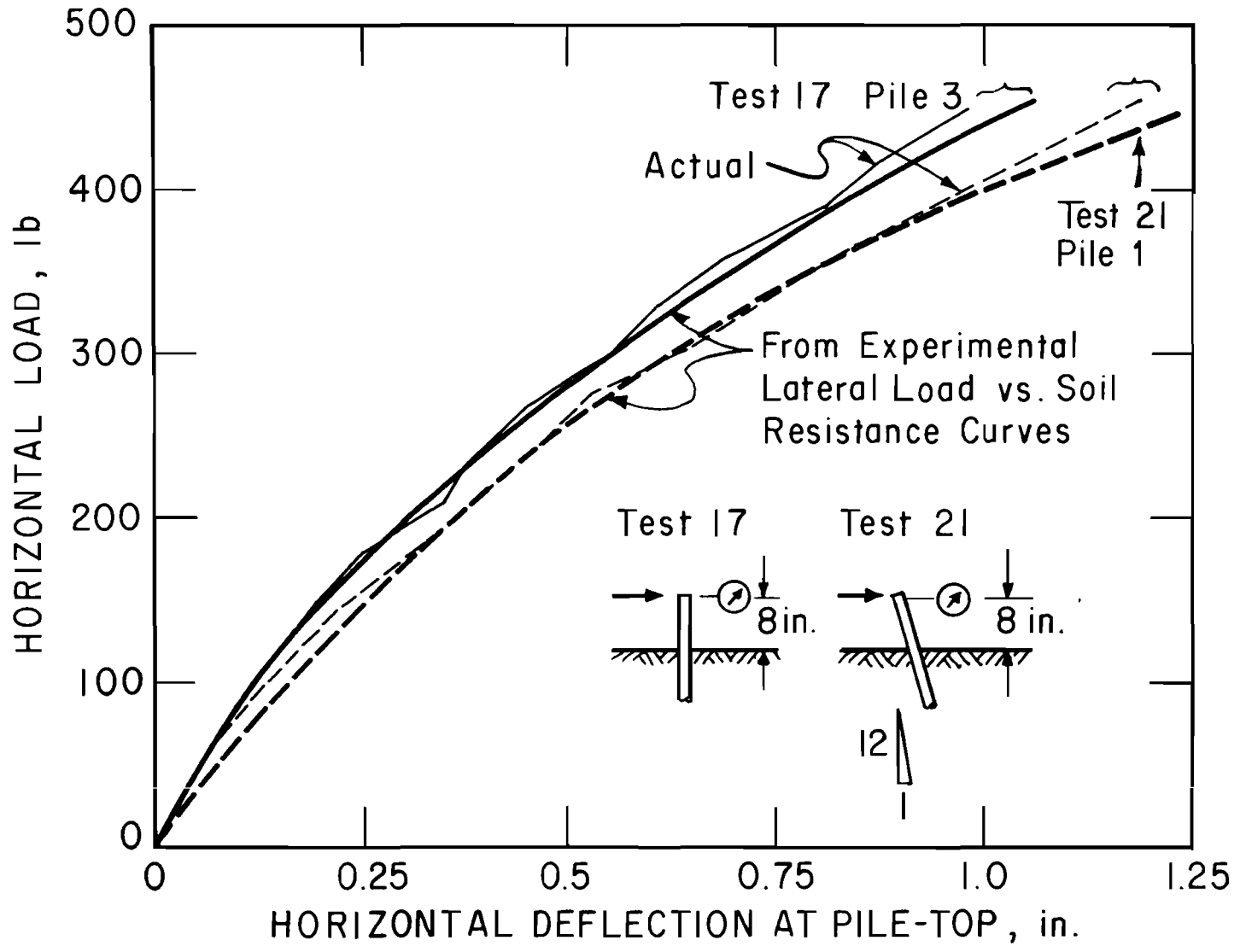


Fig. 5.26. Pile-Top Deflection from Experimental p-y Curves

density of these specimens was about 101 pcf. The difference in the value of  $\phi$  obtained from the two test series is partly due to differences in density, the main difference is thought to be related to the differences in the test procedures. The average angle of internal friction of the soil in the tank is thought to lie between  $41^\circ$  and  $47^\circ$ .

Studies of single pile behavior by use of the bilinear p-y curves (see Fig. 5.27) showed that close agreement between theory and experiment was obtained if the average angle of internal friction was selected as  $47^\circ$  (Fig. 5.28). This close agreement was desirable since it allowed the group behavior to be studied analytically without substantial error being introduced because of erroneous computation of single pile behavior.

Parker and Reese (1970) recommended p-y curves quite similar to the bilinear curves employed in the analysis except that a hyperbolic function was used to obtain a transition between the two straight lines.

Since the improved hyperbolic p-y curves were not available at the time of analysis, they are not used for this analysis. Future analysis should employ the hyperbolic curves for reasons given by Parker and Reese (1970).

The difference in behavior between the two vertical piles, Pile 3 (Test 17) and Pile 20 (Test 13) is attributed to the difference in pile locations. A series of tests, Test 13 (Pile 20), Test 14 (Pile 19), and Test 15 (Pile 18), were performed on piles on the southern end of the tank (Fig. 4.2), while the other series of tests, Test 17 (Pile 3), Test 20 (Pile 2) and Test 21 (Pile 1) were performed on piles on the northern end of the tank (Fig. 4.2). Figure 5.28 shows that experimental

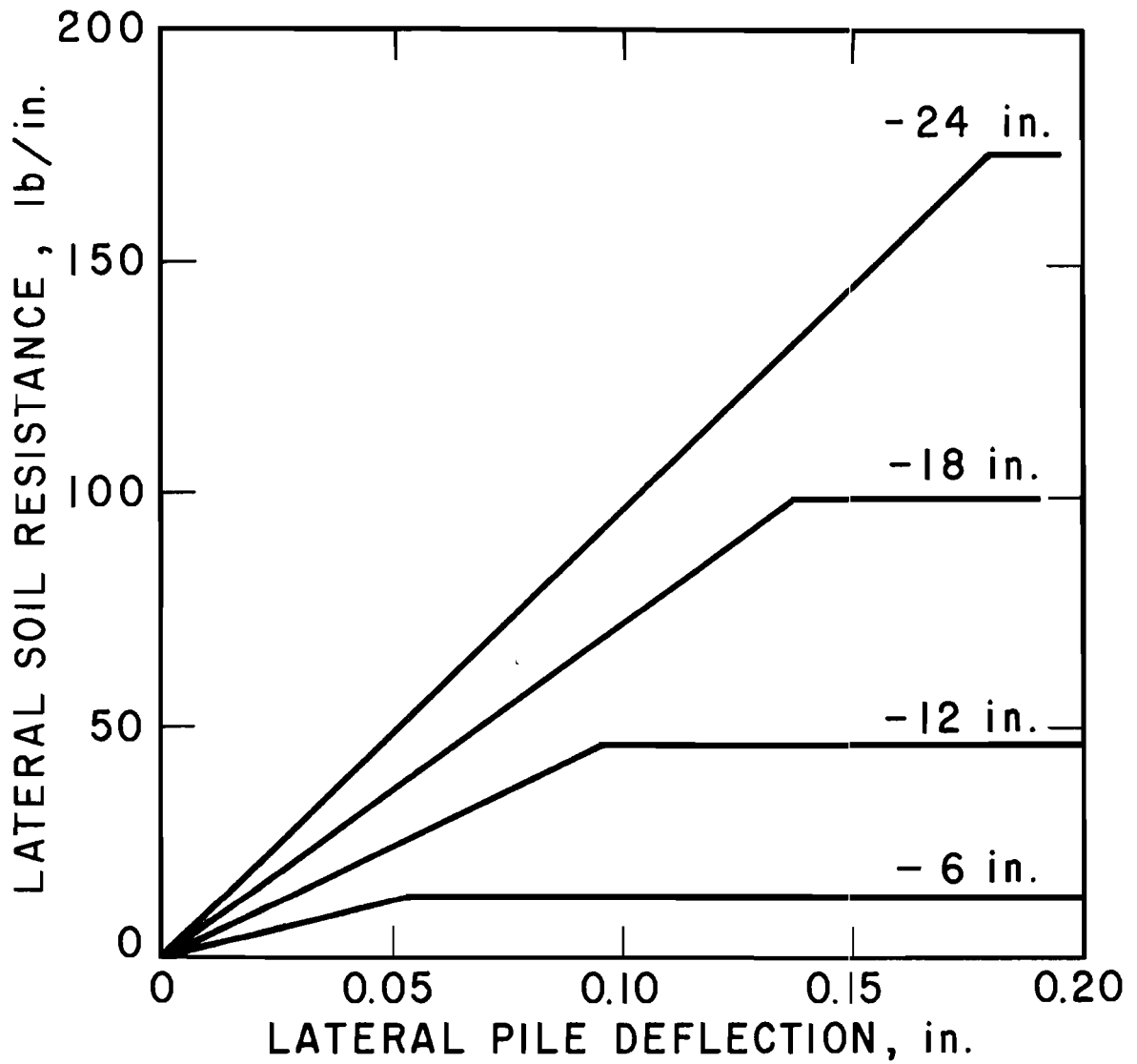


Fig. 5.27. Theoretical p-y Curves from Soil Criteria

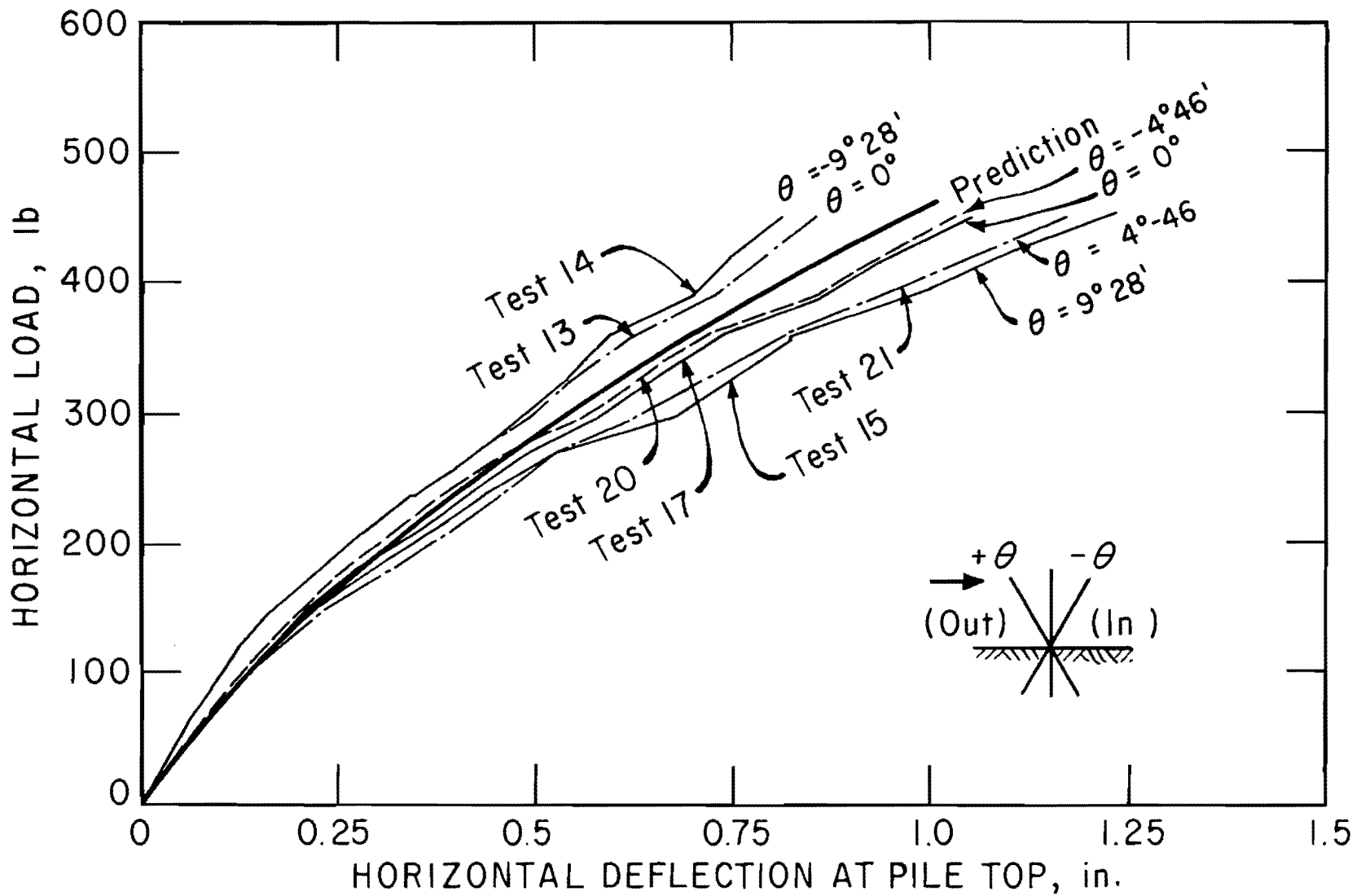


Fig. 5.28. Prediction of Pile-Top Deflection from Theoretical p-y Curves

curves of piles on the northern end are indicating larger pile-top deflection than the corresponding piles on the southern end.

The piles on the northern end were subjected to the disturbance by the running water. Although care was taken, water supplied to the tank caused a few inches scouring of sand on the northern end. Consequently, the sand was disturbed at shallow depth. The characteristics of the soil near the ground surface are most crucial in determining the behavior of a laterally loaded pile.

The variation of pile top deflections due to the batter angle will be discussed in the next section.

#### Effect of Batter

Kubo (1962) investigated the effect of batter on the behavior of laterally loaded piles. He modified the lateral soil resistance curves of a vertical pile with a modifying constant to express the effect of the pile inclination. The values of the modifying constant as a function of the batter angle were deduced from model tests in sands and also from full-scale pile loading tests. The criterion is expressed by a solid line in Fig. 5.29.

Plotted points in Fig. 5.29 show the modification factors for the batter piles tested in these experiments. The modification factors were obtained for two series of tests independently. As it is described in the preceding section, one series of tests was carried out on the northern end and the other on the southern end; each of them showed slightly different trends.

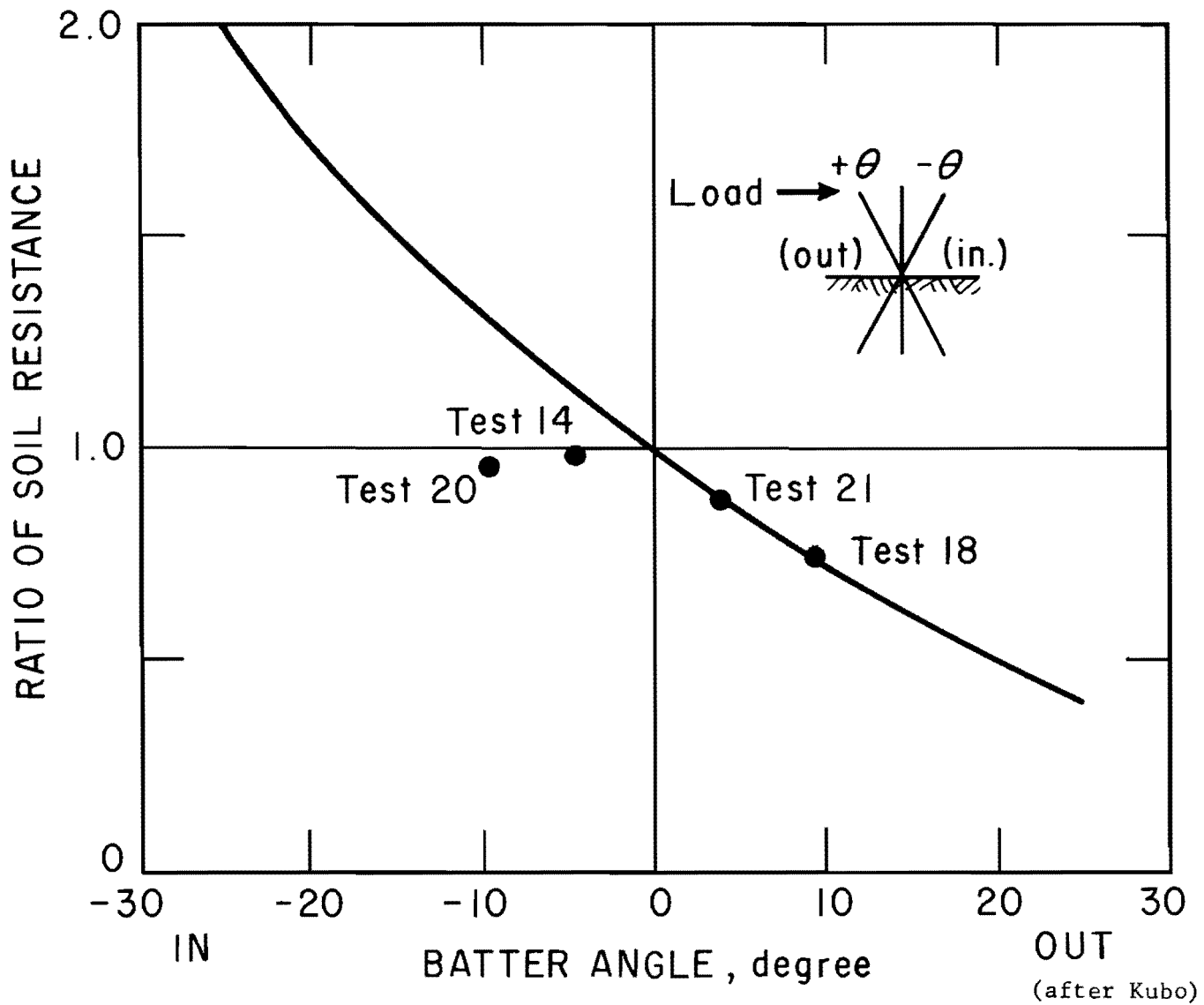


Fig. 5.29. Modification of p-y Curves for Battered Piles

The experimental modification factors were obtained after a few trial and error comparisons of the horizontal pile-top displacements at the maximum load between a vertical pile and a battered pile.

Figure 5.29 indicates that for the out-batter piles, the agreement between the empirical curve and the experiments is good, while the in-batter piles in the experiment did not show any effect of batter.

### Conclusion

The following conclusions are made concerning the analysis of experiments on laterally loaded single piles.

1. Both theoretical and experimental lateral soil resistance curves can give sufficiently accurate prediction of pile behavior.
2. The effect of disturbance of sand at shallow depth by the running water was evident.
3. The experiments support Kubo's rule for modifying the lateral soil resistance curves of out-batter piles.
4. The experiment did not reveal any difference between the behavior of a vertical pile and an in-batter pile under lateral load.

Since all lateral loading tests were performed in the relatively short time span of one month, no effect of time on the lateral behavior of piles can be adequately studied.

## CHAPTER VI

### ANALYSIS OF EXPERIMENT ON GROUPED PILE FOUNDATION

The principal objective of the experiment is establishing the correlation between single pile behavior and the behavior of a grouped pile foundation. The loading conditions on the grouped pile foundations were designed in such a way as to cover all the conceivable cases of static loading on the foundation.

The most important behavioral quantity of a grouped pile foundation is the displacement of the pile cap under the given load. The load-displacement relationships obtained in the experiment are compared with the analytical prediction.

The distribution of forces on individual piles in a foundation is another behavioral quantity to be examined. Unfortunately, almost all the strain gages on the piles were damaged during the five months submergence in the water. Comparisons were made between theory and experiment for those piles where there were surviving strain gages.

There were two test foundations, each consisting of four piles. They are designated Cap 1 and Cap 2 (Fig. 4.2). Cap 1 was tested under vertical, lateral and inclined loads. Cap 2 was subjected only to inclined loads. The analysis of test results is presented first for Cap 1 and then for Cap 2.

The analytical prediction of the behavior of the pile caps is computed by the computer program GROUP (Appendix A). The computation is



based on the experimental load-settlement curves of single piles and on theoretical lateral soil resistance curves.

### Cap 1

The grouped pile foundation, Cap 1, consisted of two vertical piles and two batter piles with 1 to 12 batter (Fig. 4.2).

The loading history of Cap 1 is shown in Fig. 6.1. Depending on the type of loading, the test is divided into three phases; namely, combined loading (Test 22-1), vertical loading (Test 22-2) and lateral loading (Test 22-3). In addition to the varying load, Cap 1 was subjected to a dead load of 500 pounds imposed by the self-weight of the cap.

Test 22-1. The foundation was loaded by four cycles of vertical load at the center of the pile group. During the last two cycles, the vertical load was kept constant at the maximum, and lateral load was applied on the level of pile tops. Under these loadings none of the piles in the foundation were loaded up to failure.

Figure 6.2 shows a plot of the vertical component of the pile-cap displacement. The upper half of the graph shows the vertical displacement curve for the vertical loading and unloading without lateral load on the pile cap. The lower half of the graph shows the vertical load 9 kips or 12 kips. The experimental curves are shown as solid lines.

Figures 6.3 and 6.4 show the horizontal and rotational components of pile-cap displacement, respectively. The displacement curves are shown only for lateral loading with a constant vertical load of 9 kips or 12 kips. The displacement curves for vertical loading are not shown,

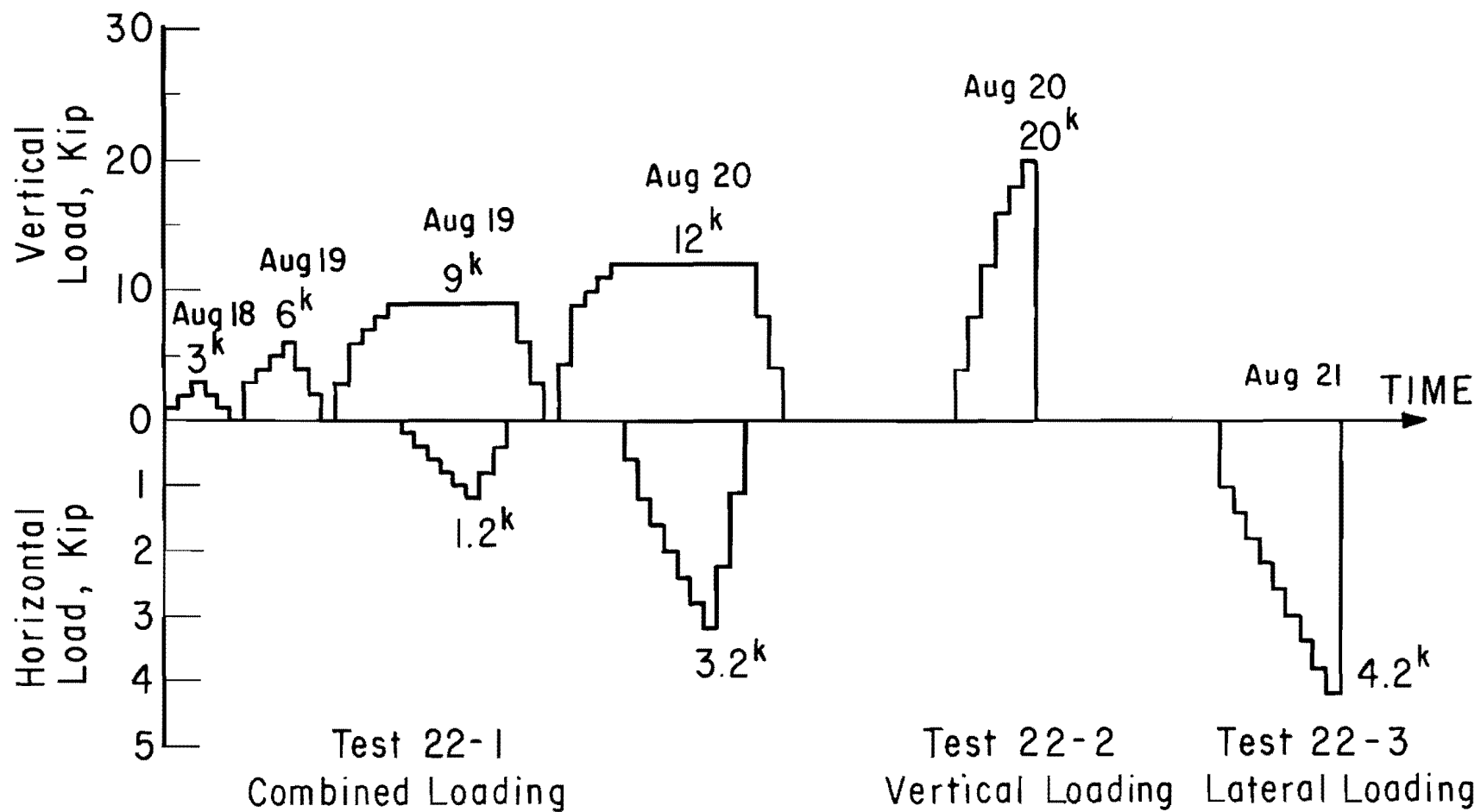


Fig. 6.1. Loading History of Cap 1

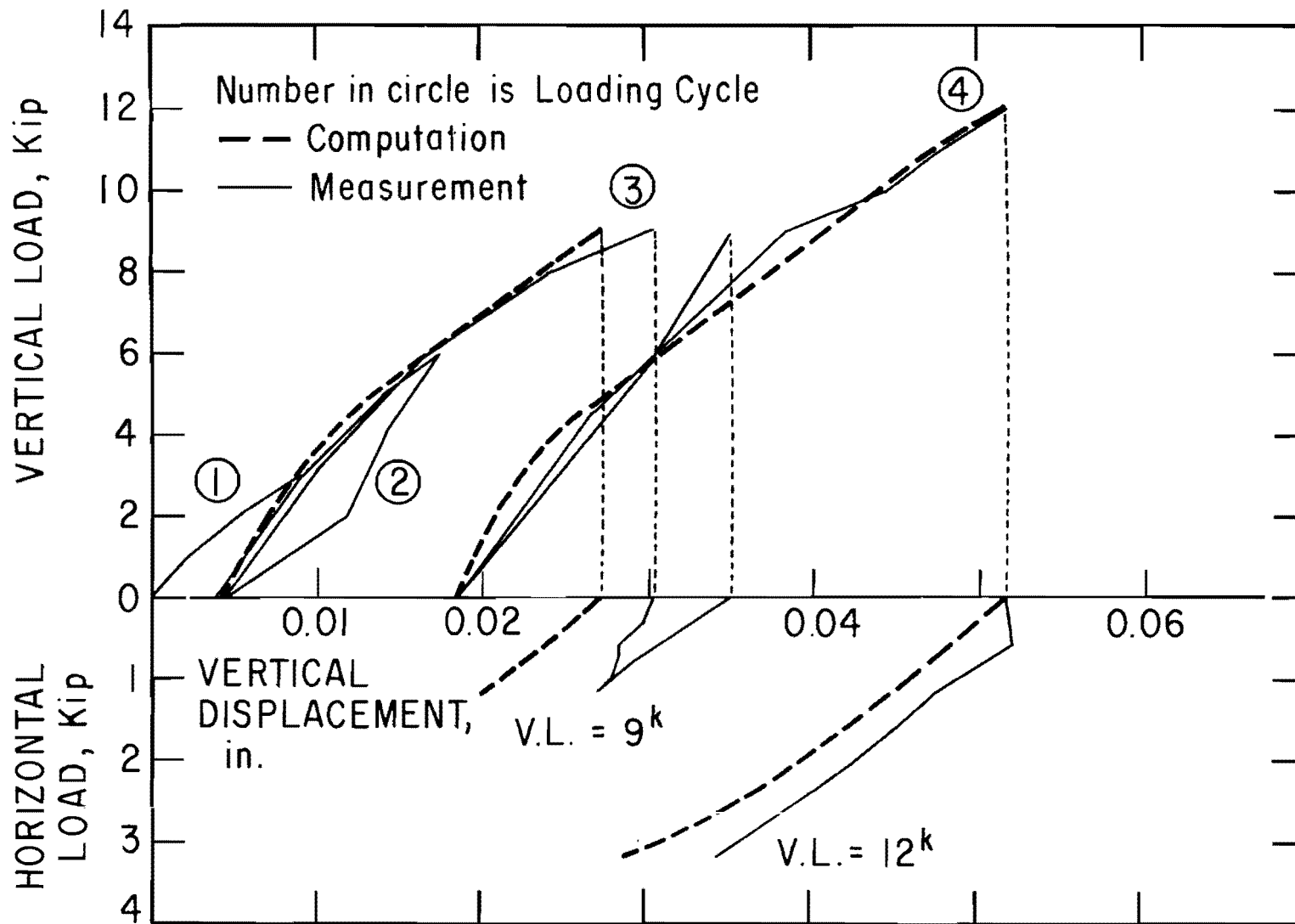


Fig. 6.2. Vertical Displacement of Cap 1 in Test 22-1

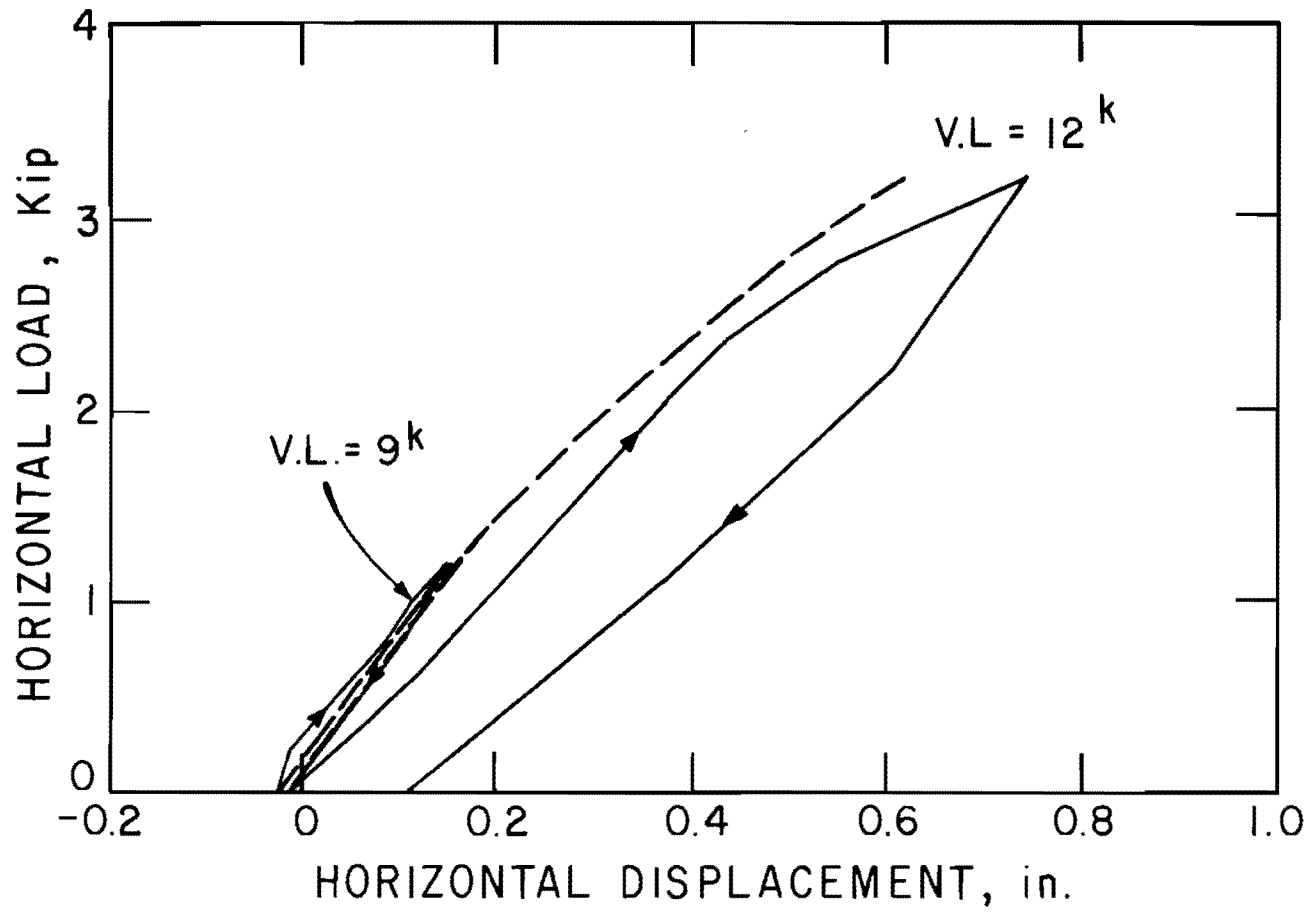


Fig. 6.3. Horizontal Displacement of Cap 1 in Test 22-1

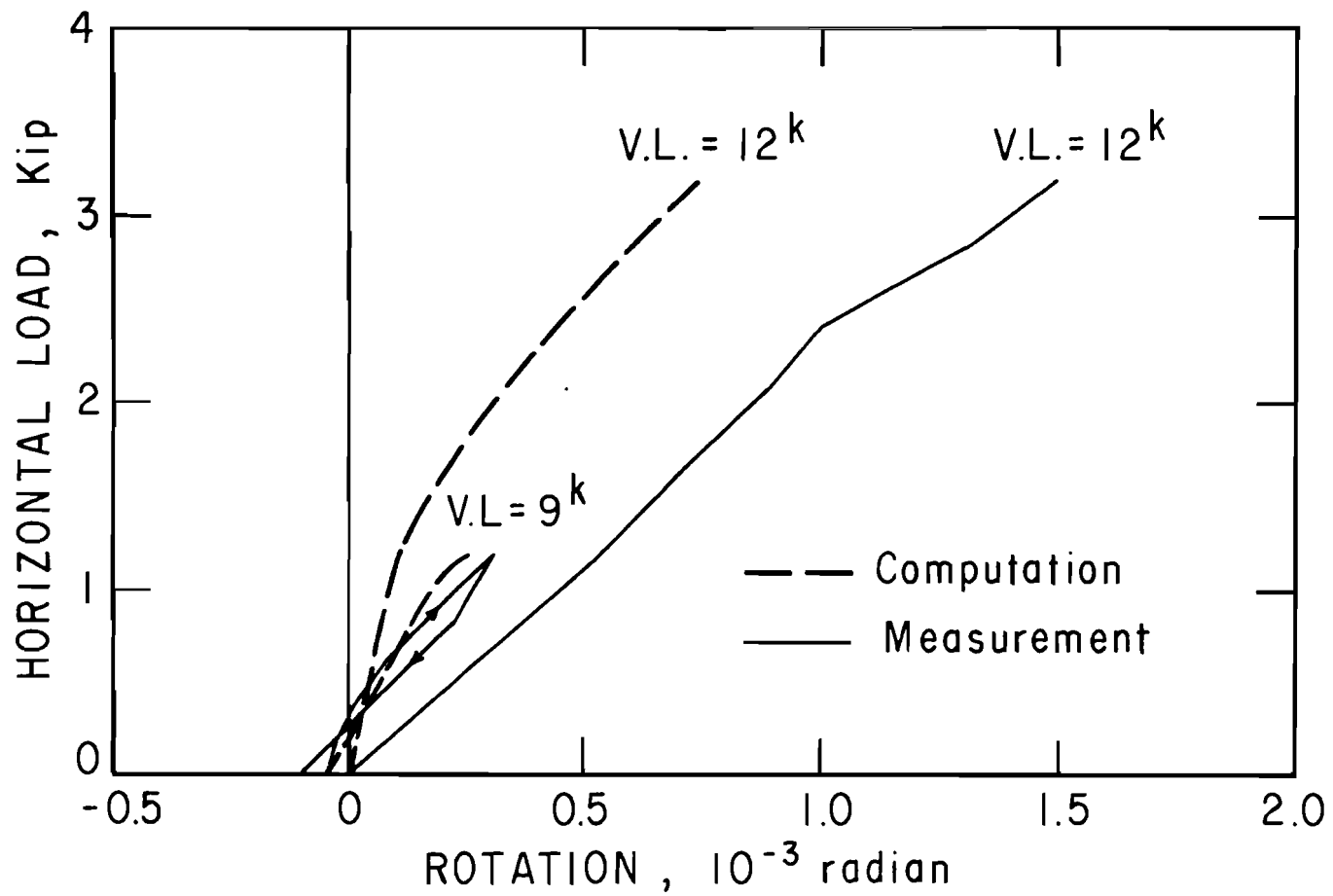


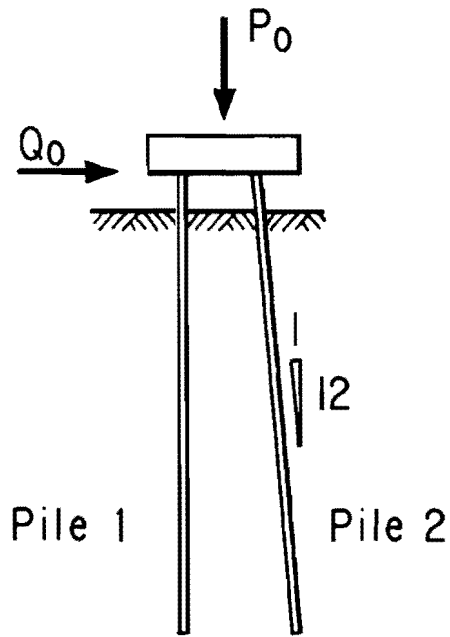
Fig. 6.4. Rotation of Cap 1 in Test 22-1

because the horizontal and rotational components of pile-cap displacement are only nominal under the vertical load alone.

The prediction of the pile-cap displacement employed the load-settlement curve of Test 23 on Pile 7 (Fig. 5.8). Test 23 was conducted soon after Test 22 on the grouped pile foundation Cap 1. Considering the change in load-displacement relationships with time (Fig. 5.9), Test 23 is considered to be the best representation of single pile behavior for use in making analysis of Test 22. Theoretical bilinear lateral soil resistance curves developed in the previous chapter (Fig. 5.27) were used for computing the lateral behavior of the vertical piles in the foundation. The modification of the lateral soil resistance curves for the out-batter pile was made in accordance with Kubo's criterion (Fig. 5.29). The out-batter pile in Cap 1 has 1 to 12 batter or a  $4^{\circ}46'$  batter angle. The correction factor for this angle is 0.86. The soil resistance curves for an out-batter pile were obtained by applying the correction factor uniformly to those of the vertical pile.

In Fig. 6.2, the analytically predicted vertical displacement curves are fitted to the third and fourth cycles of vertical loading. In each of these loading cycles a good agreement is obtained between the analytical prediction and the experimental vertical displacement curve. The experiment shows that the grouped pile foundation Cap 1 had considerable amount of permanent set in the vertical displacement after the third loading cycle.

Figure 6.5 illustrates qualitatively the mechanism of the large permanent set of the vertical displacement after the third loading



(a) Grouped Pile Foundation Cap 1

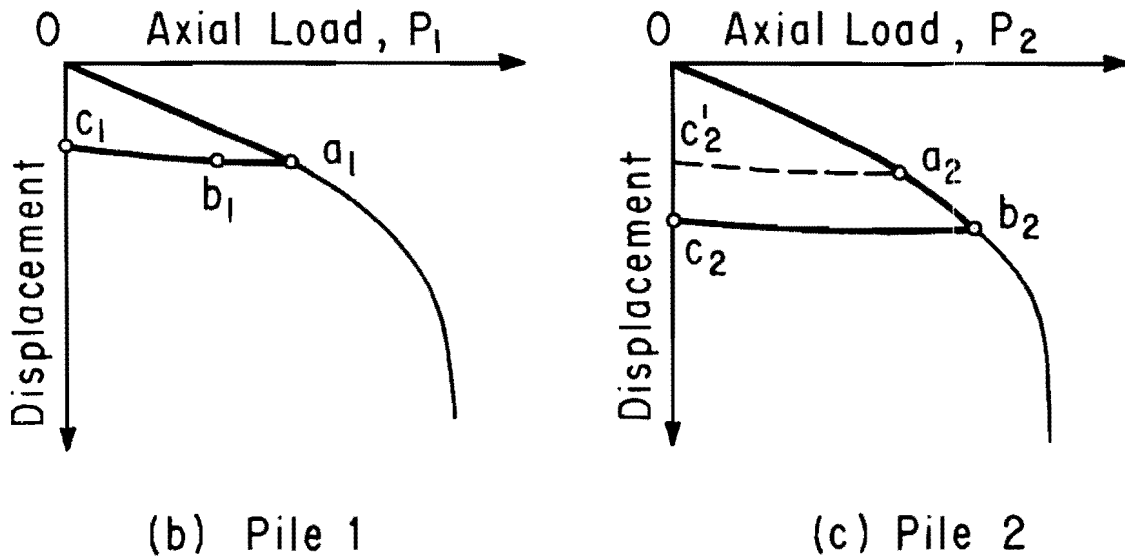


Fig. 6.5. Axial Single Pile Behavior and Pile Cap Displacement

cycle. Due to a vertical load  $P_o$  (Fig. 6.5a), Pile 1 and Pile 2 take the paths  $Oa_1$  and  $Oa_2$  in the axial load versus displacement curves (Figs. 6.5b and 6.5c). When a horizontal force  $Q_o$  (Fig. 6.5a) is added to the foundation, the paths of load displacement curve of each individual pile move to points  $b_1$  and  $b_2$ . If all the loads  $P_o$  and  $Q_o$  are removed from the foundation, the paths go to points  $C_1$  and  $C_2$ . If it were not for the horizontal load  $Q_o$ , the path of Pile 2 would be  $Oa_2c_2'$ . An excessive permanent set  $c_2c_2'$  is created in Pile 2 because of the horizontal loading on the foundation, which subsequently increased the permanent set of the vertical pile cap displacement.

The effect of permanent set in the axial behavior of a single pile is not manifest on the horizontal component of the pile-cap displacement (Fig. 6.3). Considering the small batter angle of Pile 2, the horizontal component of the permanent set in the axial pile displacement may be regarded as negligibly small.

On the other hand, the permanent set in the axial pile displacement is affecting the rotational displacement of the pile cap (Fig. 6.4). In the third loading cycle where the vertical load on the foundation was kept constant at 9 kips, a good correspondence is obtained between the experimental curve and the analytical prediction of rotation of the pile cap. However, in the fourth loading cycle, in which a constant 12 kip vertical load was maintained on the foundation, the experimental rotation angle is far greater than the analytical prediction because of the hysteresis in the axial displacement of pile.



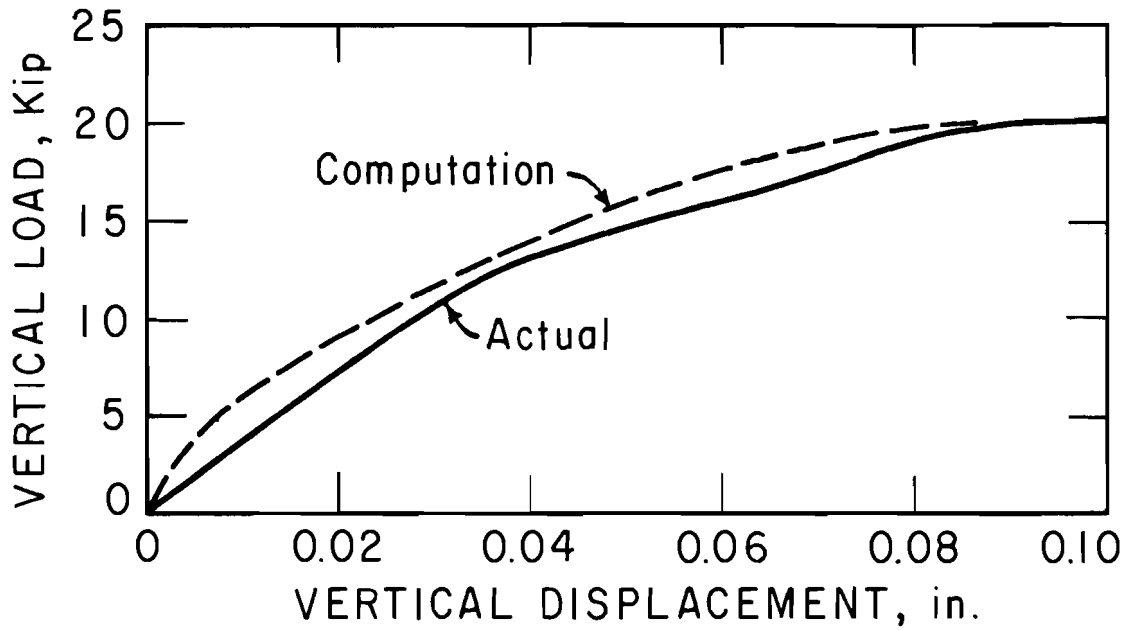
Test 22-2. In this phase of testing, Cap 1 was loaded with only the vertical load at the center of four piles. The vertical load was increased until it reached the ultimate.

Figures 6.6 shows the three components of pile-cap displacement for Test 22-2. The analytical prediction was computed by making use of the load settlement curve of Test 23 on Pile 7 (Fig. 5.8) and the theoretical lateral soil resistance curve in Fig. 5.27. These are the same conditions as those used for the prediction of Test 22-1.

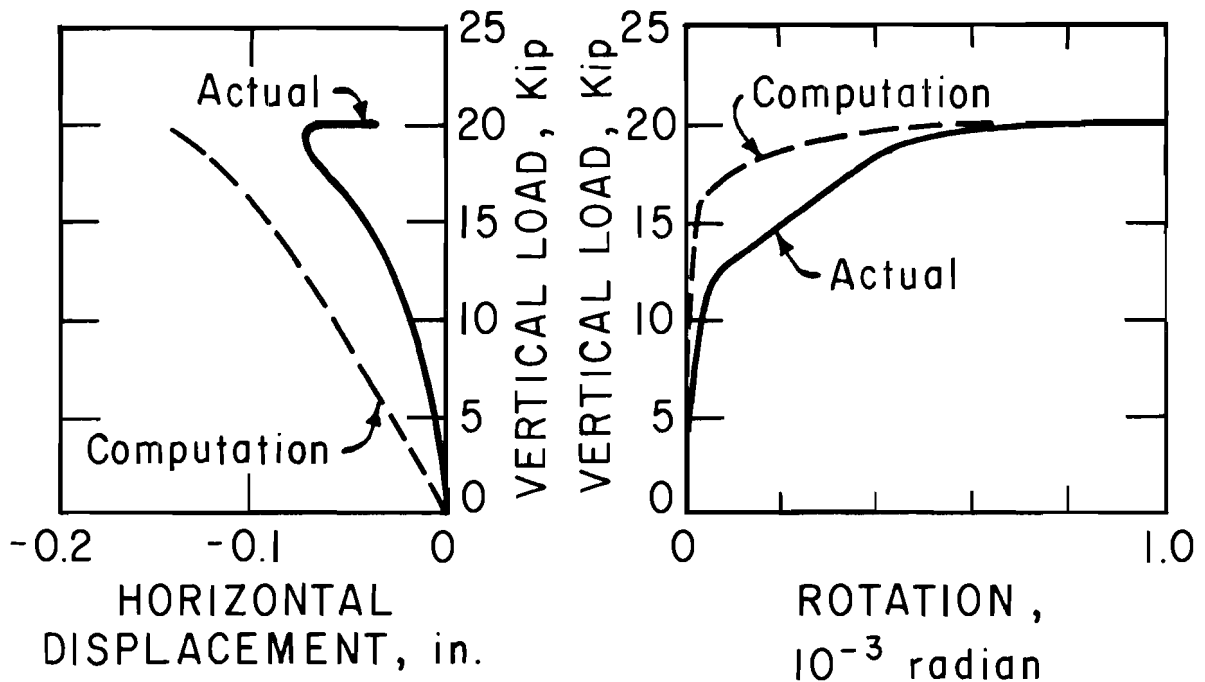
The analytical prediction of the vertical pile-cap displacement agrees well with the experimental curve (Fig. 6.6a).

Considerable discrepancies are observed between the analytical predictions and the experimental curves of the horizontal and rotational components of pile-cap displacement (Figs. 6.6b and 6.6c). There are several conceivable causes contributing to these discrepancies.

First, it must be considered that the pile cap moved during the previous test 0.7 inch in the positive direction or to the right in Fig. 6.5a. The permanent set in the horizontal displacement during the previous Test 22-1 was about 0.1 inch in the positive direction. The predicted horizontal displacement of the pile cap is 0.15 inch to the negative direction. The discrepancy in horizontal displacement curve in Fig. 6.6b may be attributed to the error in the alignment of load or to the tilting of vertical load in the counter-clockwise direction. No immediate assessment can be made as to the effect of lateral loading of a pile in the reversed direction.



(a) Vertical



(b) Horizontal

(c) Rotation

Fig. 6.6. Displacement of Cap 1 in Test 22-2

Second, consideration may be given to the disturbance in the axial behavior of a pile. Pile 2 in the grouped pile foundation Cap 1 (Fig. 6.5a) was subjected to an axial load almost equal to the ultimate bearing capacity during the previous test, while Pile 1 was subjected to an axial load well below the ultimate. Subsequently, the axial resistance of Pile 1 was reduced. The effect of reduced axial resistance in Pile 1 is reflected in the backward turn of experimental horizontal displacement curve near at the ultimate vertical load on the foundation (Fig. 6.6b).

The third reason may be found in the difference of load displacement curve between Pile 1 and Pile 2. During the previous test, Pile 1 and Pile 2 followed the load-displacement paths  $Oa_1b_1$  and  $Oa_2b_2$ , respectively (Figs. 6.7a and 6.7b). The new path for Pile 1 should be  $b_1c_1$  in Fig. 6.7a. The new path for Pile 2 is assumed to be expressed by  $b_2d_2$  in Fig. 6.7b which has smaller ultimate value than the virgin curve  $Oa_2c_2$ . Although Pile 1 may have larger ultimate bearing capacity than Pile 2, the load displacement curve of Pile 1 starts having steep slope much earlier than Pile 2. The discrepancy in the rotation curves (Fig. 6.6c) which start from a little over one-half the ultimate vertical load on the foundation, is indicative of the early occurrence of steep slope in the load displacement curve of Pile 1.

Test 22-3. This is the last test performed on Cap 1, which was loaded only by the horizontal force at the level of the pile top.

Figure 6.8 shows the displacement of the foundation. The solid lines indicate the experimental curves and the broken lines express the analytical computation.

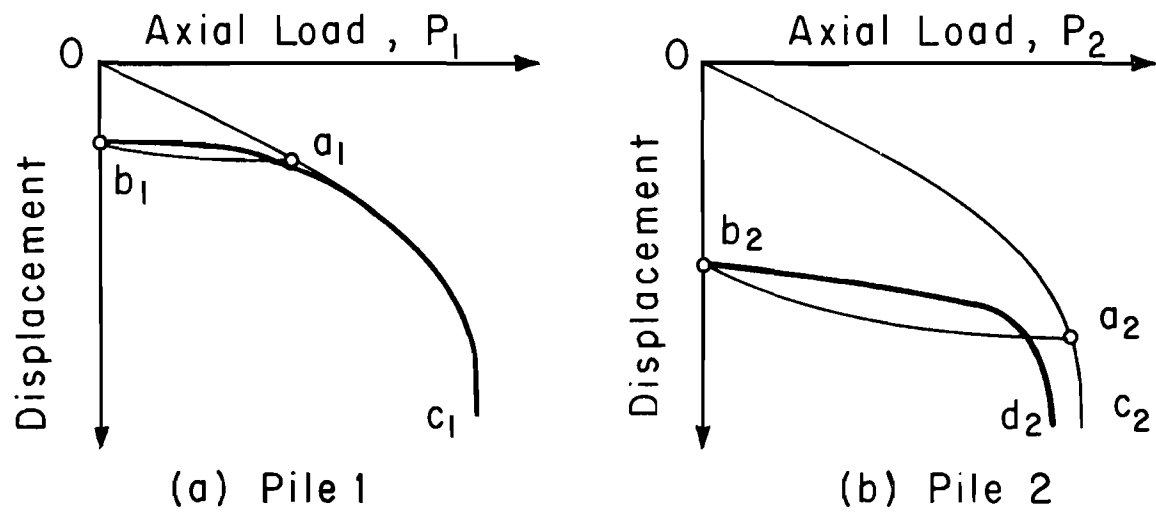


Fig. 6.7. Axial Single Pile Behavior and Pile-Cap Displacement

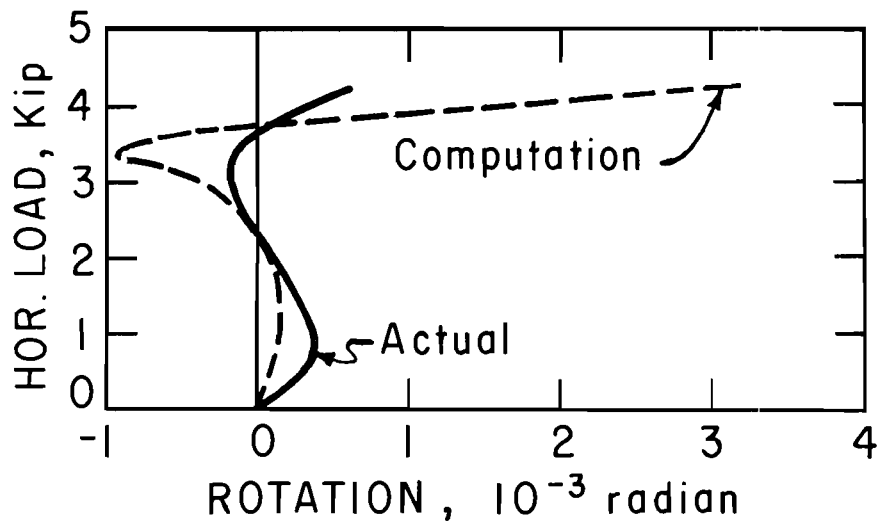
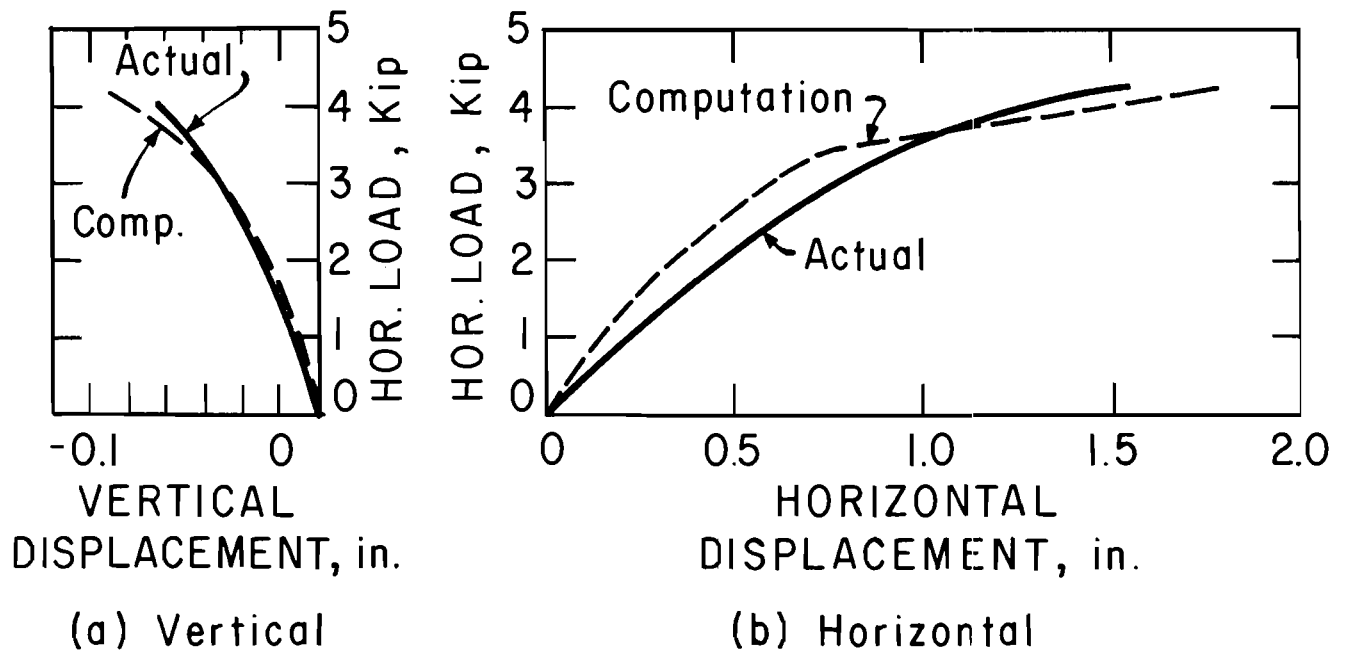


Fig. 6.8. Displacement of Cap 1 in Test 22-3

As it is discussed in Chapter V, the axial resistance of a pile is greatly reduced when a pile is loaded in the opposite direction of the previous loading to failure. Figure 6.9 plots the analytical computation of the axial forces on pile tops. It indicates that Pile 1 is subjected to uplift force immediately after the application of the horizontal load on the foundation.

Pile 1 has been loaded to failure in Test 22-2 under a downward load. Therefore, it is proper to use the uplift force versus pile-top displacement curve of Test 2 on Pile 9 (Fig. 5.3) for Pile 1. The uplift loading test, Test 2, was conducted on a pile which was once failed by a downward load. The analytical prediction of pile-cap displacement uses the same downward axial load versus displacement curve and the lateral soil resistance curves as Test 22-1 and Test 22-2.

Good correspondence between the analytical prediction and the experimental displacement curves is obtained (Fig. 6.8). The failure of the foundation is caused by the excessive horizontal displacement of the pile cap. The axial forces on pile tops are far below the ultimate axial pile resistance.

### Cap 2

The grouped pile foundation, Cap 2, consisted of four batter piles. A pair of piles makes 1 to 12 batter to the vertical and the other two piles make 1 to 6 batter to the vertical. Their arrangement is shown in Fig. 4.2.

Cap 2 was subjected to a dead load of 500 pounds and to an inclined load which made an angle  $12^\circ$  to the vertical. The inclined load had a

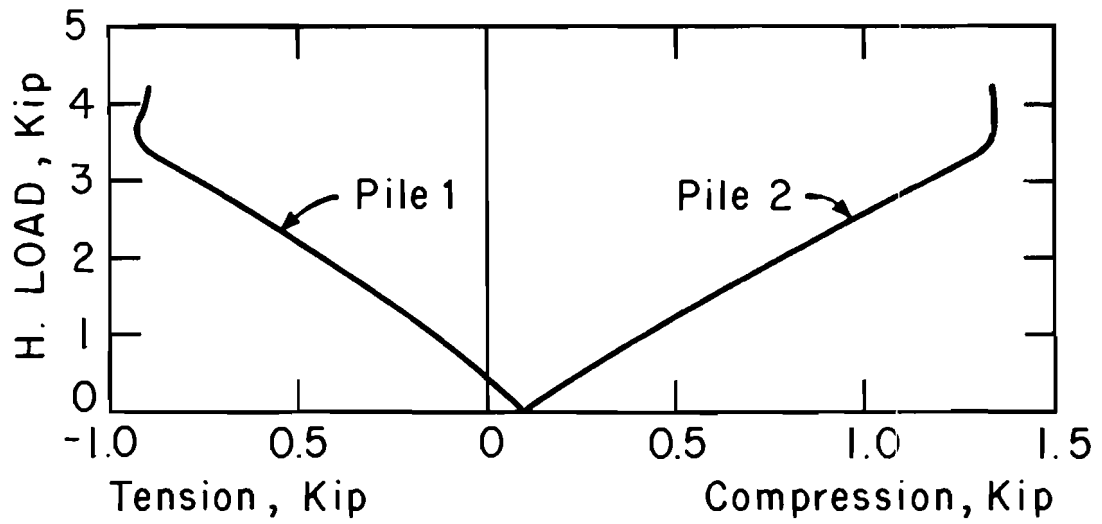


Fig. 6.9. Axial Pile and Load in Cap 1, Test 22-3

slight eccentricity of 0.43 inch with respect to the reference point on the origin of the structural coordinate system, which was selected at the center and the bottom base of the pile cap. The inclined load was increased incrementally in cycles until the foundation failed. The inclination angle  $12^\circ$  was chosen on the conception that both the vertical bearing capacity and the maximum lateral resistance of a pile might be fully mobilized at the time of foundation failure.

Displacement. Figures 6.10, 6.11, and 6.12 show the experimental load-displacement curves in solid lines and the theoretical prediction in broken lines. The analytical prediction of the load-displacement curves was made from the load-settlement curve of Test 23 on Pile 7 (Fig. 5.8) and the theoretical lateral soil resistance curves shown in Fig. 5.27. These conditions are identical to those which are used for Cap 1.

The analytical prediction of vertical displacement of grouped pile foundation, Cap 2, coincides with the envelope of experimental curve (Fig. 6.10). The experimental vertical displacement curve in Fig. 6.10 shows some irregularities in the first two loading cycles. These irregularities may be attributed to the variation in the axial behavior between individual piles. Although it is assumed in the analysis that two symmetrically arranged piles are acting in an identical manner, in actuality there must be some variation between two symmetrical piles. This assumption is verified by the observed rotation of the pile cap not only in the plane of symmetry, but also in the other planes where no rotation was assumed. The magnitude of pile-cap rotation in other planes sometimes reached as high as the rotation in the plane of symmetry.



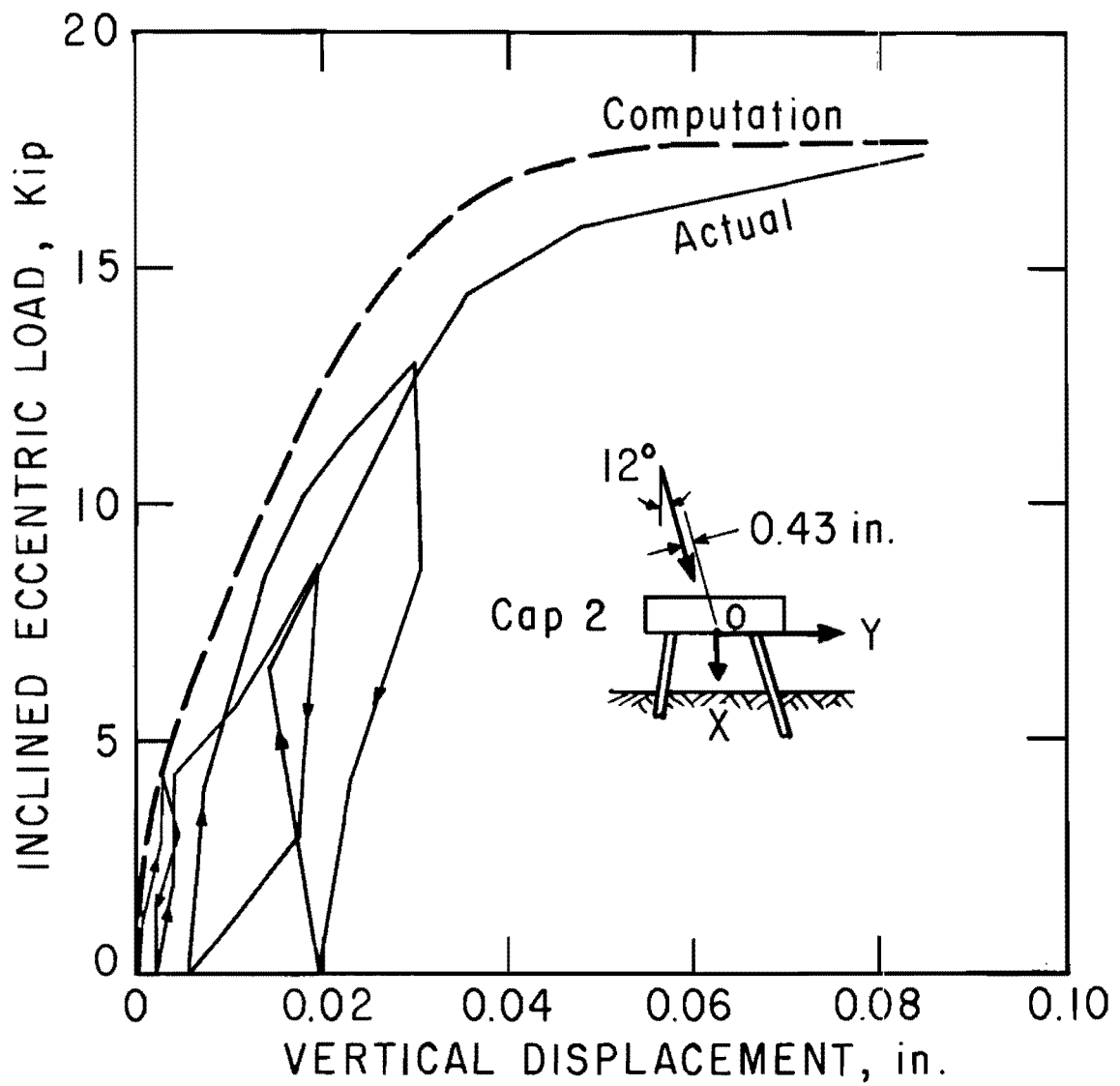


Fig. 6.10. Vertical Displacement of Cap 2

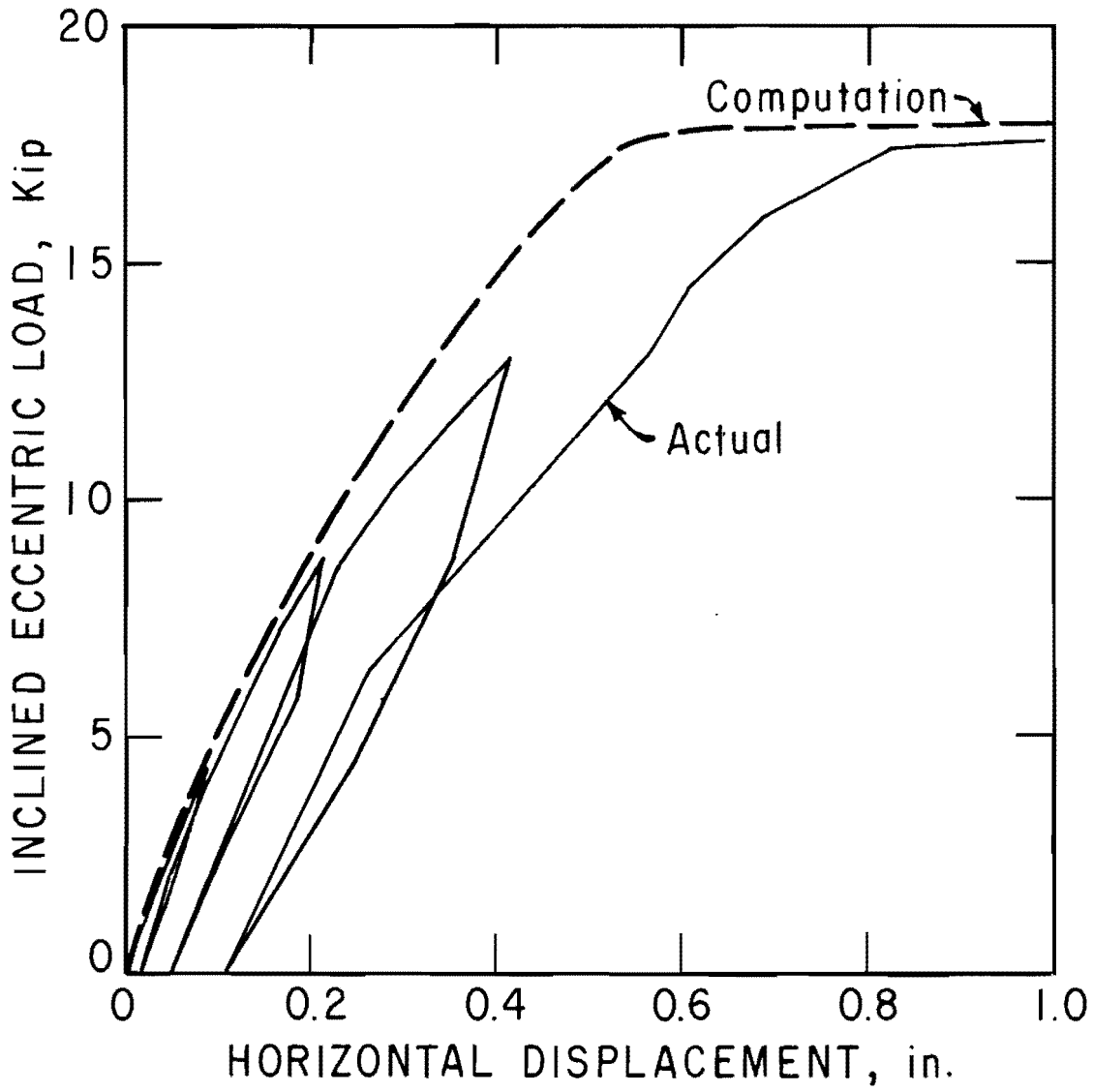


Fig. 6.11. Horizontal Displacement of Cap 2

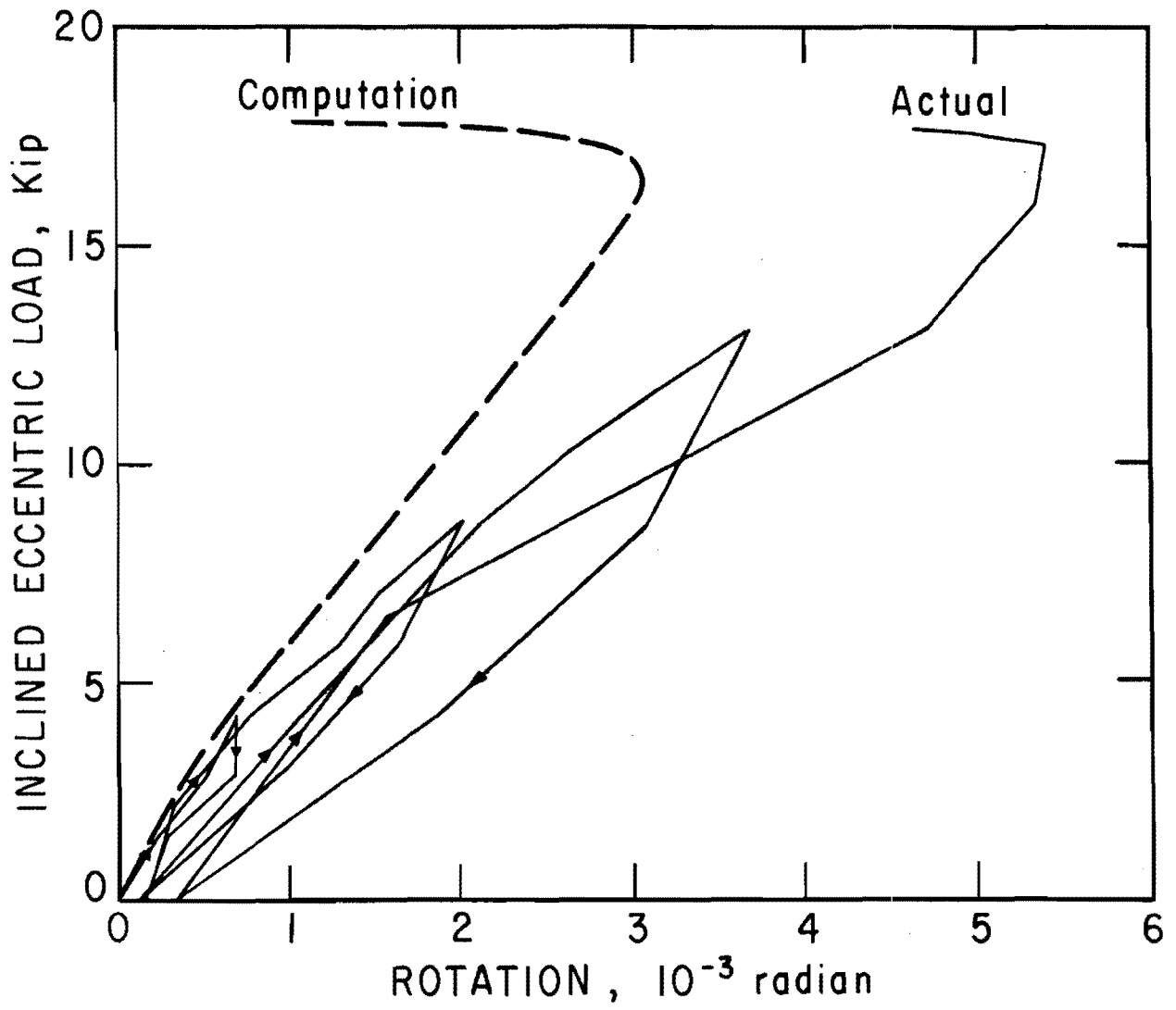


Fig. 6.12. Rotation of Cap 2

The comparison of analytical prediction with the experimental horizontal and rotational displacement curves (Figs. 6.11 and 6.12) shows a disparity for the higher loads. This disparity was caused by the change in the inclination angle of the resultant of applied load on the foundation. The inclined load on the foundation was given by a vertical jack and a horizontal jack attached at the center of four piles. The horizontal displacement of the pile cap gave some tilting to the vertical jack. The tilting of the vertical jack tended to become greater, because the loading beam for the vertical jack lacked stiffness against the horizontal force. Therefore, the inclination angle of the resultant of load on the foundation was greater at higher load than that assumed for the analytical computation.

Force. Figure 6.13 illustrates a typical example of pile reactions and force distribution within the piles, computed by the analytical method. The example shows the case where the foundation is subjected to an inclined load of 8,900 pounds which is about one-half the ultimate load. The axial soil reactions at pile tip shown in Fig. 6.15 do not mean that these forces really exist, but it merely indicates the assumption of uniform distribution of axial force in a pile, which was made to facilitate the computation of laterally loaded piles as a beam column.

The analytically computed pile forces are compared with the experimental measurements made by strain gages installed six inches below the pile tops. Figures 6.14, 6.15, and 6.16 show the load versus axial force and the bending moment relationships at these gage locations.

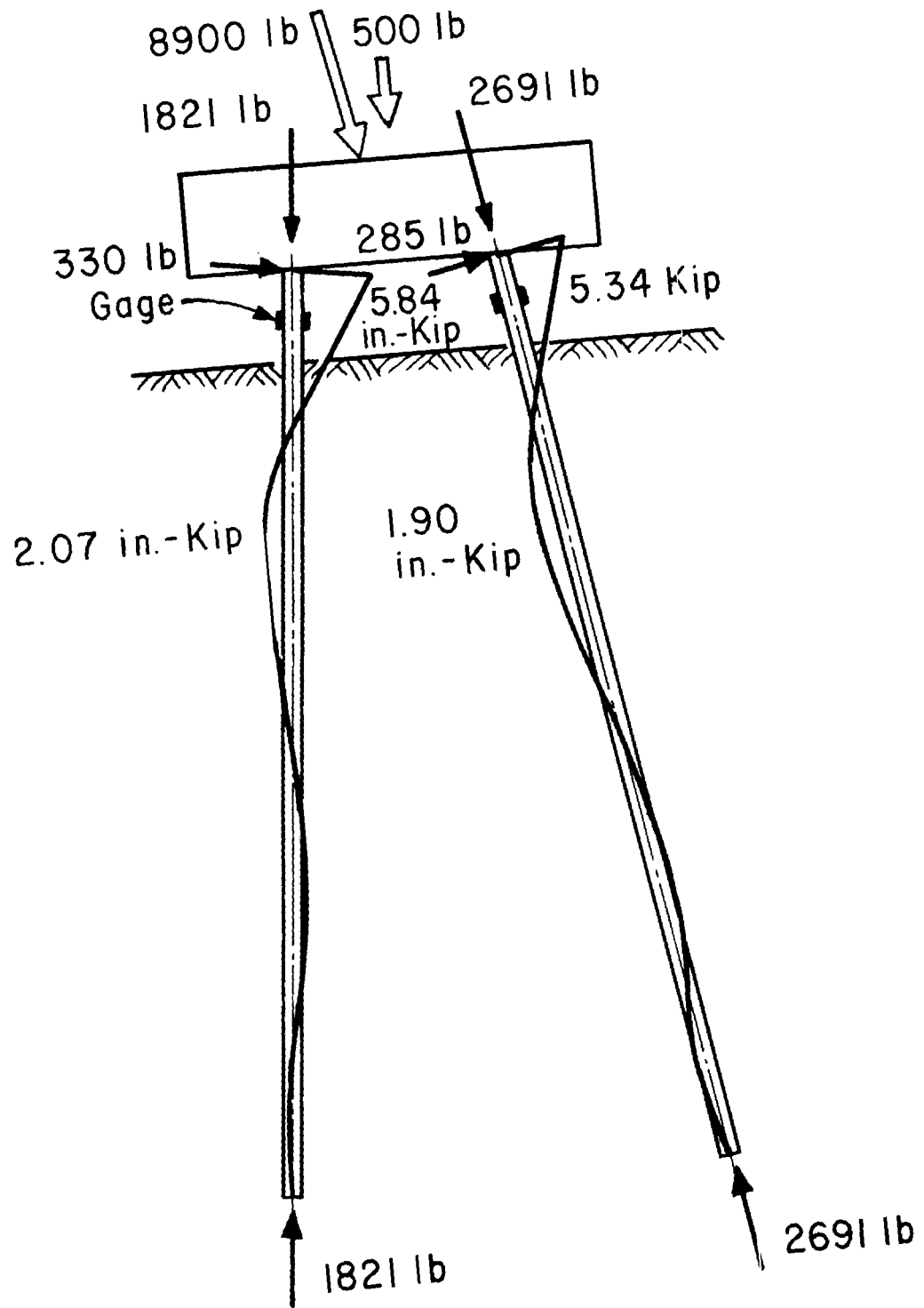


Fig. 6.13. Typical Distribution of Forces on Piles

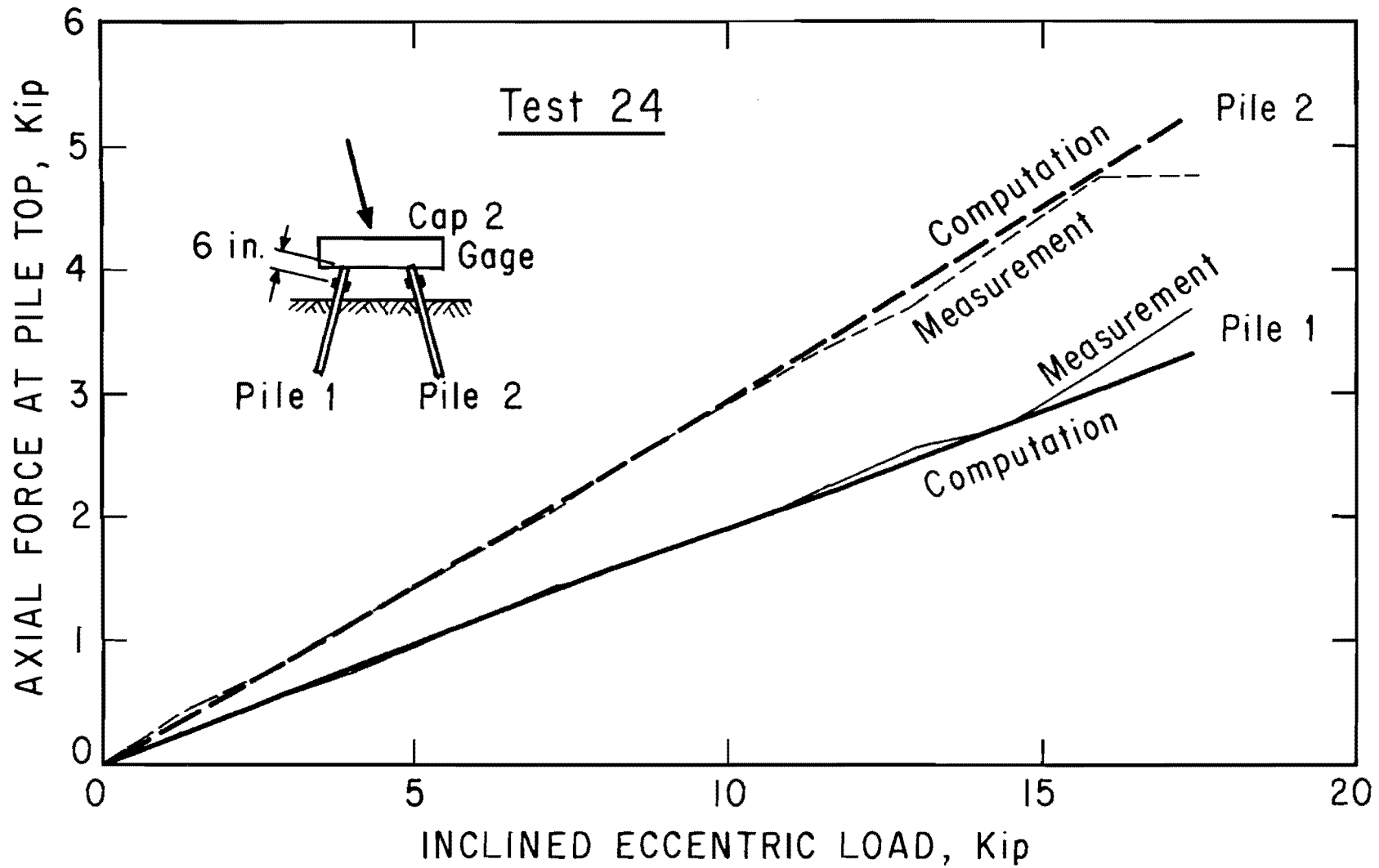


Fig. 6.14. Axial Forces at the Top of Individual Piles

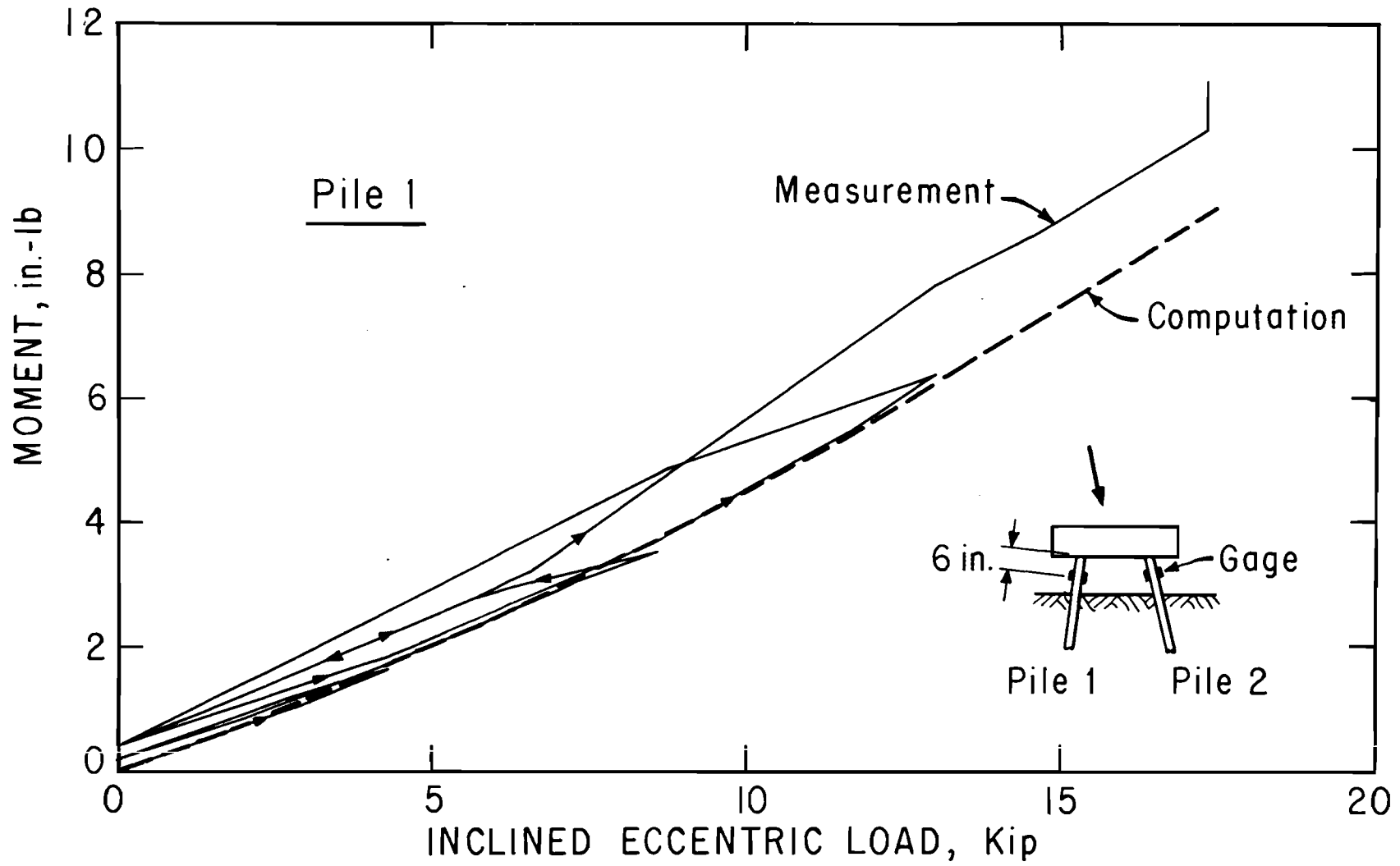


Fig. 6.15. Moment in Pile 1

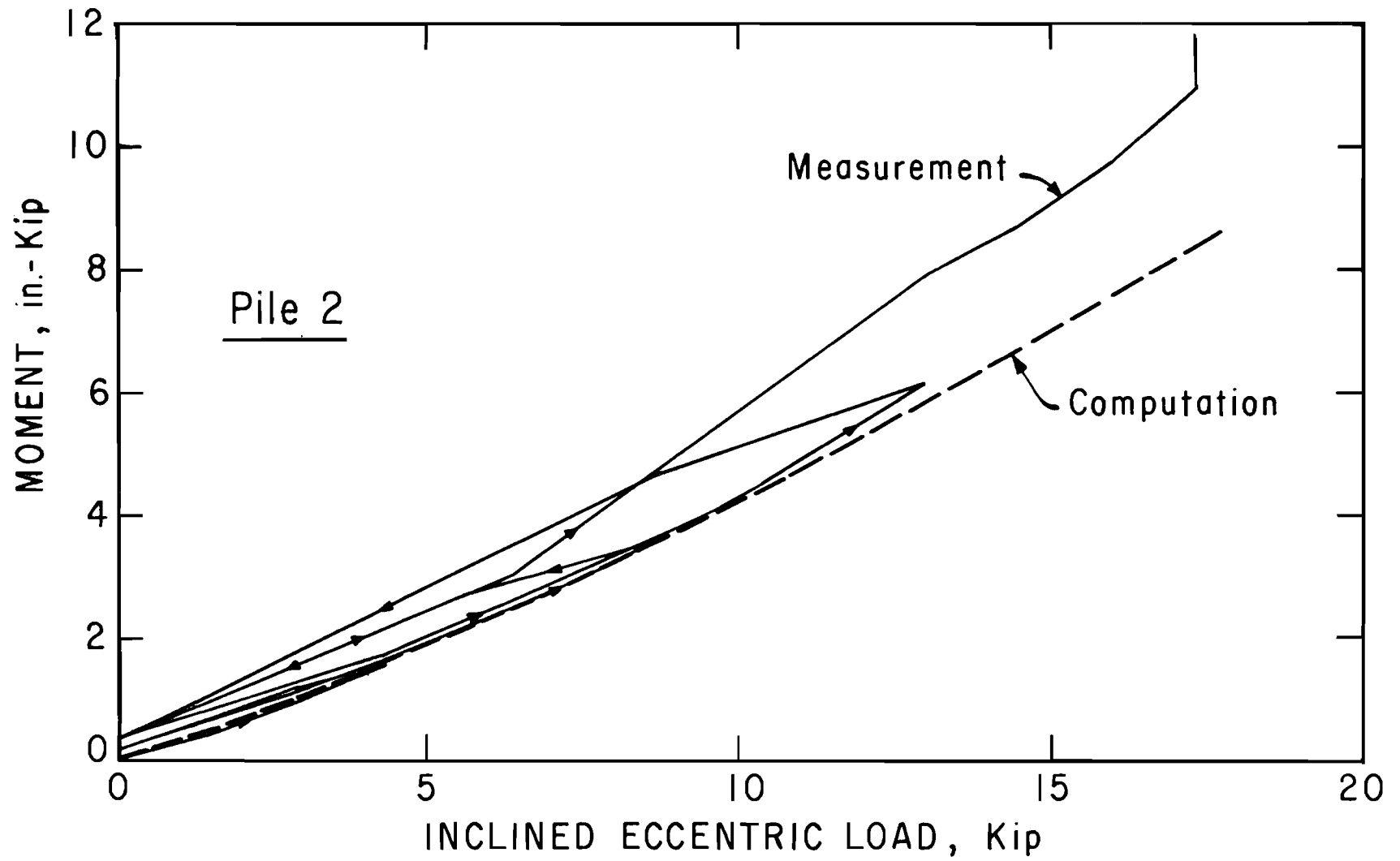


Fig. 6.16. Moment in Pile 2



Since the gages are installed at the pile portions which stand above the ground surface, the summation of axial forces in four piles must be equal to the vertical component of the resultant load. The axial forces in Fig. 6.14 are computed by applying the same normalizing factor to the two axial strain measurements in such a way as to produce equilibrium between the load and the pile reactions. The normalizing factor varied from one loading step to the other. Generally speaking, the normalizing factor becomes close to unity when the load is large. Still, in some instances the factor varied as much as 10 per cent from unity at large loads.

After the normalization of the data, the experimental measurements coincide with the theoretical prediction precisely except near the ultimate load.

The moment in the piles is computed from the bending strain measurement. In the absence of a proper way to calibrate or normalize the field data, the experimental moment is calculated by simply applying the laboratory calibration factor to the measured bending strain.

The comparison between the theoretical and the experimental moment at the gage location discloses that the computed values form the envelope for the experimental load versus moment curves (Figs. 6.15 and 6.16). For either pile the agreement between experiment and theory is good in the first three loading cycles. The deviation of the experimental value from theory is rather great in the last loading cycle in which the foundation was loaded to failure. This finding is consistent with the observed larger horizontal displacement of the pile cap.

### Discussion

The analysis of experiments on grouped pile foundations validates the analytical method of predicting the behavior of grouped pile foundations. If proper information is furnished, the analytical method is capable of making accurate predictions.

The experiment revealed that the accuracy of prediction is greatly dependent on the axial behavior of a pile. Referring to the single pile tests, the axial behavior or, in this case, the axial load versus pile-top displacement curve varies with the passage of time. It may change drastically depending on the past loading history on the pile. All these changes occurred for a pile in a sand. Seed and Reese (1957) report that the piles driven in clays showed changes in their axial behavior with the passage of time. Therefore, the importance of recognition of the axial loading history and the time of loading with regard to the time of pile installation must be stressed for any type of soil for making a realistic prediction of behavior of a grouped pile foundation.

The lateral behavior of a pile is prescribed by a set of  $p$ - $y$  curves or lateral soil resistance versus pile deflection curves given along the length of the pile. The analytical prediction employs rather simple bilinear  $p$ - $y$  curves generated after Reese's criteria. Reduction to the lateral soil resistance for out-batter piles was made according to Kubo's criteria. As the close prediction of laterally loaded single piles was made by these  $p$ - $y$  curves, no evidence was found in the analysis of grouped pile foundations that these  $p$ - $y$  curves are affecting the accuracy of prediction of behavior of a grouped pile foundation. The analysis of

the experiment is limited to the case of a submerged dense sand. However, presently available soil criteria are assumed to be capable of providing sufficiently accurate  $p$ - $y$  curves. With regard to the accuracy of  $p$ - $y$  curves, it must be remembered that the error in  $p$ - $y$  curves has only reduced effect on the prediction of pile-top reaction versus displacement relationship.

Experimental errors were induced by the misalignment of the applied load on the foundation. This problem can be solved by measuring the exact line of action of the load.

Variation between two symmetrical piles caused some experimental errors. However, its effect was not so great as to jeopardize the assumption of two-dimensionality of the foundation.

CHAPTER VII  
NUMERICAL EXAMPLES

Comparative analysis of some characteristic quantities are made for two examples of grouped pile foundations. In the first example, the effect of variation in the axial load settlement curve on the behavior of a grouped pile foundation is investigated. In the second example, the effect of the pile-top fixity to the pile cap on the total pile-cap displacement curve is examined.

The data coding and the computation results for the typical computer runs are given in Appendix A.

Example 1. Test Grouped Pile Foundation, Cap 2

Figure 7.1 shows the geometrical configuration of Cap 2. It consists of four steel pipe piles of two inches in diameter which are arranged symmetrically with respect to the plane of symmetry. These piles are rigidly connected to the pile cap. The pile properties are described in Chapter IV. Each individual pile group consists of two identical piles of 108 inches in length. All the piles are standing approximately 12 inches above the ground surface.

Cap 2 is subjected to a load inclined approximately 12 degrees in addition to a dead load of 500 pounds in the plane of symmetry. The resultant of the applied load is acting about 0.5 inch off the origin 0 of the structural coordinate system (X, Y), which is arbitrarily chosen at the center of the pile cap and level to the pile tops (Fig. 7.1) The load was increased incrementally until the foundation failed.

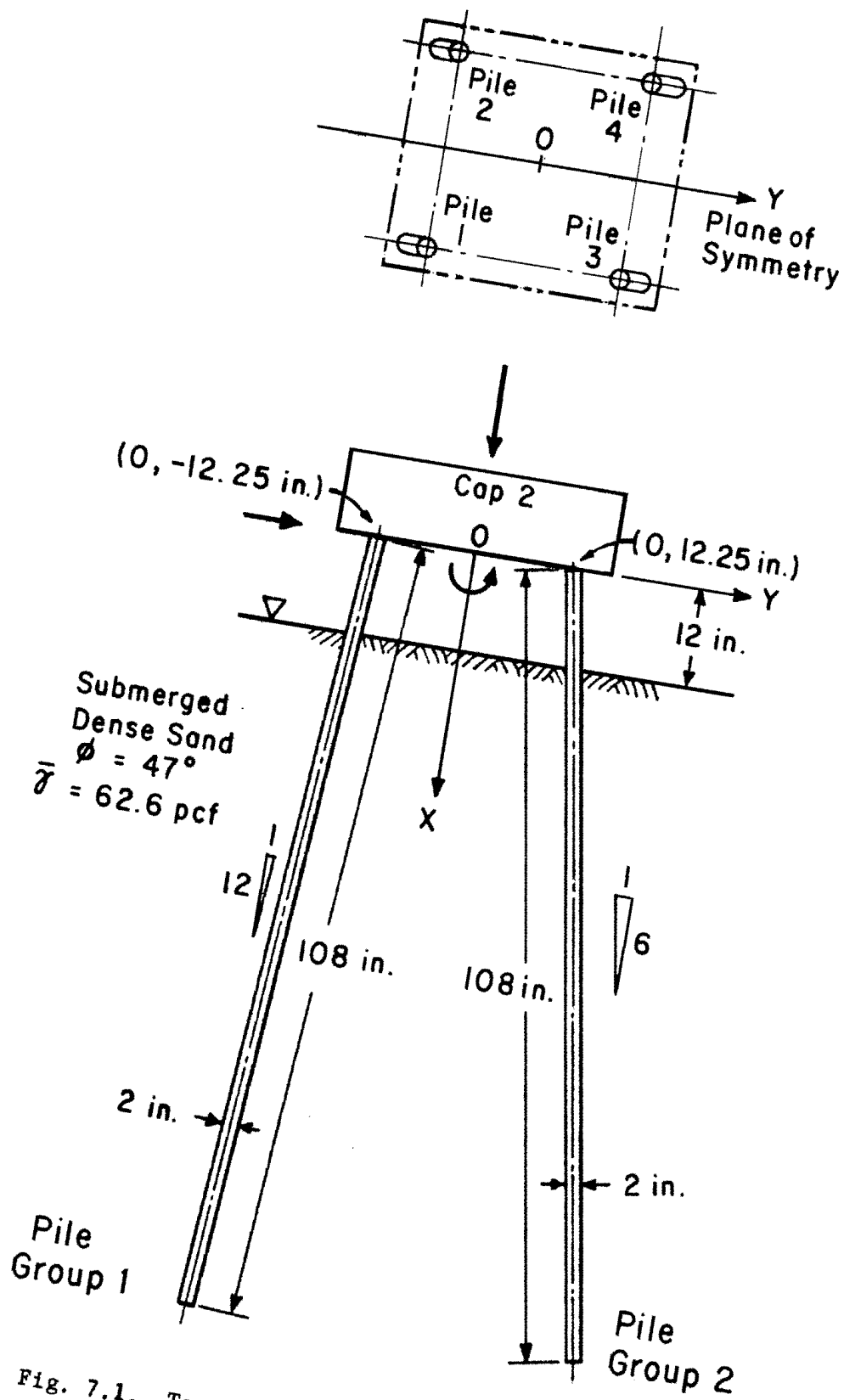


Fig. 7.1. Test Grouped Pile Foundation, Cap 2

The soil was uniform and homogeneous throughout. It consisted of a submerged dense sand with an angle of internal friction  $\phi$  of  $47^\circ$  and an effective unit weight  $\gamma$  of 62.6 pcf. A set of theoretical lateral soil resistance curves along a vertical pile are generated automatically by the computer program from the soil properties. No modification of the curves is made for an in-battered pile. The set of curves for the out-battered pile are modified. The modification of the lateral soil resistance curves is made according to Fig. 5.29. The modification factor for a 1 to 6 batter, or  $9^\circ 28'$  batter angle, is 0.73.

The computed vertical displacement curves of the pile cap are shown in Fig. 7.2. Case A was computed by making use of the axial load displacement curve of Test 22 on Pile 7 (Fig. 5.8). The ultimate bearing capacity in this test was 5,400 pounds. Case B was computed for Test 10 on Pile 5 (Fig. 5.6a) with the rest of the data remaining the same as Case A. The ultimate bearing capacity in Test 10 was 4,600 pounds. In Case C, the axial load displacement curve was replaced with that of Test 1 on Pile 9 (Fig. 5.3), in which the ultimate bearing capacity reached only 3,600 pounds.

The vertical displacement curves for Cases A, B, and C in Fig. 7.2 are almost similar to the corresponding axial load-displacement curves of single piles. It is proved quantitatively that the variation in the axial load displacement curve of a single pile is reflected by a similar variation in the prediction of behavior of grouped pile foundations.

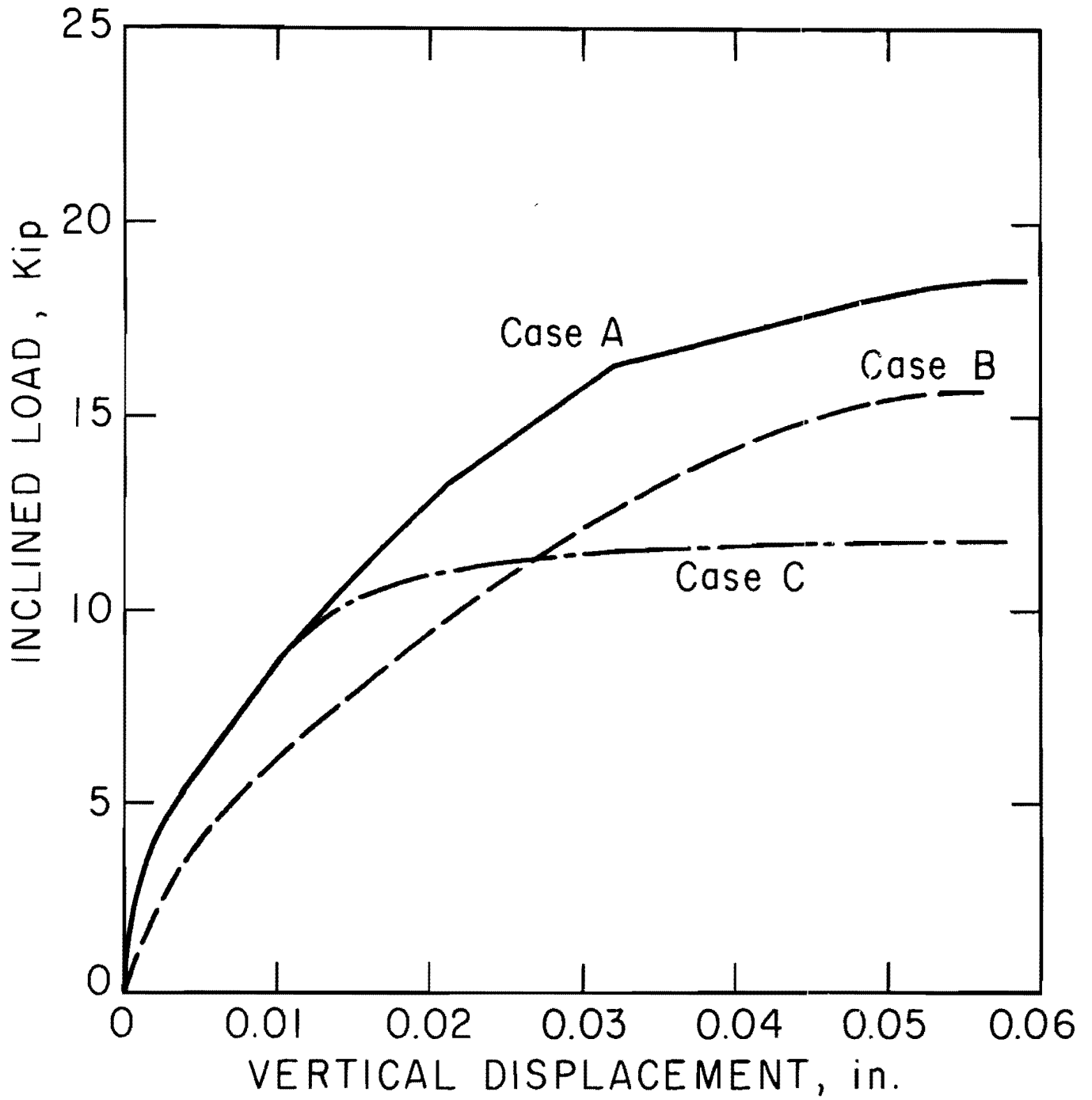


Fig. 7.2. Vertical Displacement of Cap 2

### Example 2. Copano Bay Causeway Bent

This example was taken from Parker and Cox (1969), who dealt with the foundation of one of the bents in the Copano Bay Causeway Bridge on Texas State Highway 35.

Figure 7.3 shows the configuration of the foundation. It consists of six 18-inch square prestressed concrete piles of 93 feet in length, which are assumed to be rigidly connected to the pile cap. Individual pile groups, Groups 1 and 4, consist of only one pile battered 1:4 in the plane of symmetry. Individual pile groups, Groups 2 and 3, consist of 2 piles battered 1:6 away from the plane of symmetry. However, Groups 2 and 3 are regarded as vertical piles, because the projection of these piles on the plane of symmetry is vertical. The distance from the pile top to the assumed scour line is approximately 10 feet.

The origin 0 of the structural coordinate system (X, Y) is chosen at the center of the cap and level to the pile tops.

The foundation is subjected to a vertical load of 844 kips and a horizontal load of 36.4 kips at the top of the bent which is 38.5 feet above the origin 0 of the structural coordinate system, which subsequently causes a moment of  $1.68 \times 10^4$  kip-inch around the origin 0. The computation is done for a constant vertical load of 844 kips and for a varying horizontal load at 38.5 feet above the origin 0. The horizontal load was increased until the foundation failed.

Figure 7.4 shows the section of the prestressed concrete pile. The prestressed concrete pile has an 18-inch square section with ten 0.5 inch diameter 270 k strands. The final prestress on the concrete was 718 psi.



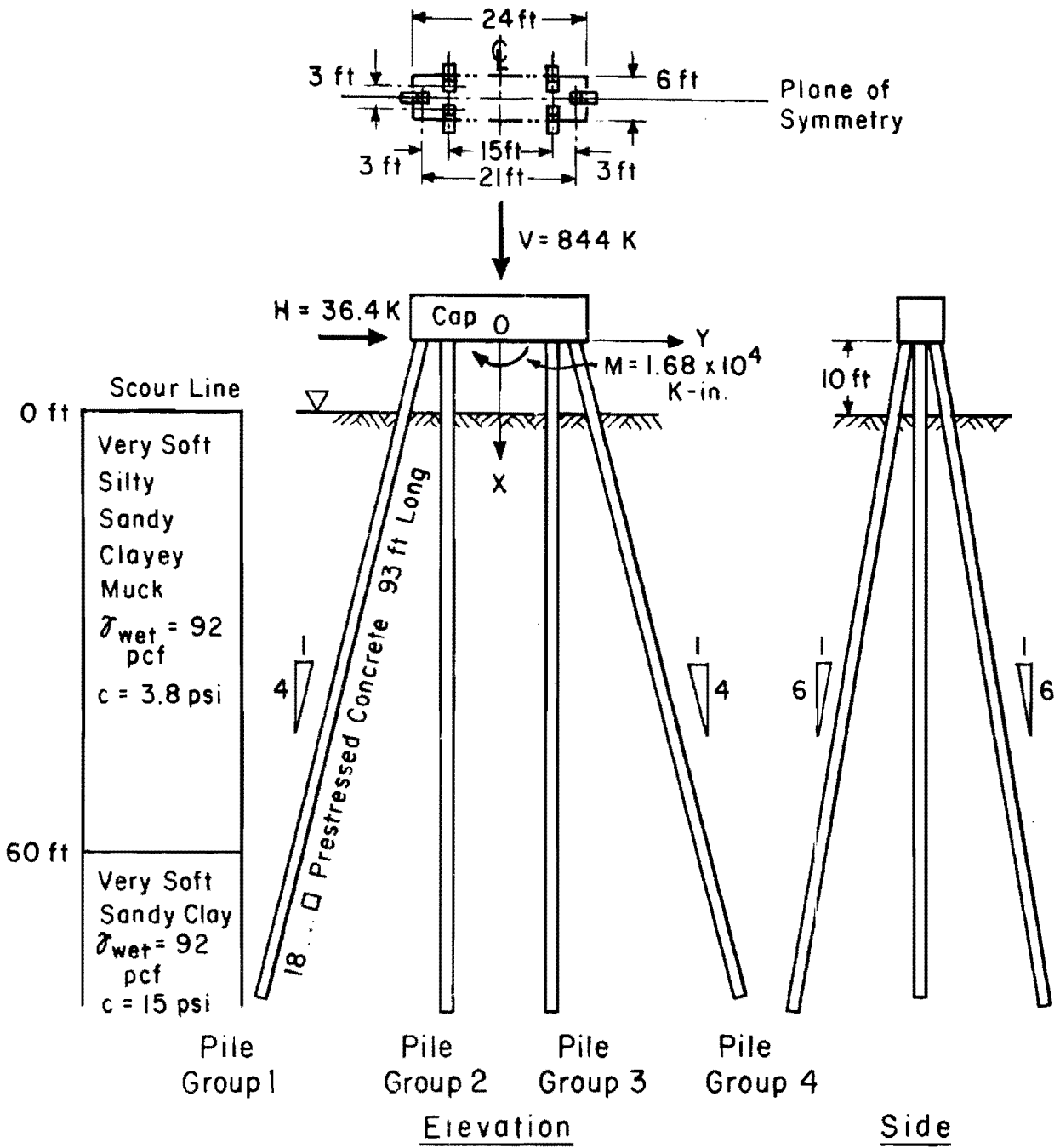


Fig. 7.3. Copano Bay Causeway Bridge Foundation

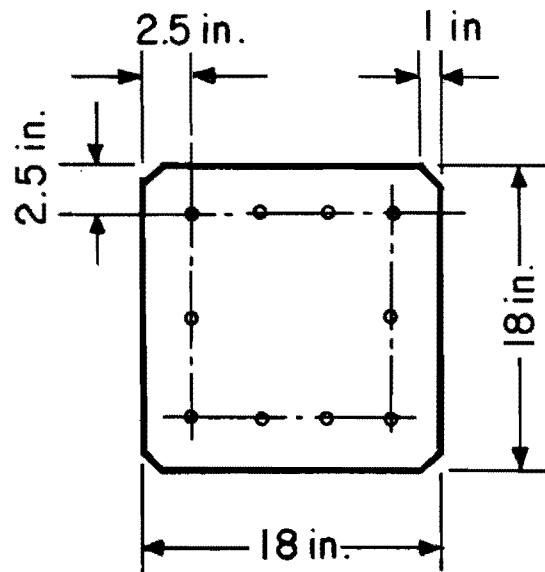


Fig. 7.4. Section of Prestressed Concrete Pile

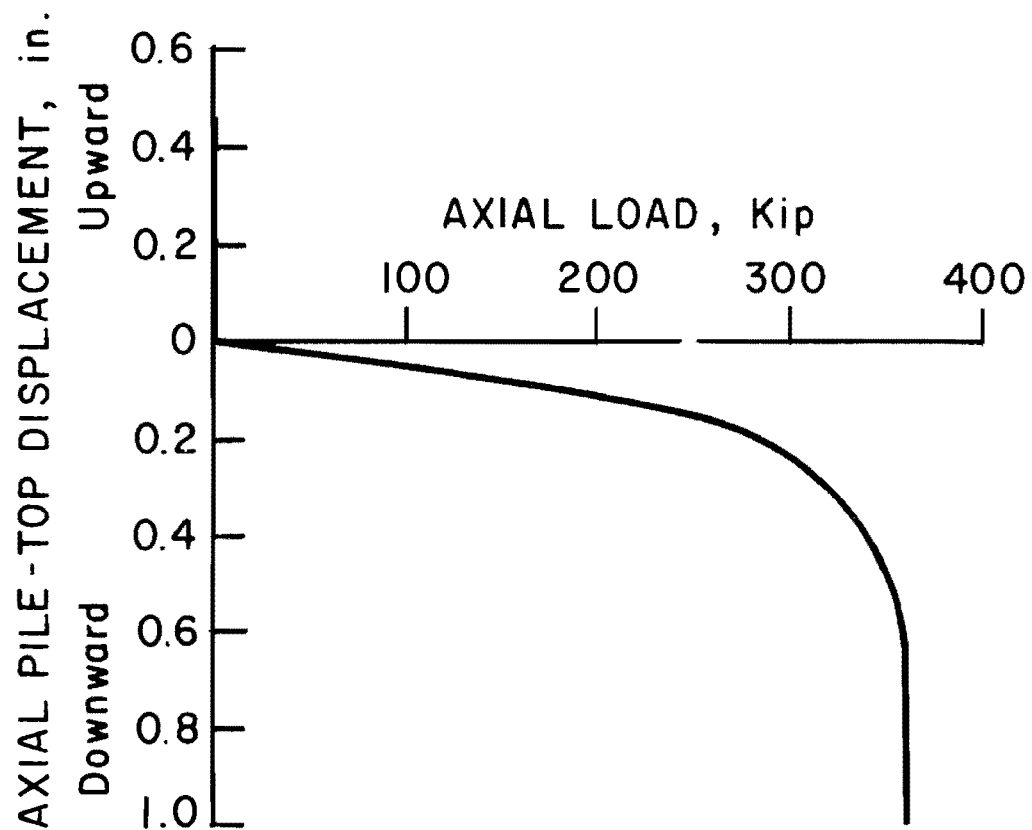


Fig. 7.5. Axial Load versus Pile-Top Displacement

The compressive strength of the concrete is assumed to be 6,000 psi. The moment of inertia of the section is 8,600 inches<sup>4</sup>. The Young's modulus of the concrete may be computed from the formula, Eq. 7.1;

$$E = 57,400 \sqrt{\sigma_c} \dots \dots \dots (7.1)$$

where

E = Young's modulus of concrete in psi, and

$\sigma_c$  = compressive strength of concrete in psi

The concrete of 6,000 psi compressive strength gives the Young's modulus  $4.44 \times 10^6$  psi. In this case the pile is regarded as linearly elastic throughout, with the assumption that the maximum stress in the pile is always in the elastic range.

The result of an axial loading test is given in Fig. 7.5. Judging from the resistance of the pile-head connection to the pile cap, no uplift resistance from each pile is assumed, as is shown in Fig. 7.5.

The theoretical lateral soil resistance curves for a vertical pile is generated automatically by the computer program from soil properties. The modification of the curves for the batter piles is made according to Fig. 5.29. The modification factor for the 1 to 6 in-batter and out-batter piles are 1.30 and 0.73, respectively.

The horizontal displacement of the pile cap is shown in Fig. 7.6. The other components of displacement, vertical and rotational, are not shown because these components are of secondary importance for this loading condition.

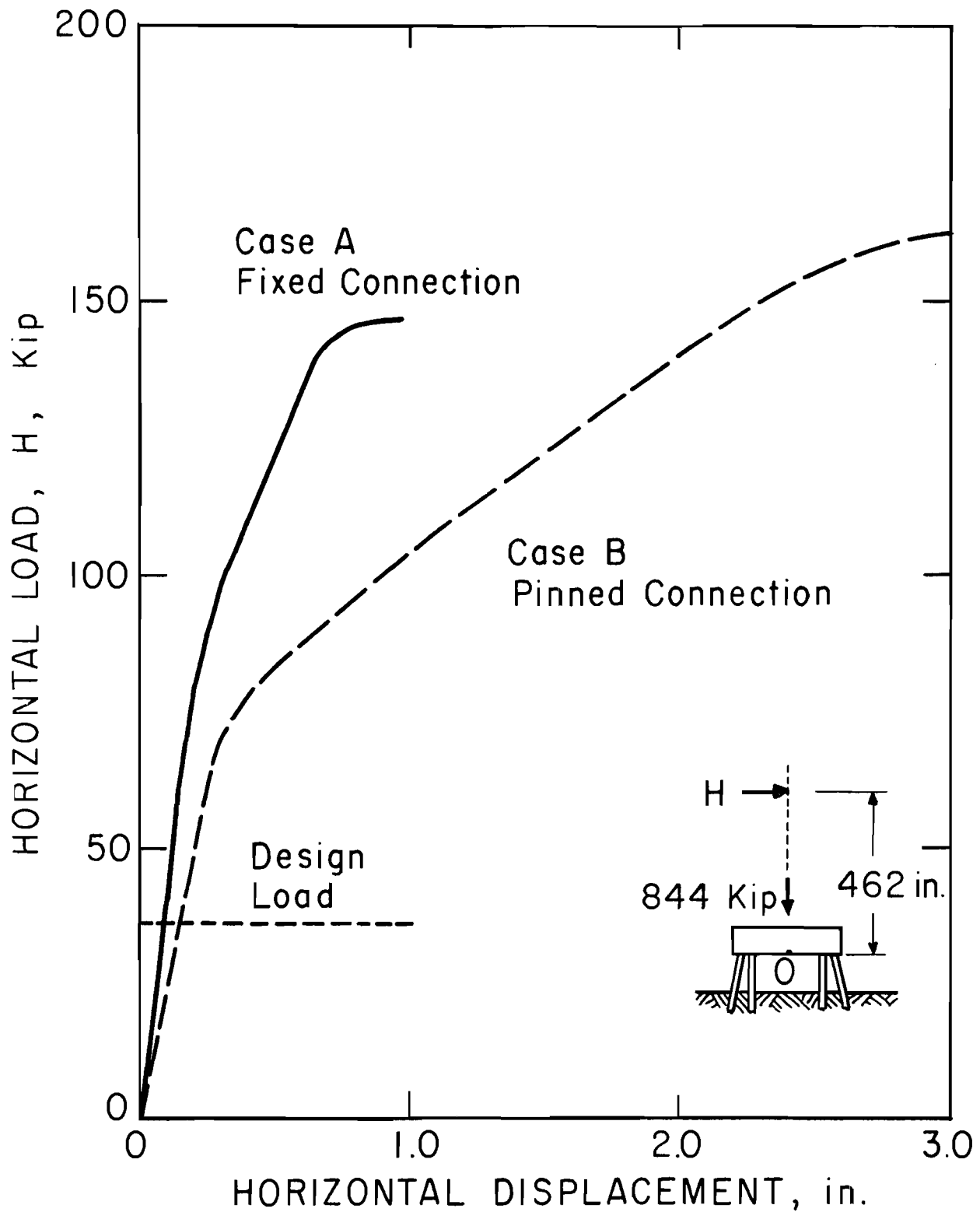


Fig. 7.6. Horizontal Pile Cap Displacement, Copano Bay Causeway Bridge Foundation

In Fig. 7.6, Case A is computed for the case where all the pile tops are fixed to the pile cap. Case B shows the horizontal displacement curve for the other extreme case where all the pile tops are connected to the pile cap by pins.

The actual fixity of the pile top to the pile cap may be assumed somewhere between these two limiting cases. The failure of the foundation for Cases A and B is caused by the failure of the piles in the axial bearing capacity. The ultimate horizontal load for the Cases A and B are almost the same, however, the difference in horizontal displacement between the two is great. The ultimate horizontal load for Case A is slightly less than that of Case B. The difference is due to the smaller lateral soil reaction for Case A, in which the axial pile resistance has a greater role in achieving the equilibrium of forces.

## CHAPTER VIII

### CONCLUSIONS AND RECOMMENDATIONS

The following conclusions are made from the analysis of grouped pile foundations.

1. The numerical successive displacement correction method is an effective way to solve the problem of a two-dimensional grouped pile foundation under an arbitrary static short-term loading.
2. The plan of the experimental program was adequate for demonstrating the validity of the theory for the behavior of a grouped pile foundation.
3. Single pile behavior as determined by experiment was used in the theory for grouped pile behavior and the theory predicted the behavior of the grouped pile foundation which agreed well with the behavior of the grouped pile foundation determined by experiment.
4. The analyses of the experiments revealed that the accuracy of prediction of the behavior of a grouped-pile foundation is critically affected by the accuracy of prediction of the axial behavior of single piles.
5. The theory for the behavior of an axially loaded pile in sand can describe only in a limited way the actual behavior.
6. The analyses of the experiments revealed that the presently available theory for a laterally loaded pile in sand can give sufficiently accurate predictions of the lateral behavior of single piles for use in the analysis of grouped pile foundations.

7. The modification for an out-battered pile can be made accurately by Kubo's criteria, while in-battered test piles did not show the effect of batter.

It is recommended that grouped pile foundations be designed by using the procedure listed below.

1. Determine subsoil conditions using standard techniques in engineering practice.
2. Generate lateral soil resistance versus deflection curves (p-y curves) using soil criteria described in Chapter III. (The computer program GROUP can generate p-y curves automatically if soil properties are specified.)
3. Modify p-y curves for out- and in-battered piles by Kubo's criteria.
4. Conduct axial loading tests at the site to obtain curves giving axial load versus displacement or make the best estimate of such curves using available theory.
5. Estimate the load on the foundation.
6. Choose a pile arrangement, pile material, and pile dimensions.
7. Run the computer program GROUP for the solution with the information obtained above.
8. Repeat Steps 6 and 7 to improve the solution.

Computer programs LLP and AXP may be used for the analysis of the lateral and the axial behavior of a single pile, respectively.

Future research is recommended in order to be able to make a more accurate prediction of the behavior of a grouped pile foundation.

Specific investigations which need to be carried out are:

1. Performing similar studies to those reported herein on grouped pile foundations in clays.
2. Investigation of the "group effect" between piles.
3. Development of more accurate methods for predicting the behavior of an axially loaded pile.
4. Examination of the interaction between the axial and lateral behavior of a pile.
5. Experiments on the full-sized grouped pile foundations.



This page replaces an intentionally blank page in the original.

-- CTR Library Digitization Team

## REFERENCES

1. Aschenbrenner, Rudolph (1967), "Three Dimensional Analysis of Pile Foundations," Journal of the Structural Division, American Society of Civil Engineers, Vol. 93, No. ST1, No. 5097, February, 1967, pp. 201-219.
2. Asplund, S. O. (1956), "Generalized Elastic Theory for Pile Groups," Publications, International Association for Bridge and Structural Engineering, Vol. 16, 1956, pp. 1-22.
3. Chang, Y. L. (1937), Discussion on "Lateral Pile-Loading Tests," by Feagin, Transactions, American Society of Civil Engineers, 1937.
4. Coyle, H. M. and Reese, L. C. (1966), "Load Transfer for Axially Loaded Piles in Clay," Journal of the Soil Mechanics and Foundations Division, American Society of Civil Engineers, Vol. 92, SM2, paper No. 4702, March, pp. 1-26.
5. Coyle, H. M. and Sulaiman, I. H. (1967), "Skin Friction for Steel Piles in Sand," Journal of the Soil Mechanics and Foundations Division, American Society of Civil Engineers, Vol. 93, SM 6, paper No. 5590, November, pp. 261.
6. D'Appolonia, E. and Romualdi, J. P. (1963), "Load Transfer in End Bearing Steel H-Piles," Journal of the Soil Mechanics and Foundations Division, American Society of Civil Engineers, Vol. 89, No. SM2, No. 3450, March, 1963, pp. 1-25.
7. Feagin, L. B. (1953), "Lateral Load Tests on Groups of Battered and Vertical Piles," Special Technical Publication No. 154, American Society of Testing and Materials, July, 1953, pp. 12-20.
8. Francis, Arthur J. (1964), "Analysis of Pile Groups with Flexural Resistance," Journal of Soil Mechanics and Foundations Division, American Society of Civil Engineers, Paper 3887, May, 1964, pp. 1-32.
9. Hansen, Bent, (1959), "Limit Design of Pile Foundations," Bygningsstatistiske Meddelelser Argang XXX, No. 2, September, 1959.
10. Hrennikoff, A. (1950), "Analysis of Pile Foundations with Battered Piles," Transactions, American Society of Civil Engineers, Vol. 115, Paper No. 2401, 1950.

11. Karol, R. H. (1960), Soils and Soil Engineering, Prentice Hall, Englewood Cliffs, New Jersey, 1960.
12. Kishida, Hideaki (1967), "Ultimate Bearing Capacity of Piles Driven into Loose Sand," Soil and Foundation, Vol. VII, No. 3, 1967.
13. Matlock, Hudson and Reese, Lymon C., (1962), "Generalized Solution for Laterally Loaded Piles," Transactions, American Society of Civil Engineers, Vol. 127, Part I, 1962, pp. 1220-1251.
14. Matlock, Hudson and Ingram, Wayne B. (1963), "Bending and Buckling of Soil Supported Structural Elements," Paper No. 32, Proceedings, Second Pan-American Conference on Soil Mechanics and Foundation Engineering, Brazil, July, 1963.
15. Matlock, Hudson (1963), "Application of Numerical Methods to Some Problems in Offshore Operations," Journal of Petroleum Technology, Vol. 15, No. 9, September, 1963, pp. 1040-1046.
16. Matlock, Hudson and Haliburton, Allan T. (1966), "Finite-Element Method of Solution for Linearly Elastic Beam-Columns," Research Report Number 56-1, Center for Highway Research, The University of Texas at Austin, Austin, Texas, September, 1966.
17. Matlock, Hudson (1970), "Correlations for Design of Laterally Loaded Piles in Soft Clay," Offshore Technology Conference, Paper No. OTC 1204, 1970.
18. Mattes, Neil S. and Poulos, Harry G. (1969), "Settlement of Single Compressible Pile," Journal of the Soil Mechanics and Foundations Division, American Society of Civil Engineers, January, 1969, No. SM1, pp. 189-207.
19. McClelland, B., and Focht, J. A., Jr. (1958), "Soil Modulus for Laterally Loaded Piles," Transactions, American Society of Civil Engineers, Vol. 123, Paper No. 2954, 1958, pp. 1049-1085.
20. McClelland, B., Focht, J. A., and Emrich, W. J. (1969), "Problems in Design and Installation of Offshore Piles," Journal of the Soil Mechanics and Foundations Division, American Society of Civil Engineers, Vol. 95, No. SM6, November 1969, pp. 1491-1514.
21. Meyerhof, G. G. (1959), "Compaction of Sands and Bearing Capacity of Piles," Journal of the Soil Mechanics and Foundations Division, American Society of Civil Engineers, Vol. 85, No. SM6, Part I, December, 1959, pp. 1-59.

22. Palmer, L. A. and Brown, P. O. (1954), "Piles Subjected to Lateral Earth Support," Special Technical Publication No. 154, American Society of Testing and Materials, July, 1953.
23. Parker, Frazier, Jr., and Cox, William R. (1969), "A Method for the Analysis of Pile Supported Foundations Considering Nonlinear Soil Behavior," Research Report No. 117-1, Center for Highway Research, The University of Texas at Austin, Austin, Texas, June 1969.
24. Parker, Frazier, Jr., and Reese, Lymon C. (1970), "Experimental and Analytical Studies of Behavior of Single Piles in Sand Under Lateral and Axial Loading," Research Report No. 117-2, Center for Highway Research, The University of Texas at Austin, Austin, Texas, November 1969.
25. Poulos, H. G. and Davis, E. G. (1968), "The Settlement Behavior of Single Axially Loaded Incompressible Piles and Piers," Geotechnique, Vol. 18, No. 3, September 1968, pp. 351-371.
26. Poulos, H. G. (1968), "Analysis of the Settlement of Pile Groups," Geotechnique, Vol. 18, 1968, pp. 449-471.
27. Poulos, H. G. and Mattes, N. S. (1969), "The Behavior of Axially Loaded End Bearing Piles," Geotechnique, Vol. 19, No. 7, June 1969, pp. 285-300.
28. Prakash, Shamsar (1961), Behavior of Pile Groups Subjected to Lateral Loads, Department of Civil Engineering, University of Illinois, Urbana, Illinois, December, 1961.
29. Radosavljević, Z. (1957), "Calcul et Essais des Pieux en Groupe," Proceedings, Fourth International Conference on Soil Mechanics and Foundation Engineering, Vol. 2, pp. 56-60, London, 1957.
30. Reese, Lymon C. (1958), Discussion on "Soil Modulus for Laterally Loaded Piles," by McClelland Focht, Transaction, American Society of Civil Engineers, Vol. 123, 1958, pp. 1071-1077.
31. Reese, Lymon C., Matlock, H., and Dunaway, Jr. (1960), "Foundation Analysis for the Bay Marchange Y-Structure," unpublished report to the California Company, May 1960.
32. Reese, Lymon C. and Matlock, Hudson (1960), "Numerical Analysis of Laterally Loaded Piles," Proceedings, Second Structural Division Conference on Electronic Computation, American Society of Civil Engineers, Pittsburg, Penn., 1960, pp. 657.

33. Reese, Lymon C. and Matlock, Hudson (1966a), "Behavior of a Two-Dimensional Pile Group Under Inclined and Eccentric Loading," Proceedings, Offshore Exploration Conference, Long Beach, California, February 1966.
34. Reese, Lymon C. (1966b), "Analysis of a Bridge Foundation Supported by Batter Piles," Proceedings, Fourth Annual Engineering and Geology and Soils Engineering Symposium, Moscow, Idaho, April 1966, p. 61.
35. Reese, Lymon C. and O'Neill, Mike W. (1967), "The Analysis of Three-Dimensional Pile Foundations Subjected to Inclined and Eccentric Loads," Proceedings of the Conference on Civil Engineering in the Oceans, American Society of Civil Engineers, September 1967, pp. 245-276.
36. Reese, Lymon C., and O'Neill, M. W. (1970), "Generalized Analysis of Pile Foundations," Journal of the Soil Mechanics and Foundations Division, American Society of Civil Engineers, Proceedings, Vol. 96, No. SM1, Paper No. 7032, January 1970, pp. 235-250.
37. Robertson, Robert N. (1961), "The Analysis of a Bridge Foundation with Batter Piles," M.S. Thesis, The University of Texas at Austin, Austin, Texas, January 1961.
38. Robinsky, E. I. and Morrison, C. F. (1964), "Sand Displacement and Compaction Around Model Friction Piles," Canadian Geotechnical Journal, Vol. 1, No. 2, March 1964, pp. 81-93.
39. Saul, William E., (1968), "Static and Dynamic Analysis of Pile Foundations," Journal of the Structural Division, American Society of Civil Engineers, Paper 5936, ST5, May 1968, pp. 1077-1100.
40. Seed and Reese (1957), "The Action of Soft Clay Along Friction Piles," Transactions, American Society of Civil Engineers, 1957, pp. 731-764.
41. Shinohara, Tomio and Kubo, Koichi (1961), "Experimental Study on the Lateral Resistance of Piles, Part 1," (In Japanese), Monthly Report of Transportation Technical Research Institute, Japan, Vol. II, No. 6, July 1961.
42. Skempton, A. W. (1951), "The Bearing Capacity of Clays," Building Research Congress, Division 1, Part III, 1951, pp. 180-189.

43. Skempton, A. W., Yassin, A. A., and Gibson, R. E. (1953), "Theorie de la force portante des pieux dans le sable," Ann. Institute, Batim., No's. 63-64, 1953.
44. Terzaghi, K. (1955), "Evaluation of Coefficients of Subgrade Reaction," Geotechnique, December, 1955.
45. Terzaghi, Karl (1956), Theoretical Soil Mechanics, John Wiley and Sons, New York, 1956, pp. 363-366.
46. Thurman, A. G. and D. Appolonia E. (1965), "Computed Movement of Friction and End Bearing Piles Embedded in Uniform and Stratified Soils." Proceedings, Sixth International Conference on Soil Mechanics and Foundation Engineering, Vol. 2, pp. 323-327.
47. Tschebotarioff, Gregory P., (1953), "The Resistance to Lateral Loading of Single Piles and of Pile Groups," Special Technical Publication No. 154, American Society of Testing and Materials, July 1953, pp. 38-48.
48. Turzynski, L. D. (1960), "Groups of Piles Under Mono-planar Forces," Structural Engineer, Vol. 38, No. 9, 1960, p. 286.
49. Vesić, A. S. (1963), "Bearing Capacity of Deep Foundations in Sand," Highway Research Record, No. 3, 1963, pp. 112-153.
50. Vesić, A. S. (1965), "Ultimate Loads and Settlements of Deep Foundations in Sand," Proceedings, Symposium on Bearing Capacity and Settlement of Foundations, National Science Foundation, Durham, North Carolina, 1965, pp. 53-58.
51. Vesić, A. S. (1968), "Experiments with Instrumental Pile Groups in Sand," Performance of Deep Foundations, Special Technical Publications No. 444, American Society for Testing Materials, 1968, pp. 177-222.
52. Walker, B. P. and Whitaker, T. (1967), "An Apparatus for Forming Uniform Beds of Sand for Model Foundation Tests," Geotechnique, Vol. 17, No. 2, June 1967, pp. 161-167.
53. Wen, R. K. L. (1955), "Model Studies of Laterally Loaded Foundations," Proceedings, Highway Research Board, Vol. 30, 1955, pp. 100-152.
54. Woodward, R. J., Lundgren, R., and Boitano, J. D. (1961), "Pile Loading Tests in Stiff Clays," Proceedings, Fifth International Conference on Soil Mechanics and Foundation Engineering, Paris, Vol. 2, 1961, pp. 177-184.

This page replaces an intentionally blank page in the original.

-- CTR Library Digitization Team

## APPENDIX A

### COMPUTER PROGRAM GROUP

#### A.1 Description of the Program

The computer program GROUP can be employed to solve for the behavior of a two-dimensional grouped pile foundation. The program is written in FORTRAN IV. It solves for the displacement of the pile cap and for the distribution of forces among and within piles for a given load. The program must be furnished with information on the load, the arrangement of individual pile groups, the dimensions and material properties of the piles, the axial pile-top displacement curves, and the lateral soil resistance curves or the soil data for the automatic generation of the lateral soil resistance curves.

The program consists of the main program GROUP and the subroutines MAKE, FVEC, AXIAL, LLP, MCURV, SOIL 2R, and MULT. The general flow diagram of the program is given on the next sheet. The function of each subprogram is described below briefly.

The main program GROUP reads in and prints out all the data which are commonly used by all the subprograms. This program performs the operation of seeking the equilibrium between the external load and the pile reactions by the successive displacement correction method.

The subroutine MAKE generates the theoretical lateral soil resistance curves from the soil data. Reese's soil criteria for sand and for clay that are introduced in Chapter IV, are the basis for this program. The



original program was written by Parker and Cox (1969). Some modifications to the program were made.

The subroutine FVEC solves for the axial and lateral reaction and for the moment at the top of individual piles.

The subroutine AXIAL interpolates the axial pile top reaction from the axial pile top displacement curve.

The subroutine LLP solves for the lateral reaction and the moment of a laterally loaded pile for the given displacement by the finite difference method.

The subroutine MCURV calculates the flexural rigidity EI at all the stations. If an interaction diagram of the yield axial force and the plastic moment is given, the subroutine resets the EI value for the plastic hinges.

The subroutine SOIL 2R interpolates the lateral soil resistance at each station from a set of lateral soil resistance curves given along the pile.

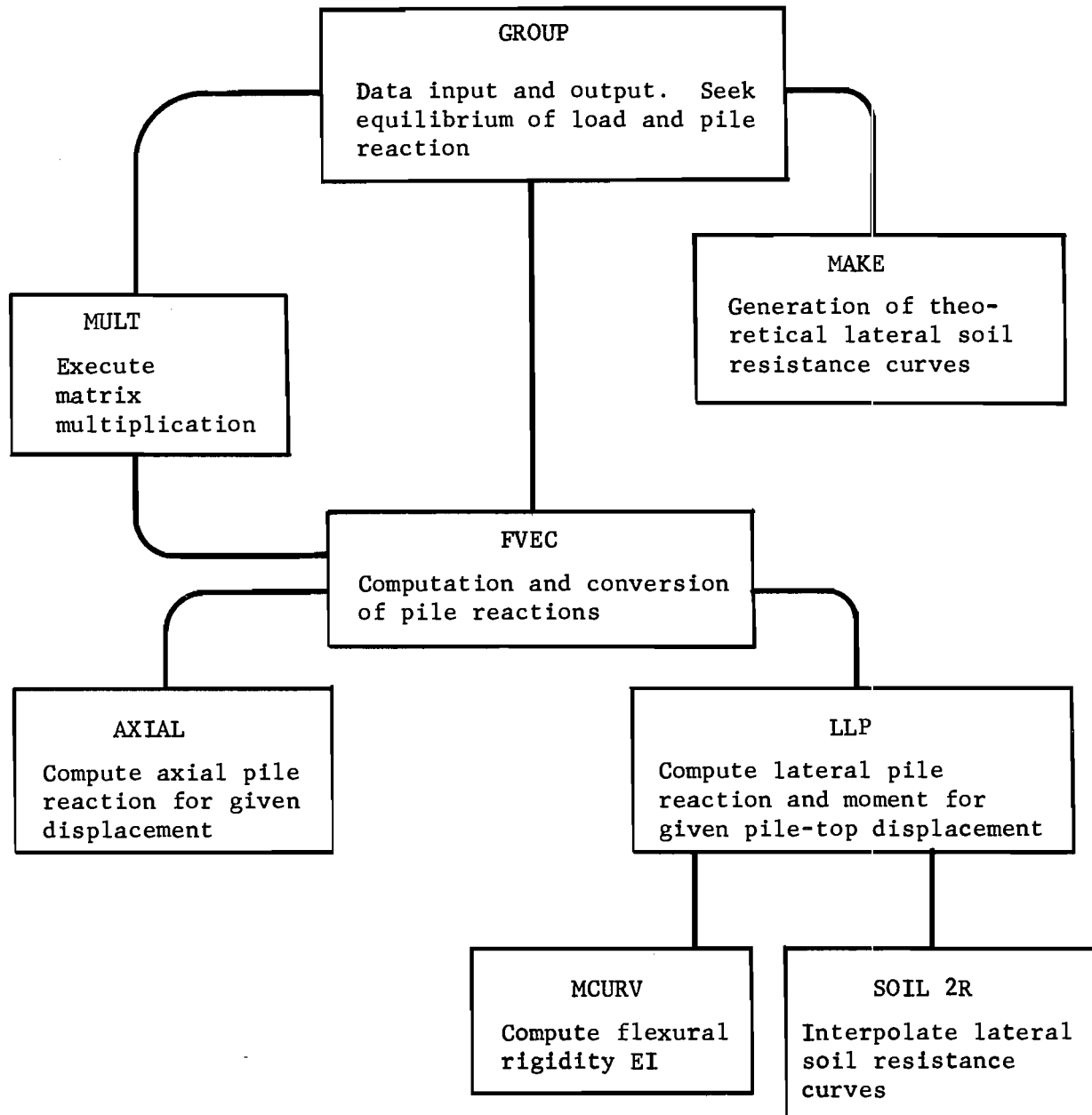
The subroutine MULT is a short program to perform the matrix multiplication.

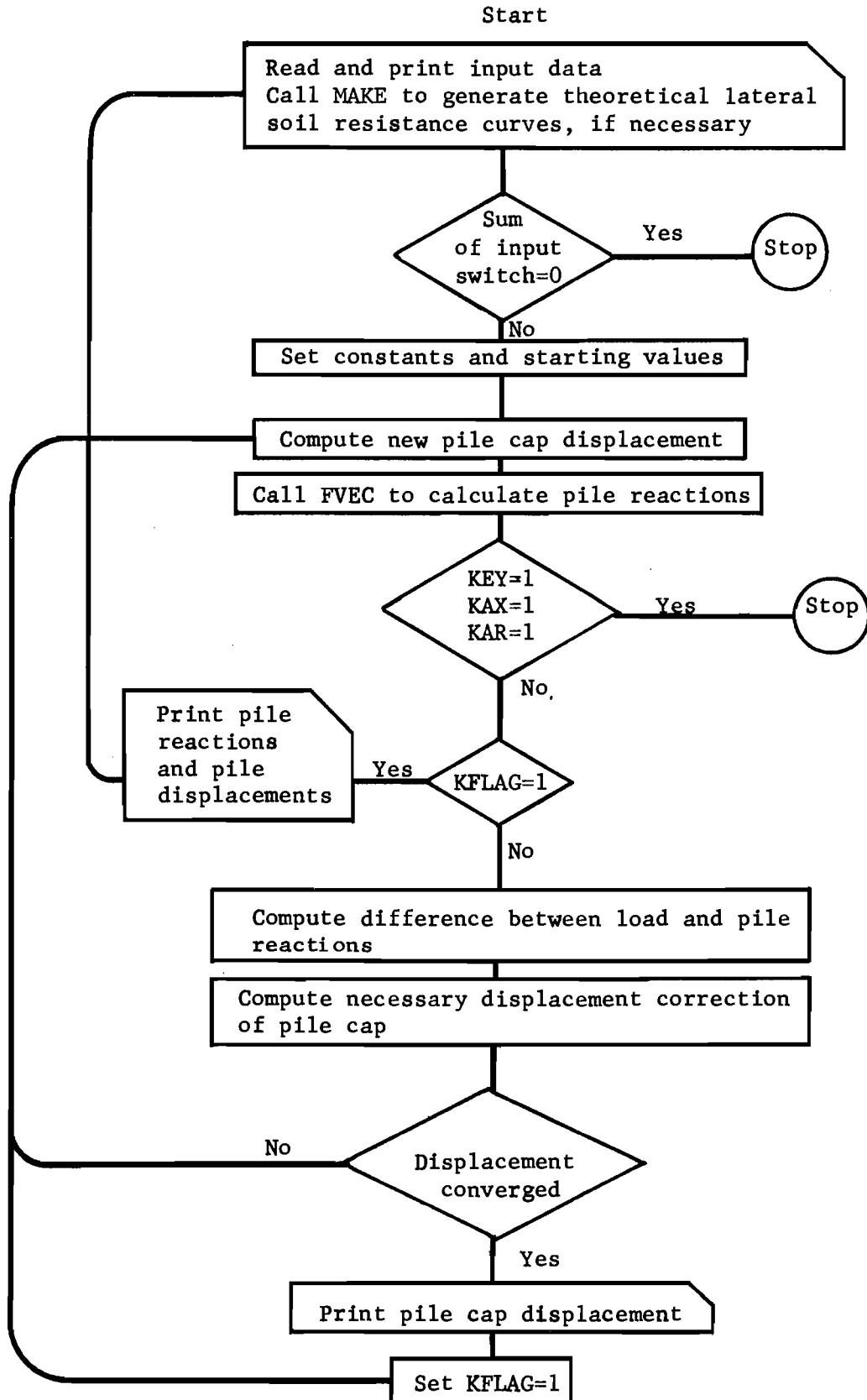
Inside the program the partial derivatives are computed for an increment of  $10^{-5}$  times unit displacement. Prior to the iteration, a pile cap is given an initial displacement of 0.01 times unit displacement in the X and Y directions. The tolerance for the convergence of displacement is set as  $10^{-5}$  times unit displacement. The iteration in the main program GROUP is stopped after 100 times. The iteration in the subroutine LLP is stopped after 1,000 times.

On the following pages are given the flow diagram of each subprogram, the glossary of notations, the listing of the program, the coding form of the input data, the example data coding and the example problem runs.

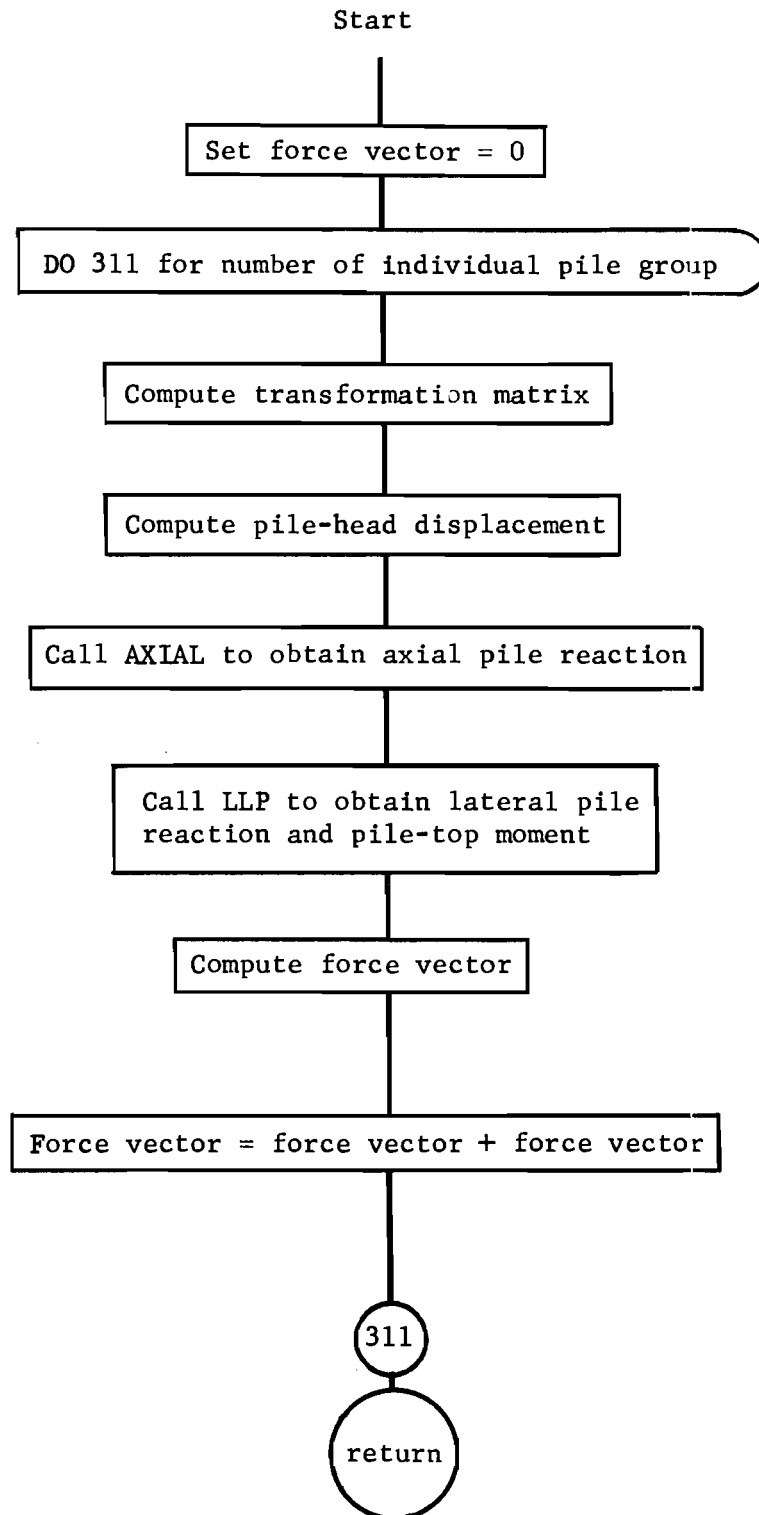
## A.2 FLOW DIAGRAMS FOR PROGRAM GROUP

## General Flow Diagram

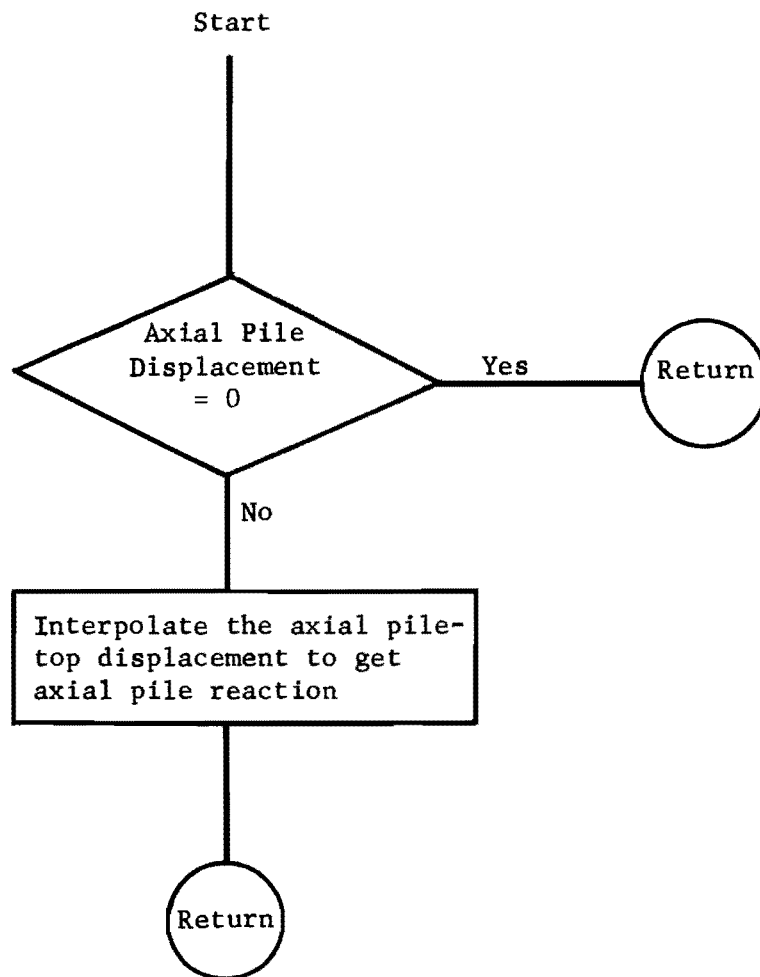




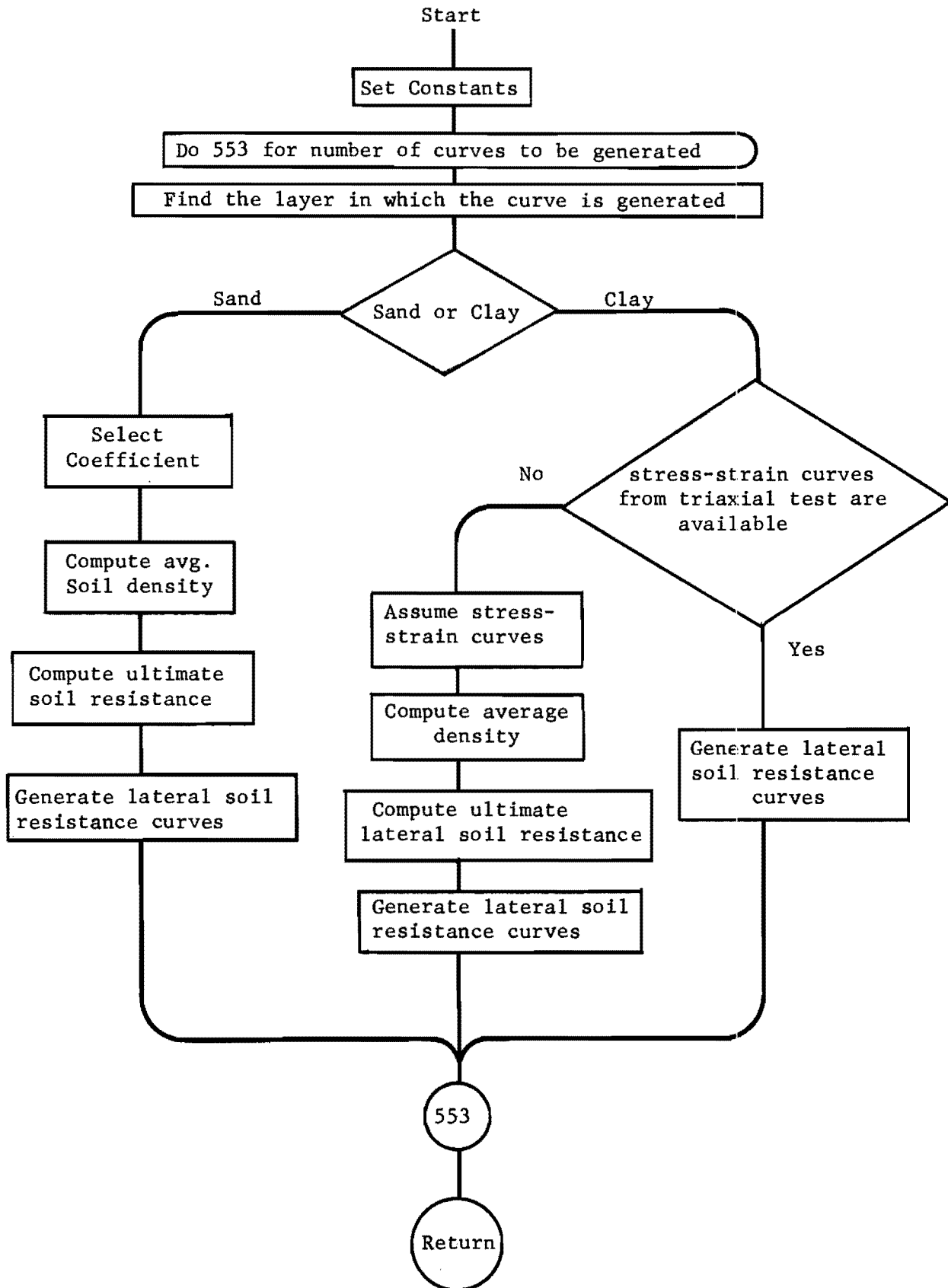
## Flow Diagram for Subroutine FVEC



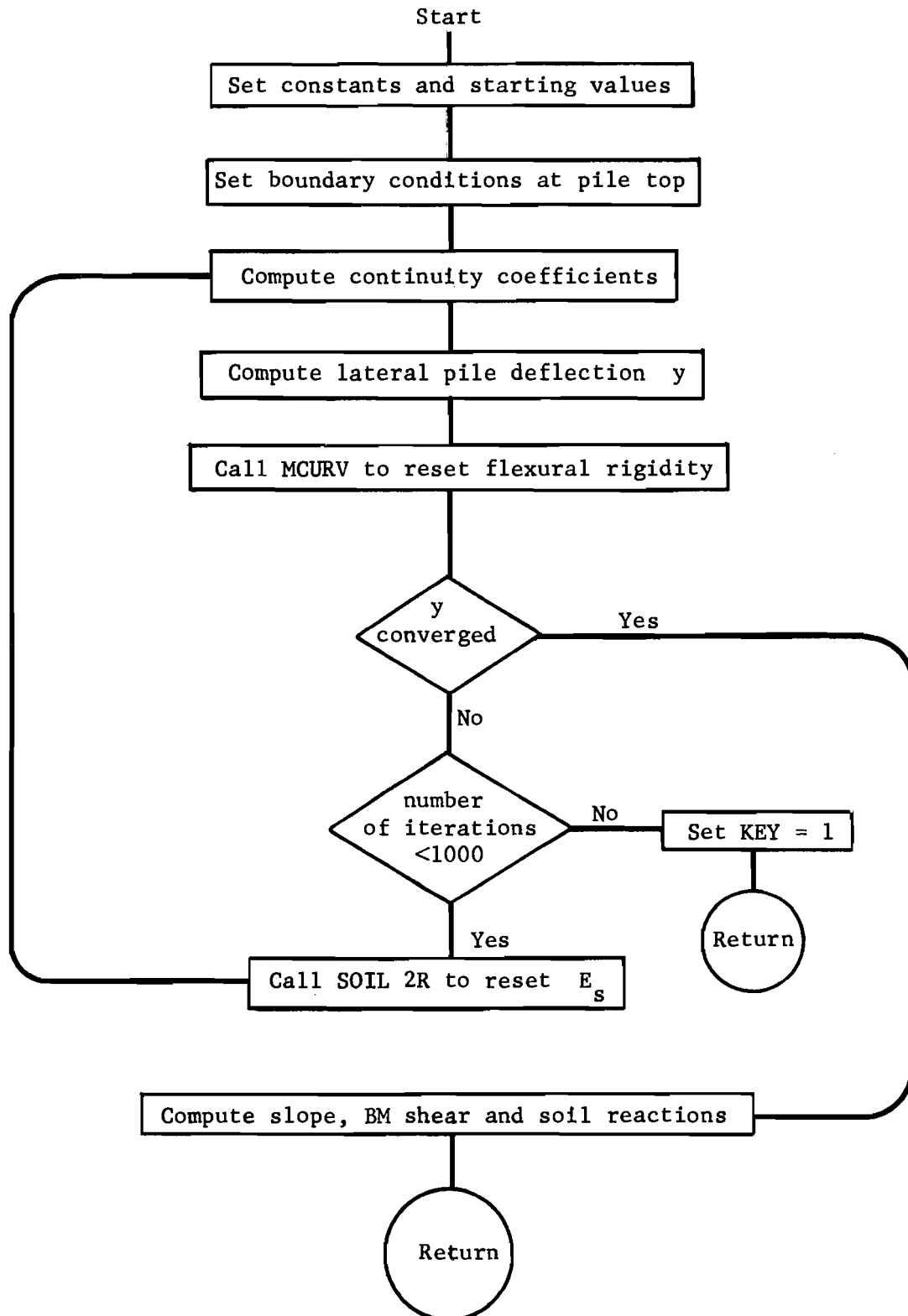
## Flow Diagram for Subroutine AXIAL



## Flow Diagram for Subroutine MAKE

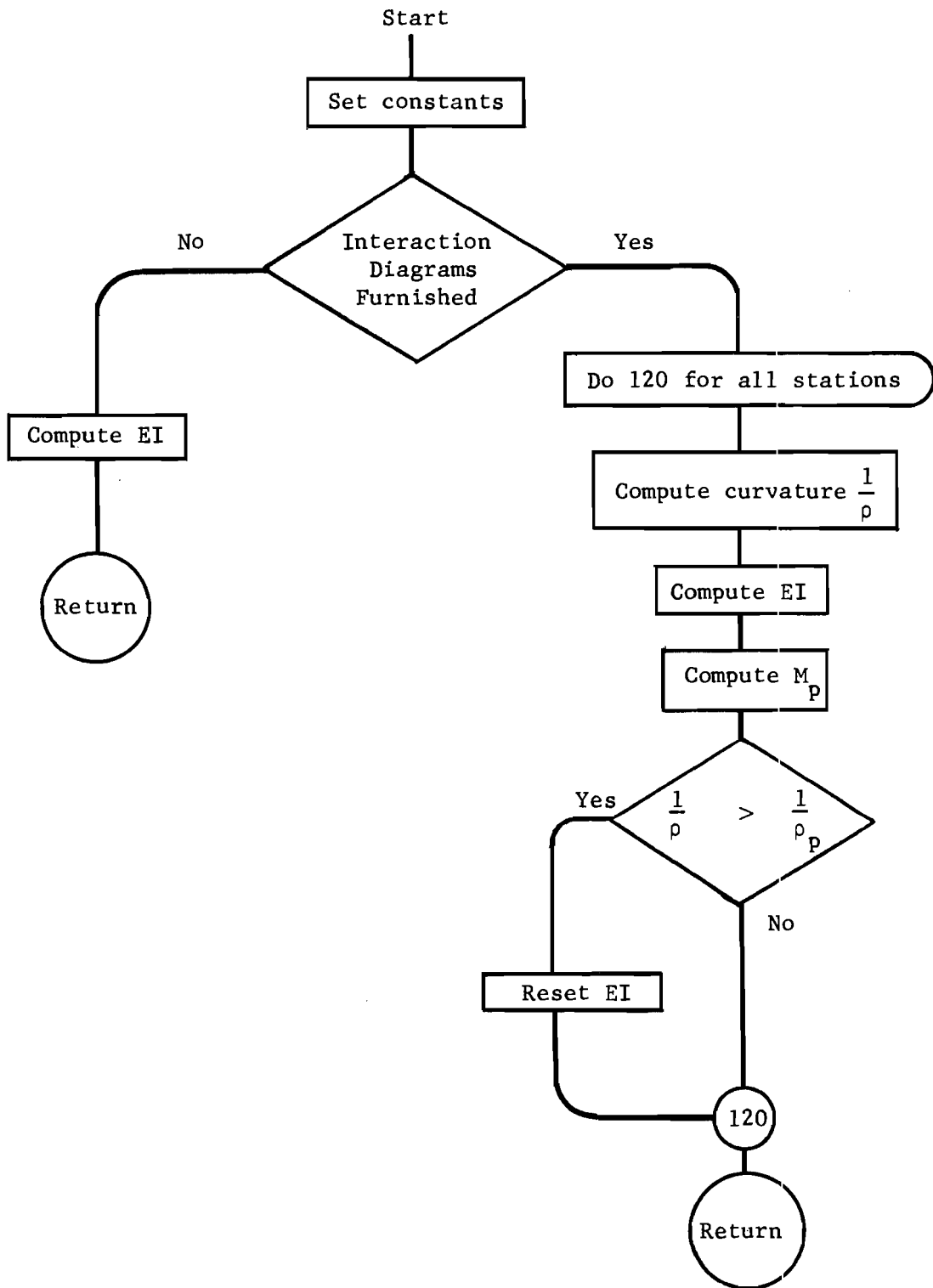


Flow Diagram for Subroutine LLP





Flow Diagram of Subroutine MCURV



## A.3 Glossary of Notations for Program GROUP

A(507)	continuity coefficient
AGAM	average soil density
ANUM(20)	alphanumeric variable to read in the title of run
AREA(20, 5)	cross-sectional area of a pile
AV(10)	Terzaghi's A coefficient
B(507)	continuity coefficient
BM(507)	bending moment in a pile
BULT(20, 5, 20)	ultimate moment in a beam-column
C(507)	continuity coefficient
COF(3,3)	cofactor of matrix SK
CURV(507)	curvature of pile
DBM(507)	shear force in a pile
DDV(3, 1)	correction vector for pile-cap displacement
DFV(3, 1)	difference between load vector and pile reaction vector
DIS1(10, 10)	distance from ground surface to the top of a soil layer
DIS2(10, 10)	distance from ground surface to the bottom of a soil layer
DIST(10, 10)	distance from ground surface to the depth when a stress-strain curve of triaxial test is given
DISTA(20)	Y coordinate of pile top (+ to right)
DISTB(20)	X coordinate of pile top (+ downward)
DPS(20)	distance from pile top to soil surface
DTC(10, 20)	distance from ground surface to where a lateral soil resistance curve is generated

DV(3, 1)	displacement vector of a pile cap
DY(507)	slope of a pile
EP50	strain in triaxial test corresponding to one-half of the ultimate deviator stress, $\sigma_{\Delta}$
ES	soil modulus or slope in the early portion of lateral soil resistance curve or secant modulus of lateral soil resistance curve
FDBET(20)	elastic rotational restraint on pile top
FKO(10)	coefficient of earth pressure at rest, K
FP(10, 10, 15)	strain in the triaxial test
FV(3, 1)	load vector
GAMMA(10, 10)	effective unit weight of a soil, $\gamma'$
HH(20)	increment length of a discretized pile
HHNN(20)	total length of a pile
ICON(10, 10)	code to specify the consistency of a clay
II(5)	number of points in an axial pile-top displacement curve
INFO(10, 10)	switch for inputting stress-strain curves of triaxial test
KA(20)	number specifying the axial pile-top displacement curve to be used
KAR	signal to notify the failure in axial soil resistance
KAX	signal to notify the axial load in excess of pile strength
KDENSE(10, 10)	code to specify the state of sand
KEY	a signal to notify the error in SOIL 2R and the failure in convergence in LLP
KFLAG	a signal to notify the end of run
KIC, KID, KIE, KIF, KIG, KIH	input switch for TABLES C, D, E, F, G, and H

KNPL	number of individual pile groups
KOC, KOD, KOE, KOF, KOH, KOJ	output switch for Tables C, D, E, F, G, H, and J
KP(20)	index specifying the pile to be used
KS(20)	index specifying the set of lateral soil resistance curves to be used
KSS(20)	index specifying the soil data to be used for generating a set of theoretical lateral soil resistance curves
KTYPE(20)	number specifying the pile material
MPLAST	signal to notify the formation of plastic hinges
NC(5)	number of lateral soil resistance curves in a set
NDS(20)	number of different sections in a pile
NINI(20, 5)	number of interaction diagrams of ultimate axial load and ultimate moment
NKS	number of sets of lateral soil resistance curves
NN(20)	number of increments into which a pile is divided
NOC(10)	number of theoretical lateral soil resistance curves in a set which are generated from soil data
NP(5, 20)	number of points in a lateral soil resistance curve
NPILE	number of types of pile
NPOINT(10, 10)	number of points in a stress-strain curve of a triaxial test
NSOILP	number of soil profiles
NSTYPE(10)	number of soil layers
P(507)	axial force in a pile
PC(5, 20, 25)	lateral soil resistance per unit length of pile
PDV(3, 1)	pile top displacement vector
PHI(10, 10)	angle of internal friction of a sand, $\phi$

POTT(20)	number of piles in an individual pile group
PUF	ultimate lateral soil resistance by flow-around failure
PULT(20, 5, 20)	ultimate axial load on a beam-column
PUW	ultimate lateral soil resistance by wedge failure
PX	axial pile reaction
Q(10)	lateral soil resistance
R(507)	flexural rigidity of a pile, EI
REACT(507)	lateral pile reaction
RES(507)	lateral soil resistance on a pile
RRI(20, 5)	flexural stiffness, EI
RV(3, 1)	pile reaction vector
RV1(3, 1)	pile reaction vector for virtual cap movement in X direction
RV2(3, 1)	pile reaction vector for virtual cap movement in Y direction
RV3(3, 1)	pile reaction vector for virtual cap rotation
S(3, 1)	pile reaction vector
SDIS	distance from ground surface
SHEARS(10, 10)	shear strength of a clay
SIG50	one-half of the ultimate deviator stress, $\sigma_{\Delta}$ in triaxial test
SIGD(10, 10, 15)	deviator stress, $\sigma_{\Delta}$ , in the triaxial test
SIZE(20, 5)	width of pile
SK(3, 3)	partial derivatives of pile reactions
SRES	summation of lateral soil resistances along the pile
SSS(5,2T)	axial pile top load

SWGAM	sum of soil weight
TC(20)	alphabetical designation of pile top connection to pile cap
THETA(20)	batter angle (+ counterclockwise from vertical)
U(3,3)	force transformation matrix
UT(3, 3)	displacement transformation matrix
XRI(20, 5)	moment of inertia, I
XS(5, 20)	distance from ground surface to the lateral soil resistance curve
XX1(20, 5)	distance from top of pile to top of pile sections
XX2(20, 5)	distance from top of pile to the bottom of pile section
Y(507)	lateral pile deflection
YC(5, 20, 25)	lateral pile deflection
YIELD(20)	yield stress
YOUNG(20)	Young's modulus
YY(507)	dummy to preserve the previous lateral pile deflection
ZZZ(5, 25)	axial pile-top displacement

#### A.4 DATA CODING FOR PROGRAM GROUP

Since the program GROUP must deal with a great number of data, careful data preparation and the correct data coding are essential for the computation.

The data are classified into the following groups.

TABLE A Title of each run

TABLE B Input and Output switches

TABLE C Load on pile cap

TABLE D Arrangement of individual pile groups

TABLE E Pile properties

TABLE F Axial pile top displacement curve

TABLE G Lateral soil resistance curve

TABLE H Soil data for theoretical lateral soil resistance curve

Input and output switches in TABLE B are necessary to eliminate inputting the identical data for the repetitive run. By setting the switch properly only the changing data have to be head in and printed out. If no new data are supplied, the data for the previous run are kept and used for the new run.

The general deck structure of the data is illustrated in the following.

##### Deck Structure of Input Data

TABLE A TITLE OF RUN, necessary for each run

Card AI one card

TABLE B INPUT OUTPUT SWITCH, necessary for each run

Card BI one card

TABLE C LOAD ON PILE CAP

If B1 = 0, skip to TABLE D

Card CI one card

TABLE D INDIVIDUAL PILE GROUP ARRANGEMENT

If B2 = 0, skip to TABLE E

Card DI one card

Card DII D1 cards

TABLE E PILE PROPERTIES

If B3 = 0, skip to TABLE F

Card EI one card

Card EII one card

Card EIII one card

If E5 = 1, 2, 2, or 5, skip E4 and E5

Card EIV one card

Card EV E14 cards

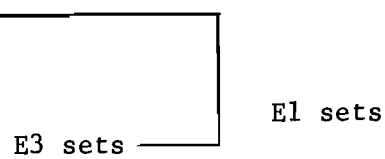


TABLE F AXIAL PILE TOP DISPLACEMENT CURVE

If B4 = 0, Skip to TABLE G

Card FI one card

Card FII one card

Card FIII F3 cards

F1 sets

TABLE G LATERAL SOIL RESISTANCE CURVE

If B5 = 0, skip to TABLE H

Card GI one card

Card GII one card

Card GIII one card

Card GIV G5 cards

G3 sets

G1 sets

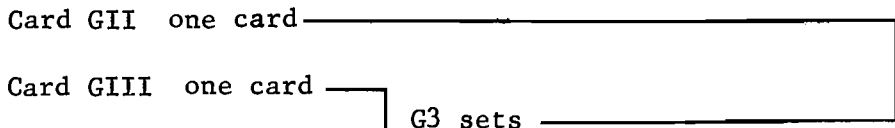




TABLE H SOIL DATA FOR THEORETICAL LATERAL SOIL RESISTANCE CURVES

If B6 = 0, Skip TABLE H

Card HI one card

Card HII one card

Card HIII H3 cards

Card HIV one card

If H13 = 0, skip H5 and H6

Card HV one card

Card HVI H15 cards

H1 sets

H4 sets

To start a new run go to TABLE A. To terminate the run, add two blank cards at the end of data.

## Data Coding Form for Program GROUP

The data cards must be stacked in proper order, as it is shown in the description of the data deck structure. Some of the cards have to be removed depending on the type of problem. All ten-space words assume E10.3 format (for example, +1.234E+05). All words with less than five spaces assume integers (for example, 6.17).

Each card is identified by an alphanumeric sign with Roman numerals (that is, BII, CIII, etc.). Each datum in a card is designated by an alphanumeric sign with Arabic numbers (for example, D3, E4 ).

The maximum value a datum can take is indicated in the following when it is necessary. In order to take larger values than indicated, the dimension statement in the program must be revised.

## TABLE A Title of run

## Card AI

A1	1 to 80	alphanumeric description of each run.
----	---------	---------------------------------------

## TABLE B Input and Output Switch

Enter 1 for inputting new data or listing the data and computation results. Enter 0 for skipping the input or listing. If there is no data input, data from the previous run are used.

## Card BI

B1	5	Input TABLE C Load
B2	10	Input TABLE D Arrangement
B3	15	Input TABLE E Pile
B4	20	Input TABLE F Axial Displacement Curve

B5	25	Input TABLE G	Lateral Soil Reaction Curves
B6	30	Input TABLE H	Soil Data
B7	45	Output TABLE C	Load
B8	50	Output TABLE D	Arrangement
B9	55	Output TABLE E	Pile
B10	60	Output TABLE F	Axial Displacement Curve
B11	65	Output TABLE G	Lateral Soil Reaction Curve
B12	70	Output TABLE H	Soil Data
B13	75	Output TABLE J	Computational Results on a Laterally Loaded Pile

Table J lists the computation results on the axial and lateral behaviors of single piles. The output switch controls the listing of distribution of deflection, slope, moment, shear and soil resistance along the piles.

TABLE C Load on Grouped Pile Foundation

Card CI

C1	1 to 10	Vertical load, pound (downward +)
C2	11 to 20	Horizontal load, pound (from left to right +)
C3	21 to 30	Moment, inch-pound (counterclockwise +)

TABLE D Individual Pile Group Arrangement

Card DI

D1	1 to 5	Number of individual pile groups (maximum 20)
----	--------	---

Card DII

D2	3 to 5	Pile head connection to pile cap. Enter PIN for pinned connection, FIX for fixed connection and RES for elastically restrained connection
----	--------	---

D3	6 to 10	Number of piles in the individual pile group. (no restriction in number)
D4	11 to 15	Index for pile. Enter E2.
D5	16 to 20	Index for axial pile-top displacement curve. Enter F2.
D6	21 to 25	Index for the set of lateral soil resistance curves. Enter G2. If the set of curves is generated from soil data (TABLE H), assign successive sequential number to the set after data in TABLE G.
D7	26 to 30	Index for the soil data for the theoretical lateral soil curves. Enter H2.
D8	31 to 40	Pile-top location, vertical coordinate, inch (downward from origin +)
D9	41 to 50	Pile-top location, horizontal coordinate, inch (right-hand side of origin +)
D10	51 to 60	Batter angle of pile, radian (counterclockwise from vertical +)
D11	61 to 70	Distance from pile to ground surface, inch
D12	71 to 80	Spring constant for an elastically restrained pile top, inch-pound. Can be left blank for PIN and FIX in D2.

TABLE E Pile Properties

## Card EI

E1	1 to 5	Number of different types of pile (maximum 20)
----	--------	--

## Card EII

E2	1 to 5	Sequential number assigned to the pile
E3	6 to 10	Number of different sections in the pile (maximum 5)
E4	11 to 15	Number of increments by which the pile is divided into finite elements (maximum 500)

E5	16 to 20	Code for pile type. Enter 1 for wide flange (strong axis), 2 for wide flange (weak axis), 3 for steel pipe, 4 for others with interaction curve and 5 for others without interaction curve. Interaction curve refers to a diagram of ultimate axial force and ultimate moment in a beam column.
E6	21 to 30	Total length of the pile, inch
E7	31 to 40	Yield stress of pile material, psi
E8	41 to 50	Young's modulus of pile material, psi

## Card EIII

E9	1 to 10	Distance from pile top to top of uniform section, inch
E10	11 to 20	Distance from pile top to bottom of uniform section, inch
E11	21 to 30	Width of pile in the section, inch
E12	31 to 40	Cross-sectional area of pile in the section, inch <sup>2</sup>
E13	41 to 50	Moment of inertia of pile in the section, inch <sup>4</sup>

## Card EIV

E14	1 to 5	Number of points in the interaction diagram (maximum 20)
-----	--------	--

Card EV Start from ( $P_u$ , 0) and end at (0,  $M_p$ )

E15	1 to 10	Ultimate axial force in a pile, pound
E16	11 to 20	Ultimate moment in a pile, inch-pound

## TABLE F Axial Pile-Top Displacement Curve

## Card FI

F1	1 to 5	Number of curves (maximum 5)
----	--------	------------------------------

## CARD FII

F2	1 to 5	Sequential number assigned to the curve
----	--------	---

F3	6 to 10	Number of points in a curve (maximum 25)
Card FIII		
F4	1 to 10	Axial load on pile top, pound (downward load +)
F5	11 to 20	Pile-top displacement, inch (downward displacement +)

TABLE G Lateral Soil Resistance Curve

## Card GI

G1	1 to 5	Number of sets of curves (maximum 5)
----	--------	--------------------------------------

## Card GII

G2	1 to 5	Sequential number assigned to the set
G3	6 to 10	Number of curves in the set (maximum 20)

## Card GIII

G4	1 to 10	Depth from ground surface to curve, inch
G5	11 to 15	Number of points in the curve. Curve input starts from ground surface and ends at pile point or deeper.

## Card GIV

G6	1 to 10	Lateral soil resistance, pound per unit length of pile
G7	11 to 20	Lateral pile deflection, inch. Point input starts from (0, 0).

TABLE H Soil Data for Theoretical Lateral Soil Resistance Curve

Card H1	1 to 5	Number of soil profiles for which a set of curves are generated (maximum 10)
---------	--------	--

## Card HII

H2	1 to 5	Sequential number assigned to the soil profile
H3	6 to 10	Number of curves to be generated

H4        11 to 15        Number of different soil strata in the profile (maximum 10)

Card HIII

H5        1 to 10        Depth from ground surface to point where a curve is generated, inch. Start from ground surface and end at pile tip or deeper.

Card HIV

H6        1 to 10        Depth from ground surface to top of soil stratum, inch

H7        11 to 20        Depth from ground surface to bottom of a soil stratum, inch

H8        21 to 30        Effective unit weight of soil, pcf. H9 and H10 are needed only for a sand.

H9        31 to 40        Angle of internal friction of a sand, degree.

H10       45 to 50        Code for the state of sand. Enter 1 for a dense sand, 2 for a medium sand, and 3 for a loose sand.

H11       51 to 60        Shear strength of a clay, psi

H12       65                Code to specify the consistency of a clay. Enter 3 for a stiff clay, 2 for a medium clay, and 1 for a soft clay.

H13       70                Switch for inputting stress-strain curves from triaxial test. Enter 1 for input, 0 for no input.

Card HV

H14       1 to 10        Depth from ground surface to point where the soil specimen was sampled, inch

H15       11 to 15        Number of points in a stress-strain curve

Card HVI

H16       1 to 10        Deviator stress, psi

H17       11 to 20        Strain. Point input starts from (0, 0).

## A.5 Listing of Program GROUP



```

PROGRAM GROUP(INPUT,OUTPUT)
DIMENSION ANUM(20), FV(3,1), SK(3,7), OFV(3,1), COF(3,3),
1 PDV(3,1), HHNN(20),DDV(3,1), RV(3,1), RV1(3,1), RV2(3,1)
2 , RV3(3,1)
COMMON / BLOCK1 / TC(20), PUTT(20), KP(20), KA(20), KS(20),
1 KSS(20), DISTB(20), DISTA(20), THETA(20),
2 UPS(20), FDBET(20), KNPI
COMMON / BLOCK2 / NN(20), HH(20), NDS(20), KTYPE(20), YIELD(20),
1 YOUNG(20)
COMMON / BLOCK3 / XX1(20, 5), XX2(20, 5), RRI(20, 5), XRI(20, 5),
1 SIZE(20,5), APFA(20,5), PULT(20,5,20),
2 BULT(20,5,20), NINT(20,5)
COMMON / BLOCK5 / NC(5), XS(5,20), NP(5,20), Yc(5,20,25),
1 PC(5,20,25)
COMMON / BLOCK6 / NOC(10), NSTYPE(10), DTC(10,20), GAMMA(10,10),
1 PHI(10,10), KNENSE(10,10), SHEARS(10,10), TCON(
2 10,10), INFO(10,10), DTS1(10,10), DLS2(10,10),
3 DIST(10,10), NPOINT(10,10), SIGD(10,10,15),
4 FP(10,10,15)
COMMON / BLOCK7 / KFLAG, KEY, KOJ, KAY, KAR
COMMON / BLOCK9 / II(5), ZZZ(5, 25), SSS(5, 25), DV(3, 1)
501 FORMAT ( 1H1 )
502 FORMAT ( 20A4 )
503 FORMAT ( 6I5, 10X, 7I5 )
504 FORMAT ( 4E10.3, 15 )
505 FORMAT ( 7X, A3, 5I5, 5E10.3 )
506 FORMAT ( 4I5, 3E10.3 )
507 FORMAT ( 4E10.3 )
508 FORMAT ( 2E10.3 )
509 FORMAT ( E10.3 )
510 FORMAT ( 5X, 20A4 )
511 FORMAT ( /// 5X, 16HTABLE C LOAD )
512 FORMAT ( / 11X, 9HV LOAD, LB, 6X, 9HH LOAD, LB, 7X, 12HMOMENT, LB-IN )
513 FORMAT ( 5X, 3E15.3 )
514 FORMAT ( /// 5X, 38HTABLE D ARRANGEMENT OF PILE GROUPS )
515 FORMAT ( / 7X, 47HGROUP CONNECT NO OF PILE PYLE NO L-S CURVE )
1 , 20HP-Y CURVE SOIL DATA )
516 FORMAT ( 5X, 15, 6X, A3, 5X, 15, 6X, 15, 4X, 14, 7X, 15, 5X, 15 )
517 FORMAT ( / 7X, 5HGROUP, 8X 7HVERT, IN, 8X, 6HHOP, IN, 3X,
1 9HSLOPE, RAD, 3X, 9HGROUND, TN, 6X, 6HSPRING )
518 FORMAT ( 5X, 15, 7X, 5E12.3 )
519 FORMAT ( /// 5X, 27HTABLE E PILE DIMENSIONS )
520 FORMAT ( / 7X, 6HPILE , 5HSEC , 5HINC , 8HMATERIAL, 5X,
1 9HLENGTH, IN, 6X, 9HYIELD, PSI, 10X, 5H , PSI )
521 FORMAT ( /// 5X, 37HTABLE F AXIAL LOAD VS SETTLEMENT )
522 FORMAT ( / 8X, 5HCURVE, 13, 10X, 13HNUM OF POINTS , 13 )
523 FORMAT ( 12X, 5HPOINT, 5X, 13HAYIAL LOAD, LB, 7X,
1 13HSETTLEMENT, IN )
524 FORMAT ( 10X, 15, 9X, E11.3, 9X, E11.3 )
525 FORMAT ( /// 5X, 22HTABLE G P-Y CURVES )
526 FORMAT ( / 7X, 3HSET, 13, 10X, 13HNUM OF CURVES, 13 )
527 FORMAT ( 8X, 5HCURVE, 13, 6X, 20HDISTANCE FROM TOP, IN, E10.3, 4X,
1 13HNUM OF POINTS, 13 )
528 FORMAT ( 12X, 5HPOINT, 9X, 4HP, LB, 16X, 4HY, IN )
529 FORMAT ( 10X, 35H(C LOAD D ARRANGEMENT E PYLE ,
1 31HP L-S G P-Y H SOIL J LLP) )
530 FORMAT ( 5X, 3I5, 18, 2X, 3E15.3 )
531 FORMAT ( E10.3, 15 )

```

```

532 FORMAT ( 5E10.3 )
533 FORMAT ( 4E10.3, 15, 5X, E10.3, 215 )
535 FORMAT ( /// 5X, 41HTABLE H      SOIL DATA FOR AUTO P-Y CURVES      )
536 FORMAT ( / 7X, 7HPROFILE, 13, 5X, 13HNUM OF CURVES, 13, 5X,
1      13HNUM OF STRATA, 13 )
537 FORMAT ( 8X, 42HDISTANCES FROM PILE TOP TO P-Y CURVES,INCH )
538 FORMAT ( 10X, 5HCURVE, 5X, 11HLOCATION,IN )
539 FORMAT ( 8X, 43HSTRATUM TYPE GAMMA,PCF  PHT,DEG  DENS ,
1      29HSHEAR,PSI  CONSIST S-S CURVE )
540 FORMAT ( 10X, 15, 6H SAND, 2E11.3, 1X )
541 FORMAT ( 10X, 15, 6H CLAY, E11.3, 17X, F11.3, 4X, 15, 6X, 15 )
542 FORMAT ( 8X, 7HSTRATUM, 13, 5X, 20HDISTANCE FROM TOP,IN, E11.3,
1      5X, 13HNUM OF POINTS, 13 )
543 FORMAT ( 10X, 5HPOINT, 10X, 10HSTRESS,PSI, 14X, 6HSTRAIN )
544 FORMAT ( 10X, 15, 5X, E11.3 )
545 FORMAT ( 7X *PILE* 2X *FROM,IN* 5X *TO,IN* 7X *D,IN* 8X *A,IN2*
1      5HA,IN2, 7X, 5HI,IN4 )
546 FORMAT ( 8X, 7HSTRATUM, 11X, 7HFROM,IN, 7X, 5HTO,IN )
547 FORMAT ( 10X, 2E15.3 )
548 FORMAT ( /// 5X, 35HTABLE B      INPUT AND OUTPUT SWITCH, 5X,
1      19H(IF 1 YES, IF 0 NO) )
549 FORMAT ( / 7X, 41HTABLE      C      D      E      F      G      H      J )
550 FORMAT ( 7X, 5HINPUT, 9I5 )
551 FORMAT ( 7X, 6HOUTPUT, 9I5 )
552 FORMAT ( 11X, 19HINTERACTION DIAGRAM, 10X, 13HNUM OF POINTS, 13, /
1      16X, 7HPULT,LB, 7X, 10HMULT,IN-LB )
553 FORMAT ( 11X, 30HLINEARLY ELASTIC PILE MATERIAL )
558 FORMAT ( / 7X, 13HNUM OF CURVES, 13 )
559 FORMAT ( / 7X, 11HNUM OF SEIS, 73 )
560 FORMAT ( / 10X, 15HNO OF ITERATION, 12 )
561 FORMAT ( / 8X, 19HSTRESS STRAIN CURVE )
564 FORMAT ( / 9X, 41HVERTICAL,IN  HORIZONTAL,IN  ROTATION,RAD )
565 FORMAT ( 5X, 3E15.3 )
566 FORMAT ( ///// 10X, 39HPILE CAP DISPL DOES NOT CONVERGE AFTER ,
1      14H100 ITERATIONS )
567 FORMAT ( ///// 10X, 39HDETERMINANT OF STIFFNESS MATRIX IS ZERO )
570 FORMAT ( 5X, 15, 5E12.3 )
576 FORMAT ( /// 5X, 19HCOMPUTATION RESULTS )
577 FORMAT ( 20X, 49H(DENSITY OF SAND      1 DENSE  2 MEDIUM  3 LOOSE)
1      )
578 FORMAT ( 20X, 50H(CONSISTENCY OF CLAY  1 STIFF  2 MEDIUM  3 SOFT )
1      )
579 FORMAT ( / 10X, 44H(MATERIAL  1 STEEL H, 2 STEEL H(WEAK AXIS), ,
1      10HSTEEL PIPE, / 20X, 27H* OTHERS WITH INT DIAGRAM,
2      , 29HS OTHERS WITHOUT INT DIAGRAM) / )
580 FORMAT ( /// 5X, 41HTABLE I      DISPLACEMENT OF GROUPED PILE ,
1      10HFOUNDATION )
581 FORMAT ( /// 5X, 42HTABLE J      COMPUTATION ON INDIVIDUAL PILE )
C-----START INPUTTING DATA
      NSOILP = 0
C-----INPUT TABLE A (TITLE OF RUN)
      100 READ 502, ( ANUM(I), I = 1, 20 )
      NKS = 0
C-----INPUT TABLE B (SWITCH FOR INPUT AND OUTPUT)
      READ 503, KIC, KID, KIE, KIF, KIG, KIH,
1      KOC, KOD, KOE, KOF, KOG, KOH, KOJ
      ITEST = KIC + KID + KIE + KIF + KIG + KIH
      IF ( ITEST .EQ. 0 ) GO TO 9999

```

```

C-----INPUT TABLE C      (LOAD)
      IF ( KIC .EQ. 0 ) GO TO 102
      READ 504, FV(1, 1), FV(2, 1), FV(3, 1)
C-----INPUT TABLE D      (PILE GROUP ARRANGEMENT)
102   IF ( KID .EQ. 0 ) GO TO 103
      READ 503, KNPL
      DO 104 I = 1, KNPL
      READ 505, TC(I), IPOTT, KP(I), KA(I), KS(I), KCS(I), UISTR(I),
1     DISTA(I), THETA(I), DPS(I), FDRFT(I)
      POTT(I) = IPOTT
104   CONTINUE
C-----INPUT TABLE E      (PILE DIMENSIONS)
103   IF ( KIE .EQ. 0 ) GO TO 115
      READ 503, NPILE
      DO 113 I = 1, NPILE
      READ 506, IDP, NDS(I), NN(I), KTYPE(I), HHNN(I), YIELD(I), YOUNG(I)
      HH(I) = HHNN(I) / NN(I)
      INDEX = NDS(I)
      DO 116 J = 1, INDEX
      READ 532, XX1(I, J), XX2(I, J), SIZE(I, J), AREA(I, J), XRI(I, J)
      RRI(I, J) = XRI(I, J) * YOUNG(I)
      MATL = KTYPE(I)
      GO TO ( 117, 117, 117, 118, 116 ), MATL
118   CONTINUE
      READ 503, NINT(I, J)
      INT = NINT(I, J)
      READ 508, ( PULT(I, J, K), BULT(I, J, K), K = 1, INT )
      GO TO 116
117   CONTINUE
      GO TO ( 185, 186, 187 ), MATL
185   SF = 1.14
      GO TO 188
186   SF = 1.50
      GO TO 188
187   SF = 1.27
188   CONTINUE
      NINT(I, J) = 2
      PULT(I, J, 1) = AREA(I, J) * YIELD(I)
      BULT(I, J, 2) = 2.0 * SF * YIELD(I) * XRI(I, J) /
1     SIZE(I, J)
      BULT(I, J, 1) = 0.0
      PULT(I, J, 2) = 0.0
116   CONTINUE
113   CONTINUE
C-----INPUT TABLE F      (AXIAL LOAD VS SETTLEMENT)
115   IF ( KIF .EQ. 0 ) GO TO 105
      READ 503, NKA
      DO 106 I = 1, NKA
      READ 503, IDEN, II(I)
      INDEX = II(I)
      READ 508, ( SSS(IDEN, J), ZZZ(IDEN, J), J = 1, INDEX )
106   CONTINUE
C-----INPUT TABLE G      (P-Y CURVES)
105   IF ( KIG .EQ. 0 ) GO TO 107
      READ 503, NKS
      DO 108 I = 1, NKS
      READ 503, IDPY, NC(I)
      INDEX = NC(I)

```

```

      DO 112 J = 1, INDEX
      READ 531, XS(IDPY, J), NP(IDPY, J)
      INDEX2 = NP(IDPY, J)
      READ 508, ( PC(IDPY, J, K), YC(IDPY, J, K), K = 1, INDEX2 )
112   CONTINUE
108   CONTINUE
C-----INPUT TABLE H      (SOIL DATA FOR AUTOMATIC GENERATION OF P-Y CURVE)
107   IF ( KIH .EQ. 0 ) GO TO 109
      READ 503, NSOILP
      DO 110 I = 1, NSOILP
      READ 503, NC, NOC(I), NSTYPE(I)
      INDEX = NOC(I)
      READ 509, ( DTC(I, J), J = 1, INDEX )
      INDEX1 = NSTYPE(I)
      DO 111 J = 1, INDEX1
      READ 533, DIS1(I, J), DIS2(I, J), GA, PI, KDENSE(I, J),
1      SHEARS(I, J), ICON(I, J), INFO(I, J)
      PHI(I, J) = PI / 57.296
      GAMMA(I, J) = GA / 1728.0
      IF ( INFO(I, J) .EQ. 0 ) GO TO 111
      READ 531, DIST(I, J), NPOINT(I, J)
      INDEX2 = NPOINT(I, J)
      READ 508, ( SIGD(I, J, K), FP(I, J, K), K = 1, INDEX2 )
111   CONTINUE
110   CONTINUE
109   CONTINUE
C-----AUTOMATIC GENERATION OF P-Y CURVES
      IF ( KIH .EQ. 0 ) GO TO 202
      DO 200 I = 1, KNPL
      IF ( KSS(I) .EQ. 0 ) GO TO 200
      CALL MAKE ( I )
200   CONTINUE
C-----START OF PRINTING OUT THE INPUT DATA
C-----OUTPUT TABLE A      (TITLE OF RUN)
202  PRINT 501
      PRINT 510, ( ANUM(I), I = 1, 20 )
C-----OUTPUT TABLE B      ( SWITCH FOR INPUT AND OUTPUT)
      PRINT 548
      PRINT 549
      PRINT 550, KIC, KID, KIE, KIF, KIG, KIH
      PRINT 551, KOC, KOD, KOE, KOF, KOG, KOH, KOJ
      PRINT 529
C-----OUTPUT TABLE C      (LOAD)
      IF ( KOC .EQ. 0 ) GO TO 170
      PRINT 541
      PRINT 512
      PRINT 513, FV(1, 1), FV(2, 1), FV(3, 1)
C-----OUTPUT TABLE D      (PILE GROUP ARRANGEMENT)
170  IF ( KOD .EQ. 0 ) GO TO 171
      PRINT 544
      PRINT 515
      DO 199 I = 1, KNPL
      IPOTT = POTT(I)
      PRINT 516, I, TC(I), IPOTT, KP(I), KA(I), KS(I), KSS(I)
199  CONTINUE
      PRINT 517
      DO 198 I = 1, KNPL
198  PRINT 518, I, DISTR(I), DISTA(I), THETA(I), DPS(I), FDBET(I)

```

```

C-----OUTPUT TABLE E      (PILE DIMENSIONS)
171  IF ( KOE .EQ. 0 ) GO TO 176
    PRINT 519
    PRINT 520
    PRINT 530, ( I, NDS(I), NN(I), KTYPE(I), RHNN(I), YIELD(I),
1     YOUNG(I), I = 1, NPILE )
    PRINT 579
    PRINT 545
      DO 197 I = 1, NPILE
        INDEX = NDS(I)
        DO 196 J = 1, INDEX
          PRINT 570, I, XX1(I, J), XX2(I, J), SIZE(I, J), AREA(I, J),
1         XRI(I, J)
          MATL = KTYPE(I)
          IF ( MATL .EQ. 5 ) GO TO 175
          INT = NINT(I, J)
          PRINT 552, INT
          PRINT 547, ( PULT(I, J, K), BULT(I, J, K), K = 1, INT )
          GO TO 196
175  PRINT 553
196  CONTINUE
197  CONTINUE
C-----OUTPUT TABLE F      (AXIAL LOAD VS SETTLEMENT)
170  IF ( KOF .EQ. 0 ) GO TO 173
    PRINT 521
    PRINT 558, NKA
      DO 174 I = 1, NKA
        PRINT 522, I, II(I)
        PRINT 523
          INDEX = II(I)
          PRINT 524, ( J, SSS(I, J), ZZZ(I, J), J = 1, INDEX )
174  CONTINUE
C-----OUTPUT TABLE G      (P-Y CURVES)
173  IF ( KOG .EQ. 0 ) GO TO 177
      MAX = NKS
      DO 183 I = 1, KNPL
        IF ( KS(I) .GE. MAX ) MAX = KS(I)
183  CONTINUE
    PRINT 525
    PRINT 559, MAX
      DO 178 I = 1, MAX
        PRINT 526, I, NC(I)
          INDEX = NC(I)
          DO 178 J = 1, INDEX
            PRINT 527, J, XS(I, J), NP(I, J)
            PRINT 528
              INDEX2 = NP(I, J)
              PRINT 524, ( K, PC(I, J, K), YC(I, J, K), K = 1, INDEX2 )
178  CONTINUE
C-----OUTPUT TABLE H      (SOIL DATA FOR AUTOMATIC GENERATION OF P-Y CURVES)
177  IF ( KOH .EQ. 0 ) GO TO 300
    PRINT 535
      DO 182 I = 1, NSOILP
        PRINT 536, I, NOC(I), NSTYPE(I)
        PRINT 537
        PRINT 538
          INDEX = NOC(I)
          PRINT 544, ( J, DTC(I, J), J = 1, INDEX )

```

```

PRINT 539
      INDEX1 = NSTYPE(I)
      DO 190 J = 1, INDEX1
        GA = GAMMA(I, J) * 1728.0
        PI = PHI(I, J) * 57.296
        IF ( PI .EQ. 0 ) GO TO 191
      PRINT 540, J, GA, PI, KDENSE(I, J)
      GO TO 190
191 PRINT 541, J, GA, SHEARS(I, J), ICON(I, J), INFO(I, J)
190 CONTINUE
      PRINT 577
      PRINT 578
      PRINT 546
      PRINT 524, ( J, DIS1(I, J), DIS2(I, J), J = 1, INDEX1 )
      DO 184 J = 1, INDEX1
        IF ( INFO(I, J) .EQ. 0 ) GO TO 184
      PRINT 561
      PRINT 542, J, DIS1(I, J), NPOINT(I, J)
      PRINT 543
          INDEX2 = NPOINT(I, J)
      PRINT 524, ( K, SIGD(I, J, K), FP(I, J, K), K = 1, INDEX2 )
184 CONTINUE
182 CONTINUE
C-----SET INITIAL DISPL VECTOR DV AND CONSTANTS
300      KFLAG = 0
          TOL = 0.00001
          KEY = 0
          KSW = 0
          ITER = 1
          DV(1, 1) = 0.0
          DV(2, 1) = 0.0
          DV(3, 1) = 0.0
          DDV(1, 1) = 0.001
          DDV(2, 1) = 0.001
          DDV(3, 1) = 0.0
C-----CORRECT THE BENT DISPLACEMENT
350      DO 302 I = 1, 3
302      DV(I, 1) = DV(I, 1) + DDV(I, 1)
C-----COMPUTE PILE REACTIONS FOR THE NEW DISPLACEMENT
      CALL FVEC ( RV )
      IF ( KEY .EQ. 1 ) GO TO 9999
      IF ( KAX .EQ. 1 ) GO TO 9999
      IF ( KAR .EQ. 1 ) GO TO 9999
      IF ( KFLAG .EQ. 1 ) GO TO 100
C-----COMPUTE THE DIFFERENCE BETWEEN LOAD AND REACTION
      DO 330 I = 1, 3
330      DV(I, 1) = FV(I, 1) - RV(I, 1)
      CONTINUE
      IF ( KEY .EQ. 1 ) GO TO 9999
C-----COMPUTE PARTIAL DERIVATIVES
      DELTA = 0.00001
      DV(1, 1) = DV(1, 1) + DELTA
      CALL FVEC ( RV1 )
      DV(1, 1) = DV(1, 1) - DELTA
      DV(2, 1) = DV(2, 1) + DELTA
      CALL FVEC ( RV2 )
      DV(2, 1) = DV(2, 1) - DELTA
      DV(3, 1) = DV(3, 1) + 0.001 * DELTA

```

```

CALL FVEC ( RV3 )
IF ( KEY .EQ. 1 ) GO TO 9999
DO 310 I = 1, 3
  SK(I, 1) = (-RV(I, 1) + RV1(T, I) ) / DELTA
  SK(I, 2) = (-RV(I, 1) + RV2(T, I) ) / DELTA
  SK(I, 3) = (-RV(I, 1) + RV3(T, I) ) / ( 0.001 * DELTA )
310 CONTINUE
C-----INVERT STRUCTURAL STIFFNESS MATRIX SK
  COF(1, 1) = SK(2, 2) * SK(3, 3) - SK(2, 3) * SK(3, 2)
  COF(1, 2) = SK(2, 3) * SK(3, 1) - SK(2, 1) * SK(3, 3)
  COF(1, 3) = SK(2, 1) * SK(3, 2) - SK(2, 2) * SK(3, 1)
  COF(2, 1) = SK(1, 3) * SK(3, 2) - SK(1, 2) * SK(3, 3)
  COF(2, 2) = SK(1, 1) * SK(3, 3) - SK(1, 3) * SK(3, 1)
  COF(2, 3) = SK(1, 2) * SK(3, 1) - SK(1, 1) * SK(3, 2)
  COF(3, 1) = SK(1, 2) * SK(2, 3) - SK(1, 3) * SK(2, 2)
  COF(3, 2) = SK(1, 3) * SK(2, 1) - SK(1, 1) * SK(2, 3)
  COF(3, 3) = SK(1, 1) * SK(2, 2) - SK(1, 2) * SK(2, 1)
  DET = 0.0
DO 320 NCOL = 1, 3
320   DET = DET + SK(1, NCOL) * COF(1, NCOL)
  IF ( DET .NE. 0.0 ) GO TO 321
PRINT 567
  GO TO 9999
321   DO 322 NROW = 1, 3
      DO 322 NCOL = 1, 3
        SK(NROW, NCOL) = COF(NCOL, NROW) / DET
322 CONTINUE
C-----COMPUTE DISPLACEMENT CORRECTION
CALL MULT ( DDV, SK, UFV, 1 )
C-----CHECK CONVERGENCE OF REACTION
DO 335 I = 1, 3
  IF ( ABS ( DDV(I, 1) ) .GE. TOL ) GO TO 331
335 CONTINUE
  GO TO 360
331   ITER = ITER + 1
  IF ( ITER .GE. 100 ) GO TO 332
  GO TO 350
332 PRINT 566
  GO TO 9999
360 PRINT 501
  PRINT 510, ( ANUM(I), I = 1, 20 )
  PRINT 576
  PRINT 580
  PRINT 564
  PRINT 565, DV(1, 1), DV(2, 1), DV(3, I)
  KFLAG = 1
  PRINT 560, ITER
  PRINT 581
  GO TO 350
9999 CONTINUE
END

```

```

SUBROUTINE FVEC ( VECTOR )
DIMENSION VECTOR(3,1), U(3,3), UT(3,3), S(3, 1), US(3, 1)
COMMON / BLOCK1 / IC(40), POTT(20), KP(20), KA(20), KS(20),
1          KSS(20), UISTR(20), DISTA(20), THETA(20),
2          UPS(20), FDBET(20), KNPI
COMMON / BLOCK7 / KFLAG, KEY, KOJ, KAV, KAR
COMMON / BLOCK8 / Y(507), ES(507), R(507), MPLAST, MUP, H, HF2, N,
1          NP4, REACT(507), BM(507)
COMMON / BLOCK9 / II(5), ZZZ(5, 25), SSS(5, 25), DV(3, 1)
COMMON / DATA1 / PDV(3, 1)
DO 310 I = 1, 3
310  VECTOR(I, 1) = 0.0
DO 311 I = 1, KNPL
    U(1, 1) = COS(THETA(I))
    U(1, 2) = -SIN(THETA(I))
    U(1, 3) = 0.0
    U(2, 1) = -U(1, 2)
    U(2, 2) = U(1, 1)
    U(2, 3) = 0.0
    U(3, 1) = DISTR(I) * U(2, 1) - DISTA(I) * U(1, 1)
    U(3, 2) = DISTR(I) * U(1, 1) + DISTA(I) * U(2, 1)
    U(3, 3) = 1.0
DO 320 J = 1, 3
DO 320 K = 1, 3
320  UT(J, K) = U(K, J)
CALL MULT ( PDV, UT, DV, 1 )
CALL AXIAL ( 1, PX )
CALL LLP ( 1, PDV(2, 1), PDV(3, 1), PX, SRES )
    S(1, 1) = PX * POTT(I)
    S(2, 1) = SRES * POTT(I)
    S(3, 1) = HM(4) * POTT(I)
CALL MULT ( US, U, S, 1 )
DO 312 J = 1, 3
312  VECTOR(J, 1) = VECTOR(J, 1) + US(J, 1)
311  CONTINUE
RETURN
END

```



```

SUBROUTINE AXIAL ( I, PX )
COMMON / BLOCK1 / TC(20), POTT(20), KP(20), KA(20), KS(20),
1      KSS(20), UISTR(20), UTSTA(20), THETA(20),
2      DPS(20), FDBET(20), KNPI
COMMON / BLOCK7 / KFLAG, KEY, KOJ, KAY, KAR
COMMON / BLOCK9 / II(5), ZZZ(5, 25), SSS(5, 25), DV(3, 1)
COMMON / DATA1 / PDV(3, 1)
562 FORMAT ( // 5X *FAILURE IN BEARING      DTLE GROUP* IS )
563 FORMAT ( // 5X *FAILURE IN PULL OUT    DTLE GROUP* IS )
      IF ( PDV(1, 1) .NE. 0 ) GO TO 317
RETURN
317      ND = KA(I)
          IT = II(ND)
          KAK = 0
          DO 302 J = 1, IT
              IF ( PDV(1, J) .LE. ZZZ(ND, J) ) GO TO 303
302      CONTINUE
          PRINT 562, I
          KAR = 1
          RETURN
303      IF ( PDV(1, 1) .GE. ZZZ(ND, 1) ) GO TO 304
          PRINT 563, I
          KAR = 1
          RETURN
304      KKK = J - 1
          PX = SSS(ND, KKK) + ( SSS(ND, J) - SSS(ND, KKK) ) *
1          ( PDV(1, 1) - ZZZ(ND, KKK) ) / ( ZZZ(ND, J) -
2          ZZZ(ND, KKK) )
          RETURN
END

```

```

SUBROUTINE MAKE ( NOP )
DIMENSION FKO(10), AV(10), W(10)
COMMON / BLCCK1 / TC(20), PUTT(20), KP(20), KA(20), KS(20),
1      KSS(20), DISTR(20), DITETA(20), THETA(20),
2      UPS(20), FDBET(20), KNOL
COMMON / BLCCK2 / NN(20), HM(20), NDS(20), KTYPE(20), YIELD(20),
1      YOUNG(20)
COMMON / BLCCK3 / XX1(20,5), XX2(20,5), RRI(20,5), XRI(20,5),
1      SIZE(20,5), AREA(20,5), PULT(20,5,20),
2      BULT(20,5,20), NINT(20,5)
COMMON / BLCCK5 / NC(5), XS(5,20), NP(5,20), Yc(5,20,25),
1      PC(5,20,25)
COMMON / BLCCK6 / NOC(10), NSTYPE(10), DTC(10,20), GAMMA(10,10),
1      PHI(10,10), KDENSE(10,10), SHEARS(10,10), ICON(
2      10,10), INFO(10,10), DIS1(10,10), DIS2(10,10),
3      DIST(10,10), NPOTNT(10,10), SIGD(10,10,15),
4      FP(10,10,15)
C-----SET CONSTANTS
      MOP = KP(NOP)
      NSET = KS(NOP)
      KSOIL = KSS(NOP)
      NSTYPEX = NSTYPE(KSOIL)
      NOCX = NOC(KSOIL)
      NDSX = NDS(MOP)
      NC(NSET) = NOCX
C-----START GENERATING A SET OF P-Y CURVES
      DO 553 IJK = 1, NOCX
          XS(NSET, IJK) = DTC(KSOIL, IJK)
C-----IDENTIFY THE SOIL LAYER
      DO 512 IFS = 1, NSTYPEX
          IF ( DIS2(KSOIL, IFS) = DTC(KSOIL, IJK) ) 512, 513, 513
          512 CONTINUE
C-----IDENTIFY IF THE LAYER IS SAND OR CLAY
          513 IF ( PHI(KSOIL, IFS) .EQ. 0 ) GO TO 528
C-----P-Y CURVES IN A SAND
C-----SET COEFFICIENT OF EARTH PRESSURE AND SLOPE OF FIRST PORTION OF P-Y CURVE
          514 IF ( KDENSE(KSOIL, IFS) .EQ. 1 ) GO TO 501
              GO TO 502
          501      FKO(IF5) = 0.40
                  AV(IF5) = 1500.0
              GO TO 510
          502      IF ( KDENSE(KSOIL, IFS) .EQ. 2 ) GO TO 503
              GO TO 504
          503      FKO(IF5) = 0.45
                  AV(IF5) = 600.0
              GO TO 510
          504      FKO(IF5) = 0.50
                  AV(IF5) = 200.0
          510 CONTINUE
C-----COMPUTE AVE DENSITY FOR CALC OVERBURDEN PRESSURE
          SWGAM = 0.0
          SDIS = 0.0
          DO 516 III = 1, IFS
              SWGAM = SWGAM + GAMMA(KSOIL, III) * ( DIS2(KSOIL, III) -
1              DIS1(KSOIL, III) )
              SDIS = SDIS + ( DIS2(KSOIL, III) - DIS1(KSOIL, III) )
          516 CONTINUE
          AGAM = SWGAM / SDIS

```

```

C-----CHOOSE PILE DIAMETER
      DO 519 IPT = 1, NDSX
      IF ( XX2(MOP, IPT) - DTC(KSOIL, IJK) ) 519, 520, 520
519      CONTINUE
520      DIA = SIZE(MOP, IPT)
C-----COMPUTE ALPHA AND ES
      ALPHA = PHI(KSOIL, IFS) / 2.0
      ES = ( AV(IFS) * AGAM * DTC(KSOIL, IJK) ) / 1.35
C-----P-Y CURVE WITH SLOPE ZERO
      IF ( ES ) 596, 596, 595
596      PC(NSET, IJK, 2) = 0.0
      YC(NSET, IJK, 2) = 1.0
      GO TO 597
C-----COMPUTE TWO ULT REG AND SELECT THE SMALLER ONE
595      PHIP = 0.7854 + PHI(KSOIL, IFS) / 2.0
      PHIM = 0.7854 - PHI(KSOIL, IFS) / 2.0
      PHIO = PHI(KSOIL, IFS)
      ALPHA = 0.5 * PHIO
      CP = TAN(PHIP) * * 2
      CA = TAN(PHIM) * * 2
      TP = TAN(PHIO)
      TB = TAN(PHIP)
      TA = TAN(ALPHA)
      CP2 = CP * CP
      CP3 = CP2 * CP
      XX = DTC(KSOIL, IJK)
      PUW = AGAM * XX * ( DIA * ( CP - CA ) + XX * TB * ( CP
      * TA + 0.5 * ( TP - TA ) ) )
      PUF = AGAM * DIA * XX * ( CP2 + CP2 * TP + TP - CA )
      IF ( PUW - PUF ) 525, 526, 526
525      PC(NSET, IJK, 2) = PUW
      GO TO 527
526      PC(NSET, IJK, 2) = PUF
C-----COMPUTE THE POINTS ON P-Y CURVE
527      YC(NSET, IJK, 2) = PC(NSET, IJK, 2) / ES
597      YC(NSET, IJK, 1) = 0.0
      PC(NSET, IJK, 1) = 0.0
      YC(NSET, IJK, 3) = 10.0 * DIA
      PC(NSET, IJK, 3) = PC(NSET, IJK, 2)
      NP(NSET, IJK) = 3
      GO TO 553
C-----P-Y CURVES IN CLAYS
C-----CHECK IF STRESS-STRAIN CURVES ARE AVAILABLE OR NOT
528      IF ( INFO(KSOIL, IFS) ) 529, 529, 540
C-----NO STRESS-STRAIN CURVES ARE AVAILABLE
C-----ASSUME STRESS-STRAIN CURVES ACCORDING TO THE CONSISTENCY OF CLAY
529      IF ( ICON(KSOIL, IFS) .EQ. 3 ) GO TO 530
      GO TO 531
530      EP50 = 0.02
      GO TO 534
531      IF ( ICON(KSOIL, IFS) .EQ. 1 ) GO TO 532
      GO TO 533
532      EP50 = 0.005
      GO TO 534
533      EP50 = 0.01
C-----COMPUTE AVE DENSITY FOR CALC OVERBURDEN PRESSURE
534      SGAM = 0.0
      SDIS = 0.0

```

```

DO 537 III = 1, IFS
  SGAM = SGAM + GAMMA(KSOIL, IJI) * ( DIS2(KSOIL, III) -
1     DIS1(KSOIL, III) )
  SDIS = SDIS + ( DIS2(KSOIL, IJI) - DIS1(KSOIL, III) )
537 CONTINUE
  AGAM = SGAM / SDIS
C-----CHOOSE PILE DIAMETER
DO 539 IPT = 1, NDSX
  IF ( XX2(MOP, IPT) - DTC(KSOIL, IJK) ) 539, 540, 540
539 CONTINUE
540 DIA = SIZE(MOP, IPT)
C-----COMPUTE TWO ULT REG AND SELECT THE SMALLER ONE
  PUW = AGAM * DIA * DTC(KSOIL, IJK) + 2.0 * SHEARS(KSOIL,
1     IFS) * DIA + 2.83 * SHEARS(KSOIL, IFS) * DTC(KSOIL,
2     IJK)
  PUF = 11.0 * SHEARS(KSOIL, IFS) * DIA
  SIG50 = SHEARS(KSOIL, IFS)
  A = 2.0 * ( ALOG10(2.0) ) + ALOG10(EPS0)
  EP100 = 10.0 ** A
  DIFF = EP100 / 10.0
  IF ( PUF - PUW ) 541, 541, 542
C-----COMPUTE POINTS ON P-Y CURVE
541 MPOINT = 12
  PC(NSET, IJK, 12) = PUF
  PC(NSET, IJK, 11) = PUF
  YC(NSET, IJK, 12) = 10.0 * DIA
  YC(NSET, IJK, 11) = EP100 * DIA
  NP(NSET, IJK) = 12
  GO TO 546
542 STUP = 9.0
DO 543 ITO = 1, 9
  EP = STUP * DIFF
  STUP = STUP - 1.0
  PSD = ALOG10(SIG50) + 0.5 * ( ALOG10(EP) - ALOG10(EP50) )
  SIGA = 10.0 ** PSD
  Q(ITO) = 5.5 * SIGA * DIA
  IF ( PUW - Q(ITO) ) 543, 544, 545
543 CONTINUE
  DIFF = DIFF / 10.0
  STUP = 9.0
DO 561 ITO = 1, 9
  EP = STUP * DIFF
  STUP = STUP - 1.0
  PSD = ALOG10(SIG50) + 0.5 * ( ALOG10(EP) - ALOG10(EP50) )
  SIGA = 10.0 ** PSD
  Q(ITO) = 5.5 * SIGA * DIA
  IF ( PUW - Q(ITO) ) 561, 562, 562
561 CONTINUE
562 NP(NSET, IJK) = 3
  PC(NSET, IJK, 3) = PUW
  YC(NSET, IJK, 3) = 10.0 * DIA
  PC(NSET, IJK, 2) = PUW
  YC(NSET, IJK, 2) = EP * DIA
  GO TO 546
544 MPOINT = 12 - ITO
  KZ = MPOINT - 1
  PC(NSET, IJK, MPOINT) = PUW
  YC(NSET, IJK, MPOINT) = 10.0 * DIA

```

```

      PC(NSET, IJK, KZ) = PUW
      YC(NSET, IJK, KZ) = EP * DIA
      NP(NSET, IJK) = MPOINT
545  GO TO 546
      MPOINT = 13 - ITO
      KF = MPOINT - 1
      PC(NSET, IJK, MPOINT) = PUW
      PC(NSET, IJK, KF) = PUW
      YC(NSET, IJK, MPOINT) = 10.0 * DIA
      YC(NSET, IJK, KF) = ( DIA * DIFF * ( 2.0 * SIUP + 3.0 ) )
1      / 2.0
      NP(NSET, IJK) = MPOINT
546  CONTINUE
      YC(NSET, IJK, 1) = 0.0
      PC(NSET, IJK, 1) = 0.0
      IM = NP(NSET, IJK) - 2
593  IF ( IM = 1 ) 594, 594, 593
      TIME = 1.0
      DO 547 JT = 2, IM
          EP = DIFF * TIME
          TIME = TIME + 1.0
          ABC = ALOG10(SIG50) + 0.5 * ( ALOG10(FP) - ALOG10(EP50) )
          DSIG = 10.0 ** ABC
          PC(NSET, IJK, JT) = 5.5 * DIA * DSIG
          YC(NSET, IJK, JT) = DIA * EP
547  CONTINUE
594  CONTINUE
      GO TO 553
C-----COMPUTE POINTS ON P-Y CURVE FROM STRESS-STRAIN CURVE
548  DO 549 IPT = 1, NDSX
      IF ( XX2(MOP, IPT) = DTC(KSOIL, IJK) ) 549, 592, 592
549  CONTINUE
592  DIA = SIZE(MOP, IPT)
      PC(NSET, IJK, 1) = 0.0
      YC(NSET, IJK, 1) = 0.0
      MZ = NPOINT(KSOIL, IFS)
      DO 552 JT = 2, MZ
          YC(NSET, IJK, JT) = DIA * FP(KSOIL, IFS, JT)
          PC(NSET, IJK, JT) = 5.5 * DIA * SIGD(KSOIL, IFS, JT)
552  CONTINUE
      IE = NPOINT(KSOIL, IFS) + 1
      YC(NSET, IJK, IE) = 10.0 * DIA
      IE1 = IE - 1
      PC(NSET, IJK, IE) = PC(NSET, IJK, IE1)
      NP(NSET, IJK) = IE
553  CONTINUE
      RETURN
      END.

```

```
SUBROUTINE MULT ( A, B, C, ISIZE )
DIMENSION A(3, 3), B(3, 3), C(3, 3)
DO 10 I = 1, 3
  DO 10 J = 1, ISIZE
    A(I, J) = 0.0
  DO 5 K = 1, 3
    A(I, J) = A(I, J) + B(I, K) + C(K, J)
5  CONTINUE
10 CONTINUE
RETURN
END
```

```

SUBROUTINE LLP ( ITYPE, YT, ALPHA, PX, SPFS )
DIMENSION A(507), B(507), C(507), DY(507), DHM(507), RES(507),
1      YY(507), P(507)
COMMON / BLOCK1 / TC(20), PUTT(20), KP(20), KA(20), KS(20),
1      KSS(20), UISTR(20), DISTA(20), THETA(20),
2      OPS(20), FDBET(20), KNPL
COMMON / BLOCK2 / NN(20), HH(20), NDS(20), KTYPE(20), YIELD(20),
1      YOUNG(20)
COMMON / BLOCK3 / XX1(20, 5), XX2(20, 5), RRI(20, 5), XRI(20, 5),
1      SIZE(20,5), AREA(20,5), PULT(20,5,20),
2      BULT(20,5,20), NINT(20,5)
COMMON / BLOCK7 / KFLAG, KEY, KOJ, KAY, KAR
COMMON / BLOCK8 / Y(507), ES(507), R(507), MPLAST, MOP, H, HE2, N,
1      NP4, REAC(507), RM(507)
COMMON / DATA / PDV(J, 1)
520 FORMAT ( 10X *NO OF ITERATION* I5 )
551 FORMAT ( 10X *STA* 4X *X,IN* 8X *Y,IN* 8X *DY/DX* 7X *M, LB-IN* 5X
1      *DY/DX* 7X *P, LB-IN* )
552 FORMAT ( 7X, I5, 2X, 6E12.3 )
553 FORMAT ( / 10X *PILE TOP DISPLACEMENTS AND REACTIONS* )
554 FORMAT ( 13X *X,IN* 8X *Y,IN* 8X *DY/DX* 7X *AXIAL, LB* 4X
1      *LAT, LB* 6X *BM, LB-IN* )
555 FORMAT ( 10X, 6E12.3 )
556 FORMAT ( // 10X *LATERALLY LOADED PILE* )
580 FORMAT ( / 10X *PLASTIC HINGE IS FORMED IN GROUP* I5 )
1501 FORMAT ( ///// 10X *EI DOES NOT COVER TOTAL LENGTH OF PILE* I5 )
1502 FORMAT ( ///// 10X *NO CLOSURE OF A LLP AFTER 1000 ITERATIONS*
1      10X *PILE GROUP* I3 )
1503 FORMAT ( // 7X *PILE GROUP* I3 )
1506 FORMAT ( / 5X *PLASTIC HINGES AT STATION* )
1507 FORMAT ( 10X, 14I5 )
C-----START EXECUSION OF PROGRAM
C-----COMPUTE CONSTANTS AND INDEXES
      MOP = KP(ITYPE)
      ITER = 1
      K = 1
      TOLP = 0.00001
      PIN = 3MPIN
      FIX = 3MFIX
      G = FDBET(ITYPE)
      H = HH(MOP)
      N = NN(MOP)
      H2 = H * H
      HE2 = H * H
      HE3 = HE2 * H
      HE4 = HE2 * HE2
      NP3 = N + 3
      NP4 = N + 4
      NP5 = N + 5
      NP6 = N + 6
      NP7 = N + 7
C-----CLEAR THE STORAGE PLACES
      DO 1000 J = 1, NP7
          R(J) = 0.0
          Y(J) = 0.0
          ES(J) = 0.0
          P(J) = 0.0
1000      CONTINUE

```

```

C-----COMPUTE INITIAL ES (ES = KX * K = 1.0) AND FLEXURAL STIFFNESS EI = R
  DO 1001 J = 4, NP4
    XJ = J - 4
    P(J) = PX
    ES(J) = 1.0 * XJ * H
    R(J) = RHI(MOP, 1)
  1001 CONTINUE
C-----SET RECURSION COEFFICIENTS AT STATIONS 1, 2 AND 4
  A(1) = 0.0
  R(1) = 0.0
  C(1) = 0.0
  A(2) = 0.0
  R(2) = 0.0
  C(2) = 0.0
  A(4) = YT
  R(4) = 0.0
  C(4) = 0.0
C-----RECURSION COEFFICIENT AT STATION 3
  IF ( TC .EQ. FIX ) GO TO 1011
  IF ( TC .EQ. PIN ) GO TO 1012
C-----ELASTICALLY RESTRAINED TOP
  DENOM = G * H + 2.0 * R(4)
  A(3) = ( 4.0 * R(4) * YT - 2.0 * ALPHA * G * HE2 ) /
  1 DENOM
  R(3) = 0.0
  C(3) = ( G * H - 2.0 * R(4) ) / DENOM
  GO TO 1013
C-----FIXED TOP
  1011 A(3) = -2.0 * ALPHA * H
  R(3) = 0.0
  C(3) = 1.0
  GO TO 1013
C-----PINNED TOP
  1012 A(3) = 2.0 * YT
  R(3) = 0.0
  C(3) = -1.0
  1013 CONTINUE
C-----COMPUTE RECURSION COEFFICIENTS AT ALL STATIONS
  1023 DO 1029 J = 5, NP5
    AA = R(J - 1)
    BB = -2.0 * R(J - 1) - 2.0 * P(J) + P(J) * HE2
    CC = R(J - 1) + 4.0 * R(J) + R(J + 1) - 2.0 * P(J) * HE2
  1 +ES(J) * HE4
    DD = -2.0 * R(J) - 2.0 * R(J + 1) + P(J) * HE2
    EE = R(J + 1)
C-----COMPUTE RECURSION COEFFICIENTS AT EACH STATION J
  E = AA * B(J - 2) + BB
  DENOM = E * B(J - 1) + AA * C(J - 2) + CC
  IF ( DENOM .NE. 0 ) GO TO 1021
C-----IF DENOM IS ZERO BEAM DOES NOT EXIST n = 0
  D = 0.0
  GO TO 1022
  1021 D = -1.0 / DENOM
  1022 C(J) = D * EE
  R(J) = D * ( E * C(J - 1) + DD )
  A(J) = D * ( E * A(J - 1) + AA * A(J - 2) )
  1029 CONTINUE
C-----PRESERVE PREVIOUS Y AND COMPUTE NEW Y

```



```

DO 1035 J = 4, NP4
1035   YY(J) = Y(J)
      Y(NP6) = 0.0
      Y(NP7) = 0.0
DO 1030 L = 3, NP7
      J = N + 8 - L
      Y(J) = A(J) + B(J) * Y(J+1) + C(J) * Y(J+2)
1030   CONTINUE
C-----RESET EI VALUES
CALL MCURV
IF ( KAX .EQ. 0 ) GO TO 1031
RETURN
1031   CONTINUE
C-----CHECK FOR CLOSURE OF DEFLECTION Y AT ALL STATIONS
DO 1040 J = 4, NP4
      IF ( ABS ( YY(J) - Y(J) ) .GE. TOLP ) GO TO 1050
1040   CONTINUE
      IF ( KFLAG .EQ. 0 ) GO TO 1039
      IF ( MPLAST .EQ. 0 ) GO TO 1039
PRINT 580, ITYPE
1039   CONTINUE
      GO TO 1060
1050   ITER = ITER + 1
      IF ( ITER .LE. 1000 ) GO TO 1051
PRINT 1502, ITYPE
      KEY = 1
RETURN
C-----COMPUTE NEW SET OF ES VALUES
1051 CALL SOIL 2R ( ITYPE )
      GO TO 102J
C-----COMPUTE SLOPE, BM, SHEAR AND REACTION
1060   CONTINUE
      BM(2) = 0.0
      BM(NP6) = 0.0
DO 1071 J = 3, NP5
      DY(J) = ( Y(J+1) - Y(J-1) ) / H2
      RM(J) = - R(J) * ( Y(J-1) - 2.0 * Y(J) + Y(J+1) ) / HE2
1071   CONTINUE
DO 1072 J = 3, NP5
      DBM(J) = - ( BM(J+1) - BM(J-1) ) / H2 + P(J) * DY(J)
1072   CONTINUE
C-----SUM UP SOIL REACTION
DO 1008 J = 4, NP4
1008   RES(J) = ES(J) * Y(J)
      SRES = 0.0
DO 1100 K = 4, NP4
      IF ( K .EQ. 4 ) GO TO 1109
      IF ( K .EQ. NP4 ) GO TO 1109
      SRES = SRES + RES(K) * H
      GO TO 1100
1109   SRES = SRES + RES(K) * H / 2.0
1100   CONTINUE
      IF ( KFLAG .EQ. 0 ) GO TO 1075
PRINT 1503, ITYPE
PRINT 553
PRINT 554
PRINT 555, PDV(1, 1), Y(4), DY(4), PX, SRES, BM(4)
      IF ( KOJ .EQ. 0 ) GO TO 1075

```

```
C-----PRINT OUT ALL THE PILE STATIONS
PRINT 556
PRINT 551
      DBM(4) = SRES
DO 1073 J = 4, NP4
      ISTA = J - 4
      ZI = ISTA
      X = ZI * H
PRINT 552, ISTA, X, Y(J), DY(J), BM(J), DBM(J), RES(J)
1073  CONTINUE
PRINT 520, ITER
1075  CONTINUE
RETURN
END
```

```

SUBROUTINE MOURV
DIMENSION CURV(507)
COMMON / RLOCK1 / TC(20), PUTT(20), KP(20), KA(20), KS(20),
1 KSS(20), DISTB(20), DISTA(20), THETA(20),
2 DPS(20), FDBET(20), KNPI
COMMON / RLOCK2 / NN(20), HM(20), NDS(20), KTYPE(20), YIELD(20),
1 YOUNG(20)
COMMON / RLOCK3 / XX1(20, 5), XX2(20, 5), RRI(20, 5), XRI(20, 5),
1 SIZE(20,5), AREA(20,5), PULT(20,5,20),
2 BULT(20,5,20), NINT(20,5)
COMMON / RLOCK7 / KFLAG, KEY, KOJ, KAY, KAR
COMMON / RLOCK8 / Y(507), ES(507), R(507), MPLAST, MOP, H, HE2, N,
1 NP4, REACT(507), BM(507)
COMMON / DATA1 / PDV(3, 1)
501 FORMAT ( /// 5X *AXIAL LOAD EXCEEDS PILE STRENGTH* )
C-----SET CONSTANTS
      AX = ABS ( PDV(3, 1) )
      KAX = 0
      MATL = KTYPE(MOP)
      NDSX = NDS(MOP)
      MPLAST = 0
      IF ( MATL .EQ. 5 ) GO TO 101
      GO TO 102
C-----LINEARLY ELASTIC PILE MATERIAL
101  CONTINUE
      DO 110 I = 4, NP4
          X = I - 4
          XSTA = X * H
      DO 111 J = 1, NDSX
          IF ( XX2(MOP, J) .GE. XSTA ) GO TO 112
111  CONTINUE
112  R(I) = RRI(MOP, J)
110  CONTINUE
      RETURN
C-----BILINEARLY ELASTIC PILE MATERIAL
102  CONTINUE
      DO 120 I = 4, NP4
          C = ( Y(1+1) - 2.0 * Y(I) + v(I-1) ) / HE2
          CURV(I) = ABS ( C )
C-----CHECK IF AXIAL LOAD EXCEEDS PILE STRENGTH
          IF ( AX .LE. PULT( MOP, 1, 1 ) ) GO TO 121
          PRINT 5,1
          KAX = 1
      RETURN
121  CONTINUE
C-----DETERMINE THE PILE SECTION
      X = I - 4
      XSTA = X * H
      DO 122 J = 1, NDSX
          IF ( XX2(MOP, J) .GE. XSTA ) GO TO 123
122  CONTINUE
123  R(I) = RRI(MOP, J)
          INT = NINT(MOP, J)
          DO 130 K = 2, INT
              IF ( PULT(MOP, J, K) .LE. AX ) GO TO 131
130  CONTINUE
131  BMP = BULT(MOP, J, K) + ( BULT(MOP, J, K-1) - BULT(MOP, J,
1      , K) ) * ( AX - PULT(MOP, J, K) ) /

```

```
      2          ( PULT(MOP, J, K-1) - PULT(MOP, J, K) )
C-----CHECK IF MOMENT EXCEEDS PLASTIC MOMENT
      RM = R(I) * CURV(I)
      IF ( RM .GT. BMP ) GO TO 133
      GO TO 120
133      R(I) = BMP / CURV(I)
      MPLAST = 1
120      CONTINUE
      RETURN
      END
```

```

SUBROUTINE SOIL 2H ( NOP )
DIMENSION EST(20)
COMMON / BLOCK1 / TC(20), POTT(20), KP(20), KA(20), KS(20),
1      KSS(20), UISTA(20), DISTA(20), THETA(20),
2      UPS(20), FDBET(20), KNPI
COMMON / BLOCK2 / NN(20), HH(20), NDS(20), KTYPE(20), YIELD(20),
1      YOUNG(20)
COMMON / BLOCK5 / NC(5), XS(5,20), NP(5,20), YC(5,20,25),
1      PC(5,20,25)
COMMON / BLOCK7 / KFLAG, KEY, KOJ, KAX, KAR
COMMON / BLOCK8 / Y(507), ES(507), R(507), MPLAST, MOP, H, HE2, N,
1      NP4, REACT(507), RM(507)
3000 FORMAT( // 52H      P-Y CURVES DO NOT EXTEND THE LENGTH OF THE PILE
1      )
C-----SET CONSTANT
      NSET = KS(NOP)
C-----START COMPUTING ES VALUES
      K = 2
      DO 3090 J = 4, NP4
          ZJ = J - 4
          Z = ZJ * H - DPS(NUP)
C-----CHECK IF THE STATION IS ABOVE GROUND SURFACE IF SO SET ES = 0
      IF ( / ) 3010, 3015, 3015
3010      ES(J) = 0.0
      GO TO 3090
C-----FIND THE P-Y CURVES LOCATING ABOVE AND BELOW THE GIVEN STATION
3015      IF ( XS(NSET, K) - Z ) 3020, 3027, 3030
3020      K = K + 1
      IF ( K = NC(NSET) ) 3015, 3015, 3025
3025 PRINT 3000
      KEY = J
3026 RETURN
3027      M = K
      GO TO 3035
3030      M = K - 1
3035      YA = ABS ( Y(J) )
      IF ( YA - 1.0E-10 ) 3036, 3037, 3037
3036      YA = 1.0E-10
C-----FIND POINTS BEHIND AND AHEAD OF GIVEN Y ON EACH P-Y CURVE AND COMPUTE
C      ES ON EACH CURVE BY LINEAR INTERPOLATION
3037      DO 3070 I = M, K
          L = 2
3040      IF ( YC(NSET, I, L) - YA ) 3045, 3055, 3060
3045      L = L + 1
      IF ( L = NP(NSET, I) ) 3040, 3040, 3050
3050      P1 = PC(NSET, I, L-1)
      GO TO 3065
3055      P1 = PC(NSET, I, L)
      GO TO 3065
3060      P1 = PC(NSET, I, L) - ( PC(NSET, I, L) - PC(NSET, I, L-1)
1          ) * ( YC(NSET, I, L) - YA ) / ( YC(NSET, I, L) -
2          YC(NSET, I, L-1) )
3065      EST(I) = P1 / YA
3070      CONTINUE
C-----INTERPOLATE BETWEEN CURVES FOR ES VALUE
      IF ( K = M ) 3075, 3075, 3080
3075      ES(J) = EST(K)
      GO TO 3090

```

```
3080          ES(J) = ( EST(K) - ( EST(K) - EST(M) ) * ( XS(NSET, K) -  
1          Z ) / ( XS(NSET, K) - XS(NSET, M) ) )  
3090          CONTINUE  
          RETURN  
          END
```

## A.6 Example Run for Program GROUP

Some of the typical runs for the two examples in Chapter VII are shown in the following.

## Example 1. Cap 2.

The example runs show two cases.

1. Foundation is subjected only to the dead load, 500 pounds.
2. Foundation is subjected to an inclined load very close to the ultimate.

## Example 2. Copano Bay.

The computation is made for two cases of loading in the foundation.

1. Foundation is subjected only to the vertical load, 844 kips.
2. Foundation is subjected to both the vertical load, 844 kips, the design lateral load 86.4 kips and the design moment  $-1.68 \times 10^7$  inch-pounds.











## CAP 2 ULTIMATE BEARING CAPACITY 5400 LB

TABLE H INPUT AND OUTPUT SWITCH (IF 1 YES, IF 0 NO)

TABLE	C	D	E	F	G	H	J
INPUT	1	1	1	1	1	1	
OUTPUT	1	1	1	1	1	1	0
	(C LOAD	D ARRANGEMENT	E PILE	F L-S	G P-Y	H SOIL	J LLP)

TABLE C LOAD

V LOAD, LB	H LOAD, LB	MOMENT, LB-IN
5.000E+02	0.	0.

TABLE D ARRANGEMENT OF PILE GROUPS

GROUP	CONNECT	NO OF PILE	PILE NO	L-S CURVE		
1	FIX	2	1	1	2	1
2	FIX	2	1	1	1	0
GROUP	VERT, IN	HOR, IN	SLOPE, RAD	GROUND, IN	SPRING	
1	0.	1.225E+01	1.652E-01	1.200E+01	0.	
2	0.	-1.225E+01	-8.390E-02	1.200E+01	0.	

TABLE E PILE DIMENSIONS

PILE	SEC	INC	MATERIAL	LENGTH, IN	YIFLD, PSI	E, PSI
1	1	30	3	1.080E+02	6.400E+04	2.900E+07

(MATERIAL 1 STEEL H, 2 STEEL H (WEAK AXIS), STEEL PIPE  
4 OTHERS WITH INT DIAGRAM, 5 OTHERS WITHOUT INT DIAGRAM)

PILE	FROM, IN	TO, IN	D, IN	A, IN <sup>2</sup>	A, IN <sup>2</sup>	I, IN <sup>4</sup>
1	0.	1.080E+02	2.000E+00	3.800E-01	1.850E-01	
INTERACTION DIAGRAM		MULT, IN-LB		NUM OF POINTS		
	PULT, LB					
	2.432E+04		0.			
	0.		1.504E+04			

TABLE F AXIAL LOAD VS SETTLEMENT

NUM OF CURVES 3

CURVE	1	NUM OF POINTS	15
POINT	AXIAL LOAD, LB	SETTLEMENT, IN	
1	-5.400E+03	-2.000E+01	
2	-5.400E+03	-1.000E-01	
3	-5.000E+03	-7.200E-02	
4	-4.000E+03	-4.600E-02	
5	-3.000E+03	-2.800E-02	
6	-2.000E+03	-1.600E-02	

7	-1.000E+03	-4.000E-03
8	0.	0.
9	1.000E+03	4.000E-03
10	2.000E+03	1.600E-02
11	3.000E+03	2.800E-02
12	4.000E+03	4.600E-02
13	5.000E+03	7.200E-02
14	5.400E+03	1.000E-01
15	5.400E+03	2.000E+01

CURVE 2                      NUM OF POINTS 13

POINT	AXIAL LOAD, LB	SETTLEMENT, IN
1	-4.600E+03	-2.000E+01
2	-4.600E+03	-8.700E-02
3	-4.200E+03	-7.000E-02
4	-3.000E+03	-4.000E-02
5	-2.000E+03	-2.200E-02
6	-1.000E+03	-7.000E-03
7	0.	0.
8	1.000E+03	7.000E-03
9	2.000E+03	2.200E-02
10	3.000E+03	4.000E-02
11	4.200E+03	7.000E-02
12	4.600E+03	8.700E-02
13	4.600E+03	2.000E+01

CURVE 3                      NUM OF POINTS 11

POINT	AXIAL LOAD, LB	SETTLEMENT, IN
1	-3.600E+03	-2.000E+01
2	-3.400E+03	-4.500E-02
3	-3.000E+03	-3.300E-02
4	-2.000E+03	-1.300E-02
5	-1.000E+03	-2.000E-03
6	0.	0.
7	1.000E+03	2.000E-03
8	2.000E+03	1.300E-02
9	3.000E+03	3.300E-02
10	3.400E+03	4.500E-02
11	3.600E+03	2.000E+01

TABLE 6      P-Y CURVES

NUM OF SETS 2

SET 1                      NUM OF CURVES 6

CURVE	DISTANCE FROM TOP, IN	NUM OF POINTS
1	0.	2
POINT	P, LB	Y, IN
1	0.	0.
2	0.	2.000E+01
2	6.000E+00	NUM OF POINTS 3
POINT	P, LB	Y, IN
1	0.	0.
2	9.480E+00	5.300E-02
3	9.480E+00	2.000E+01
3	1.200E+01	NUM OF POINTS 3
POINT	P, LB	Y, IN
1	0.	0.
2	3.350E+01	9.500E-02
3	3.350E+01	2.000E+01
4	1.800E+01	NUM OF POINTS 3

POINT	P, LB	Y, IN	
1	0.	0.	
2	7.240E+01	1.370E-01	
3	7.240E+01	2.000E+01	
CURVE 5	DISTANCE FROM TOP, IN	2.400E+01	NUM OF POINTS 3
POINT	P, LB	Y, IN	
1	0.	0.	
2	1.260E+02	1.260E-01	
3	1.260E+02	2.000E+01	
CURVE 6	DISTANCE FROM TOP, IN	9.600E+01	NUM OF POINTS 3
POINT	P, LB	Y, IN	
1	0.	0.	
2	1.541E+03	5.470E-01	
3	1.541E+03	2.000E+01	
SET 2	NUM OF CURVES	6	
CURVE 1	DISTANCE FROM TOP, IN	0.	NUM OF POINTS 3
POINT	P, LB	Y, IN	
1	0.	0.	
2	0.	1.000E+00	
3	0.	2.000E+01	
CURVE 2	DISTANCE FROM TOP, IN	6.000E+00	NUM OF POINTS 3
POINT	P, LB	Y, IN	
1	0.	0.	
2	1.284E+01	5.316E-02	
3	1.284E+01	2.000E+01	
CURVE 3	DISTANCE FROM TOP, IN	1.200E+01	NUM OF POINTS 3
POINT	P, LB	Y, IN	
1	0.	0.	
2	4.595E+01	9.512E-02	
3	4.595E+01	2.000E+01	
CURVE 4	DISTANCE FROM TOP, IN	1.800E+01	NUM OF POINTS 3
POINT	P, LB	Y, IN	
1	0.	0.	
2	9.932E+01	1.371E-01	
3	9.932E+01	2.000E+01	
CURVE 5	DISTANCE FROM TOP, IN	2.400E+01	NUM OF POINTS 3
POINT	P, LB	Y, IN	
1	0.	0.	
2	1.730E+02	1.790E-01	
3	1.730E+02	2.000E+01	
CURVE 6	DISTANCE FROM TOP, IN	9.600E+01	NUM OF POINTS 3
POINT	P, LB	Y, IN	
1	0.	0.	
2	2.113E+03	5.469E-01	
3	2.113E+03	2.000E+01	

TABLE H SOIL DATA FOR AUTO P-Y CURVES

PROFILE	1	NUM OF CURVES	6	NUM OF STRATA	1		
DISTANCES FROM PILE TOP TO P-Y CURVES, INCH							
CURVE	LOCATION, IN						
1	0.						
2	6.000E+00						
3	1.200E+01						
4	1.800E+01						
5	2.400E+01						
6	9.600E+01						
STRATUM	TYPE	GAMMA, PCF	PHI, DEG	DENS	SHFAR, PSI	CONSIST	S-S CURVE
1	SAND	6.260E+01	4.680E+01	1			

STRATUM	(DENSITY OF SAND			1 DENSE	2 MEDIUM	3 LOOSE)
	(CONSISTENCY OF CLAY			1 STIFF	2 MEDIUM	3 SOFT )
	FROM, IN			TO, IN		
1	0.			9.600E+01		

CAP 2      ULTIMATE BEARING CAPACITY 5400 LB

COMPUTATION RESULTS

TABLE I      DISPLACEMENT OF GROUPED PILE FOUNDATION

VERTICAL, IN	HORIZONTAL, IN	ROTATION, RAD
6.027E-04	-2.305E-03	-2.182E-05

NO OF ITERATION 2

TABLE J      COMPUTATION ON INDIVIDUAL PILE

PILE GROUP 1

PILE TOP DISPLACEMENTS AND REACTIONS

X, IN	Y, IN	DY/DX	AXIAL, LB	LAT, LB	BM, LB-IN
4.794E-04	-2.410E-03	-2.177E-05	1.19E+02	-4.749E+00	-7.786E+01

PILE GROUP 2

PILE TOP DISPLACEMENTS AND REACTIONS

X, IN	Y, IN	DY/DX	AXIAL, LB	LAT, LB	BM, LB-IN
5.272E-04	-2.262E-03	-2.177E-05	1.31E+02	-4.000E+00	-6.854E+01



## CAP 2 INCLINED LOAD IS VARIED

TABLE B INPUT AND OUTPUT SWITCH (IF 1 YES, IF 0 NO)

TABLE	C	D	E	F	G	H	J
INPUT	1	0	0	0	0	0	
OUTPUT	1	0	0	0	0	0	1
	(C LOAD	D ARRANGEMENT	E PILE	F L-S	G P-Y	H SOIL	J LLP)

TABLE C LOAD

V LOAD, LB	H LOAD, LB	MOMENT, LB-IN
1.777E+04	3.700E+03	7.800E+03

CAP 2 INCLINED LOAD IS VARIED

## COMPUTATION RESULTS

TABLE 1 DISPLACEMENT OF GROUPED PILE FOUNDATION

VERTICAL, IN	HORIZONTAL, IN	ROTATION, RAD
5.094E-01	1.431E+00	-2.855E-02

NO OF ITERATION 8

TABLE 2 COMPUTATION ON INDIVIDUAL PILE

PILE GROUP 1

## PILE TOP DISPLACEMENTS AND REACTIONS

X, IN	Y, IN	OY/OX	AXIAL, LB	L, T, LB	M, LB-IN
1.083E+00	1.271E+00	-2.856E-02	5.400E+03	6.040E+02	1.095E+04

## LATERALLY LOADED PILE

STA	X, IN	Y, IN	OY/OX	M, LB-IN	OM/OX	P, LB/IN
0	0.	1.271E+00	-2.856E-02	1.095E+04	6.040E+02	0.
1	3.000E+00	1.154E+00	-3.496E-02	8.147E+03	6.033E+02	0.
2	7.200E+00	1.019E+00	-3.945E-02	5.242E+03	6.033E+02	0.
3	1.080E+01	8.704E-01	-4.197E-02	2.269E+03	6.033E+02	0.
4	1.440E+01	7.166E-01	-4.249E-02	-7.335E+02	5.941E+02	5.136E+00
5	1.800E+01	5.645E-01	-4.101E-02	-2.660E+03	5.617E+02	1.284E+01
6	2.160E+01	4.213E-01	-3.765E-02	-6.377E+03	4.798E+02	3.270E+01
7	2.520E+01	2.934E-01	-3.263E-02	-8.578E+03	3.190E+02	5.662E+01
8	2.880E+01	1.863E-01	-2.642E-02	-9.938E+03	5.750E+01	8.864E+01
9	3.240E+01	1.032E-01	-1.972E-02	-1.007E+04	-2.546E+02	8.476E+01
10	3.600E+01	4.432E-02	-1.339E-02	-8.872E+03	-4.843E+02	4.281E+01
11	3.960E+01	0.441E-03	-8.043E-03	-7.057E+03	-5.750E+02	7.600E+00
12	4.320E+01	-1.360E-02	-3.985E-03	-5.044E+03	-5.579E+02	-1.707E+01
13	4.680E+01	-2.165E-02	-1.222E-03	-3.191E+03	-4.721E+02	-3.060E+01
14	5.040E+01	-2.239E-02	4.168E-04	-1.692E+03	-3.547E+02	-3.461E+01
15	5.400E+01	-1.885E-02	1.193E-03	-6.205E+02	-2.351E+02	-3.186E+01
16	5.760E+01	-1.380E-02	1.385E-03	4.666E+01	-1.721E+02	-2.534E+01
17	6.120E+01	-8.872E-03	1.241E-03	2.848E+02	-5.491E+01	-1.757E+01
18	6.480E+01	-4.871E-03	9.469E-04	4.903E+02	-4.652E+00	-1.035E+01
19	6.840E+01	-2.054E-03	6.297E-04	4.551E+02	2.238E+01	-4.664E+00
20	7.200E+01	-3.372E-04	3.584E-04	2.536E+02	3.224E+01	-8.144E-01
21	7.560E+01	5.258E-04	1.602E-04	2.370E+02	3.128E+01	1.346E+00
22	7.920E+01	8.164E-04	3.555E-05	1.346E+02	2.488E+01	2.208E+00
23	8.280E+01	7.817E-04	-2.947E-05	5.917E+01	1.690E+01	2.228E+00
24	8.640E+01	0.047E-04	-5.328E-05	1.180E+01	9.633E+00	1.809E+00
25	9.000E+01	3.981E-04	-5.313E-05	-1.226E+01	4.126E+00	1.250E+00
26	9.360E+01	2.217E-04	-4.231E-05	-1.997E+01	5.661E-01	7.281E-01
27	9.720E+01	9.346E-05	-2.958E-05	-1.799E+01	-1.321E+00	3.205E-01
28	1.008E+02	8.707E-06	-1.965E-05	-1.161E+01	-1.954E+00	3.112E-02
29	1.044E+02	-4.800E-05	-1.418E-05	-4.678E+00	-1.689E+00	-1.785E-01
30	1.080E+02	-9.341E-05	-1.261E-05	-0.	-7.178E-01	-3.610E-01

NO OF ITERATION 8

## PILE GROUP 2

## PILE TOP DISPLACEMENTS AND REACTIONS

X,IN	Y,IN	DY/DX	AXIAL,LR	LAT,LB	BM,LB-IN
3.906E-02	1.440E+00	-2.856E-02	3.614E+03	6.714E+02	1.218E+04

## LATERALLY LOADED PILE

STA	X,IN	Y,IN	DY/DX	M,LR-IN	DM/DX	P,LB/IN
0	0.	1.440E+00	-2.856E-02	1.218E+04	6.714E+02	0.
1	3.600E+00	1.322E+00	-3.577E-02	9.340E+03	6.705E+02	0.
2	7.200E+00	1.182E+00	-4.106E-02	6.420E+03	6.705E+02	0.
3	1.080E+01	1.026E+00	-4.437E-02	3.444E+03	6.705E+02	0.
4	1.440E+01	8.626E-01	-4.567E-02	4.375E+02	6.637E+02	3.792E+00
5	1.800E+01	6.976E-01	-4.497E-02	-2.527E+03	6.398E+02	9.480E+00
6	2.160E+01	5.388E-01	-4.234E-02	-5.339E+03	5.797E+02	2.389E+01
7	2.520E+01	3.928E-01	-3.793E-02	-7.792E+03	4.624E+02	4.128E+01
8	2.880E+01	2.657E-01	-3.207E-02	-9.655E+03	2.718E+02	6.462E+01
9	3.240E+01	1.619E-01	-2.528E-02	-1.050E+04	-1.343E+01	9.384E+01
10	3.600E+01	8.368E-02	-1.830E-02	-1.022E+04	-3.330E+02	8.368E+01
11	3.960E+01	3.914E-02	-1.196E-02	-8.647E+03	-5.428E+02	3.288E+01
12	4.320E+01	-2.447E-03	-6.832E-03	-6.620E+03	-5.968E+02	-2.892E+00
13	4.680E+01	-1.905E-02	-3.084E-03	-4.550E+03	-5.479E+02	-2.424E+01
14	5.040E+01	-2.465E-02	-6.332E-04	-2.755E+03	-4.438E+02	-3.361E+01
15	5.400E+01	-2.361E-02	7.514E-04	-1.372E+03	-3.215E+02	-3.433E+01
16	5.760E+01	-1.924E-02	1.353E-03	-4.210E+02	-2.062E+02	-2.974E+01
17	6.120E+01	-1.387E-02	1.445E-03	1.472E+02	-1.118E+02	-2.268E+01
18	6.480E+01	-8.844E-03	1.253E-03	4.216E+02	-4.347E+01	-1.527E+01
19	6.840E+01	-4.840E-03	9.464E-04	4.937E+02	-1.647E-01	-8.799E+00
20	7.200E+01	-2.030E-03	6.306E-04	4.474E+02	2.265E+01	-3.874E+00
21	7.560E+01	-2.999E-04	3.641E-04	3.470E+02	3.070E+01	-5.996E-01
22	7.920E+01	5.917E-04	1.685E-04	2.358E+02	2.955E+01	1.237E+00
23	8.280E+01	9.135E-04	4.289E-05	1.386E+02	2.374E+01	1.993E+00
24	8.640E+01	9.005E-04	-2.578E-05	6.605E+01	1.647E+01	2.046E+00
25	9.000E+01	7.279E-04	-5.445E-05	1.939E+01	9.691E+00	1.720E+00
26	9.360E+01	5.085E-04	-5.923E-05	-5.144E+00	4.349E+00	1.248E+00
27	9.720E+01	3.015E-04	-5.299E-05	-1.344E+01	7.226E-01	7.671E-01
28	1.008E+02	1.270E-04	-4.453E-05	-1.173E+01	-1.260E+00	3.346E-01
29	1.044E+02	-1.919E-05	-3.874E-05	-5.548E+00	-1.769E+00	-5.233E-02
30	1.080E+02	-1.520E-04	-3.688E-05	0.	-9.038E-01	-4.281E-01

NO OF ITERATION 7

COPANO BAY      VERTICAL LOAD ALONE      FIXED CONNECTION

TABLE H      INPUT AND OUTPUT SWITCH      (IF 1 YES, IF 0 NO)

TABLE	C	D	E	F	G	H	J
INPUT	1	1	1	1	0	1	
OUTPUT	1	1	1	1	1	1	0
	(C LOAD	L ARRANGEMENT		E PILE	F L-S	G P-Y	H SOIL    J LLP)

TABLE C      LOAD

V LOAD, LB	H LOAD, LB	MOMENT, LB-IN
8.440E+05	0.	0.

TABLE D      ARRANGEMENT OF PILE GROUPS

GROUP	CONNCT	NO OF PILE	PILE NO	L-S CURVE		
1	FIX	1	1	1	1	1
2	FIX	2	1	1	1	1
3	FIX	2	1	1	1	1
4	FIX	1	1	1	1	1

GROUP	VERT, IN	HOR, IN	SLOPE, RAD	GROUND, IN	SPRING
1	0.	-1.260E+02	-2.440E-01	1.200E+02	0.
2	0.	-9.000E+01	0.	1.200E+02	0.
3	0.	9.000E+01	0.	1.200E+02	0.
4	0.	1.260E+02	2.440E-01	1.200E+02	0.

TABLE F      PILE DIMENSIONS

PILE	SEC	INC	MATERIAL	LENGTH, IN	YTFLD, PSI	E, PSI
1	1	30	5	1.116E+03	6.000E+03	4.440E+06

(MATERIAL 1 STEEL H, 2 STEEL H (WEAK AXIS), STEEL PIPE  
4 OTHERS WITH INT DIAGRAM, 5 OTHERS WITHOUT INT DIAGRAM)

PILE	FROM, IN	TO, IN	D, IN	A, IN <sup>2</sup>	I, IN <sup>4</sup>
1	0.	1.116E+03	1.800E+01	3.240E+02	8.600E+03

LINEARLY ELASTIC PILE MATERIAL

TABLE F      AXIAL LOAD VS SETTLEMENT

NUM OF CURVES 1

CURVE 1	NUM OF POINTS 11	
POINT	AXIAL LOAD, LB	SETTLEMENT, IN
1	0.	-2.000E+01
2	0.	0.
3	4.000E+04	3.000E-02
4	8.000E+04	4.000E-02
5	1.000E+05	5.000E-02

6	1.200E+05	6.000E-02
7	2.400E+05	1.400E-01
8	2.600E+05	1.600E-01
9	2.800E+05	1.900E-01
10	3.600E+05	6.500E-01
11	3.000E+05	1.000E+01

TABLE G P-y CURVES

NUM OF SETS 1

SET 1	NUM OF CURVES 9		
CURVE 1	DISTANCE FROM TOP, IN 0.		NUM OF POINTS 3
POINT	P, LB	Y, IN	
1	0.	0.	
2	3.600E-02	4.320E-02	
3	3.600E-02	1.800E+02	
CURVE 2	DISTANCE FROM TOP, IN 6.000E+01		NUM OF POINTS 12
POINT	P, LB	Y, IN	
1	0.	0.	
2	6.261E-02	1.440E-01	
3	8.855E-02	2.880E-01	
4	1.084E-01	4.320E-01	
5	1.252E-01	5.760E-01	
6	1.400E-01	7.200E-01	
7	1.534E-01	8.640E-01	
8	1.657E-01	1.008E+00	
9	1.771E-01	1.152E+00	
10	1.878E-01	1.296E+00	
11	1.980E-01	1.440E+00	
12	1.980E-01	1.800E+02	
CURVE 3	DISTANCE FROM TOP, IN 6.100E+01		NUM OF POINTS 12
POINT	P, LB	Y, IN	
1	0.	0.	
2	2.379E+02	1.440E-01	
3	3.305E+02	2.880E-01	
4	4.121E+02	4.320E-01	
5	4.759E+02	5.760E-01	
6	5.320E+02	7.200E-01	
7	5.828E+02	8.640E-01	
8	6.295E+02	1.008E+00	
9	6.730E+02	1.152E+00	
10	7.138E+02	1.296E+00	
11	7.524E+02	1.440E+00	
12	7.524E+02	1.800E+02	
CURVE 4	DISTANCE FROM TOP, IN 9.600E+01		NUM OF POINTS 12
POINT	P, LB	Y, IN	
1	0.	0.	
2	2.379E+02	1.440E-01	
3	3.305E+02	2.880E-01	
4	4.121E+02	4.320E-01	
5	4.759E+02	5.760E-01	
6	5.320E+02	7.200E-01	
7	5.828E+02	8.640E-01	
8	6.295E+02	1.008E+00	
9	6.730E+02	1.152E+00	
10	7.138E+02	1.296E+00	
11	7.524E+02	1.440E+00	
12	7.524E+02	1.800E+02	
CURVE 5	DISTANCE FROM TOP, IN 1.320E+02		NUM OF POINTS 12

POINT	P, LB	Y, IN
1	0.	0.
2	2.379E+02	1.440E-01
3	3.305E+02	2.880E-01
4	4.121E+02	4.320E-01
5	4.759E+02	5.760E-01
6	5.320E+02	7.200E-01
7	5.828E+02	8.640E-01
8	6.295E+02	1.008E+00
9	6.730E+02	1.152E+00
10	7.138E+02	1.296E+00
11	7.524E+02	1.440E+00
12	7.524E+02	1.800E+02

CURVE 6 DISTANCE FROM TOP, IN 1.680E+02 NUM OF POINTS 12

POINT	P, LB	Y, IN
1	0.	0.
2	2.379E+02	1.440E-01
3	3.305E+02	2.880E-01
4	4.121E+02	4.320E-01
5	4.759E+02	5.760E-01
6	5.320E+02	7.200E-01
7	5.828E+02	8.640E-01
8	6.295E+02	1.008E+00
9	6.730E+02	1.152E+00
10	7.138E+02	1.296E+00
11	7.524E+02	1.440E+00
12	7.524E+02	1.800E+02

CURVE 7 DISTANCE FROM TOP, IN 2.040E+02 NUM OF POINTS 12

POINT	P, LB	Y, IN
1	0.	0.
2	2.379E+02	1.440E-01
3	3.305E+02	2.880E-01
4	4.121E+02	4.320E-01
5	4.759E+02	5.760E-01
6	5.320E+02	7.200E-01
7	5.828E+02	8.640E-01
8	6.295E+02	1.008E+00
9	6.730E+02	1.152E+00
10	7.138E+02	1.296E+00
11	7.524E+02	1.440E+00
12	7.524E+02	1.800E+02

CURVE 8 DISTANCE FROM TOP, IN 2.400E+02 NUM OF POINTS 12

POINT	P, LB	Y, IN
1	0.	0.
2	2.379E+02	1.440E-01
3	3.305E+02	2.880E-01
4	4.121E+02	4.320E-01
5	4.759E+02	5.760E-01
6	5.320E+02	7.200E-01
7	5.828E+02	8.640E-01
8	6.295E+02	1.008E+00
9	6.730E+02	1.152E+00
10	7.138E+02	1.296E+00
11	7.524E+02	1.440E+00
12	7.524E+02	1.800E+02

CURVE 9 DISTANCE FROM TOP, IN 9.960E+02 NUM OF POINTS 12

POINT	P, LB	Y, IN
1	0.	0.
2	9.392E+02	1.440E-01
3	1.328E+03	2.880E-01
4	1.627E+03	4.320E-01
5	1.878E+03	5.760E-01

6	2.100E+03	7.200E-01
7	2.301E+03	8.640E-01
8	2.405E+03	1.008E+00
9	2.600E+03	1.152E+00
10	2.818E+03	1.296E+00
11	2.970E+03	1.440E+00
12	2.970E+03	1.800E+02

TABLE H SOIL DATA FOR AUTO P-Y CURVES

PROFILE 1	NUM OF CURVES 9	NUM OF STRATA 3	
DISTANCES FROM PILE TOP TO P-Y CURVES, INCH			
CURVE	LOCATION, IN		
1	0.		
2	6.000E+01		
3	6.100E+01		
4	9.600E+01		
5	1.320E+02		
6	1.680E+02		
7	2.040E+02		
8	2.400E+02		
9	9.960E+02		
STRATUM	TYPE	GAMMA, PCF	
1	CLAY	0.	
2	CLAY	3.000E+01	
3	CLAY	3.000E+01	
		(DENSITY OF SAND)	
		(CONSISTENCY OF CLAY	
		1 DENSE 2 MEDIUM 3 LOOSE)	
		1 STIFF 2 MEDIUM 3 SOFT)	
STRATUM	FROM, IN	TO, IN	
1	0.	6.000E+01	
2	6.000E+01	8.940E+02	
3	8.940E+02	1.000E+03	
		PHI, DEG	
		DENS	
		SHFAR, PSI	
		CONSIST	
		S-S CURVE	
			-0
			-0
			-0

COPANO BAY      VERTICAL LOAD ALONE      FIXED CONNECTION

COMPUTATION RESULTS

TABLE I      DISPLACEMENT OF GROUPED PILE FOUNDATION

VERTICAL, IN	HORIZONTAL, IN	ROTATION, RAD
7.542E-02	-6.502E-08	1.995E-08
NO OF ITERATION 3		

TABLE J      COMPUTATION ON INDIVIDUAL PILE

PILE GROUP 1

PILE TOP DISPLACEMENTS AND REACTIONS

X, IN	Y, IN	DY/DX	AXIAL, LB	LAT, LB	BM, LB-IN
7.319E-02	1.822E-02	1.000E-08	1.398E+05	3.792E+02	5.195E+04

PILE GROUP 2

PILE TOP DISPLACEMENTS AND REACTIONS

X, IN	Y, IN	DY/DX	AXIAL, LB	LAT, LB	BM, LB-IN
7.542E-02	5.091E-15	1.000E-08	1.431E+05	2.196E+02	4.268E+00

PILE GROUP 3

PILE TOP DISPLACEMENTS AND REACTIONS

X, IN	Y, IN	DY/DX	AXIAL, LB	LAT, LB	BM, LB-IN
7.542E-02	5.091E-15	1.000E-08	1.431E+05	2.196E+02	4.268E+00

PILE GROUP 4

PILE TOP DISPLACEMENTS AND REACTIONS

X, IN	Y, IN	DY/DX	AXIAL, LB	LAT, LB	BM, LB-IN
7.319E-02	-1.822E-02	1.000E-08	1.398E+05	-3.791E+02	-5.193E+04



COPANO BAY      DESIGN LOAD      FIXED CONNECTION

TABLE H      INPUT AND OUTPUT SWITCH      (IF 1 YES, IF 0 NO)

TABLE	C	D	E	F	G	H	J
INPUT	1	0	0	0	0	0	
OUTPUT	1	0	0	0	0	0	1
	(C LOAD	D ARRANGEMENT	E PILE	F L-S	G PLY	H SOIL	J LLP)

TABLE C      LOAD

V LOAD, LB	H LOAD, LB	MOMENT, LB-IN
4.440E+05	3.040E+04	-1.680E+07

## COPANO BAY DESIGN LOAD FIXED CONNECTION

## COMPUTATION RESULTS

TABLE I DISPLACEMENT OF GROUPED PILE FOUNDATION

VERTICAL, IN	HORIZONTAL, IN	ROTATION, RAD
7.649E-02	9.214E-02	-9.399E-05
NO OF ITERATION 5		

TABLE J COMPUTATION ON INDIVIDUAL PILE

## PILE GROUP 1

## PILE TOP DISPLACEMENTS AND REACTIONS

X, IN	Y, IN	DY/DX	AXIAL, LB	LAT, LB	HM, LB-IN
4.047E-02	1.050E-01	-9.400E-05	8.095E+04	1.942E+03	2.507E+05

## LATERALLY LOADED PILE

STA	X, IN	Y, IN	DY/DX	M, LB-IN	DM/DX	P, LB/IN
0	0.	1.050E-01	-9.400E-05	2.507E+05	1.942E+03	0.
1	3.720E+01	9.099E-02	-3.027E-04	1.778E+05	1.942E+03	0.
2	7.440E+01	8.251E-02	-4.402E-04	1.044E+05	1.942E+03	0.
3	1.116E+02	6.424E-02	-5.060E-04	2.046E+04	1.942E+03	0.
4	1.488E+02	4.487E-02	-4.999E-04	-4.315E+04	1.941E+03	2.408E-02
5	1.860E+02	2.705E-02	-4.220E-04	-1.148E+05	1.110E+03	4.470E+01
6	2.232E+02	1.347E-02	-3.026E-04	-1.282E+05	-1.357E+02	2.226E+01
7	2.604E+02	4.530E-03	-1.873E-04	-1.085E+05	-6.891E+02	7.495E+00
8	2.976E+02	-4.650E-04	-9.639E-05	-7.810E+04	-8.142E+02	-7.682E-01
9	3.348E+02	-2.636E-03	-3.471E-05	-4.852E+04	-7.184E+02	-4.355E+00
10	3.720E+02	-3.048E-03	1.012E-06	-2.482E+04	-5.399E+02	-5.271E+00
11	4.092E+02	-2.560E-03	1.717E-05	-8.346E+03	-3.481E+02	-5.042E+00
12	4.464E+02	-1.770E-03	2.006E-05	1.178E+03	-1.816E+02	-3.910E+00
13	4.836E+02	-1.023E-03	1.751E-05	5.287E+03	-6.224E+01	-2.505E+00
14	5.208E+02	-4.676E-04	1.205E-05	5.914E+03	7.741E+00	-1.257E+00
15	5.580E+02	-1.264E-04	6.842E-06	4.784E+03	3.800E+01	-3.700E-01
16	5.952E+02	4.146E-05	2.988E-06	3.128E+03	4.244E+01	1.313E-01
17	6.324E+02	9.595E-05	6.636E-07	1.644E+03	3.392E+01	3.269E-01
18	6.696E+02	9.083E-05	-4.337E-07	6.083E+02	2.168E+01	3.312E-01
19	7.068E+02	8.368E-05	-7.441E-07	2.889E+01	1.091E+01	2.475E-01
20	7.440E+02	3.547E-05	-6.568E-07	-2.082E+02	3.589E+00	1.464E-01
21	7.812E+02	1.481E-05	-4.374E-07	-2.421E+02	-3.363E-01	6.467E-02
22	8.184E+02	2.928E-06	-2.290E-07	-1.858E+02	-1.790E+00	1.348E-02
23	8.556E+02	-2.226E-06	-8.481E-08	-1.107E+02	-1.840E+00	-1.078E-02
24	8.928E+02	-3.382E-06	-7.025E-09	-4.939E+01	-1.320E+00	-1.720E-02
25	9.300E+02	-2.748E-06	2.295E-08	-1.214E+01	-7.277E-01	-1.463E-02
26	9.672E+02	-1.675E-06	2.648E-08	4.891E+00	-2.822E-01	-9.318E-03
27	1.004E+03	-7.783E-07	1.971E-08	9.015E+00	-2.492E-02	-4.517E-03
28	1.042E+03	-2.086E-07	1.197E-08	6.864E+00	8.253E-02	-1.260E-03
29	1.079E+03	1.124E-07	7.193E-09	2.947E+00	9.283E-02	7.062E-04
30	1.116E+03	3.266E-07	5.757E-09	9.349E-14	4.008E-02	2.130E-03
NO OF ITERATION		3				

## PILE GROUP 2

## PILE TOP DISPLACEMENTS AND REACTIONS

X,IN	Y,IN	DY/DX	AXIAL,LR	LAT,LB	BM,LB-IN
6.803E-02	9.214E-02	-9.400E-05	1.321E+05	1.652E+03	2.138E+05

## LATERALLY LOADED FILE

STA	X,IN	Y,IN	DY/DX	M,LR-IN	DM/DX	P,LB/IN
0	0.	9.214E-02	-9.400E-05	2.138E+05	1.652E+03	0.
1	3.720E+01	8.477E-02	-2.719E-04	1.514E+05	1.652E+03	0.
2	7.440E+01	7.192E-02	-3.886E-04	8.821E+04	1.652E+03	0.
3	1.116E+02	5.586E-02	-4.436E-04	2.462E+04	1.652E+03	0.
4	1.488E+02	3.892E-02	-4.365E-04	-2.909E+04	1.652E+03	2.499E-02
5	1.860E+02	2.339E-02	-3.675E-04	-1.026E+05	9.327E+02	3.864E+01
6	2.232E+02	1.157E-02	-2.029E-04	-1.121E+05	-1.416E+02	1.912E+01
7	2.604E+02	3.823E-03	-1.622E-04	-9.462E+04	-6.148E+02	6.317E+00
8	2.976E+02	-4.974E-04	-8.305E-05	-8.305E+04	-4.795E+02	-8.218E-01
9	3.348E+02	-2.356E-03	-2.945E-05	-4.209E+04	-6.293E+02	-3.892E+00
10	3.720E+02	-2.688E-03	1.489E-06	-2.142E+04	-4.705E+02	-4.649E+00
11	4.092E+02	-2.245E-03	1.537E-05	-7.074E+03	-3.018E+02	-4.420E+00
12	4.464E+02	-1.545E-03	1.824E-05	1.195E+03	-1.561E+02	-3.412E+00
13	4.836E+02	-8.880E-04	1.536E-05	4.716E+03	-5.215E+01	-2.174E+00
14	5.208E+02	-4.020E-04	1.052E-05	5.216E+03	8.388E+00	-1.081E+00
15	5.580E+02	-1.050E-04	5.939E-06	4.195E+03	3.421E+01	-3.075E-01
16	5.952E+02	3.989E-05	2.566E-06	2.729E+03	3.758E+01	1.263E-01
17	6.324E+02	8.589E-05	5.427E-07	1.425E+03	2.978E+01	2.926E-01
18	6.696E+02	8.026E-05	-4.041E-07	5.187E+02	1.890E+01	2.927E-01
19	7.068E+02	5.583E-05	-6.641E-07	1.502E+01	9.417E+00	2.170E-01
20	7.440E+02	3.086E-05	-5.796E-07	-1.885E+02	3.013E+00	1.273E-01
21	7.812E+02	1.271E-05	-3.831E-07	-2.149E+02	-3.866E-01	5.549E-02
22	8.184E+02	2.352E-06	-1.988E-07	-1.635E+02	-1.620E+00	1.083E-02
23	8.556E+02	-2.083E-06	-7.230E-08	-9.628E+01	-1.634E+00	-1.009E-02
24	8.928E+02	-3.028E-06	-4.647E-09	-4.261E+01	-1.160E+00	-1.539E-02
25	9.300E+02	-2.428E-06	2.100E-08	-1.004E+01	-6.330E-01	-1.293E-02
26	9.672E+02	-1.465E-06	2.360E-08	4.691E+00	-2.409E-01	-8.153E-03
27	1.004E+03	-6.725E-07	1.737E-08	8.114E+00	-1.661E-02	-3.903E-03
28	1.042E+03	-1.735E-07	1.044E-08	6.097E+00	7.548E-02	-1.049E-03
29	1.079E+03	1.045E-07	6.205E-09	2.601E+00	8.277E-02	6.562E-04
30	1.116E+03	2.882E-07	4.938E-09	0.	3.561E-02	1.879E-03

NO OF ITERATION 3

## PILE GROUP 3

## PILE TOP DISPLACEMENTS AND REACTIONS

X,IN	Y,IN	DY/DX	AXIAL,LR	LAT,LB	BM,LB-IN
8.495E-02	9.214E-02	-9.400E-05	1.574E+05	1.643E+03	2.138E+05

## LATERALLY LOADED FILE

STA	X,IN	Y,IN	DY/DX	M,LR-IN	DM/DX	P,LB/IN
0	0.	9.214E-02	-9.400E-05	2.138E+05	1.643E+03	0.
1	3.720E+01	8.477E-02	-2.719E-04	1.515E+05	1.643E+03	0.
2	7.440E+01	7.191E-02	-3.887E-04	8.832E+04	1.643E+03	0.
3	1.116E+02	5.585E-02	-4.438E-04	2.467E+04	1.643E+03	0.
4	1.488E+02	3.890E-02	-4.367E-04	-3.913E+04	1.643E+03	2.497E-02
5	1.860E+02	2.336E-02	-3.677E-04	-1.027E+05	9.244E+02	3.860E+01
6	2.232E+02	1.154E-02	-2.630E-04	-1.122E+05	-1.483E+02	1.907E+01
7	2.604E+02	3.794E-03	-1.622E-04	-9.472E+04	-6.196E+02	6.268E+00

8	2.976E+02	-5.232E-04	-8.292E-05	-6.801E+04	-7.202E+02	-8.646E-01
9	3.348E+02	-2.376E-03	-2.928E-05	-4.271E+04	-6.311E+02	-3.925E+00
10	3.720E+02	-2.702E-03	1.654E-06	-2.140E+04	-4.711E+02	-4.673E+00
11	4.092E+02	-2.253E-03	1.551E-05	-7.037E+03	-3.017E+02	-4.436E+00
12	4.464E+02	-1.548E-03	1.833E-05	1.224E+03	-1.550E+02	-3.420E+00
13	4.836E+02	-5.884E-04	1.542E-05	4.755E+03	-5.154E+01	-2.175E+00
14	5.208E+02	-4.009E-04	1.055E-05	5.244E+03	8.965E+00	-1.078E+00
15	5.580E+02	-1.035E-04	5.943E-06	4.272E+03	3.465E+01	-3.031E-01
16	5.952E+02	4.125E-05	2.559E-06	2.736E+03	3.788E+01	1.306E-01
17	6.324E+02	8.585E-05	5.318E-07	1.425E+03	2.922E+01	2.959E-01
18	6.696E+02	8.081E-05	-4.138E-07	5.160E+02	1.894E+01	2.947E-01
19	7.068E+02	5.607E-05	-6.709E-07	1.164E+01	9.401E+00	2.179E-01
20	7.440E+02	3.090E-05	-5.834E-07	-1.977E+02	2.977E+00	1.275E-01
21	7.812E+02	1.266E-05	-3.846E-07	-2.167E+02	-4.222E-01	5.529E-02
22	8.184E+02	2.283E-06	-1.990E-07	-1.644E+02	-1.646E+00	1.051E-02
23	8.556E+02	-2.141E-06	-7.188E-08	-9.657E+01	-1.649E+00	-1.037E-02
24	8.928E+02	-3.065E-06	-4.113E-09	-4.255E+01	-1.166E+00	-1.558E-02
25	9.300E+02	-2.447E-06	2.142E-08	-9.862E+00	-6.339E-01	-1.303E-02
26	9.672E+02	-1.471E-06	2.386E-08	4.841E+00	-2.745E-01	-8.185E-03
27	1.004E+03	-5.718E-07	1.748E-08	8.230E+00	-1.465E-02	-3.999E-03
28	1.042E+03	-1.707E-07	1.047E-08	6.156E+00	7.706E-02	-1.032E-03
29	1.079E+03	1.072E-07	6.196E-09	2.620E+00	8.372E-02	6.735E-04
30	1.116E+03	2.902E-07	4.920E-09	-4.674E-14	3.598E-02	1.893E-03

NO OF ITERATION 3

## PILE GROUP 4

## PILE TOP DISPLACEMENTS AND REACTIONS

X, IN	Y, IN	DY/DX	AXIAL LR	LAT. LR	BM, LB-IN
1.080E-01	6.807E-02	-9.400E-05	1.920E+05	1.135E+03	1.452E+05

## LATERALLY LOADED PILE

STA	X, IN	Y, IN	DY/DX	M, LB-IN	DM/DX	P, LB/IN
0	0.	6.807E-02	-9.400E-05	1.452E+05	1.135E+03	0.
1	3.720E+01	6.195E-02	-2.143E-04	1.018E+05	1.135E+03	0.
2	7.440E+01	5.213E-02	-2.919E-04	5.766E+04	1.135E+03	0.
3	1.110E+02	4.023E-02	-3.264E-04	1.316E+04	1.135E+03	0.
4	1.488E+02	2.784E-02	-3.175E-04	-3.143E+04	1.134E+03	1.788E-02
5	1.860E+02	1.660E-02	-2.653E-04	-7.578E+04	6.240E+02	2.743E+01
6	2.232E+02	8.105E-03	-1.886E-04	-8.164E+04	-1.353E+02	1.339E+01
7	2.604E+02	2.567E-03	-1.155E-04	-6.841E+04	-4.633E+02	4.241E+00
8	2.976E+02	-4.914E-04	-5.843E-05	-4.883E+04	-5.271E+02	-8.120E-01
9	3.348E+02	-1.780E-03	-2.002E-05	-3.003E+04	-4.572E+02	-2.942E+00
10	3.720E+02	-1.981E-03	1.957E-06	-1.509E+04	-3.388E+02	-3.426E+00
11	4.092E+02	-1.635E-03	1.164E-05	-4.793E+03	-2.152E+02	-3.219E+00
12	4.464E+02	-1.115E-03	1.345E-05	1.085E+03	-1.095E+02	-2.462E+00
13	4.836E+02	-5.340E-04	1.119E-05	3.548E+03	-3.485E+01	-1.552E+00
14	5.208E+02	-2.819E-04	7.596E-06	3.838E+03	8.120E+00	-7.579E-01
15	5.580E+02	-5.893E-05	4.239E-06	3.052E+03	2.597E+01	-2.018E-01
16	5.952E+02	3.347E-05	1.795E-06	1.966E+03	2.775E+01	1.060E-01
17	6.324E+02	5.462E-05	3.438E-07	1.073E+03	2.169E+01	2.202E-01
18	6.696E+02	5.905E-05	-3.238E-07	3.576E+02	1.359E+01	2.153E-01
19	7.068E+02	4.053E-05	-4.968E-07	-2.383E+00	6.651E+00	1.575E-01
20	7.440E+02	2.709E-05	-4.253E-07	-1.444E+02	2.026E+00	9.114E-02
21	7.812E+02	8.883E-06	-2.775E-07	-1.592E+02	-3.903E-01	3.878E-02
22	8.184E+02	1.446E-06	-1.418E-07	-1.193E+02	-1.235E+00	6.659E-03
23	8.556E+02	-1.668E-06	-4.994E-08	-6.931E+01	-1.209E+00	-8.080E-03
24	8.928E+02	-2.270E-06	-1.543E-09	-2.004E+01	-8.441E-01	-1.154E-02
25	9.300E+02	-1.783E-06	1.628E-08	-6.535E+00	-4.529E-01	-9.490E-03
26	9.672E+02	-1.059E-06	1.757E-08	3.886E+00	-1.669E-01	-5.890E-03

27	1.004E+03	-4.756E-07	1.269E-08	6.130E+00	-5.980E-03	-2.760E-03
28	1.042E+03	-1.147E-07	7.503E-09	4.513E+00	5.825E-02	-6.933E-04
29	1.079E+03	8.260E-08	4.377E-09	1.904E+00	6.149E-02	5.190E-04
30	1.116E+03	4.109E-07	3.450E-09	4.674E-14	2.625E-02	1.376E-03
NO OF ITERATION		J				

NOTE: As stated on pages 45 and 46 of this report, the lateral reaction at the top of the pile is obtained by summation of soil reactions along the pile (Eq. 2.68). The shear at other stations is obtained by difference equation techniques (Eq. 2.65). Because of the two computational techniques, there may be, in some instances, too large a difference between the shear at the top station and that at the next station below. Experience has shown that such a difficulty is encountered rarely and apparently is associated with problems that are ill-conditioned. When such a difficulty occurs, two steps can be taken to resolve the difficulty. The first step is to rerun the problem with a larger number of increments. The input merely needs to be modified. The next step is to use a finer closure tolerance (TOL and TOLP in the program) and a higher precision in computing deflection and shear. In order to take the latter step, it will be necessary to make adjustments in the internal program. The use of one or both of these techniques should eliminate the difficulty.

## APPENDIX B

### COMPUTER PROGRAM LLP

#### B.1 Description of the Program

The program LLP solves for the deflection and for the distribution of forces in a laterally loaded single pile for a given pile-cap displacement or for given pile-top forces.

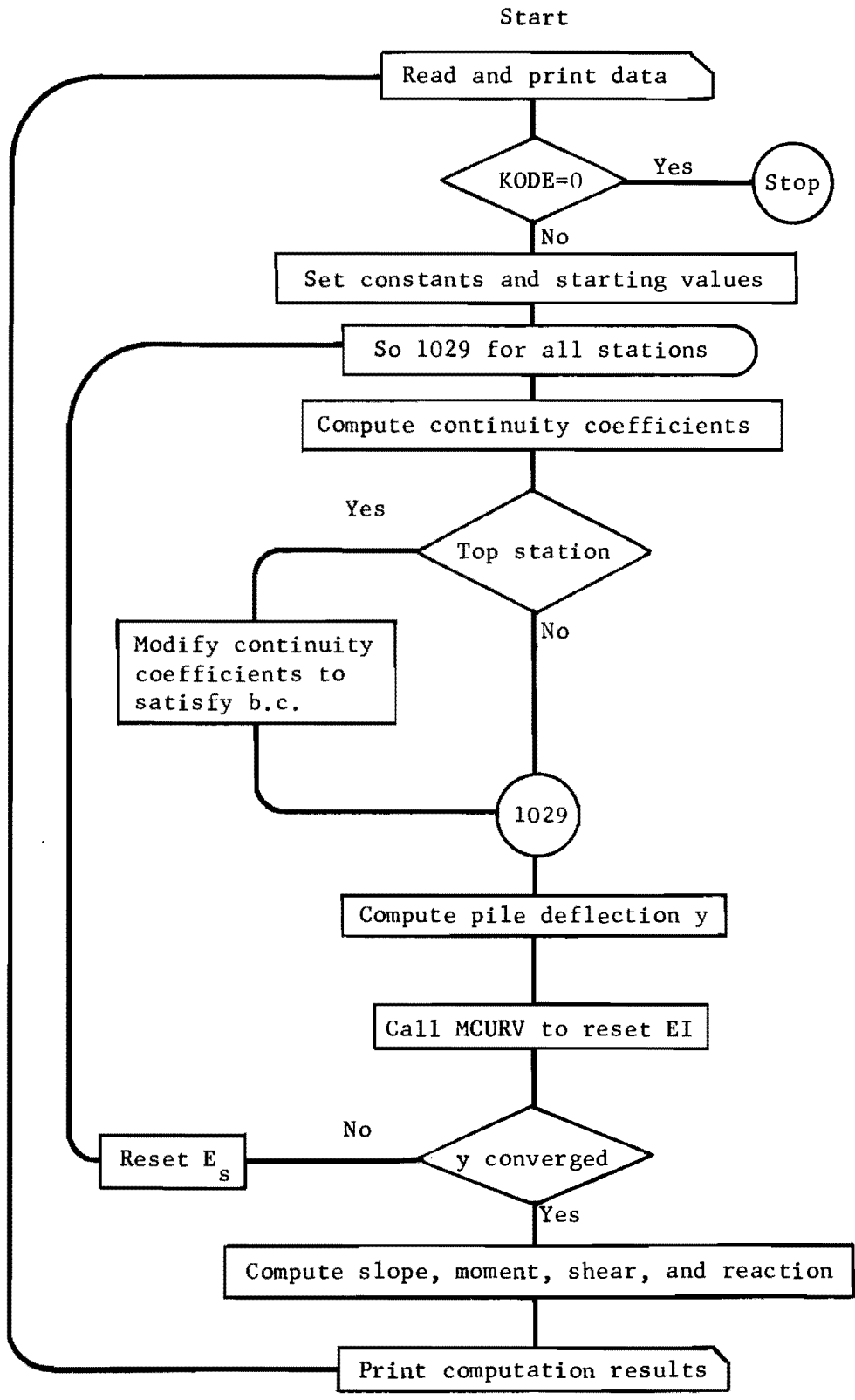
Simple bilinear moment-curvature relationships can be used for non-linear pile material. Thus, the behavior of a laterally loaded pile can be predicted even after the formation of plastic hinges in the pile.

The program LLP consists of the main program LLP and the subroutines MCURV and SOIL 2R. The main program LLP performs the data input and output and solves the finite difference equations, the theory of which is given in Chapter III. The subroutine MCURV computes the flexural rigidity,  $EI$ , of the pile and resets  $EI$  for the plastic moment. The subroutine SOIL 2R interpolates the soil modulus or the secant modulus of the lateral soil resistance curve.

The main program LLP is used in the program GROUP (Appendix A) as a subroutine. The description of subroutines MCURV and SOIL 2R have already been given in the section on program GROUP (Appendix A).

B.2 Flow Diagram for Program LLP

Flow Diagram for Main Program LLP



## B.3 Glossary of Notation for Program LLP

A(507)	continuity coefficient
B(507)	continuity coefficient
BC1, BC2	first and second boundary condition
BM(507)	bending moment in a pile
C(507)	continuity coefficient
DBM(507)	shear in a pile
DPS	distance from pile top to ground surface
DY(507)	slope of a pile
ES(507)	secant modulus in a lateral soil resistance curve
G	spring constant for the elastic restraint on pile top
H	increment length of a discretized pile
KODE	code to specify the displacement boundary condition or the force boundary condition
KTYPE	code to specify the pile material
MPLAST	signal to notify the formation of plastic hinges
N	number of elements in a discretized pile
NC	number of lateral soil resistance curves
NDS	number of different sections in a pile
NEWPL	input switch for new pile data
NEWPY	input switch for a set of new lateral soil resistance curves
NP(20)	number of points in a lateral soil resistance curve
P(507)	axial force in a pile



PC(20, 25)	lateral soil reaction
PX	axial load on pile top
R(507)	flexural rigidity EI at discretized stations
RES(507)	lateral soil reaction per unit length of a pile
RRI(5)	flexural rigidity EI in different pile section
RUN(20)	alphanumeric variable to store the title
SIZE(5)	width of a pile
TC	alphanumeric code for pile top connection to pile cap
XRI(5)	moment of inertia
XS(20)	distance from ground surface to depth where a lateral soil resistance curve is given
XX1(5)	distance from ground surface to the top of a pile section
XX2(5)	distance from ground surface to the bottom of a pile section
Y(507)	lateral pile deflection
YC(20, 25)	lateral pile deflection
YIELD(5)	yield moment
YOUNG	Young's modulus of pile material
YY(507)	dummy to store the previous computation of y

#### B.4 Data Coding for Program LLP

The input data for the program LLP are classified as follows.

TABLE A Title of the run

TABLE B Boundary condition and input switches

TABLE C Pile properties

TABLE D Lateral soil resistance curves

For the repetitive run with the same pile properties or the same lateral soil resistance curves, TABLE C or TABLE D can be omitted by setting the input switches properly.

The general deck structure of the input data is shown in the following.

##### Deck Structure of Input Data for Program LLP

TABLE A TITLE OF RUN, necessary for each run

Card AI one card

TABLE B BOUNDARY CONDITIONS AND INPUT SWITCHES, necessary for each run

Card BI one card

TABLE C PILE PROPERTIES

If B6 = 0, skip TABLE C

Card CI one card

Card CII C3 cards

TABLE D LATERAL SOIL REACTION CURVES

If B7 = 0, skip TABLE D

Card DI one card

Card DII one card  D1 sets

Card DIII D3 card

To start a new run, immediately continue TABLE A of next run. To terminate the run, attach two blank cards at the end of deck.

## Data Coding Form for Program LLP

The general instructions for data coding may be referred to A.4.

## TABLE A Title of Run

## Card AI

A1 1 to 80 Alphanumeric description of each run

## TABLE B Boundary Conditions and Input Switches

## Card BI

B5 specifies the type of boundary conditions to be entered in B1 and B2. If B5 = 1, displacement b.c. must be entered. If B5 = 2, force b.c. must be entered.

- B1 1 to 10 First b.c. Enter lateral pile top deflection, inch (to right +) if B5 = 1. Enter lateral force, pounds (to right +) if B5 = 2.
- B2 11 to 20 Second b.c. Enter slope of pile cap, radian (anti-clockwise +) if B5 = 1. Enter moment, inch-pound (anti-clockwise +) if B5 = 2.
- B3 21 to 30 Axial load on pile top, pound (downward +)
- B4 33 to 35 Code to specify the type of pile connection to pile cap. Enter PIN for a pinned-connection. FIX for a fixed connection and RES for an elastically restrained connection. Leave blank for B5 = 2.
- B5 40 Code to specify the type of b.c. to be entered in B1 and B2. If B5 = 1, displacement b.c. are specified. If B5 = 2, force b.c. are specified.
- B6 45 Switch for inputting pile properties. If B6 = 1, TABLE C must be furnished. If B6 = 0, TABLE C is skipped.
- B7 50 Switch for inputting lateral soil resistance curves. If B7 = 1, TABLE D must be furnished. If B7 = 0, TABLE D is skipped.
- B8 51 to 60 Spring constant for the elastic restraint by pile cap, inch-pound. Leave blank for B4 = PIN and FIX.

TABLE C Pile Properties

## Card CI

C1	1 to 10	Total length of pile, inch
C2	11 to 15	Number of increment by which a pile is divided into finite elements (maximum 500)
C3	16 to 20	Number of different sections in the pile (maximum 5)
C4	21 to 30	Young's modulus of pile material, psi
C5	31 to 40	Ultimate moment, inch-pound. Ultimate moment must correspond to the axial force in B3.
C6	41 to 50	Distance from pile top to ground surface, inch

## Card CII

Different sections in a pile are listed from top to bottom.

C7	1 to 10	Distance from pile top to top of a pile section, inch
C8	11 to 20	Distance from pile top to bottom of a pile section, inch
C9	21 to 30	Width of pile in the section, inch
C10	31 to 40	Moment of inertia in the section, inch <sup>4</sup>

TABLE D Lateral Soil Resistance Curves

## Card DI

D1	1 to 5	Number of curves (maximum 20)
----	--------	-------------------------------

## Card DII

D2	1 to 10	Depth from ground surface to point where a curve is given, inch
D3	11 to 15	Number of points in a curve (maximum 25)

## Card DIII

D4	1 to 10	Lateral soil resistance, pound per inch
D5	11 to 20	Lateral pile deflection, inch

## B.5 Listing of Program LLP

```

PROGRAM LLP(INPUT,OUTPUT)
DIMENSION A(507), H(507), C(507), DY(507), BM(507), UDM(507),
1 RES(507), YY(507), P(507), YRI(5), RIN(20)
COMMON / BLOCK1 / H, N, NDS, XX1(5), YX2(5), RPI(5), SIZE(5),
1 HE2, NP4, DPS, YIELD(5), YOUNG
COMMON / BLOCK2 / NC, XS(20), NP(20), YC(20,25), PC(20,25)
COMMON / BLOCK3 / Y(507), ES(507), R(507), MPLAST
501 FORMAT ( 20A4 )
502 FORMAT ( 3E10.3, 2X, A3, 3I5, E10.3 )
503 FORMAT ( E10.3, 2I5, 3E10.3 )
504 FORMAT ( 5E10.3 )
505 FORMAT ( I5 )
506 FORMAT ( E10.3, I5 )
507 FORMAT ( 2E10.3 )
510 FORMAT ( IHI, 5X, 20A4 )
511 FORMAT ( /// 5X, 41HTABLE B PILE TOP CONDITION AND INPUT ,
1 6HSWITCH )
512 FORMAT ( / 12X, 6HDEF,IN, 5X, 5HSLOPE, 6X, 10HAXIAL L,LR,
1 9H CONNec , 5HCODE , 5HT-C 6HT-D ,
2 12HSPRING M/RAD )
513 FORMAT ( 10X, 3E11.3, 2X, A3, 1X, 3I5, 3X, E11.3 )
514 FORMAT ( / 12X, 10HLAT L,LR , 12HRM ,B-TN , 11HAXIAL L,LR ,
1 8HCONNec , 5HCODE , 5HT-C , 5HT-D ,
2 12HSPRING M/RAD )
515 FORMAT ( / 15X, 41H(CODE = 1 FOR GIVEN SET OF DEF AND SLOPE) /
1 15X, 43H(CODE = 2 FOR GIVEN SET OF LOAD AND MOMENT) )
516 FORMAT ( 15X, 46H(T-C, T-D IF 1 NEW DATA ARE FURNISHED IF 0 NO .
1 11HDATA INPUT) )
520 FORMAT ( /// 5X, 42HTABLE C PREVIOUS PILE PROPERTIES ARE USED )
521 FORMAT ( /// 5X, 27HTABLE C PILE PROPERTIES )
522 FORMAT ( / 7X, 10HLENGTH,IN , 10HINCREMENT , 7HSECTION, 7X,
1 5HE,PSI, 6X, 5HGL,IN )
523 FORMAT ( 5X, E11.3, I6, I9, 2E12.3 )
524 FORMAT ( / 9X 9HSECTION , 11HFROM,IN , 5HT0,TN, 6X,
1 11HWIDTH,TN , 9HI,TN4 . 11HWULT,IN-LB )
525 FORMAT ( 8X, I5, 3X, 5E11.3 )
530 FORMAT ( /// 5X, 37HTABLE D PREVIOUS P-Y CURVES ARE USED )
531 FORMAT ( /// 5X, 39HTABLE D P-Y CURVES NO OF CURVES, I3 )
532 FORMAT ( / 10X, 5HCURVE, I3, 7X, 21HDIST FROM PILE TOP,IN, E11.3,
1 5X, 12HNO OF POINTS, I3 )
533 FORMAT ( 15X, 5HPOINT, 9X, 4HY,TN, 10X, 7HP,LR/IN )
534 FORMAT ( 13X, I5, 2X, 2E15.3 )
540 FORMAT ( /// 5X, 38HDOES NOT CONVERGE AFTER 999 ITERATIONS )
541 FORMAT ( /// 5X, 25HPLASTIC HINGES ARE FORMED )
542 FORMAT ( /// 9X, 20HNUMBER OF ITERATIONS, I5 )
550 FORMAT ( /// 5X, 31HTABLE E COMPUTATION RESULTS )
551 FORMAT ( / 6X, 3HSTA, 10X, 4HX,IN, 8X, 4HY,IN, 7X, 5HDY/DX, I1X,
1 1HM, 7X, 5HDM/DX, 5X, 7HP,LR/IN )
552 FORMAT ( 4X, I5, 2X, 6E12.3 )
553 FORMAT ( /// 7X, 25HSUM OF SOIL RESISTANCE,LR, E11.3 )
C-----READ IN INPUT DATA
100 READ 501, ( RUN(I), I = 1, 20 )
C-----PILE TOP CONDITION AND INPUT SWITCH
READ 502, BC1, BC2, PX, TC, KODE, NEWPL, NEWPY, G
IF ( KODE .EQ. 0 ) GO TO 9999
IF ( NEWPL .EQ. 0 ) GO TO 101
READ 503, HN, N, NDS, YOUNG, DPS
XN = N

```

```

      H = HN / XN
      DO 102 I = 1, NDS
    READ 504, XX1(I), XX2(I), SIZE(I), XRI(I), YIELD(I)
      XRI(I) = XRI(I) * YOUNG
102  CONTINUE
101  IF ( NEWPY .EQ. 0 ) GO TO 103
    READ 505, NC
      DO 104 I = 1, NC
    READ 506, XS(I), NP(I)
      INDEX = NP(I)
    READ 507, ( YC(I, J), PC(I, J), J = 1, INDEX )
104  CONTINUE
103  CONTINUE
C-----PRINT OUT INPUT DATA
    PRINT 510, ( HUN(I), I = 1, 20 )
    PRINT 511
      IF ( KODE .EQ. 1 ) GO TO 111
      GO TO 112
111 PRINT 512
    PRINT 513, BC1, BC2, PX, TC, KODE, NEWPL, NEWPV, G
      GO TO 113
112 PRINT 514
    PRINT 513, BC1, BC2, PX, TC, KODE, NEWPL, NEWPY, G
113  CONTINUE
    PRINT 515
    PRINT 516
      IF ( NEWPL .EQ. 0 ) GO TO 120
      GO TO 121
120 PRINT 520
      GO TO 122
121 PRINT 521
    PRINT 522
    PRINT 523, HN, N, NDS, YOUNG, DPS
    PRINT 524
    PRINT 525, ( I, XX1(I), XX2(I), SIZE(I), XRI(I), YIELD(I), I = 1,
1  NDS )
122  CONTINUE
      IF ( NEWPY .EQ. 0 ) GO TO 130
      GO TO 131
130 PRINT 530
      GO TO 132
131 PRINT 531, NC
      DO 133 I = 1, NC
    PRINT 532, I, XS(I), NP(I)
      INDEX = NP(I)
    PRINT 533
    PRINT 534, ( J, YC(I, J), PC(I, J), J = 1, INDEX )
133  CONTINUE
132  CONTINUE
C-----START EXECUSION OF PROGRAM
C-----COMPUTE CONSTANTS AND INDEXES
      ITER = 1
      K = 1
      TOLP = 0.00001
      PIN = 3HPIN
      FIX = 3HFIX
      H2 = H + H
      HE2 = H * H

```



```

HE3 = HE2 * H
HE4 = HE2 * HE2
NP3 = N + 3
NP4 = N + 4
NP5 = N + 5
NP6 = N + 6
NP7 = N + 7
C-----CLEAR THE STORAGE PLACES
DO 1000 J = 1, NP7
R(J) = 0.0
Y(J) = 0.0
ES(J) = 0.0
P(J) = 0.0
1000 CONTINUE
C-----COMPUTE INITIAL ES (ES = KX, K = 1.0) AND FLEXURAL STIFFNESS EI = R
DO 1001 J = 4, NP4
XJ = J - 4
P(J) = PX
ES(J) = 1.0 * XJ * H
R(J) = RHI(1)
1001 CONTINUE
C-----SET RECURSION COEFFICIENTS AT STATIONS 1, 2 AND 4
A(1) = 0.0
R(1) = 0.0
C(1) = 0.0
A(2) = 0.0
R(2) = 0.0
C(2) = 0.0
C-----COMPUTE RECURSION COEFFICIENTS AT ALL STATIONS
1023 DO 1029 J = 3, NP5
AA = R(J - 1)
BB = -2.0 * R(J - 1) + 2.0 * R(J) + P(J) * HE2
CC = R(J - 1) + 4.0 * R(J) + R(J + 1) - 2.0 * P(J) * HE2
+ES(J) * HE4
DD = -2.0 * R(J) - 2.0 * R(J + 1) + P(J) * HE2
EE = R(J + 1)
C-----COMPUTE RECURSION COEFFICIENTS AT EACH STATION J
E = AA * B(J - 2) + BB
DENOM = E * B(J - 1) + AA * C(J - 2) + CC
IF ( DENOM .NE. 0 ) GO TO 1021
C-----IF DENOM IS ZERO BEAM DOES NOT EXIST D = 0
D = 0.0
GO TO 1022
1021 D = -1.0 / DENOM
1022 C(J) = D * EE
R(J) = D * ( E * C(J - 1) + DD )
A(J) = D * ( E * A(J - 1) + AA * A(J - 2) )
IF ( J .NE. 3 ) GO TO 1024
IF ( KODE .EQ. 2 ) GO TO 1025
C-----STATION 3 FOR GIVEN DEFLECTION AND SLOPE
IF ( TC .EQ. FIX ) GO TO 1011
IF ( TC .EQ. PIN ) GO TO 1012
C-----ELASTICALLY RESTRAINED TOP
DENOM = G * H + 2.0 * R(4)
A(3) = ( 4.0 * R(4) * RC1 - 2.0 * BC2 * G * HE2 ) / DENOM
R(3) = 0.0
C(3) = ( G * H - 2.0 * R(4) ) / DENOM
GO TO 1013

```

```

C-----FIXED TOP
1011      A(3) = -2.0 * BC2 * H
          B(3) = 0.0
          C(3) = 1.0
          GO TO 1013
C-----PINNED TOP
1012      A(3) = 2.0 * BC1
          B(3) = 0.0
          C(3) = -1.0
          GO TO 1013
1013      CONTINUE
          GO TO 1029
C-----STATION 3 FOR GIVEN LOAD AND MOMENT
1025      A(3) = A(3) + D * HE3 * BC2 / H
          GO TO 1029
1024      IF ( J .NE. 4 ) GO TO 1029
          IF ( KODE .EQ. 2 ) GO TO 1027
C-----STATION 4 FOR GIVEN DEFLECTION AND SLOPE
          A(4) = BC1
          B(4) = 0.0
          C(4) = 0.0
          GO TO 1029
C-----STATION 4 FOR GIVEN LOAD AND MOMENT
1027      A(4) = A(4) - D * HE3 * ( BC2 / H + BC1 )
1029      CONTINUE
C-----PRESERVE PREVIOUS Y AND COMPUTE NEW Y
          DO 1035 J = 4, NP4
1035      YY(J) = Y(J)
          Y(NP6) = 0.0
          Y(NP7) = 0.0
          DO 1030 L = 3, NP7
          J = N + 8 - L
          Y(J) = A(J) + B(J) * Y(J+1) + C(J) * Y(J+2)
1030      CONTINUE
C-----RESET EI VALUES
          CALL MCURV
C-----CHECK FOR CLOSURE OF DEFLECTION Y AT ALL STATIONS
          DO 1040 J = 4, NP4
1040      IF ( ABS ( YY(J) - Y(J) ) .GE. TOLP ) GO TO 1050
          CONTINUE
          GO TO 1060
1050      ITER = ITER + 1
          IF ( ITER .LE. 999 ) GO TO 1051
          PRINT 540
          GO TO 9999
C-----COMPUTE NEW SET OF ES VALUES
1051      CALL SOIL 2R
          GO TO 1023
C-----COMPUTE SLOPE, BM AND SHEAR
1060      CONTINUE
          BM(2) = 0.0
          BM(NP6) = 0.0
          DO 1071 J = 3, NP5
          RES(J) = ES(J) * Y(J)
          DY(J) = ( Y(J+1) - Y(J-1) ) / H2
          BM(J) = - R(J) * ( Y(J-1) - 2.0 * Y(J) + Y(J+1) ) / HE2
1071      CONTINUE
          DO 1072 J = 3, NP5

```

```

                                DBM(J) = - ( BM(J+1) - BM(J-1) ) / H2 + P(J) * DY(J)
1072      CONTINUE
C-----SUM UP SOIL REACTION
                                SRES = 0.0
                                DO 1100 K = 4, NP4
                                IF ( K .EQ. 4 ) GO TO 1109
                                IF ( K .EQ. NP4 ) GO TO 1109
                                SRES = SRES + RES(K) * H
                                GO TO 1100
1109      SRES = SRES + RES(K) * H / 2.0
1100      CONTINUE
C-----PRINT OUT ALL THE PILE STATIONS
                                PRINT 550
                                PRINT 551
                                DBM(4) = SRES
                                DO 1073 J = 4, NP4
                                ISTA = J - 4
                                ZI = ISTA
                                X = ZI * H
                                PRINT 552, ISIA, X, Y(J), DY(J), BM(J), DBM(J), RES(J)
1073      CONTINUE
                                PRINT 553, SRES
                                PRINT 542, ITER
                                IF ( MPLAST .EQ. 0 ) GO TO 1074
                                PRINT 541
1074      GO TO 100
9999      CONTINUE
END

```

```

SUBROUTINE M CURV
DIMENSION CURV(507)
COMMON / BLOCK1 / H, N, NDS, XX1(5), XX2(5), RRI(5), SIZE(5),
1      HE2, NP4, DPS, YIELD(5), YOUNG
COMMON / BLOCK2 / NC, XS(20), NP(20), YC(20,25), PC(20,25)
COMMON / BLOCK3 / Y(507), ES(507), R(507), MPLAST
500 FORMAT ( /// 5X *EI VALUE DOES NOT COVER THE PILE* )
C-----SET CONSTANTS
      MPLAST = 0
C-----COMPUTE CURVATURE FROM STA 4 TO NP4
      DO 120 I = 4, NP4
        C = ( Y(I+1) - 2.0 * Y(I) + Y(I-1) ) / HE2
        CURV(I) = ABS ( C )
120    CONTINUE
C-----CALC NEW EI VALUE
      Y = 0.0
      DO 130 I = 4, NP4
        DO 100 J = 1, NDS
          IF ( XX2(J) .GE. X ) GO TO 101
100    CONTINUE
101      R(I) = RRI(J)
          BMP = YIELD(J)
C-----COMPUTE CURVATURE CORRESPONDING TO MOMENT
          CURVP = BMP / R(I)
C-----CHECK PLASTIC STATE
          IF ( CURV(I) .GE. CURVP ) GO TO 110
          GO TO 111
110      R(I) = BMP / CURV(I)
          MPLAST = 1
111    CONTINUE
          X = X + H
130    CONTINUE
      RETURN
      END

```

```

SUBROUTINE SOIL 2R
DIMENSION EST(24)
COMMON / BLOCK1 / H, N, NOS, XX1(5), YX2(5), RPI(5), SIZE(5),
1 HE2, NP4, DPS, YIELD(5), YOUNG
COMMON / BLOCK2 / NC, XS(20), NP(20), YC(20,25), PC(20,25)
COMMON / BLOCK3 / Y(507), ES(507), R(507), MPLAST
3000 FORMAT( // 52H P-Y CURVES DO NOT EXTEND THE LENGTH OF THE PILE
1 )
3001 FORMAT( / 35H *****PROBLEM IS ABANDONED***** / )
C-----START COMPUTING ES VALUES
K = 2
DO 3090 J = 4, NP4
7J = J - 4
Z = ZJ * H - DPS
C-----CHECK IF THE STATION IS ABOVE GROUND SURFACE IF SO SET ES = 0
IF ( Z ) 3010, 3015, 3015
3010 ES(J) = 0.0
GO TO 3090
C-----FIND THE P-Y CURVES LOCATING ABOVE AND BELOW THE GIVEN STATION
3015 IF ( XS(K) = Z ) 3020, 3027, 3030
3020 K = K + 1
IF ( K = NC ) 3015, 3015, 3025
3025 PRINT 3000
PRINT 3001
3026 RETURN
3027 M = K
GO TO 3035
3030 M = K - 1
3035 YA = AHS ( Y(J) )
IF ( YA = 1.0E-10 ) 3030, 3037, 3037
3030 YA = 1.0E-10
C-----FIND POINTS BEHIND AND AHEAD OF GIVEN Y ON EACH P-Y CURVE AND COMPUTE
C ES ON EACH CURVE BY LINEAR INTERPOLATION
3037 DO 3070 I = M, K
L = 2
3040 IF ( YC(I, L) = YA ) 3045, 3055, 3060
3045 I = L + 1
IF ( L = NP(I) ) 3040, 3040, 3050
3050 P1 = PC(I, L-1)
GO TO 3065
3055 P1 = PC(I, L)
GO TO 3065
3060 P1 = PC(I, L) - ( PC(I, L) - PC(I, L-1) ) * (YC(I, L) - YA
1 ) / ( YC(I, L) - YC(I, L-1) )
3065 EST(I) = P1 / YA
3070 CONTINUE
C-----INTERPOLATE BETWEEN CURVES FOR ES VALUE
IF ( K = M ) 3075, 3075, 3080
3075 ES(J) = EST(K)
GO TO 3090
3080 ES(J) = ( EST(K) - ( EST(K) - EST(M) ) * ( XS(K) - Z ) /
1 ( XS(K) - XS(M) ) )
3090 CONTINUE
RETURN
END

```

### B.6 Example Run for Program LLP

Computations for one of the laterally loaded test piles (Test 17, Pile 3) are shown in the following.

The properties of the test pile are described in Chapter IV. A set of experimental lateral soil resistance curves (Fig. 5.25) is used. The ultimate moment  $M_p$  is arbitrarily set as 5,000 inch-pound for an axial force of 1,000 pounds.

The computation is done for four different types of boundary conditions at pile top.

1. Horizontal pile-cap displacement, 0.2 inch  
 Rotation of pile cap,  $10^{-3}$  radian  
 Type of connection to pile cap, pinned
2. Horizontal pile-cap displacement, 0.2 inch  
 Rotation of pile cap,  $10^{-3}$  radian  
 Type of connection to pile cap, fixed
3. Horizontal pile-cap displacement, 0.2 inch  
 Rotation of pile cap,  $10^{-3}$  radian  
 Elastic restraint from pile, cap inch-pound per radian  
 Type of connection to pile cap, elastic restraint
4. Horizontal load on pile top, pound  
 Moment around pile top, inch-pound

Next follows the listing of the input data for four consecutive runs and their computation results.







## LATERAL SOIL RESISTANCE CURVE FROM TEST 17 PILE 3 DISPL R.C. PINNED

TABLE B PILE TOP CONDITION AND INPUT SWITCH

DEF, IN	SLOPE	AXIAL L, LB	CONNEC	CODE	T-C	T-D	SPRING M/RAD
2.000E-01	1.000E-03	1.000E+03	PIN	1	1	1	0.

(CODE = 1 FOR GIVEN SET OF DEF AND SLOPE)  
 (CODE = 2 FOR GIVEN SET OF LOAD AND MOMENT)  
 (T-C, T-D IF 1 NEW DATA ARE FURNISHED IF 0 NO DATA INPUT)

TABLE C PILE PROPERTIES

LENGTH, IN	INCREMENT	SECTION	E, PSI	GI, IN	
1.040E+02	50	1	2.900E+07	8.000E+00	
SECTION	FROM, IN	TO, IN	WIDTH, IN	I, IN <sup>4</sup>	MULT, IN-LB
1	0.	1.040E+02	2.000E+00	1.850E-01	6.000E+03

TABLE D P-Y CURVES NO OF CURVES 6

CURVE	1	DIST FROM PILE TOP, IN	0.	NO OF POINTS	5
POINT	Y, IN	P, LB/IN			
1	0.	0.			
2	1.000E-01	0.			
3	2.000E-01	0.			
4	3.000E-01	0.			
5	1.000E+01	0.			
CURVE	2	DIST FROM PILE TOP, IN	6.000E+00	NO OF POINTS	5
POINT	Y, IN	P, LB/IN			
1	0.	0.			
2	2.000E-02	7.500E+00			
3	6.500E-02	1.250E+01			
4	3.000E-01	1.600E+01			
5	1.000E+01	1.600E+01			
CURVE	3	DIST FROM PILE TOP, IN	1.200E+01	NO OF POINTS	5
POINT	Y, IN	P, LB/IN			
1	0.	0.			
2	2.000E-02	2.000E+01			
3	4.500E-02	3.000E+01			
4	2.000E-01	4.400E+01			
5	1.000E+01	4.400E+01			
CURVE	4	DIST FROM PILE TOP, IN	1.800E+01	NO OF POINTS	5
POINT	Y, IN	P, LB/IN			
1	0.	0.			
2	2.000E-02	3.000E+01			
3	5.000E-02	4.300E+01			
4	1.000E-01	5.800E+01			
5	1.000E+01	5.800E+01			
CURVE	5	DIST FROM PILE TOP, IN	2.400E+01	NO OF POINTS	5
POINT	Y, IN	P, LB/IN			
1	0.	0.			

	2	2.000E-02	3.000E+01
	3	3.500E-02	5.000E+01
	4	5.000E-02	6.600E+01
	5	1.000E+01	6.600E+01
CURVE	6	DIST FROM PILE TOP, IN	9.600E+01
POINT		Y, IN	P, LB/TN
	1	0.	0.
	2	2.000E-02	3.000E+01
	3	3.500E-02	5.000E+01
	4	5.000E-02	6.600E+01
	5	1.000E+01	6.600E+01

TABLE E COMPUTATION RESULTS

STA	X, IN	Y, IN	DY/DX	M	DM/DX	P, LB/IN
0	0.	2.000E-01	-1.036E-02	1.101E-09	1.417E+02	0.
1	2.080E+00	1.784E-01	-1.030E-02	-3.161E+02	1.416E+02	0.
2	4.160E+00	1.571E-01	-1.012E-02	-6.319E+02	1.416E+02	0.
3	6.240E+00	1.303E-01	-9.813E-03	-9.472E+02	1.416E+02	0.
4	8.320E+00	1.103E-01	-9.385E-03	-1.262E+03	1.409E+02	7.074E-01
5	1.040E+01	9.730E-02	-8.836E-03	-1.572E+03	1.347E+02	5.192E+00
6	1.248E+01	7.956E-02	-8.171E-03	-1.859E+03	1.194E+02	9.495E+00
7	1.456E+01	6.331E-02	-7.403E-03	-2.103E+03	9.489E+01	1.412E+01
8	1.664E+01	4.876E-02	-6.552E-03	-2.285E+03	6.010E+01	1.934E+01
9	1.872E+01	3.605E-02	-5.648E-03	-2.380E+03	1.631E+01	2.276E+01
10	2.080E+01	2.527E-02	-4.726E-03	-2.376E+03	-3.176E+01	2.346E+01
11	2.288E+01	1.639E-02	-3.826E-03	-2.248E+03	-7.730E+01	2.033E+01
12	2.496E+01	9.352E-03	-2.985E-03	-2.070E+03	-1.122E+02	1.322E+01
13	2.704E+01	3.978E-03	-2.232E-03	-1.814E+03	-1.321E+02	5.967E+00
14	2.912E+01	6.714E-04	-1.584E-03	-1.530E+03	-1.385E+02	1.007E-01
15	3.120E+01	-2.610E-03	-1.046E-03	-1.244E+03	-1.345E+02	-3.915E+00
16	3.328E+01	-4.284E-03	-6.159E-04	-9.747E+02	-1.237E+02	-6.426E+00
17	3.536E+01	-5.172E-03	-2.850E-04	-7.321E+02	-1.090E+02	-7.758E+00
18	3.744E+01	-5.470E-03	-4.183E-05	-5.225E+02	-8.238E+01	-8.205E+00
19	3.952E+01	-5.346E-03	1.269E-04	-3.480E+02	-7.550E+01	-8.019E+00
20	4.160E+01	-4.942E-03	2.347E-04	-2.079E+02	-5.945E+01	-7.413E+00
21	4.368E+01	-4.370E-03	2.943E-04	-9.948E+01	-4.493E+01	-6.555E+00
22	4.576E+01	-3.718E-03	3.174E-04	-1.976E+01	-3.231E+01	-5.577E+00
23	4.784E+01	-3.050E-03	3.143E-04	3.605E+01	-2.175E+01	-4.574E+00
24	4.992E+01	-2.410E-03	2.933E-04	7.204E+01	-1.323E+01	-3.616E+00
25	5.200E+01	-1.829E-03	2.615E-04	9.232E+01	-6.620E+00	-2.744E+00
26	5.408E+01	-1.323E-03	2.241E-04	1.007E+02	-1.703E+00	-1.984E+00
27	5.616E+01	-8.973E-04	1.851E-04	1.003E+02	1.760E+00	-1.346E+00
28	5.824E+01	-5.528E-04	1.474E-04	9.411E+01	4.022E+00	-8.292E-01
29	6.032E+01	-2.841E-04	1.128E-04	8.422E+01	5.328E+00	-4.262E-01
30	6.240E+01	-8.343E-05	8.246E-05	7.242E+01	5.901E+00	-1.251E-01
31	6.448E+01	5.888E-05	5.679E-05	6.001E+01	5.940E+00	8.833E-02
32	6.656E+01	1.528E-04	3.586E-05	4.795E+01	5.609E+00	2.292E-01
33	6.864E+01	2.081E-04	1.943E-05	3.683E+01	5.046E+00	3.121E-01
34	7.072E+01	2.336E-04	7.046E-06	2.703E+01	4.357E+00	3.504E-01
35	7.280E+01	2.374E-04	-1.826E-06	1.873E+01	3.623E+00	3.560E-01
36	7.488E+01	2.260E-04	-7.774E-06	1.195E+01	2.900E+00	3.390E-01
37	7.696E+01	2.050E-04	-1.138E-05	6.635E+00	2.227E+00	3.075E-01
38	7.904E+01	1.787E-04	-1.318E-05	2.641E+00	1.629E+00	2.680E-01
39	8.112E+01	1.502E-04	-1.365E-05	-1.958E-01	1.116E+00	2.253E-01
40	8.320E+01	1.219E-04	-1.321E-05	-2.058E+00	6.913E-01	1.829E-01
41	8.528E+01	9.525E-05	-1.221E-05	-3.126E+00	3.525E-01	1.429E-01
42	8.736E+01	7.112E-05	-1.091E-05	-3.575E+00	9.297E-02	1.067E-01
43	8.944E+01	4.987E-05	-9.526E-06	-3.559E+00	-9.577E-02	7.481E-02

44	9.152E+01	3.149E-05	-8.213E-06	-3.216E+00	-2.227E-01	4.724E-02
45	9.360E+01	1.571E-05	-7.072E-06	-2.666E+00	-2.963E-01	2.356E-02
46	9.568E+01	2.070E-06	-6.165E-06	-2.013E+00	-3.241E-01	3.105E-03
47	9.776E+01	-9.943E-06	-5.515E-06	-1.344E+00	-2.118E-01	-1.491E-02
48	9.984E+01	-2.087E-05	-5.111E-06	-7.386E-01	-2.637E-01	-3.131E-02
49	1.019E+02	-3.120E-05	-4.916E-06	-2.682E-01	-1.825E-01	-4.681E-02
50	1.040E+02	-4.132E-05	-4.864E-06	-0.	-6.933E-02	-6.198E-02

SUM OF SOIL RESISTANCE, LH 1.417E+02

NUMBER OF ITERATIONS 7

## LATERAL SOIL RESISTANCE CURVE FROM TEST 17 PILE 3 DISPL H.C. FIXED

TABLE H PILE TOP CONDITION AND INPUT SWITCH

DEF, IN	SLOPE	AXIAL L, LB	CONNEC	CODE	T-C	T-D	SPRING M/RAD
2.000E-01	1.000E-03	1.000E+03	FIX	1	0	0	0.

(CODE = 1 FOR GIVEN SET OF DEF AND SLOPE)

(CODE = 2 FOR GIVEN SET OF LOAD AND MOMENT)

(T-C, T-D IF 1 NEW DATA ARE FURNISHED IF 0 NO DATA INPUT)

TABLE C PREVIOUS PILE PROPERTIES ARE USED

TABLE D PREVIOUS P-Y CURVES ARE USED

TABLE F COMPUTATION RESULTS

STA	X, IN	Y, IN	DY/DX	M	DM/DX	P, LB/IN
0	0.	2.000E-01	1.000E-03	5.000E+03	3.669E+02	0.
1	2.080E+00	1.936E-01	-3.900E-03	4.232E+03	3.665E+02	0.
2	4.160E+00	1.838E-01	-5.391E-03	3.459E+03	3.668E+02	0.
3	6.240E+00	1.712E-01	-6.582E-03	2.684E+03	3.668E+02	0.
4	8.320E+00	1.564E-01	-7.471E-03	1.906E+03	3.661E+02	7.392E-01
5	1.040E+01	1.401E-01	-8.060E-03	1.130E+03	3.596E+02	5.447E+00
6	1.248E+01	1.229E-01	-8.352E-03	3.742E+02	3.436E+02	9.976E+00
7	1.456E+01	1.053E-01	-8.360E-03	-3.344E+02	3.174E+02	1.519E+01
8	1.664E+01	8.809E-02	-8.105E-03	-9.791E+02	2.787E+02	2.210E+01
9	1.872E+01	7.163E-02	-7.619E-03	-1.527E+03	2.264E+02	2.818E+01
10	2.080E+01	5.639E-02	-6.945E-03	-1.952E+03	1.629E+02	3.288E+01
11	2.288E+01	4.274E-02	-6.133E-03	-2.234E+03	9.305E+01	3.426E+01
12	2.496E+01	3.088E-02	-5.242E-03	-2.365E+03	2.319E+01	3.291E+01
13	2.704E+01	2.073E-02	-4.327E-03	-2.352E+03	-4.281E+01	3.054E+01
14	2.912E+01	1.288E-02	-3.444E-03	-2.205E+03	-9.466E+01	1.932E+01
15	3.120E+01	6.602E-03	-2.634E-03	-1.973E+03	-1.250E+02	9.903E+00
16	3.328E+01	1.918E-03	-1.923E-03	-1.696E+03	-1.383E+02	2.878E+00
17	3.536E+01	-1.398E-03	-1.322E-03	-1.405E+03	-1.392E+02	-2.097E+00
18	3.744E+01	-3.581E-03	-8.321E-04	-1.122E+03	-1.314E+02	-5.372E+00
19	3.952E+01	-4.800E-03	-4.474E-04	-8.620E+02	-1.182E+02	-7.289E+00
20	4.160E+01	-5.443E-03	-1.577E-04	-6.325E+02	-1.021E+02	-8.164E+00
21	4.368E+01	-5.516E-03	4.972E-05	-4.377E+02	-8.505E+01	-8.274E+00
22	4.576E+01	-5.236E-03	1.886E-04	-2.785E+02	-6.828E+01	-7.854E+00
23	4.784E+01	-4.731E-03	2.722E-04	-1.529E+02	-5.273E+01	-7.097E+00
24	4.992E+01	-4.104E-03	3.131E-04	-5.709E+01	-3.894E+01	-6.155E+00
25	5.200E+01	-3.429E-03	3.223E-04	1.037E+01	-2.719E+01	-5.143E+00
26	5.408E+01	-2.703E-03	3.093E-04	5.647E+01	-1.753E+01	-4.144E+00
27	5.616E+01	-2.142E-03	2.820E-04	8.440E+01	-9.882E+00	-3.213E+00
28	5.824E+01	-1.590E-03	2.465E-04	9.876E+01	-4.061E+00	-2.384E+00
29	6.032E+01	-1.117E-03	2.074E-04	1.025E+02	1.616E-01	-1.675E+00
30	6.240E+01	-7.267E-04	1.684E-04	9.895E+01	3.038E+00	-1.090E+00
31	6.448E+01	-4.104E-04	1.316E-04	9.058E+01	4.821E+00	-6.246E-01
32	6.656E+01	-1.791E-04	9.869E-05	7.944E+01	5.750E+00	-2.686E-01
33	6.864E+01	-5.839E-06	7.028E-05	6.707E+01	6.038E+00	-8.758E-03
34	7.072E+01	1.133E-04	4.670E-05	5.441E+01	5.871E+00	1.700E-01
35	7.280E+01	1.884E-04	2.780E-05	4.285E+01	5.400E+00	2.826E-01

36	7.488E+01	2.290E-04	1.324E-05	3.227E+01	4.749E+00	3.435E-01
37	7.696E+01	2.435E-04	2.501E-06	2.315E+01	4.012E+00	3.653E-01
38	7.904E+01	2.394E-04	-5.007E-06	1.559E+01	3.258E+00	3.591E-01
39	8.112E+01	2.227E-04	-9.884E-06	9.571E+00	2.538E+00	3.340E-01
40	8.320E+01	1.983E-04	-1.271E-05	4.901E+00	1.881E+00	2.974E-01
41	8.528E+01	1.698E-04	-1.400E-05	1.694E+00	1.307E+00	2.547E-01
42	8.736E+01	1.400E-04	-1.423E-05	-5.032E-01	8.234E-01	2.100E-01
43	8.944E+01	1.106E-04	-1.379E-05	-1.791E+00	4.324E-01	1.659E-01
44	9.152E+01	8.284E-05	-1.298E-05	-2.340E+00	1.310E-01	1.240E-01
45	9.360E+01	5.659E-05	-1.206E-05	-2.390E+00	-8.622E-02	8.488E-02
46	9.568E+01	3.246E-05	-1.120E-05	-2.051E+00	-2.251E-01	4.869E-02
47	9.776E+01	9.982E-06	-1.051E-05	-1.500E+00	-2.913E-01	1.497E-02
48	9.984E+01	-1.128E-05	-1.005E-05	-8.828E-01	-2.893E-01	-1.693E-02
49	1.019E+02	-3.184E-05	-9.816E-06	-3.382E-01	-2.220E-01	-4.776E-02
50	1.040E+02	-5.212E-05	-9.751E-06	-5.378E-13	-0.106E-02	-7.818E-02

SUM OF SOIL RESISTANCE\*LB 3.669E+02

NUMBER OF ITERATIONS 24

PLASTIC HINGES ARE FORMED

## LATERAL SOIL RESISTANCE CURVE FROM TEST 17 PILE 3      DI&lt;PI&gt; R.C. RESTRAINED

TABLE H      PILE TOP CONDITION AND INPUT SWITCH

DEF, IN	SLOPE	AXIAL L, LB	CONNEC	CODE	T-C	T-D	SPRING M/RAD
2.000E-01	1.000E-03	1.000E+03	REG	1	0	0	1.000E+05

(CODE = 1 FOR GIVEN SET OF DEF AND SLOPE)

(CODE = 2 FOR GIVEN SET OF LOAD AND MOMENT)

(T-C, T-D IF 1 NEW DATA ARE FURNISHED IF 0 NO DATA INPUT)

TABLE C      PREVIOUS PILE PROPERTIES ARE USED

TABLE D      PREVIOUS P-LY CURVES ARE USED

TABLE E      COMPUTATION RESULTS

STA	X, IN	Y, IN	DY/DX	M	DM/UX	P, LB/IN
0	0.	2.000E-01	-8.817E-03	9.817E+02	1.880E+02	0.
1	2.080E+00	1.813E-01	-9.118E-03	5.720E+02	1.880E+02	0.
2	4.160E+00	1.621E-01	-9.261E-03	1.618E+02	1.880E+02	0.
3	6.240E+00	1.427E-01	-9.244E-03	-2.485E+02	1.880E+02	0.
4	8.320E+00	1.236E-01	-9.068E-03	-4.586E+02	1.872E+02	7.132E-01
5	1.040E+01	1.050E-01	-8.734E-03	-1.065E+03	1.810E+02	5.238E+00
6	1.248E+01	8.728E-02	-8.247E-03	-1.448E+03	1.656E+02	9.581E+00
7	1.456E+01	7.071E-02	-7.619E-03	-1.788E+03	1.407E+02	1.443E+01
8	1.664E+01	5.558E-02	-6.872E-03	-2.065E+03	1.048E+02	2.003E+01
9	1.872E+01	4.212E-02	-6.035E-03	-2.253E+03	5.818E+01	2.482E+01
10	2.080E+01	3.048E-02	-5.146E-03	-2.372E+03	5.775E+00	2.557E+01
11	2.288E+01	2.071E-02	-4.249E-03	-2.299E+03	-4.692E+01	2.509E+01
12	2.496E+01	1.280E-02	-3.385E-03	-2.155E+03	-9.183E+01	1.810E+01
13	2.704E+01	6.631E-03	-2.594E-03	-1.971E+03	-1.210E+02	9.946E+00
14	2.912E+01	2.015E-03	-1.897E-03	-1.662E+03	-1.345E+02	3.022E+00
15	3.120E+01	-1.201E-03	-1.308E-03	-1.379E+03	-1.357E+02	-1.892E+00
16	3.328E+01	-3.425E-03	-8.264E-04	-1.103E+03	-1.284E+02	-5.138E+00
17	3.536E+01	-4.679E-03	-4.481E-04	-8.485E+02	-1.157E+02	-7.049E+00
18	3.744E+01	-5.289E-03	-1.627E-04	-6.238E+02	-1.001E+02	-7.934E+00
19	3.952E+01	-5.376E-03	4.211E-05	-4.328E+02	-8.346E+01	-8.064E+00
20	4.160E+01	-5.114E-03	1.796E-04	-2.764E+02	-6.709E+01	-7.671E+00
21	4.368E+01	-4.629E-03	2.628E-04	-1.570E+02	-5.189E+01	-6.943E+00
22	4.576E+01	-4.021E-03	3.040E-04	-5.945E+01	-3.840E+01	-6.031E+00
23	4.784E+01	-3.304E-03	3.140E-04	8.076E+00	-2.688E+01	-5.866E+00
24	4.992E+01	-2.714E-03	3.020E-04	5.378E+01	-1.740E+01	-4.072E+00
25	5.200E+01	-2.108E-03	2.758E-04	8.166E+01	-0.874E+00	-3.162E+00
26	5.408E+01	-1.507E-03	2.414E-04	9.500E+01	-4.141E+00	-2.351E+00
27	5.616E+01	-1.104E-03	2.034E-04	9.900E+01	5.556E-02	-1.656E+00
28	5.824E+01	-7.210E-04	1.653E-04	9.664E+01	2.872E+00	-1.082E+00
29	6.032E+01	-4.102E-04	1.294E-04	8.863E+01	4.646E+00	-6.243E-01
30	6.240E+01	-1.828E-04	9.711E-05	7.785E+01	5.581E+00	-2.742E-01
31	6.448E+01	-1.218E-05	6.926E-05	6.582E+01	5.885E+00	-1.827E-02
32	6.656E+01	1.053E-04	4.610E-05	5.366E+01	5.740E+00	1.580E-01
33	6.864E+01	1.796E-04	2.753E-05	4.214E+01	5.295E+00	2.694E-01
34	7.072E+01	2.149E-04	1.321E-05	3.175E+01	4.672E+00	3.298E-01
35	7.280E+01	2.345E-04	2.641E-06	2.276E+01	3.963E+00	3.518E-01

36	7.488E+01	2.308E-04	-4.732E-06	1.527E+01	2.237E+00	3.463E-01
37	7.696E+01	2.148E-04	-9.490E-06	9.272E+00	2.542E+00	3.223E-01
38	7.904E+01	1.914E-04	-1.219E-05	4.659E+00	1.908E+00	2.871E-01
39	8.112E+01	1.641E-04	-1.334E-05	1.284E+00	1.353E+00	2.462E-01
40	8.320E+01	1.359E-04	-1.339E-05	-1.027E+00	8.854E-01	2.038E-01
41	8.528E+01	1.084E-04	-1.272E-05	-2.455E+00	5.043E-01	1.626E-01
42	8.736E+01	8.246E-05	-1.163E-05	-3.177E+00	2.057E-01	1.244E-01
43	8.944E+01	6.006E-05	-1.036E-05	-3.359E+00	-1.738E-02	9.010E-02
44	9.152E+01	3.987E-05	-9.097E-06	-3.148E+00	-1.733E-01	5.981E-02
45	9.360E+01	2.222E-05	-7.968E-06	-2.676E+00	-2.702E-01	3.333E-02
46	9.568E+01	6.727E-06	-7.050E-06	-2.058E+00	-3.153E-01	1.009E-02
47	9.776E+01	-7.108E-06	-6.381E-06	-1.394E+00	-3.147E-01	-1.066E-02
48	9.984E+01	-1.982E-05	-5.461E-06	-7.748E-01	-2.727E-01	-2.973E-02
49	1.019E+02	-3.141E-05	-5.756E-06	-2.840E-01	-1.920E-01	-4.786E-02
50	1.040E+02	-4.376E-05	-5.701E-06	-2.689E-13	-7.397E-02	-6.565E-02

SUM OF SOIL RESISTANCE, LH 1.880E+02

NUMBER OF ITERATIONS 8

## LATERAL SOIL RESISTANCE CURVE FROM TEST 17 PILE 3      FORCE R.C.

TABLE H      PILE TOP CONDITION AND INPUT SWITCH

LAT L, LB	BM LB-IN	AXIAL L, LB	CONNEC	CODE	T-C	T-U	SPRING M/RAD
1.000E+02	1.500E+03	1.000E+03		2	0	0	0.

(CODE = 1 FOR GIVEN SET OF DEF AND SLOPE)

(CODE = 2 FOR GIVEN SET OF LOAD AND MOMENT)

(T-C, T-U IF 1 NEW DATA ARE FURNISHED IF A NO DATA INPUT)

TABLE C      PREVIOUS PILE PROPERTIES ARE USED

TABLE D      PREVIOUS P-Y CURVES ARE USED

TABLE E      COMPUTATION RESULTS

STA	X, IN	Y, IN	DY/DX	M	DM/DX	P, LB/IN
0	0.	2.046E-02	9.635E-04	1.500E+03	1.013E+02	0.
1	2.080E+00	2.186E-02	4.225E-04	1.291E+03	1.013E+02	0.
2	4.160E+00	2.222E-02	-3.716E-05	1.091E+03	1.013E+02	0.
3	6.240E+00	2.170E-02	-4.152E-04	8.604E+02	1.013E+02	0.
4	8.320E+00	2.049E-02	-7.112E-04	6.576E+02	1.008E+02	4.029E-01
5	1.040E+01	1.875E-02	-9.253E-04	4.470E+02	9.749E+01	2.812E+00
6	1.248E+01	1.694E-02	-1.060E-03	2.482E+02	8.972E+01	4.660E+00
7	1.456E+01	1.434E-02	-1.122E-03	6.933E+01	7.841E+01	6.212E+00
8	1.664E+01	1.198E-02	-1.119E-03	-8.269E+01	4.386E+01	7.784E+00
9	1.872E+01	9.691E-03	-1.064E-03	-2.010E+02	4.704E+01	8.390E+00
10	2.080E+01	7.549E-03	-9.702E-04	-2.828E+02	2.994E+01	8.052E+00
11	2.288E+01	5.645E-03	-8.515E-04	-3.205E+02	1.428E+01	7.000E+00
12	2.496E+01	4.007E-03	-7.206E-04	-3.467E+02	1.112E+00	5.663E+00
13	2.704E+01	2.647E-03	-5.883E-04	-3.372E+02	-8.907E+00	3.971E+00
14	2.912E+01	1.500E-03	-4.626E-04	-3.171E+02	-1.547E+01	2.339E+00
15	3.120E+01	7.229E-04	-3.440E-04	-2.747E+02	-1.903E+01	1.084E+00
16	3.328E+01	1.077E-04	-2.505E-04	-2.334E+02	-2.033E+01	1.615E-01
17	3.536E+01	-3.173E-04	-1.682E-04	-1.912E+02	-2.000E+01	-4.789E-01
18	3.744E+01	-5.720E-04	-1.019E-04	-1.509E+02	-1.857E+01	-8.880E-01
19	3.952E+01	-7.431E-04	-5.044E-05	-1.144E+02	-1.649E+01	-1.115E+00
20	4.160E+01	-8.018E-04	-1.227E-05	-8.254E+01	-1.408E+01	-1.203E+00
21	4.368E+01	-7.941E-04	1.456E-05	-5.585E+01	-1.159E+01	-1.191E+00
22	4.576E+01	-7.413E-04	3.202E-05	-3.426E+01	-9.197E+00	-1.112E+00
23	4.784E+01	-6.609E-04	4.205E-05	-1.745E+01	-7.010E+00	-9.913E-01
24	4.992E+01	-5.604E-04	4.639E-05	-4.923E+00	-5.095E+00	-8.495E-01
25	5.200E+01	-4.679E-04	4.658E-05	3.935E+00	-3.482E+00	-7.018E-01
26	5.408E+01	-3.726E-04	4.392E-05	9.754E+00	-2.170E+00	-5.589E-01
27	5.616E+01	-2.852E-04	3.949E-05	1.375E+01	-1.144E+00	-4.278E-01
28	5.824E+01	-2.083E-04	3.409E-05	1.448E+01	-7.744E-01	-3.125E-01
29	6.032E+01	-1.433E-04	2.837E-05	1.485E+01	1.742E-01	-2.150E-01
30	6.240E+01	-9.033E-05	2.276E-05	1.407E+01	5.388E-01	-1.355E-01
31	6.448E+01	-4.866E-05	1.757E-05	1.270E+01	7.556E-01	-7.299E-02
32	6.656E+01	-1.723E-05	1.298E-05	1.100E+01	8.584E-01	-2.584E-02
33	6.864E+01	5.334E-06	9.066E-06	9.183E+00	8.769E-01	8.000E-03
34	7.072E+01	2.049E-05	5.853E-06	7.301E+00	8.366E-01	3.073E-02
35	7.280E+01	2.968E-05	3.310E-06	5.727E+00	7.584E-01	4.452E-02



36	7.488E+01	3.426E-05	1.376E-06	4.250F+00	6.586F-01	5.139E-02
37	7.696E+01	3.541E-05	-2.772E-08	2.993F+00	5.499E-01	5.311E-02
38	7.904E+01	3.414E-05	-9.882E-07	1.942E+00	4.414E-01	5.122E-02
39	8.112E+01	3.130E-05	-1.592E-06	1.152E+00	3.393E-01	4.695E-02
40	8.320E+01	2.752E-05	-1.921E-06	5.440F-01	2.476F-01	4.128E-02
41	8.528E+01	2.331E-05	-2.048E-06	1.141F-01	1.683E-01	3.496E-02
42	8.736E+01	1.900E-05	-2.038E-06	-1.646E-01	1.023E-01	2.850E-02
43	8.944E+01	1.483E-05	-1.945E-06	-3.200E-01	4.953E-02	2.224E-02
44	9.152E+01	1.041E-05	-1.809E-06	-3.788E-01	9.378E-03	1.637E-02
45	9.360E+01	7.301E-06	-1.665E-06	-3.645E-01	-1.903E-02	1.095E-02
46	9.568E+01	3.986E-06	-1.534E-06	-3.045E-01	-3.664E-02	5.979E-03
47	9.776E+01	9.188E-07	-1.432E-06	-2.205E-01	-4.429E-02	1.378E-03
48	9.984E+01	-1.971E-06	-1.364E-06	-1.282E-01	-4.265E-02	-2.956E-03
49	1.019E+02	-4.757E-06	-1.330E-06	-4.870E-02	-3.215E-02	-7.136E-03
50	1.040E+02	-7.504E-06	-1.321E-06	-6.722E-14	-1.303E-02	-1.126E-02

SUM OF SOIL RESISTANCE\*LM 1.613F+02

NUMBER OF ITERATIONS 6

See note on page 262

## APPENDIX C

### COMPUTER PROGRAM AXP

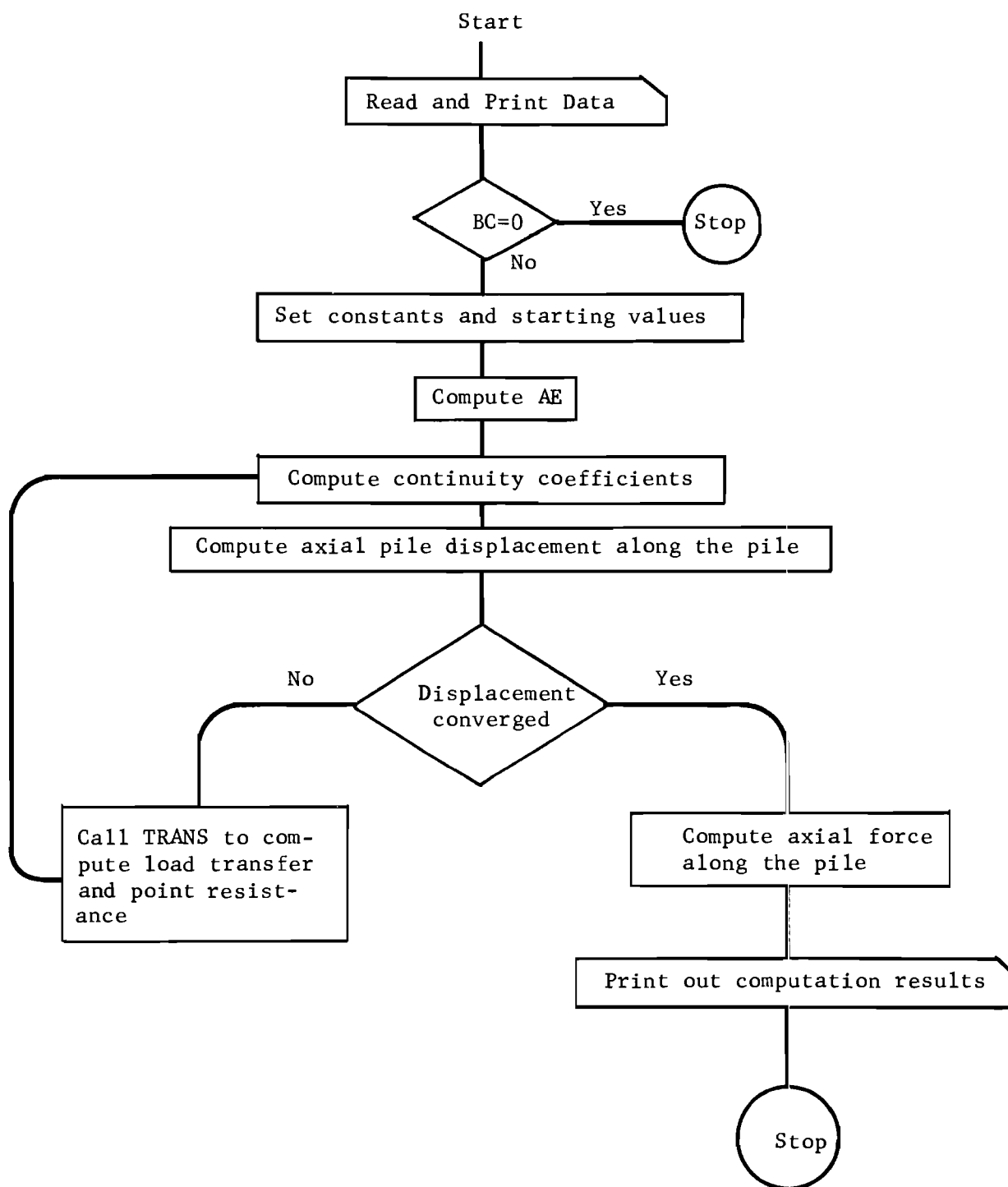
#### C.1 Description of the Program

The computer program AXP solves for the pile-top displacement and for the axial force within a single pile for a given pile-top load or for a forced pile-top displacement.

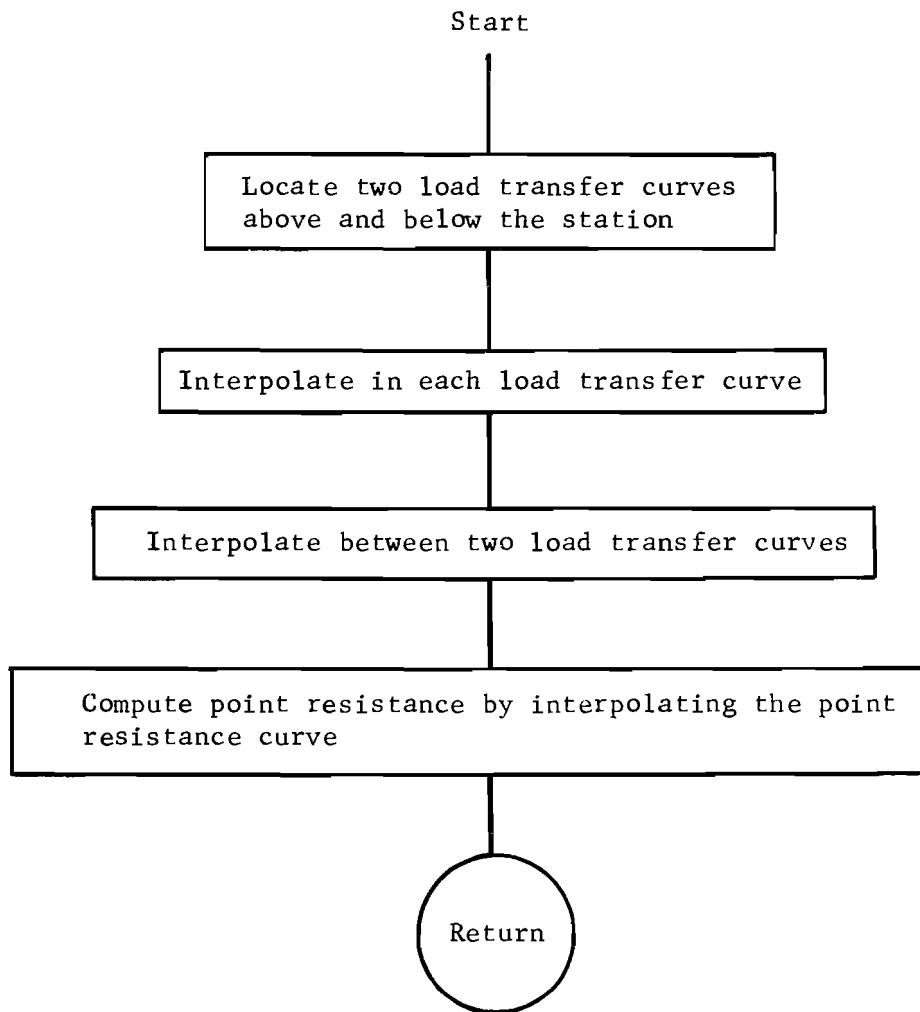
The program consists of the main program AXP and the subroutine TRANS. The theory of infinite difference method employed in the main program AXP is developed in Chapter IV. The subroutine TRANS interpolates the load transfer and the point resistance from the given curves.

The program AXP is capable of dealing with both downward loading and upward loading.

## Flow Diagrams for Main Program AXP



## Flow Diagram for Subroutine TRANS



## C.3 Glossary of Notation for Program AXP

A(103)	continuity coefficient
AE(103)	product of cross-sectional area of a pile and the Young's modulus
AREA(5)	cross-sectional area of a pile
B(103)	continuity coefficient
BC	boundary condition at pile top
BETA(103)	secant modulus of load transfer curve
CIRC(5)	circumference of a pile
DEPTH(11)	distance from pile top to depth where a load transfer curve is given
DISPL(11, 20)	pile displacement
GAM	secant modulus of point resistance curve
H	increment length of a discretized pile
HN	total length of a pile
INC	number of discretized element of a pile
KEEP	input switch for repetitive data
KFLAG	signal to notify the excessive pile displacement
KPOINT	number of points in a point resistance curve
NBC	code to specify the force boundary condition or the displacement boundary condition
NDS	number of different sections in a pile
NLT	number of load transfer curves
NPOINT(11)	number of points in a load transfer curve
PER(103)	perimeter of pile at discrete station
PR(20)	point resistance

Q(103)	axial force in a pile
SETTL(20)	pile tip settlement
TITLE(20)	alphanumeric variable to store the title of run
TR(11, 20)	load transfer on a pile
XX1(5)	distance from pile top to top of a pile section
XX2(5)	distance from pile top to bottom of a pile section
Y(103)	axial pile displacement
YK(103)	dummy to keep the previous axial pile displacement
YOUNG	Young's modulus

## C.4 Data Coding for Program AXP

The input data for the program AXP consists of the following groups.

TABLE A Title of the run

TABLE B Boundary condition at pile top

TABLE C Pile properties

TABLE D Load transfer curves

TABLE E Point resistance curves

TABLES A and B must be furnished for each run. TABLES C, D, and E can be omitted for the repetitive run by properly setting the input switch, in which case the data from the previous run are used.

The general deck structure of the input data are shown in the following.

## Deck Structure of Input Data for Program AXP

TABLE A TITLE OF RUN

Card AI one card

TABLE B BOUNDARY CONDITION AT PILE TOP AND INPUT SWITCH

Card BI one card

TABLE C PILE PROPERTIES

If B2 = 0, skip TABLES C, D, and E

Card CI one card

Card CII C3 cards

TABLE D LOAD TRANSFER CURVES

Card DI one card

Card DII one card  D1 sets

Card DIII D3 cards

## TABLE E POINT RESISTANCE CURVE

Card EI one card

Card EII E1 cards

To start a new run immediately continue TABLE A of next run. To stop the run add two blank cards at the end of data deck.



## Data Coding Form for Program AXP

The general instructions for data coding may be referred to A.4.

## TABLE A Title of Run

## Card AI

A1 1 to 80 Alphanumeric description of each run

## TABLE B Boundary Condition and Input Switch

## Card BI

B1 5 Code to specify the type of boundary condition to be entered in B3. If B1 = 1, force b.c. is entered. If B1 = 2, displacement b.c. is entered.

B2 10 Switch for inputting the subsequent data. If B2 = 1, TABLES C, D, and E must be furnished. If B2 = 0, no input for TABLES C, D, and E, in which case the data from previous run are used.

B3 11 to 20 Boundary condition. Enter axial load on pile top, pound (downward +), if B1 = 1. Enter pile top displacement, in (downward +), if B1 = 2.

## TABLE C Pile Properties

If B2 = 0, skip TABLES C, D, and E

## Card CI

C1 1 to 10 Total length of pile, inch

C2 11 to 15 Number of increment by which the pile is divided into finite elements (maximum 100)

C3 16 to 20 Number of different sections in the pile (maximum 5)

C4 21 to 30 Young's modulus of pile material, psi

## Card CII

Different sections in a pile are listed from top to bottom

C5	1 to 10	Depth from ground surface to top of a pile section, inch
C6	11 to 20	Depth from ground surface to bottom of a pile section
C7	21 to 30	Cross-sectional area, inch <sup>2</sup>
C8	31 to 40	Perimeter of pile, inch

TABLE D Load Transfer Curves

## Card DI

D1 1 to 5 Number of load transfer curves (maximum 10)

## Card DII

The load transfer curve is listed from pile top to tip or deeper. For the pile portion standing above the ground surface, assume 0 load transfer.

D2 1 to 10 Depth from pile top to point where a curve is given, inch

D3 11 to 15 Number of points in a curve (maximum 20)

## Card DIII

List the point in the order of from negative or zero displacement to positive displacement.

D4 1 to 10 Load transfer, psi (acting upward on pile wall +)

D5 11 to 20 Pile displacement, inch (downward +)

TABLE E Point Resistance Curve

## Card EI

E1 1 to 5 Number of points in the curve (maximum 20)  
Start listing the point from (0, 0)

## Card EII

E2 1 to 10 Point resistance, pound (upward +)

E3 11 to 20 Pile tip movement, inch (downward +)

C.5 Listing of Program AXP

```

PROGRAM AXP (INPUT,OUTPUT)
DIMENSION TITLE(20), XX1(5), XX2(5), AREA(5), CIRC(5), YK(103),
1      A(103), B(103), AE(103), Q(103), PER(103)
COMMON / BLOCK1 / INC, INCL, H, BETA(103), GAM, INC2, INC3, KFLAG
COMMON / BLOCK2 / NLT, DEPTH(11), NPOINT(11), TR(11, 20),
1      DISPL(11,20), KPOINT, O(20), SETTLE(20), Y(103)
C-----AXIALLY LOADED PILE WRITTEN BY KATS AMOSHIKA      AUGUST 1970
C      NBC = 1 FOR LOAD AT PILE TOP      NBC = 2 FOR DISPL AT PILE TOP
501 FORMAT ( 20A4 )
502 FORMAT ( 4E10.3 )
503 FORMAT ( E10.3, 2I5, E10.3 )
504 FORMAT ( 1H1, 5X, 20A4 )
505 FORMAT ( //10A, 16HLOAD AT PILE TOP, F15.3, 4H 1H )
506 FORMAT ( / 11A, 9HLENGTH,IN, 4X, 11HINCREMENT , 13HNO OF SECTION,
1      8X, 9HYOUNG,PSI )
507 FORMAT ( 5X, E15.3, 5X, I5, 8X, I5, 7X, F15.3 )
508 FORMAT ( / 13A, 7HSECTION, 6X, 7HFROM,IN, 10X, 5HTO,IN, 8X,
1      9HAREA,SQIN, 6X, 9HCIRCUM,IN )
509 FORMAT ( 12X, I5, 3X, 4E15.3 )
510 FORMAT ( / 9X, 3HSTA, 6X, 8HDEPTH,IN, 7X, 8HDISPL,IN, 7X,
1      8HFORCE,LB, 4X, 11HTRANS,PSI )
511 FORMAT ( 6X, I5, 4E15.3 )
512 FORMAT ( / 10A, 27HMODULUS OF POINT RESISTANCE, F15.3, 7H LR/IN )
513 FORMAT ( 2I5, E10.3 )
514 FORMAT ( / 10A, 15HNO OF ITERATION, I5 )
515 FORMAT ( / 10A, 24HDISPLACEMENT AT PILE TOP, E15.3, 6H INCH )
520 FORMAT ( I5 )
522 FORMAT ( F10.3, I5 )
523 FORMAT ( 2E10.3 )
530 FORMAT ( /// 5X, 20HLOAD TRANSFER CURVES )
531 FORMAT ( 10A, 16HNUMBER OF CURVES, I5 )
532 FORMAT ( 8X, I5, 12HDEPTH,INCH, E11.3, 4X, 13HNUM OF POINTS, I5 )
533 FORMAT ( 32A, 8HLOAD,PSI, 12X, 8HDISPL,IN )
534 FORMAT ( /// 5X, 22HPOINT RESISTANCE CURVE )
535 FORMAT ( 10X, 16HNUMBER OF POINTS, I5 )
536 FORMAT ( 27X, 13HRESISTANCE,LB, 9X, 11HTIP MOVF,IN )
537 FORMAT ( 15A, I5, 2E20.3 )
540 FORMAT ( ///// 5X, 40HPREVIOUS DATA FOR PILE AND SOIL ARE USED.//)
541 FORMAT ( /// 5X, 37HCOMPUTATION OF DISPLACEMENT AND FORCE )
542 FORMAT ( ///// 5X, 39HDOES NOT CONVERGE AFTER 1000 ITERATIONS )
C-----START READING DATA
100 READ 501, ( TITLE(I), I = 1, 20 )
READ 513, NBC, KEEP, BC
IF ( BC .EQ. 0 ) GO TO 9999
IF ( KEEP .EQ. 0 ) GO TO 160
READ 503, HA, INC, NDS, YOUNG
READ 502, ( XA1(I), XX2(I), AREA(I), CIRC(I), I = 1, NDS )
C-----READ IN LOAD TRANSFER CURVES
READ 520, NLT
NLT1 = NLT + 1
DO 171 I = 2, NLT1
READ 522, DEPTH(I), NPOINT(I)
INDEX = NPOINT(I)
READ 523, ( TR(I, J), DISPL(I, J), J = 1, INDEX )
171 CONTINUE
C-----READ IN POINT RESISTANCE CURVE
READ 520, KPOINT
READ 523, ( PR(I), SETTLE(I), I = 1, KPOINT )

```

```

160     CONTINUE
C-----PRINT OUT DATA
      PRINT 504, ( TITLE(I), I = 1, 20 )
      IF ( NRC .EQ. 1 ) GO TO 104
      GO TO 105
104 PRINT 505, HC
      GO TO 106
105 PRINT 515, HC
106     CONTINUE
      IF ( KEEP .EQ. 0 ) GO TO 161
      GO TO 162
161 PRINT 540
      GO TO 163
162     CONTINUE
      PRINT 506
      PRINT 507, FN, INC, NDS, YOUNG
      PRINT 508
      PRINT 509, ( 1, XX1(I), XX2(I), ARFA(I), CIRC(I), I = 1, NDS )
C-----PRINT OUT LOAD TRANSFER CURVES
      PRINT 530
      PRINT 531, NLT
      DO 107 I = 2, NLT1
          IM1 = I - 1
          PRINT 532, IM1, DEPTH(I), NPOINT(I)
          INDEX = NPOINT(I)
          PRINT 533
          PRINT 537, ( J, TR(I, J), DISPL(I, J), J = 1, INDEX )
107     CONTINUE
C-----PRINT OUT POINT RESISTANCE CURVE
      PRINT 534
      PRINT 535, KPOINT
      PRINT 536
      PRINT 537, ( 1, PR(I), SETTLE(I), I = 1, KPOINT )
163     CONTINUE
C-----SET INITIAL VALUES AND CONSTANTS
      KFLAG = 0
      INC1 = INC + 1
      INC2 = INC + 2
      INC3 = INC + 3
      ITER = 0
      TOL = 0.00000001
      GAM = 1000000.0
      XINC = INC
      H = MN / XINC
      HE2 = H * H
      DEPTH(1) = -1.0
      NPOINT(1) = 2
      TR(1, 1) = 0.0
      TR(1, 2) = 0.0
      DISPL(1, 1) = -100.0
      DISPL(1, 2) = 100.0
      DO 101 I = 2, INC2
          BETA(I) = 0.0
          YK(I) = 0.0
          XI = I - 2
          Z = XI * H
      DO 102 J = 1, NDS
          IF ( Z .LE. XX2(J) ) GO TO 103

```

```

102 CONTINUE
103     AE(I) = YOUNG * AREA(J)
        PER(I) = CIRC(J)
101 CONTINUE
        AE(1) = AE(2)
        AE(INC3) = AE(INC2)
C-----START SOLUTION OF DIFFERENCE EQUATION
110 CONTINUE
        DO 119 I = 2, INC2
            AA = 0.25 * AE(I+1) + AE(I) - 0.25 * AE(I-1)
            BB = -BETA(I) * PER(I) * HE2 - 2.0 * AE(I)
            CC = -0.25 * AE(I+1) + AE(I) + 0.25 * AE(I-1)
            IF ( I .EQ. 2 ) GO TO 110
            GO TO 111
110     IF ( NBC .EQ. 1 ) GO TO 114
            GO TO 115
114         DENOM = -BB
            A(2) = BC * H / AE(2)
            R(2) = 1.0
            GO TO 119
115         A(2) = BC
            R(2) = 0.0
            GO TO 119
111     IF ( I .EQ. INC2 ) GO TO 112
            DENOM = -BB - CC * AE(I-1)
            A(I) = CC * A(I-1) / DENOM
            R(I) = AA / DENOM
            GO TO 119
C-----CALC Y AT LAST STATION
112     DENOM = GAM * H / AE(INC2) + 1.0 - R(INC1)
            Y(INC2) = A(INC1) / DENOM
119 CONTINUE
C-----SOLVE FOR Y AT ALL STATIONS
        DO 129 I = 1, INC
            J = INC2 - I
            Y(J) = A(J) + R(J) * Y(J+1)
129 CONTINUE
C-----CHECK CONVERGENCE OF Y
        DO 139 I = 2, INC2
            DDD = ABS ( Y(I) - YK(I) )
            IF ( DDD .GE. TOL ) GO TO 131
139 CONTINUE
            GO TO 141
131 CALL TRANS
            IF ( KFLAG .EQ. 1 ) GO TO 9999
            DO 133 J = 2, INC2
133         YK(J) = Y(J)
            ITER = ITER + 1
            IF ( ITER .GE. 1000 ) GO TO 9998
            GO TO 116
C-----COMP AXIAL FORCE
141 CONTINUE
            DO 149 I = 3, INC1
                Q(I) = AE(I) * ( Y(I-1) - Y(I+1) ) / ( 2.0 * H )
149 CONTINUE
                Q(INC2) = GAM * Y(INC2)
                IF ( NBC .EQ. 1 ) 142, 143
142         Q(2) = BC

```

```
          GO TO 144
14J      Q(2) = AE(2) * ( Y(2) - Y(3) ) / H
144      CONTINUE
C-----PRINT OUT COMP RESULTS
        PRINT 541
        PRINT 510
          DO 159 I = 2, INC2
            ISTA = I - 2
            XISTA = ISTA
            Z = XISTA * H
159      PRINT 511, ISTA, Z, Y(I), Q(I), BETA(I)
        CONTINUE
        PRINT 512, GAM
        PRINT 514, ITER
        GO TO 100
9998    PRINT 542
9999    CONTINUE
        END
```

```

SUBROUTINE TRANS
DIMENSION Z(11)
COMMON / BLOCK1 / INC, INCL, H, BETA(103), GAM, INC2, INC3, KFLAG
COMMON / BLOCK2 / NLT, DEPTH(11), NPOINT(11), TR(11, 20),
1 DISPL(11,20), KPOINT, DP(20), SETTLE(20), Y(103)
524 FORMAT ( // // // // 5X *LOAD TRANS CURVE IS NOT GIVEN AT PILE TIP* )
525 FORMAT ( // // // // 5X *PILE DISPLACEMENT IS EXCESSIVE* )
526 FORMAT ( // // // // 5X *TIP MOVEMENT IS EXCESSIVE* )
C-----START COMPUTING BETA
DO 110 I = 2, INC2
    XMULT = I - 2
    STA = H * XMULT
    NLT1 = NLT + 1
    DO 111 J = 2, NLT1
        IF ( STA .LE. DEPTH(J) ) GO TO 112
111    CONTINUE
        PRINT 524
        KFLAG = 1
    RETURN
112    CONTINUE
C-----INTERPOLATION IN EACH CURVE
    JM1 = J - 1
    DO 120 K = JM1, J
        INDEX = NPOINT(K)
        DO 121 L = 2, INDEX
            IF ( Y(I) .LE. DISPL(K, L) ) GO TO 122
121    CONTINUE
            PRINT 525
            KFLAG = 1
        RETURN
122    CONTINUE
        XINT = DISPL(K, L) - DISPL(K, L-1)
        YINT = TR(K, L) - TR(K, L-1)
        Z(K) = TR(K, L-1) + ( YINT / XINT ) * ( Y(I) - DISPL(K,
1 L-1) )
120    CONTINUE
C-----INTERPOLATION BETWEEN TWO CURVES
    CINT = DEPTH(J) - DEPTH(JM1)
    DIF = Z(J) - Z(JM1)
    SKIN = Z(JM1) + ( DIF / CINT ) * ( STA - DEPTH(JM1) )
    BETA(I) = SKIN / Y(I)
110    CONTINUE
C-----START COMPUTING GAMMA
DO 130 I = 2, KPOINT
    IF ( Y(INC2) .LE. SETTLE(I) ) GO TO 131
130    CONTINUE
    PRINT 526
    KFLAG = 1
    RETURN
131    XINT = SETTLE(I) - SETTLE(I-1)
        YINT = PR(I) - PR(I-1)
        PRES = PR(I-1) + ( YINT / XINT ) * ( Y(INC2) - SETTLE(I-1)
1 )
        GAM = PRES / Y(INC2)
    RETURN
END

```



### C.6 Example Run for Program AXP

An example computation is made for a 2-inch diameter steel-pipe pile of 99 inches in length. The properties of the pile are listed in Chapter IV. Experimental load transfer curves computed by Parker and Reese (Figs. 5.11 and 5.12) are used. It is assumed that there is no point resistance.

Example runs are made for four different types of boundary conditions.

1. Downward load at pile top, 1,000 pounds.
2. Uplift force at pile top, 1,000 pounds.
3. Downward displacement at pile top, 0.05 inch.
4. Upward displacement at pile top, 0.05 inch.

The listing of input data for the consecutive runs is shown next, which is followed by the computation results.







LOAD TRANSFER CURVES FROM PARKER AND REESE FOR E B.C.

LOAD AT PILE TOP 1.000E+03 LB

LENGTH, IN 9.900E+01 INCREMENT 25 NO OF SECTION 1 YOUNG, PSI 5.900E+07

SECTION 1 FROM, IN 0. TO, IN 9.900E+01 AREA, SQ IN 7.800E-01 CIRCUM, IN 6.280E+00

LOAD TRANSFER CURVES  
NUMBER OF CURVES 8

DEPTH, INCH,	LOAD, PSI	NUM OF POINTS	DISP, IN
1	0.	2	-2.000E+01
2	0.	2	2.000E+01
2DEPTH, INCH,	3.000E+00	2	2.000E+01
1	0.	2	-2.000E+01
2	0.	2	2.000E+01
3DEPTH, INCH,	1.500E+01	10	1.000E+01
1	0.	10	-2.000E+01
2	-5.000E-02	10	-5.000E-02
3	-9.000E-01	10	-2.000E-02
4	-6.500E-01	10	-1.000E-02
5	0.	10	0.
6	1.000E+00	10	1.000E-02
7	1.400E+00	10	2.000E-02
8	1.050E+00	10	4.000E-02
9	5.500E-01	10	6.000E-02
10	1.000E-02	10	1.000E+01
4DEPTH, INCH,	3.300E+01	10	1.000E+01
1	-2.350E+00	10	-2.000E+01
2	-2.350E+00	10	-3.500E-02
3	-2.000E+00	10	-1.000E-02
4	-1.300E+00	10	-1.000E-02
5	0.	10	0.
6	2.100E+00	10	1.000E-02
7	3.100E+00	10	2.000E-02
8	4.500E+00	10	4.000E-02
9	5.500E+00	10	6.000E-02
10	7.000E+00	10	1.000E+01
5DEPTH, INCH,	5.100E+01	11	1.000E+01
1	-3.300E+00	11	-2.000E+01
2	-3.300E+00	11	-3.200E-02
3	-4.850E+00	11	-2.000E-02
4	-4.850E+00	11	-1.000E-02
5	-2.400E+00	11	-7.000E-03
6	0.	11	0.
7	2.000E+00	11	2.500E-03
8	4.000E+00	11	1.250E-02
9	5.000E+00	11	2.000E-02
10	7.600E+00	11	6.000E-02
11	8.000E+00	11	1.000E+01
6DEPTH, INCH,	6.900E+01	13	1.000E+01
1	0.	13	0.

1	0.	-2.000E+01
2	-8.350E+00	-5.000E-02
3	-9.000E+00	-4.000E-02
4	-9.000E+00	-3.500E-02
5	-8.300E+00	-2.500E-02
6	-6.750E+00	-1.500E-02
7	-3.300E+00	-5.000E-03
8	0.	0.
9	4.000E+00	8.000E-03
10	5.900E+00	2.000E-02
11	8.000E+00	4.000E-02
12	9.800E+00	6.000E-02
13	1.000E+01	1.000E+01
7DEPTH, INCH,	8.700E+01	NUM OF POINTS 10
	LOAD, PSI	DISPL, IN
1	-1.000E+01	-2.000E+01
2	-4.200E+00	-2.500E-02
3	-6.500E+00	-1.000E-02
4	-4.250E+00	-5.000E-03
5	0.	0.
6	4.000E+00	8.000E-03
7	5.900E+00	2.000E-02
8	8.000E+00	4.000E-02
9	9.800E+00	6.000E-02
10	1.000E+01	1.000E+01
8DEPTH, INCH,	9.900E+01	NUM OF POINTS 10
	LOAD, PSI	DISPL, IN
1	-1.000E+01	-2.000E+01
2	-4.200E+00	-2.500E-02
3	-6.500E+00	-1.000E-02
4	-4.250E+00	-5.000E-03
5	0.	0.
6	4.000E+00	8.000E-03
7	5.900E+00	2.000E-02
8	8.000E+00	4.000E-02
9	9.800E+00	6.000E-02
10	1.000E+01	1.000E+01

POINT RESISTANCE CURVE

NUMBER OF POINTS	RESISTANCE, LB	TIP MOVE, IN
1	0.	-1.000E+01
2	0.	0.
3	0.	1.000E+01

COMPUTATION OF DISPLACEMENT AND FORCE

STA	DEPTH, IN	DISPL, IN	FORCE, LB	L TRANS, PSI
0	0.	9.228E-03	1.000E+03	0.
1	3.960E+00	8.868E-03	9.991E+02	8.000E+00
2	7.920E+00	8.510E-03	9.939E+02	4.100E+01
3	1.188E+01	8.154E-03	9.821E+02	7.400E+01
4	1.584E+01	7.804E-03	9.644E+02	1.051E+02
5	1.980E+01	7.461E-03	9.422E+02	1.293E+02
6	2.376E+01	7.127E-03	9.165E+02	1.535E+02
7	2.772E+01	6.802E-03	8.879E+02	1.777E+02
8	3.168E+01	6.489E-03	8.566E+02	2.019E+02
9	3.564E+01	6.187E-03	8.215E+02	2.441E+02

10	3.960E+01	5.898E-03	7.808F+02	2.996E+02
11	4.356E+01	5.625E-03	7.336F+02	2.606E+02
12	4.752E+01	5.371E-03	6.798F+02	4.272E+02
13	5.148E+01	5.137E-03	6.198F+02	4.922E+02
14	5.544E+01	4.925E-03	5.576F+02	5.034E+02
15	5.940E+01	4.736E-03	4.968F+02	5.089E+02
16	6.336E+01	4.568E-03	4.379F+02	5.089E+02
17	6.732E+01	4.421E-03	3.813F+02	5.037E+02
18	7.128E+01	4.294E-03	3.269F+02	5.000E+02
19	7.524E+01	4.187E-03	2.742F+02	5.000E+02
20	7.920E+01	4.097E-03	2.227F+02	5.000E+02
21	8.316E+01	4.026E-03	1.722E+02	5.000E+02
22	8.712E+01	3.974E-03	1.224F+02	5.000E+02
23	9.108E+01	3.938E-03	7.324F+01	5.000E+02
24	9.504E+01	3.921E-03	2.438F+01	5.000E+02
25	9.900E+01	3.921E-03	0.	5.000E+02

MODULUS OF POINT RESISTANCE      0.      LR/TN

NO OF ITERATION      7

## LOAD TRANSFER CURVES FROM PARKER AND REESE

FORCE H.C.

LOAD AT PILE TOP -1.000E+03 LB

PREVIOUS DATA FOR PILE AND SOIL ARE USED

## COMPUTATION OF DISPLACEMENT AND FORCE

STA	DEPTH, IN	DISPL, IN	FORCE, LB	L TRANS, PSI
0	0.	-9.359E-03	-1.000E+03	0.
1	3.960E+00	-8.999E-03	-9.995E+02	4.727E+00
2	7.920E+00	-8.640E-03	-9.963E+02	2.423E+01
3	1.188E+01	-8.283E-03	-9.892E+02	4.373E+01
4	1.584E+01	-7.929E-03	-9.786E+02	6.240E+01
5	1.980E+01	-7.580E-03	-9.651E+02	7.800E+01
6	2.376E+01	-7.236E-03	-9.493E+02	2.360E+01
7	2.772E+01	-6.898E-03	-9.315E+02	1.092E+02
8	3.168E+01	-6.566E-03	-9.120E+02	1.248E+02
9	3.564E+01	-6.242E-03	-8.893E+02	1.612E+02
10	3.960E+01	-5.927E-03	-8.614E+02	2.080E+02
11	4.356E+01	-5.623E-03	-8.283E+02	2.549E+02
12	4.752E+01	-5.332E-03	-7.904E+02	3.017E+02
13	5.148E+01	-5.055E-03	-7.484E+02	3.512E+02
14	5.544E+01	-4.794E-03	-7.012E+02	4.211E+02
15	5.940E+01	-4.551E-03	-6.483E+02	4.909E+02
16	6.336E+01	-4.328E-03	-5.903E+02	5.606E+02
17	6.732E+01	-4.127E-03	-5.278E+02	6.304E+02
18	7.128E+01	-3.949E-03	-4.619E+02	6.841E+02
19	7.524E+01	-3.795E-03	-3.941E+02	7.259E+02
20	7.920E+01	-3.666E-03	-3.248E+02	7.677E+02
21	8.316E+01	-3.561E-03	-2.540E+02	8.095E+02
22	8.712E+01	-3.483E-03	-1.813E+02	8.500E+02
23	9.108E+01	-3.431E-03	-1.082E+02	8.500E+02
24	9.504E+01	-3.405E-03	-3.599E+01	8.500E+02
25	9.900E+01	-3.405E-03	0.	8.500E+02

MODULUS OF POINT RESISTANCE 0. LB/TN

NO OF ITERATION 3



LOAD TRANSFER CURVES FROM PARKER AND REESE      DISPLACEMENT 8.C.  
 DISPLACEMENT AT PILE TOP      5.000E-02 INCH

PREVIOUS DATA FOR PILE AND SOIL ARE USED

COMPUTATION OF DISPLACEMENT AND FORCE

STA	DEPTH, IN	DISPL, IN	FORCE, LB	L TRANS, PSI
0	0.	5.000E-02	3.008F+03	0.
1	3.960E+00	4.892E-02	3.008E+03	1.352E+00
2	7.920E+00	4.784E-02	3.002F+03	7.320E+00
3	1.188E+01	4.676E-02	2.990E+03	1.394E+01
4	1.584E+01	4.569E-02	2.968E+03	2.383F+01
5	1.980E+01	4.463E-02	2.931E+03	4.362E+01
6	2.376E+01	4.358E-02	2.872E+03	6.356E+01
7	2.772E+01	4.256E-02	2.793E+03	8.363E+01
8	3.168E+01	4.158E-02	2.695E+03	1.038E+02
9	3.564E+01	4.063E-02	2.582E+03	1.181E+02
10	3.960E+01	3.972E-02	2.458E+03	1.294E+02
11	4.356E+01	3.886E-02	2.326E+03	1.410E+02
12	4.752E+01	3.805E-02	2.186E+03	1.530E+02
13	5.148E+01	3.729E-02	2.037E+03	1.654E+02
14	5.544E+01	3.658E-02	1.880E+03	1.767E+02
15	5.940E+01	3.594E-02	1.715E+03	1.879E+02
16	6.336E+01	3.535E-02	1.544E+03	1.991E+02
17	6.732E+01	3.483E-02	1.365E+03	2.101E+02
18	7.128E+01	3.437E-02	1.182E+03	2.156E+02
19	7.524E+01	3.398E-02	9.984E+02	2.168E+02
20	7.920E+01	3.365E-02	8.156E+02	2.179E+02
21	8.316E+01	3.339E-02	6.336E+02	2.188E+02
22	8.712E+01	3.320E-02	4.521E+02	2.195E+02
23	9.108E+01	3.307E-02	2.711E+02	2.199E+02
24	9.504E+01	3.300E-02	9.034E+01	2.201E+02
25	9.900E+01	3.300E-02	0.	2.201E+02

MODULUS OF POINT RESISTANCE      0.      LB/IN

NO OF ITERATION      10

LOAD TRANSFER CURVES FROM PARKER AND REESE      DISPLACEMENT b.c.  
 DISPLACEMENT AT PILE TOP      -5.000E-02    INCH

PREVIOUS DATA FOR PILE AND SOIL ARE USED

COMPUTATION OF DISPLACEMENT AND FORCE

STA	DEPTH, IN	DISPL, IN	FORCE, LB	L TRANS, PSI
0	0.	-5.000E-02	-2.764E+03	0.
1	3.960E+00	-4.901E-02	-2.764E+03	1.276E+01
2	7.920E+00	-4.801E-02	-2.763E+03	0.075E+01
3	1.188E+01	-4.702E-02	-2.761E+03	2.115E+00
4	1.584E+01	-4.603E-02	-2.757E+03	5.748E+00
5	1.980E+01	-4.504E-02	-2.744E+03	1.702E+01
6	2.376E+01	-4.406E-02	-2.719E+03	2.850E+01
7	2.772E+01	-4.309E-02	-2.682E+03	4.022E+01
8	3.168E+01	-4.213E-02	-2.633E+03	5.217E+01
9	3.564E+01	-4.119E-02	-2.575E+03	6.043E+01
10	3.960E+01	-4.028E-02	-2.510E+03	6.699E+01
11	4.356E+01	-3.939E-02	-2.440E+03	7.381E+01
12	4.752E+01	-3.853E-02	-2.366E+03	8.089E+01
13	5.148E+01	-3.769E-02	-2.284E+03	9.159E+01
14	5.544E+01	-3.688E-02	-2.182E+03	1.276E+02
15	5.940E+01	-3.612E-02	-2.050E+03	1.650E+02
16	6.336E+01	-3.541E-02	-1.886E+03	2.037E+02
17	6.732E+01	-3.477E-02	-1.691E+03	2.431E+02
18	7.128E+01	-3.420E-02	-1.474E+03	2.625E+02
19	7.524E+01	-3.371E-02	-1.251E+03	2.673E+02
20	7.920E+01	-3.330E-02	-1.026E+03	2.722E+02
21	8.316E+01	-3.297E-02	-7.999E+02	2.769E+02
22	8.712E+01	-3.272E-02	-5.720E+02	2.812E+02
23	9.108E+01	-3.256E-02	-3.432E+02	2.826E+02
24	9.504E+01	-3.247E-02	-1.144E+02	2.833E+02
25	9.900E+01	-3.247E-02	0.	2.833E+02

MODULUS OF POINT RESISTANCE      0.      LB/TN

NO OF ITERATION    13

This page replaces an intentionally blank page in the original.

-- CTR Library Digitization Team

APPENDIX D

DISPLACEMENT MEASUREMENT OF PILE CAP

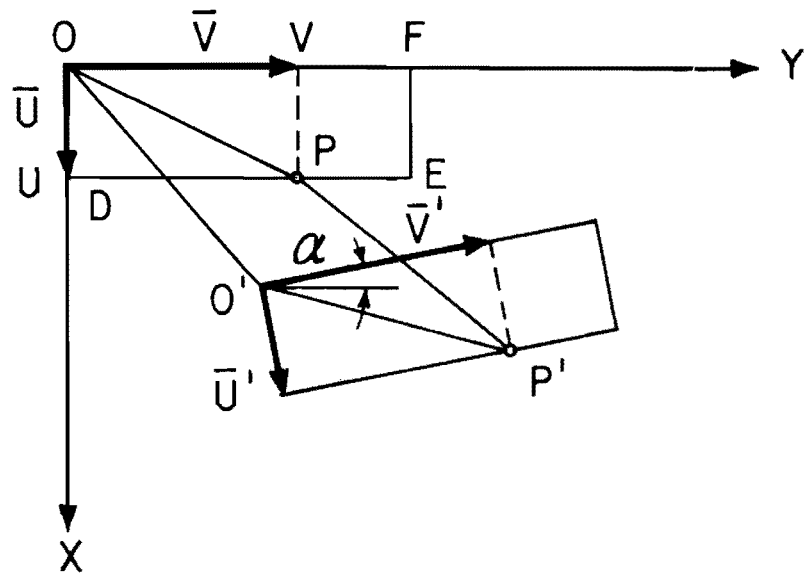
Figure D.1 illustrates the method of computing the two-dimensional displacement of the reference point P on the pile cap from the dial gage readings. Figure D.1a shows the pile cap before and after the displacement. The upper left corner of the pile cap before displacement coincides with the origin of the structural coordinate system. The position of reference point P is expressed as the sum of the two vectors  $\bar{U}$  and  $\bar{V}$ . After displacement, the new position of the corner is expressed by a vector  $\bar{O}O'$ . The new position of the reference point is designated by  $P'$ , which is the sum of vectors  $\bar{O}O'$ ,  $\bar{U}'$ , and  $\bar{V}'$ . Therefore, the displacement of the reference point P is expressed by Eq. D.1.

$$\overline{PP'} = (\overline{O}O' + \bar{U}' + \bar{V}') - (\bar{U} + \bar{V}) \dots \dots \dots (D.1)$$

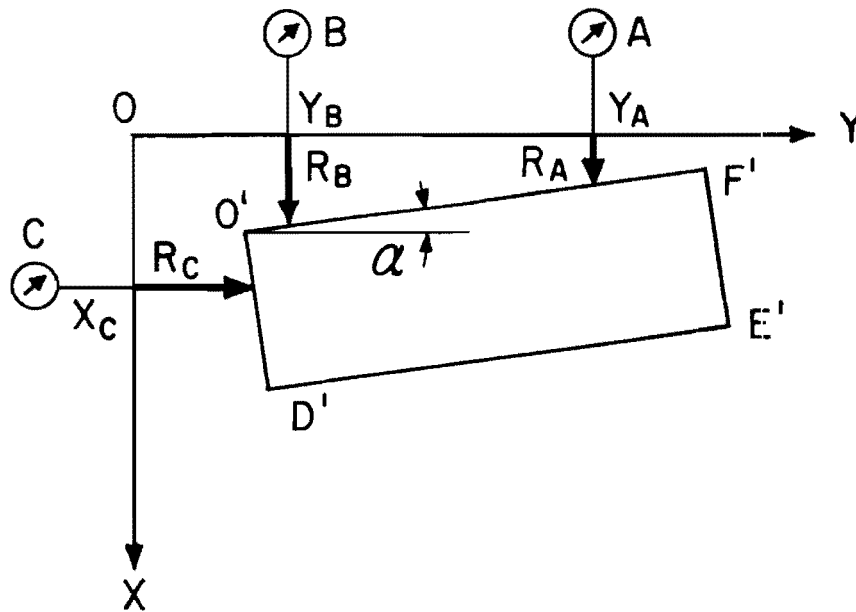
Each dial gage reading  $R_A$ ,  $R_B$ , or  $R_C$  in Fig. D.1b represents the average reading of more than two gages. The rotation angle  $\alpha$  is immediately determined by readings  $R_A$  and  $R_B$ .

$$\alpha = \frac{R_B - R_A}{Y_A - Y_B} \dots \dots \dots (D.2)$$

The vector  $\bar{O}O'$  is determined by solving for the intersection point of two lines  $O'D'$  (Eq. D.3) and  $O'F'$  (Eq. D.4) crossing perpendicular to each other.



(a) Displacement of Pile Cap



(b) Dial Gage Reading

Fig. D.1.. Measurement of Pile-Cap Displacement

$$y = \tan \alpha x + b_1 \dots \dots \dots (D.3)$$

$$x = \tan \alpha y + b_2 \dots \dots \dots (D.4)$$

therefore,

$$OO' = \frac{b_2 - b_1 \tan \alpha}{1 + \tan^2 \alpha} \frac{b_1 + b_2 \tan \alpha}{1 + \tan^2 \alpha} \dots \dots \dots (D.5)$$

Constants  $b_1$  and  $b_2$  are solved from the conditions that  $O'D'$  passes point  $(X_c, R_c)$  and  $O'F'$  passes point  $(R_B, Y_B)$ .

$$b_1 = R_c - X_c \tan \alpha \dots \dots \dots (D.6)$$

$$b_2 = R_B + Y_B \tan \alpha \dots \dots \dots (D.7)$$

The vectors  $\bar{U}'$  and  $\bar{V}'$  are expressed by Eqs. D.8 and D.9

$$U' = (U \cos \alpha \quad U \sin \alpha) \dots \dots \dots (D.8)$$

$$V' = (-V \sin \alpha \quad V \cos \alpha) \dots \dots \dots (D.9)$$

This page replaces an intentionally blank page in the original.

-- CTR Library Digitization Team

## THE AUTHORS

Katsuyuki Awoshika was a graduate research assistant with the Center for Highway Research of The University of Texas at Austin from March 1, 1968, to October 31, 1970. He has had experience in the areas of structural engineering and foundation engineering, and his special interest is in the problems of soil-structure interaction systems. He is currently engaged in research in the area of steel structures at the Nippon Kokan K. K. (Japan Steel and Tube Corporation), Tokyo, Japan.

No picture available.

Lymon C. Reese is Professor and Chairman of the Department of Civil Engineering at The University of Texas at Austin. His specialization is in the area of soil mechanics and foundation engineering. He was the recipient of the Thomas A. Middlebrooks Award of the American Society of Civil Engineers in 1958. One of his primary interests has been in the design of offshore structures and pile foundations. In recent years he has become well known for his research in the application of the finite element method of analysis to problems in soil and rock mechanics. He holds memberships in numerous professional and learned societies and is a Registered Professional Engineer in Texas.

